
# Towards a Pharmacology Intervention for Malignant Catarrhal Fever in Cattle

Thesis submitted in accordance with the requirements of the University of Liverpool for the degree of Doctor in Philosophy

By

Ishtar Adana Mohammed Alethari

**2019**

# Author's Declaration

Apart from the help and advice acknowledged, this thesis represents the unaided work of the author

……

Ishtar Adnan Mohammed Alethari

2019

This research was carried out in the Department of Infection Biology, University of Liverpool.

# Supervisor's Certification

We certify that the thesis entitled "Towards a Pharmacology Intervention for Malignant Catarrhal Fever in Cattle" was prepared under our supervision at the Department of Infection Biology, Institute of Infection and Global Health, Faculty of Health and Life Sciences, University of Liverpool as partial fulfilment of the requirements of University of the Liverpool for the degree of Doctor in Philosophy.

Signature:

Name: Prof James Stewart

Title: Chair of Molecular Virology

Address: Department of Infection Biology

Institute of Infection and Global Health

University of Liverpool

Liverpool Science Park IC2

146 Brownlow Hill

Liverpool L3 5RF

E-mail: j.p.stewart@liverpool.ac.uk

Date:

# Acknowledgements

First and foremost, I would like to thank Allah for his-never ending grace, mercy and provision during what ended up being one of the toughest times of my life. Second, I would like to express my sincere gratitude to my advisor Prof James Stewart for the continuous support of my PhD study, for his patience, motivation, and immense knowledge. His guidance helped me in all the time of research and writing of this thesis. I could not have imagined having a better advisor and mentor for my PhD study. My sincere thanks also goes to Dr Vivien Bubb from Institute of Translational Medicine who worked actively to provide me with the protected academic time to pursue this goal and for her brilliance help in writing.

Next I would like to thank my truly outstanding director Dr Neil Black for his leadership and support to complete my study. Also I would like to thank my brilliant and truly friend Sanaria for her amazing and lovely friendship. I would like to thank my colleagues for their wonderful collaboration. You support me greatly and were always willing to help me. I was always a pleasure to coming to work every day with such lovely and engaging people. Also I would like to thank Dr Stuart Armstrong for his proteomic genius and guidance. A big thank to Dr Jordan, the postdoc in our team for his help in colocalisation analysis, thesis formatting and for his support. I will not forget Dr Janine Coombes who help me too much in confocal images and spend lots of her time to help, all thanks to her. I am also grateful to the lovely technical team in the Infection Biology of IGH, at the University of Liverpool, Mrs Catherine Hartley, Mrs Catherine Glover and Dr Jennifer Mullin who always provided me extensive personal and professional guidance and taught me a great deal about both scientific research and life in general, thanks for everything. I would like to thank my colleague Mohammed for his support.

Again bid thanks to Dr Isabel who support me and help my emotionally and practically. Big thank to Dr Nadine for her help and guidance.

Many thanks to my sponsor, University of Al-Qadisiyah, Ministry of Higher Education and Scientific Research in Iraq (MOHESR) and the Iraqi Cultural Attaché, London for providing this opportunity and supporting me financially and enabling me to obtain this degree.

A very special gratitude goes to my family; my mother, my brother and my sisters for their emotional support, love and guidance which was with me in my life all the time. I would also like to send a special thanks to the person who wished to see me I take this degree, who is the most important part in my education, my deceased father. Lastly, a huge thanks to my lovely husband Zaki who grateful support me and help me to pass this hard time and to reach to this point, also I would like to thank my three flowers my lovely daughters; Shams, Shahad and Fatima to be in my life.

# Abstract

Malignant catarrhal fever (MCF) is a frequently lethal disease, which is characterised by high fever, depression, profuse nasal discharge, corneal opacity, as well as hyperaemic to ulcerative lesions in the mucosa of the respiratory tract. This leads to ocular and nasal discharge, diarrhoea. Severe inflammation of the conjunctival, oral, and nasal mucosa is accompanied by necrosis in the oral and nasal cavities sometimes extending into the oesophagus and trachea. MCF in general is sporadic, affecting individual animals within a group, but occasionally can cause high losses in the herd.

MCF in domestic cattle is caused by two γ-herpesviruses namely ovine herpesvirus 2 (OvHV-2) and alcelaphine herpesvirus 1 (AlHV-1). AlHV-1 is endemic in wildebeest (*Connochaetes taurinus)* in Africa where it causes wildebeest associated malignant catarrhal fever (WA-MCF). Whereas OvHV-2 is endemic in sheep populations worldwide and causes sheep associated malignant catarrhal fever (SA-MCF).

MCF is characterized by marked T cell hyperplasia and proliferation of unrestricted cytotoxic large granular lymphocytes (LGLs) which leads to necrosis of infiltrated tissues. These LGLs can be grown out in culture and contain OvHV-2 in a latent form. Little is known about the underlying molecular basis of MCF pathogenesis or what controls the differences in clinical outcome of infection in two closely-related host species.

The overall aim of this project was to understand better the interactions between OvHV-2 and cellular proteins during latency to identify possible druggable targets that could be used for MCF therapy. All γ-herpesviruses express a protein during latency called latency-associated nuclear antigen (LANA). This protein in other herpesviruses is a master-regulator of virus latency. It tethers virus genome to host chromatin and ensures genome

replication during latency as well as interacting with cellular proteins to control cell replication and also innate defence mechanisms. OvHV-2 has been shown to encode and express a LANA protein (oLANA) during latency in LGLs. The specific aim of this project was to determine the interactions of oLANA with cellular proteins which would give insight into pathogenesis as well as targets for therapeutic intervention. To do this, co-immunoprecipitatioin in HEK 293T cells was combined with label-free quantitative mass spectrometry to identify binding partners. A GFP-tagged recombinant oLANA lacking the central repetitive domain (GFP-oLANAΔ) was used as bait with GFP-trap technology to pull down cellular partners and then co-precipitants were analysed by mass spectrometry. Eight cellular proteins were identified as potential binding partners in this process. Of these, only histone H1 was validated by co immunoprecipitation and western blotting. While two others CCDC12 and Rad50 were shown to co-localise with oLANA by immunofluorescence and confocal microscopy. These results confirm, as other LANAs, a chromatin binding role for oLANA. They also give potential cellular targets for future investigation and therapeutic intervention.

# List of abbreviations

| | |
|---|---|
| AIHV-1 | Alcelaphine herpesvirus 1 |
| AlHV-2 | Alcelaphine herpes virus 2 |
| APS | Ammonium persulfate |
| BLAST | Basic Local Alignment Sequence Tool |
| BMCF | Bovine malignant catarrhal fever |
| BoHV-1 | Bovine herpesvirus 1 |
| BoHV-6 | Bovine herpesvirus 6 |
| Bp | Base pair |
| BVD | Bovine virus diarrhoea |
| CaCl2 | Calcium chloride |
| cGAS | cGMP-AMP synthase |
| CIAP | calf intestinal alkaline phosphatase |
| CID | collisional induced dissociation |
| CMV | Cytomegalovirus |
| CpHV-2 | Caprine herpesvirus 2 |
| CTLs | Cytotoxic T lymphocytes |
| DMEM | Dulbecco's Modified Eagle's Medium - high |
| DNA | Deoxyribonucleic acid |
| dNTPs | Deoxyribonucleotide triphosphate |
| dsDNA | Double-stranded DNA |
| dsDNA BR | Double-stranded DNA broad range |
| E gene | Early |
| *E. coli* | *Escherichia coli* |
| EB | Elution buffer |
| EBNA1 | Epstein-Barr nuclear antigen |
| EBV | Epstein-Barr virus |
| ECL | Enhanced chemoluminescence |
| EDTA | Ethylenediaminetetraacetic acid |
| EHV-2 | Equid herpesvirus 2 |

| | |
|---|---|
| EHV-5 | Equid herpesvirus 5 |
| ELISA | Enzyme-linked immunosorbent assay |
| FBS | Foetal bovine serum |
| gB | Glycoprotein B |
| gD | Glycoprotein D |
| GFP | Green fluorescence protein |
| gH | Glycoprotein H |
| gl | Glycoprotein L |
| GMP | Genome maintenance protein |
| HEK | Human embryonic kidney |
| HEPES | 4-(2-Hydroxyethyl)piperazine-1-ethanesulfonic acid |
| HHV-4 | Human herpesvirus 4 |
| HHV-6 | Human herpesvirus 6 |
| HHV-7 | Human herpesvirus 7 |
| HipHV-1 | Hippotragine herpesvirus 1 |
| Hr(s) | Hour, hours |
| HRL | Horseradish peroxidase-linked |
| HSV-1 | Herpes simplex virus 1 |
| HSV-2 | Herpes simplex virus 2 |
| HVS | Herpesvirus saimiri |
| Ibex-MCFV | Ibex malignant catarrhal fever virus |
| IBR | Infectious bovine rhinotracheitis |
| IEGs | Immediate early genes |
| IL-2 | Interleukin-2 |
| IgG | Immunoglobulin G |
| Kb | Kilo base |
| kDa | Kilo Dalton |
| KSHV | Kaposi's sarcoma-associated herpesvirus |
| L | Late |
| LANA | Latency-Associated Nuclear Antigen |
| LGLs | large granular lymphocytes |

| | |
|---|---|
| LRTs | Long terminal repeats |
| MCF | Malignant Catarrhal Fever |
| MCFVs | Malignant catarrhal fever viruses |
| MCFV-WTD | White-tailed deer |
| MHC | Major Histocompatibility complex |
| MHCI | Major histocompatibility class I |
| MHCII | Major histocompatibility class II |
| MHV-68 | Murine gammaherpesvirus 68 |
| MQ | MaxQuant |
| MuHV-4 | Murid herpesvirus 4 |
| NK | Natural killer |
| NLS | Nuclear localization signal |
| NSAIDs | Nonsteroidal anti-inflammatory drugs |
| OIE | World Organisation for Animal Health |
| ORF 73 | Open reading frame 73 |
| ORFs | Open reading frames |
| OvHV-2 | Ovine herpesvirus 2 |
| PAGE | SDS-polyacrylamide gel electrophoresis |
| PBL | peripheral blood lymphocyte |
| PBMCs | Peripheral blood mononuclear cells |
| PBMNC | polymorphonuclear leukocytes |
| PBS | Dulbecco's Phosphate Buffered Saline |
| PCR | Polymerase Chain Reaction |
| PEI | Polyethlenimine |
| PFA | Paraformaldehyde |
| PIPA buffer | Radioimmunoprecipitation assay buffer |
| PRRs | Pattern recognition receptors |
| pSRG | Vesicular stomatitis virus G protein |
| RNA | Ribonucleic acid |
| RT | Room temperature |
| S.O.C | Super Optimal broth with Catabolite repression |

| | |
|---|---|
| SA-MCF | Sheep associated MCF |
| SDS | Sodium dodecyl sulphate |
| SOX | shutoff and exonuclease |
| TAE | Tris-acetate-EDTA |
| TBS | Tris-buffered saline |
| TBS-T | Tris-buffered saline -Tween 20 |
| TEMED | N,N,N′,N′-Tetramethylethylenediamine |
| TFA | trifluoroacetic acid |
| TNF | Tumour necrosis factor |
| U | Unit |
| UV | Ultraviolet |
| V | Volt |
| VP-16 | Etoposide, VePesid |
| VZV | Varicella-zoster virus |
| WA-MCF | Wildebeest associated MCF |
| Xg | Times gravity |
| γHVs | Gamma herpesvirus |
| NF-κB | Nuclear factor kappa-light-chain-enhancer of activated B cells |

# Table of Contents

# List of figures

# List of tables

# Chapter one: Introduction

# 1.1 *Herpesviridae*

The first description of the word 'herpes' was given about 2600 years ago. The family name is derived from the Greek word 'herpein', meaning 'to creep', referring to the latent, recurring infections typical of this group of viruses (Mettenleiter and Sobrino, 2008). The *Herpesviridae* family has a large number of viruses which generally share a common structure, with icosahedral capsid symmetry and a relatively large double-stranded linear DNA genome encoding 100–200 genes. Herpesviruses are a group of double-stranded DNA viruses which belong to the main order *Herpesvirales,* which includes three main subfamilies: *Alloherpesviridae*, *Herpesviridae* and *Malacoherpesviridae*. These are widely distributed in the animal kingdom (Davison, 2010).

The *Herpesviridae* family consists of the herpesviruses of mammals, birds and reptiles. These viruses are widespread in vertebrate species, have a strong effect on humans and almost all animal species, and cause serious diseases, which have effects on the organisms' health and epidemiological condition. These viruses also have economic importance in food production. Herpesviruses are usually hosted in a species-specific way by their natural hosts (McGeoch *et al.*, 2006). The *Herpesviridae* family can cause a range of clinical diseases in different species, including infectious bovine rhinotracheitis (IBR), a major respiratory disease of cattle, and the fatal lymphoproliferative disease, malignant catarrhal fever (MCF) of cattle (Ababneh *et al.*, 2014).

## 1.1.1 Structure and biological features of herpesviruses

### 1.1.1.1 Structure of herpesviruses

The most important biological feature of herpesviruses is the distinct morphology of the virion (virus particle); it is 120–300 nm in diameter and is composed of a unique four-layered structure: the core, the capsid, the tegument and the envelope. The core contains the large linear double-stranded DNA which integrates into the host cell chromosome; this is enclosed by an icosahedral capsid about 120–230 kb in size, which includes 162 capsomers (capsid subunits) and which encloses the viral genome. This capsid is surrounded by an amorphous globular material layer (proteinaceous matrix) called the tegument, which is further surrounded by a lipid bilayer called the envelope, containing viral glycoprotein spikes (Maclachlan *et al.*, 2016) (Figure 1-1). The genome of herpesviruses is complex, with unique and repeated regions of DNA.

The herpesvirus DNA is double-stranded and linear, but it is circularised as an episome during latency, and this episome remains inside the nucleus of the host cells. It maintains itself by tethering into the host chromosome during genome segregation into daughter cells during cell division (Stenglein *et al.*, 2009).

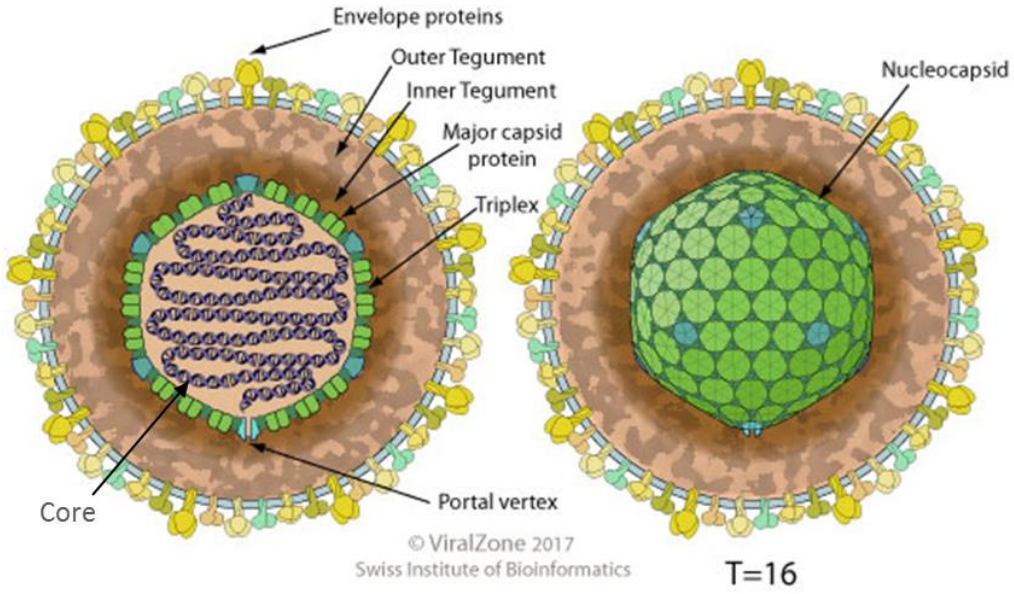


**Figure 1- 1. Schematic diagram of *Herpesviridae* virion.**
Virions are enveloped, spherical to pleomorphic, 150-200 nm in diameter, T=16 icosahedral symmetry. Capsid consists of 162 capsomers and is surrounded by an amorphous tegument. Glycoprotein complexes are embedded in the lipid envelope (**https://viralzone.expasy.org/176?outline=all_by_species**)

### 1.1.1.2 Biological features of herpesviruses

*Herpesviridae* family members share some common features, including the following. First, they share a complex double-stranded DNA genome encoding a number of enzymes involved in protein processing, DNA synthesis, and nucleic acid metabolism, which varies between different members. Secondly, DNA synthesis, capsid formation and virus gene transcription take place in the nucleus of the host cell. Third, viruses require a distraction method in the host cell to complete the viral replicative processes, which are usually characterised by lysis of the infected host cell. Also, each virus has its own host range, which may vary considerably both in nature and in the laboratory. And finally, the virus is able to persist in a latent form within the host to establish a long-term latent host infection (Christian *et al.*, 2012). During latent infection, the virus shuts down its activity inside

infected cells, thus evading the immune system and producing progeny virus DNA which remains within the host cell as episomal DNA (Pellet and Roizman, 2013).

These characteristics give herpesviruses the ability to place/maintain their main reservoir in latently infected organisms. *Herpesviridae* family members are distributed in nature in such a way that one or more herpesviruses can affect one or more species (Pellet and Roizman, 2013).

### 1.1.1.3 Herpesvirus genomes

Herpesvirus DNA genomes are composed of double-stranded DNA organised in a number of open reading frames (ORFs) which encode a range of from 70 to more than 200 proteins. *Herpesviridae* family members have repeated sequences which are organised proportionally according to the genera of the herpesviruses. Each virus has a unique long and short sequence region. In gamma-herpesviruses such as Kaposi's sarcoma herpesvirus (KSHV), the DNA genome has a symmetric terminal sequence at both ends, while in other members such as EBV, unrelated repeat sequences (internal repeats) are present within the genome (Modrow *et al.*, 2013).

## 1.1.2 Herpesvirus classification

The *Herpesviridae* family is divided into three distinct subfamilies according to their genome sequence arrangement, their host-replication behaviour, their biological properties and similarities in the functions of important viral proteins (Davison *et al.*, 2009a; Davison, 2010). The three subfamilies are, *Alphaherpesvirinae*, *Betaherpesvirinae* and *Gammaherpesvirinae,* according to their common genetic and biological properties and an analysis of their double-strand DNA (Pellet and Roizman, 2013). These are shown in

Table (1-1) as well as in Figure (1-2). Many members of the *Alphaherpesvirinae* and the *Gammaherpesvirinae* are of very great importance in veterinary medicine.

The most recent classification of herpesviruses has been updated, and its usage is recommended by the International Committee on Taxonomy of Viruses; http://www.ictvonline.org.

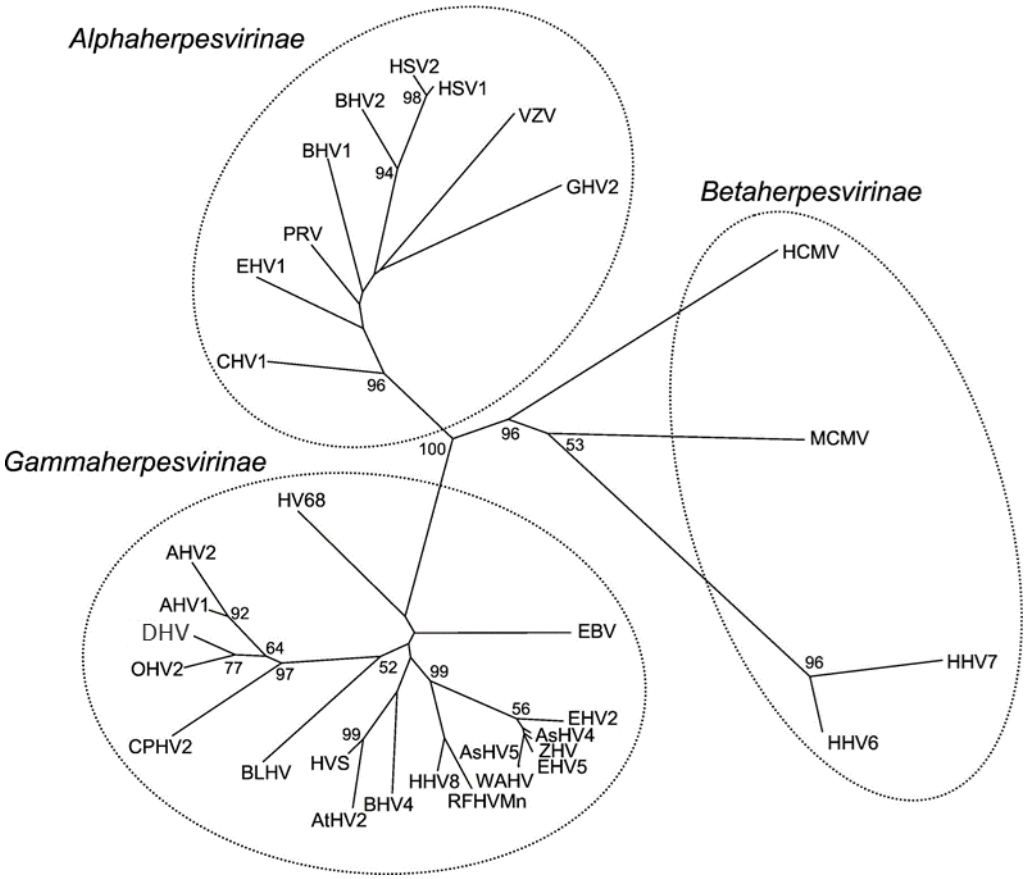


**Figure 1- 2. A Phylogenetic tree for the DNA polymerase gene proteins of representative *alpha-, beta-,* and *gammaherpesviruses.***

Bootstrap values of greater than 50 are shown, and the branch lengths represent relative genetic distances (Kleiboeker *et al.*, 2002).Bootstrapping values indicate how many times the same branch was observed when repeating the phylogenetic reconstruction on a re-sampled set of data

| Name[a] | Acronym[b] | Common name[c] |
|---|---|---|
| **Order *Herpesvirales*** | | |
| **Family *Herpesviridae*** | | |
| **Subfamily:** | | |
| **I. *Alphaherpesvirinae*** | | |
| *1- Iltovirus* Genus: | | |
| *Gallid alphaherpesvirus* 1 | GaHV1 | Infectious laryngotracheitis virus |
| *Psittacid alphaherpesvirus* 1 | PsHV1 | Pacheco's disease virus |
| *2- Mardivirus* Genus: | | |
| *Columbid alphaherpesvirus* 1 | CoHV1 | None Pigeon herpesvirus |
| *Gallid alphaherpesvirus* 2 | GaHV2 | Marek's disease virus type 1 |
| *Gallid alphaherpesvirus* 3 | GaHV3 | Marek's disease virus type 2 |
| *Meleagrid alphaherpesvirus* 1 | MeHV1 | Turkey herpesvirus |
| *3- Simplexvirus* Genus: | | |
| *Ateline alphaherpesvirus* 1 | AtHV1 | Spider monkey herpesvirus |
| *Bovine alphaherpesvirus* 2 | BoHV2 | Bovine mammillitis virus |
| *Cercopithecine alphaherpesvirus* 2 | CeHV2 | SA8 |
| *Human alphaherpesvirus* 1 | HHV1 | Herpes simplex virus type 1 |
| *Human alphaherpesvirus* 2 | HHV2 | Herpes simplex virus type 2 |
| *Macacine alphaherpesvirus* 1 | McHV1 | B-virus |
| *Macropodid herpesvirus* 1 | MaHV1 | Parma wallaby herpesvirus |
| *Macropodid herpesvirus* 2 | MaHV2 | Dorcopsis wallaby herpesvirus |
| *Papiine herpesvirus* 2 | PaHV2 | Herpesvirus papio 2 |
| *Saimiriine herpesvirus* 1 | SaHV1 | Marmoset herpesvirus |
| *4- Varicellovirus* Genus: | | |
| *Bovine alphaherpesvirus* 1 | BoHV1 | Infectious bovine rhinotracheitis virus |
| *Bovine alphaherpesvirus* 5 | BoHV5 | Bovine encephalitis herpesvirus |
| *Bubaline alphaherpesvirus* 1 | BuHV1 | Water buffalo herpesvirus |
| *Canid alphaherpesvirus* 1 | CaHV1 | Canine herpesvirus |
| *Caprine alphaherpesvirus* 1 | CpHV1 | Goat herpesvirus |

| | | |
|---|---|---|
| *Cercopithecine alphaherpesvirus* 9 | CeHV9 | Simian varicella virus |
| *Cervid alphaherpesvirus* 1 | CvHV1 | Red deer herpesvirus |
| *Cervid alphaherpesvirus* 2 | CvHV2 | Reindeer herpesvirus |
| *Equid alphaherpesvirus* 1 | EHV1 | Equine abortion virus |
| *Equid herpesvirus* 3 | EHV3 | Equine coital exanthema virus |
| *Equid herpesvirus* 4 | EHV4 | Equine rhinopneumonitis virus |
| *Equid herpesvirus* 8 | EHV8 | Asinine herpesvirus 3 |
| *Equid herpesvirus* 9 | EHV9 | Gazelle herpesvirus |
| *Felid herpesvirus* 1 | FeHV1 | Feline rhinotracheitis virus |
| *Human herpesvirus* 3[e] | HHV3 | Varicella-zoster virus |
| *Phocid herpesvirus* 1 | PhoHV1 | Harbour seal herpesvirus |
| *Suid herpesvirus* 1 | SuHV1 | Pseudorabies virus |
| *5*- Unassigned Genus: | | |
| *Chelonid alphaherpesvirus* 5 | ChHV5 | Chelonid fibropapilloma-associated |
| *Chelonid herpesvirus* 6 | ChHV6 | Lung–eye–trachea disease-associated virus |
| Tentative species in the genus *Equid herpesvirus* 6 | EHV6 | Asinine herpesvirus 1 |
| **I. *Betaherpesvirinae*** | | |
| 1- *Cytomegalovirus* Genus: | | |
| *Cercopithecine betaherpesvirus* 5 | 5 CeHV5 | African green monkey cytomegalovirus |
| *Human betaherpesvirus* 5 | HHV5 | Human cytomegalovirus |
| *Macacine betaherpesvirus* 3 | McHV3 | Rhesus cytomegalovirus |
| *Panine betaherpesvirus* 2 | PnHV2 | Chimpanzee cytomegalovirus |
| Tentative species in the genus *Aotine betaherpesvirus* 1 | AoHV1 | Herpesvirus aotus type 1 |
| *Aotine betaherpesvirus* 3 | AoHV3 | Herpesvirus aotus type 3 |
| 2- *Muromegalovirus* Genus: | | |
| *Murid betaherpesvirus* 1 | MuHV1 | Mouse cytomegalovirus |
| *Murid betaherpesvirus* 2 | MuHV2 | Rat cytomegalovirus |
| 3- *Proboscivirus* Genus: | | |
| *Elephantid betaherpesvirus* | ElHV1 | Elephant endotheliotropic herpesvirus |

| | | |
|---|---|---|
| Unassigned species in the subfamily *Caviid herpesvirus* 2 | CavHV2 | Guinea pig cytomegalovirus |
| *Suid herpesvirus* 2 | SuHV2 | Pig cytomegalovirus |
| *Tupaiid herpesvirus* 1 | 1 TuHV1 | Tree shrew herpesvirus |
| 4- *Roseolovirus* Genus: | | |
| *Human betaherpesvirus* 7 | HHV7 | Human herpesvirus 7 |
| *Human betaherpesvirus* 6 | HHV6 | Human herpesvirus 6 |
| 5- Unassigned Genus: | | |
| *Caviid betaherpesvirus* 2 | CavHV2 | Guinea pig cytomegalovirus |
| *Suid betaherpesvirus* 2 | SuHV2 | Pig cytomegalovirus |
| *Tupaiid betaherpesvirus* 1 | TuHV1 | Tree shrew herpesvirus |
| **II. *Gammaherpesvirinae*** | | |
| 1- *Lymphocryptovirus* Genus: | | |
| *Callitrichine gammaherpesvirus* 3 | CalHV3 | Marmoset lymphocryptovirus |
| *Cercopithecine gammaherpesvirus* 14 | CeHV14 | African green monkey EBV-like virus |
| *Gorilline gammaherpesvirus* 1 | GoHV1 3 | Gorilla herpesvirus |
| *Human gammaherpesvirus* 4 | HHV4 | Epstein-Barr virus |
| *Macacine herpesvirus* 4 | McHV4 | Rhesus lymphocryptovirus |
| *Panine gammaherpesvirus* 1 | PnHV1 | Herpesvirus pan |
| *Papiine gammaherpesvirus* 1 | PaHV1 | Herpesvirus papio |
| *Pongine gammaherpesvirus* 2 | PoHV2 | Orangutan herpesvirus |
| 2- *Rhadinovirus* Genus: | | |
| *Ateline herpesvirus* 2 | AtHV2 | Herpesvirus ateles strain 810 |
| *Ateline herpesvirus* 3 | AtHV3 | Herpesvirus ateles strain 73 |
| *Bovine herpesvirus* 4 | BoHV4 | Movar virus |
| *Human herpesvirus* 8 | HHV8 | Kaposi's sarcoma-associated herpesvirus |
| *Macacine herpesvirus* 5 | McHV5 | Rhesus rhadinovirus |
| *Murid herpesvirus* 4 | MuHV4 | Murine gammaherpesvirus 68 |
| *Saimiriine herpesvirus* 2 | SaHV2 | Herpesvirus saimiri |
| Tentative species in the genus *Leporid herpesvirus* 1 | Tentative 1 LeHV1 | Cottontail rabbit herpesvirus |

| | | |
|---|---|---|
| *Leporid herpesvirus* | 2 LeHV2 | Herpesvirus cuniculi |
| *Leporid herpesvirus* 3 | 3 LeHV3 | Herpesvirus sylvilagus |
| *Marmodid herpesvirus* 1 | MarHV1 | Woodchuck herpesvirus |
| 3- *Macavirus* Genus: | | |
| *Alcelaphine herpesvirus* 1 | AlHV1 | Malignant catarrhal fever virus |
| *Alcelaphine herpesvirus* 2 | AlHV2 | Hartebeest malignant catarrhal fever virus |
| *Bovine herpesvirus* 6 | BoHV6 | Bovine lymphotropic herpesvirus |
| *Caprine herpesvirus* 2 | CpHV2 | Caprine herpesvirus 2 |
| *Hippotragine herpesvirus* 1 | HiHV1 | Roan antelope herpesvirus |
| *Ovine herpesvirus* 2 | OvHV2 | Sheep-associated malignant catarrhal fever virus |
| *Suid herpesvirus* 3 | SuHV3 | Porcine lymphotropic herpesvirus 1 |
| *Suid herpesvirus* 4 | SuHV4 | Porcine lymphotropic herpesvirus 2 |
| *Suid herpesvirus* 5 | SuHV5 | Porcine lymphotropic herpesvirus 3 |
| 4- *Percavirus* Genus: | | |
| *Equid gammaherpesvirus* 2 | EHV2 | Equine herpesvirus 2 |
| *Equid gammaherpesvirus* 5 | EHV5 | Equine herpesvirus 5 |
| *Mustelid gammaherpesvirus* 1 | MusHV1 | Badger herpesvirus |
| Unassigned species in the subfamily *Equid herpesvirus* 7 | EHV7 | Asinine herpesvirus 2 |
| *Phocid herpesvirus* 2 | PhoHV2 | Phocid herpesvirus 2 |
| *Saguinine herpesvirus* 1 | 1 SgHV1 | Callitrichine herpesvirus 1 Herpesvirus saguinus |
| Unassigned species in the family *Iguanid herpesvirus* 2 | 2 IgHV2 | Iguana herpesvirus |
| Unassigned viruses in the family *Acciptrid herpesvirus* 1 | 1 AcHV1 | Bald eagle herpesvirus |
| *Anatid herpesvirus* 1 | 1 AnHV1 | Duck plague herpesvirus |
| *Boid herpesvirus* 1 | BoiHV1 | Boa herpesvirus |
| *Callitrichine herpesvirus* 2 | CalHV2 | Marmoset cytomegalovirus |
| *Caviid herpesvirus* 1 | CavHV1 | Guinea pig herpesvirus |
| *Caviid herpesvirus* 3 | CavHV3 | Guinea pig herpesvirus 3 |

| | | |
|---|---|---|
| *Cebine herpesvirus* 1 | CbHV1 | Capuchin herpesvirus AL-5 |
| *Cebine herpesvirus* 2 | 2 CbHV2 | Capuchin herpesvirus AP-18 |
| *Cercopithecine herpesvirus* 3 | CeHV3 | SA6 |
| *Cercopithecine herpesvirus* 4 | CeHV4 | SA15 |
| *Chelonid herpesvirus* 1 | ChHV1 | Grey patch disease-associated virus |
| *Chelonid herpesvirus* 2 | ChHV2 | Pacific pond turtle herpesvirus |
| *Chelonid herpesvirus* 3 | ChHV3 | Painted turtle herpesvirus |
| *Chelonid herpesvirus* 4 | ChHV4 | Argentine turtle herpesvirus |
| *Ciconiid herpesvirus* 1 | CiHV1 | Black stork herpesvirus |
| *Cricetid herpesvirus* 1 | CrHV1 | Hamster herpesvirus |
| *Elapid herpesvirus* 1 | EpHV1 | Indian cobra herpesvirus |
| *Erinaceid herpesvirus* 1 | ErHV1 | European hedgehog herpesvirus |
| *Falconid herpesvirus* 1 | FaHV1 | Falcon inclusion body disease virus |
| *Gruid herpesvirus* 1 | GrHV1 | Crane herpesvirus |
| *Iguanid herpesvirus* 1 | IgHV1 | Green iguana herpesvirus |
| *Lacertid herpesvirus* 1 | LaHV1 | Green lizard herpesvirus |
| *Macacine herpesvirus* 6 | McHV6 | Rhesus leukocyte-associated herpesvirus strain 1 |
| *Macacine herpesvirus* 7 | McHV7 | Herpesvirus cyclopis |
| *Murid herpesvirus* 3 | MuHV3 | Mouse thymic herpesvirus |
| *Murid herpesvirus* 5 | MuHV5 | Field mouse herpesvirus |
| *Murid herpesvirus* 6 | MuHV6 | Sand rat nuclear inclusion agent |
| *Ovine herpesvirus* 1 | OvHV1 | Sheep pulmonary adenomatosis-associated Herpesvirus |
| *Perdicid herpesvirus* 1 | PdHV1 | Bobwhite quail herpesvirus |
| *Phalacrocoracid herpesvirus* 1 | PhHV1 | Cormorant herpesvirus |
| *Procyonid herpesvirus* 1 | PrHV1 | Kinkajou herpesvirus |
| *Sciurid herpesvirus* 1 | ScHV1 | Ground squirrel cytomegalovirus |
| *Sciurid herpesvirus* 2 | ScHV2 | Ground squirrel herpesvirus |
| *Sphenicid herpesvirus* 1 | SpHV1 | Black footed penguin herpesvirus |

| | | |
|---|---|---|
| *Strigid herpesvirus* 1 | StHV1 | Owl hepatosplenitis virus |

**Table 1- 1. The order of *Herpesviridae***

a: Species of the family *Herpesviridae* (ICTV; http://www. ictvonline.org). Formal taxonomic names are in italicized font.

b: Acronyms apply to viruses, not species, and have no taxonomic standing. A hyphen may be included prior to the number

c: Where the name has changed, the former name is given. Where the name is new, the word "None" is given. Where the name has not changed, no information is given

Currently, a great many types of viruses have been identified, and it seems that this number will increase further with the discovery of new species. *Herpesviridae* family has at least nine human viruses and 28 viruses of animal species which have importance in medical and veterinary practice.

### 1.1.2.1 *Alphaherpesvirinae*

The *Alphaherpesvirinae* subfamily is characterised by its ability to infect a wide (variable) range of hosts, including mammals (human and animal), birds and reptiles. The family's members are characterised by rapid growth and proliferation in cell cultures, short replicative cycles in a host (18 h) and the ability to infect different types of cells with efficient lysis of the infected cell. This ability includes such things as fibroblasts in culture, epithelial cells and the establishment and maintenance of latent infections in sensory ganglia (Pellet and Roizman, 2013). Members of this subfamily are often referred to as neurotropic herpesviruses (which infect nervous system tissue). The most well-known human herpesviruses for this subfamily are the herpes simplex virus 1 (HSV-1), the herpes simplex virus 2 (HSV-2) and the varicella-zoster virus. However, the most important viruses in this subfamily of veterinary medicine are; bovine herpesvirus 2 (BoHV-2) which causes lumpy skin disease, bovine herpesvirus 1 (BoHV-1) which causes infectious bovine

rhinotracheitis in cattle, gallid herpesvirus 2 which causes Marek's disease in poultry, see Table (1-1).

### 1.1.2.2 *Betaherpesvirinae*

The *Betaherpesvirinae* subfamily of viruses have slightly different features from alphaherpesviruses. They are narrow-spectrum cells (e.g. lymphoid cells and kidney and secretory glands), they have a fairly restricted host range and they are slower to replicate in cell cultures. Furthermore, unlike alphaherpesviruses, they have a long reproductive cycle in the infected host, which often results in the development of a carrier state. The infection is established in lymphocytes, secretory glands and the cells of the kidney, as well as other cell types. Infected cells then become enlarged (cytomegaly) (Davison, 2010). Viruses of this subfamily can establish latency inside immune cells associated with monocyte series (Modrow *et al.*, 2013). The human herpesviruses *Cytomegalovirus* (CMV), HHV-6 and HHV-7 are members of this subfamily.

### 1.1.2.3 *Gammaherpesvirinae*

Viruses of this subfamily have a limited host range. They are lymphotropic, have a specific affinity for either T or B lymphocytes (Riaz *et al.*, 2014) and have a predominant specificity for lymphoblastoid cells, where they replicate and establish latency. The period of the replication cycle is variable according to the virus type. Viruses in this subfamily appear to favour the initial establishment of latency, while only a subset support lytic replication compared to alpha or beta herpesviruses, which undergo lytic replication (Ackermann, 2006). *Gammaherpesvirinae* include both animal and human viruses such as Epstein-Barr virus (EBV), Kaposi's sarcoma-associated herpesvirus (KSHV) in humans and malignant catarrhal fever in cattle.

Gammaherpesviruses share some common features, including the structure of some proteins (Ackermann, 2006; McGeoch *et al.*, 2006; Fields *et al.*, 2007). A significant feature of gammaherpesviruses is to create a latent infection in the memory of lymphocytes, which results in less visible tissue damage (Yin *et al.*, 2003). Generally, a gammaherpesvirus infection depends not only on the virus itself but also on the target animal species and the type of cell infection.

The subfamily *Gammaherpesvirinae* comprises four separate genera. The first is *Lymphocryptovirus*, which to date has been found only in primate hosts. This genus includes *human herpesvirus 4* (HHV-4), also known as Epstein-Barr virus (EBV), which was first found in a lymphoblastoid cell line from a B cell lymphoma in 1964 (Epstein *et al.*, 1964). The second is *Macavirus*, which are of veterinary importance and include malignant catarrhal fever viruses (MCFVs), which are described in further detail in section (1.2.2) below. Third is the genus *Percavirus*, including *Equid herpesvirus 2* (EHV-2) and *Equid herpesvirus 5* (EHV-5), which were transferred from the genus *Rhadinovirus.* These viruses cause upper respiratory tract disease in horses; latency is established in B cells in the respiratory tract and transmission takes place via the respiratory system (Ackermann, 2006; Ackermann, 2005a). Finally, the fourth is the genus *Rhadinovirus*, which are found in an enormous range of mammals. This group includes *human herpesvirus 8* (KSHV), which was first found in a Kaposi's sarcoma in an AIDS patient (Davison *et al.*, 2009b).

### 1.1.3 Herpesviruses life cycle

The herpesviruses life cycle is divided into two different stages in the host: the lytic stage and the latent stage (Riaz *et al.*, 2017). A herpesvirus infection begins when the virus attaches to the target cell surface and binds to specific host receptors (glycoproteins),

initiating viral entry. During virus fusion and entry into the cytoplasm, the virus loses its envelope, viral components are liberated and the capsid is translocated into the cell nucleus through the nuclear pores. The viral genome can then be injected into the nucleus and viral DNA begins a highly controlled cascade of gene expression in three kinetic stages: immediate early, early and late. The capsid is then covered with a shell originating from the inner nuclear membrane, which is later replaced with a vesicular membrane of the trans-Golgi apparatus. This modifies the protein envelope. As a result of this modification, the viral particles are enveloped and egress from the host cell membrane by cell-to-cell spread and exocytosis, thereby preserving the existence of the viruses in nature (Stenglein *et al.*, 2009; Riaz *et al.*, 2017).

### 1.1.3.1 Attachment and entry

Herpesviruses must first attach to host cells in order to enter them. Specific glycoproteins (gB, gH and gL) and the binding receptor gD (which determines fusion pathways) are present in the viral envelope of herpesviruses. These glycoproteins interact with the target molecules present on the host cell membrane and allow the viral capsid and tegument proteins to enter the host cell's cytoplasm (Riaz *et al.*, 2017). Most herpesviruses enter a host cell by fusing with the plasma membrane, but some also use the endocytic pathway for viral entry (Connolly *et al.*, 2011). After fusion, the virus, which is inserted in the host cell membrane, undergoes extensive compositional changes by refolding, and starts releasing its contents into the host cell cytoplasm (Stampfer *et al.*, 2010; Russell *et al.*, 2013). During entry, the outer tegument is released into the cytoplasm, while the inner tegument proteins remain associated with the capsid and are transported, along with the nucleocapsid, to the nucleus. The virus then initiates the replication

mechanism by changing the cellular machinery, either by using the host cell to synthesise viral components such as VP16 in HSV-1, by host shut-off components such as SOX in KSHV or by immediate early gene activation (Mettenleiter *et al.*, 2006).

### 1.1.3.2 The lytic stage of herpesviruses

The lytic stage involves virus replication and the release of infectious virus particles from the infected cell, which can then spread and infect new cells in the host. At this stage of infection, there is regular expression of viral genes, genome replication, virion assembly, egress and transmission, which results in the establishment of sensory neuronal latency; this in turn allows the virus to replicate and causes recrudescent disease whenever the immune system is suppressed. The lytic stage starts with transcription of a sequential set of genes, including: immediate early genes (IEGs) or α genes, which are involved in initiating viral DNA replication and enhancing the expression of later lytic genes; early (E) or β genes, which work in DNA replication and control cellular activities such as RNA polymerase II; and late (L) or γ lytic products, which are structural proteins and include the capsid and glycoproteins incorporated in the viral envelope (Grinde, 2013) (see Figure 1-3). A number of proteins can be categorised as structural, such as glycoproteins. Non-structural proteins, however, are necessary for successful replication. Unlike some other viruses, herpesviruses have more than one structural glycoprotein embedded in its envelope. These glycoproteins play an important role in host cell entry either by endocytosis or fusion of plasma membrane (Adler *et al.*, 2017). The common glycoproteins found in all herpesviruses are gB, gH, gL and gM that required and sufficient for viral entry into host cells. However, Modrow *et al*. (2013) indicated that some herpesviruses have additional unique glycoproteins present in the host cell membrane and/or embedded

within the virus envelope. Some glycoproteins, such as gH/gL, are expressed as heterodimers, which play an important role in inducing remodelling in host cell fusion activity and thus viral internalisation (Spear *et al.*, 2000). Other glycoproteins such as gD are also recruited to play specific roles, such as cell tropism specification, receptor binding and/or enhancing gH/gL binding (Eisenberg *et al.*, 2012). The new transcribed viral DNA will pack into the nucleus of the infected cells to start the viral gene cascade into uninfected cells (Mettenleiter *et al.*, 2006). In the end, mature virions fuse with the cell membrane of the infected cell and bud into extracellular spaces (Mettenleiter *et al.*, 2006).

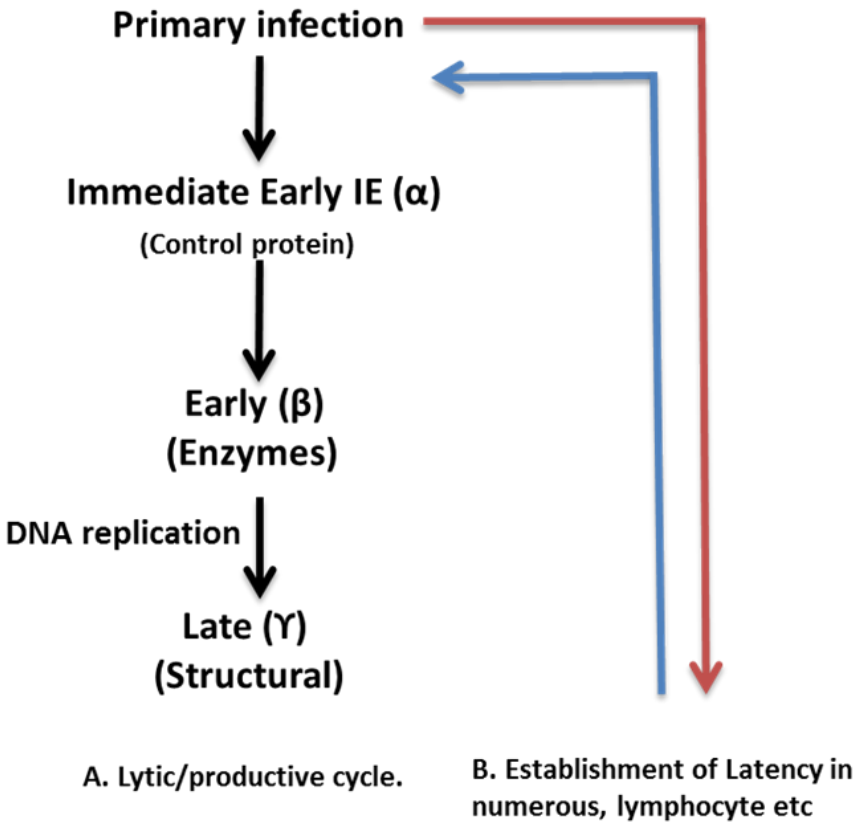


**Figure 1- 3 . Schematic diagram of the lifecycle of a typical herpesvirus. (Riaz *et al.*, 2017)**

### 1.1.3.3 The latent stage of herpesviruses

Gammaherpesviruses are known to be capable of true latency which is the ability of a pathogenic virus to lie dormant (latent) within a cell in a hidden or inactive phase, denoted as part of the viral life cycle, which is an important feature of infection and disease caused by many herpesviruses (O'Toole *et al.*, 1997). This persistent infection is present without causing clinically significant damage to the carrier animal; however, the virus can reactivate the lytic mode, resulting in the transmission of infectious viruses—for example, to other cattle and susceptible species (Baxter *et al.*, 1997). This latency stage is a unique feature of herpesviruses; it predominantly affects the T cells and endothelial cells of the host species (Barton *et al.*, 2011). Infected cells retain the virus from one generation to the next and can also convert the infected cells into latent infection cells. During a latent infection, the entire viral genome is harboured in a circular closed covalent form called an episome in the nucleus of the host cell: there is limited expression of a small subset of viral genes or no gene expression, few numbers of viral antigens are produced and no viral replication occurs (Riaz *et al.*, 2017). The latent virus is able to reactivate following a number of stimuli, including cellular stress, exposure to UV and immunosuppression or tissue damage, after which viral replication and new infectious virion production occurs (Doboro *et al.*, 2016). α-viruses establish latent infections in neurons, while γ-herpesviruses are markedly lymphotropic; however, the β-herpesviruses are more variable (Ackermann, 2006). Herpesviruses establish latency using different mechanisms depending on the open reading frames (ORFs). In certain viruses, unique ORFs are expressed, such as Epstein-Barr nuclear antigen (EBNA1) (Sivachandran *et al.*, 2012) in EBV, or latency-associated nuclear antigen (LANA) in KSHV (Hu *et al.*, 2002). These genes maintain their latent form by

tethering the virus episome to the host chromosome during mitosis in cell division to evade the immune system (Leight and Sugden, 2000; Grundhoff and Ganem, 2003).

Innate and adaptive (Lymphocytes represent the most important effector cells of the adaptive immune system) immunity play important protective roles by combating herpesvirus infection. The γ-herpesviruses actively antagonize the innate and adaptive antiviral responses, thereby efficiently establishing latent or persistent infections, during virus entry. Sensor molecules called toll-like receptors (TLRs) at the cell surface are expressed. These sensors recognize molecules characteristic of pathogens, including their DNA genomes. Although the cytosolic DNA-sensing pathway is activated during viral infection but herpesviruses have developed multiple mechanisms to attenuate host antiviral machinery and to facilitate viral infection and replication including suppression of MHC-I- and MHC-II-restricted antigen presentation, impairment cell functions, activation of viral-specific regulatory T cells, and induction of inhibitory cytokines, for instance HSV-1 able to evade the antiviral responses through DNA-sensor-mediated at both the recognition level through multiple DNA sensors and innate immune signalling through the STING-TBK1-IRF3 or NF-κB axis , (Figure 1-4) (Hu and Usherwood, 2014; Zheng, 2018).

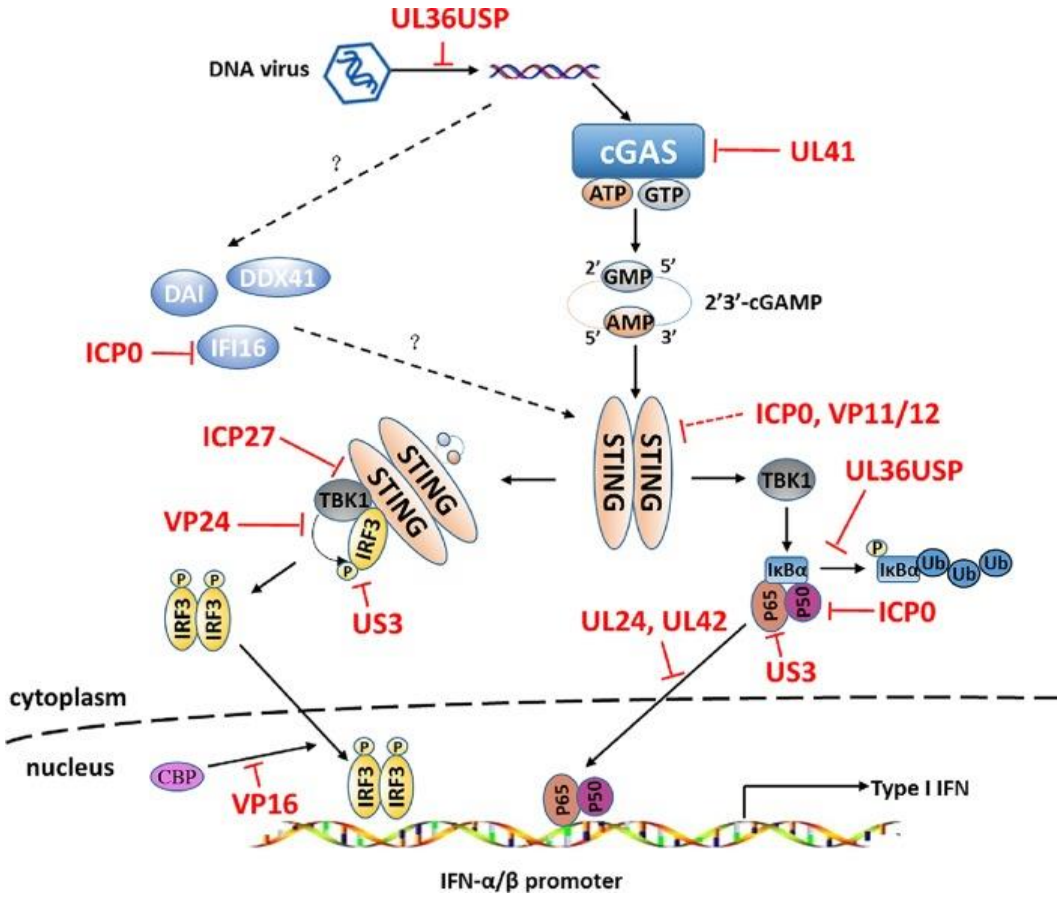


**Figure 1- 4. Evasion of the DNA-sensor-mediated IFN-I signal pathway by HSV-1.**
Cytosolic DNA sensors, such as cGAS, IFI16, DDX41, and DAI, recognize double-stranded DNA in the cytosol and trigger IFN-I production through transmission of a series of signals. HSV-1 can targeted the DNA-sensor-mediated IFN-I signal pathway through multiple steps, including both DNA-sensor-mediated viral recognition and subsequent signalling. Solid lines indicate confirmed interactions between host molecules and HSV-1 proteins. Dashed lines indicate uncertain interactions. CBP, CREB-binding protein; P, phosphate; Ub, ubiquitin (Zheng, 2018).

cGAS is the main cytosolic DNA sensor which is essential for IFN production and the establishment of a host antiviral state; therefore, herpesviruses such as HSV-1 must evolve certain strategies to antagonize the cGAS/STING pathway for effective infection. The interplay between herpesviruses and host antiviral innate immunity is very intricate, with viral proteins targeting multiple steps of the cellular DNA-sensor-mediated antiviral signal

pathway. In general, the latency and reactivation strategies of herpesviruses are crucial strategies these viruses use to survive in nature (Oehmig *et al.*, 2004). There is no common pattern of herpesvirus gene expression, which is required in establishing and maintaining latency and in reactivation.

## 1.2 Malignant catarrhal fever (MCF)

Animal diseases have been observed and studied since ancient times. Viral infections, for instance, cause health issues in animals; while methods have been discovered to manage or eradicate some of these infections, researchers are still trying to develop treatments and vaccines for others (Moore *et al.*, 2010). The study of animal diseases is of great importance because of the economic losses caused by these diseases and because of the possible transmission of the pathogenic factors causing the diseases to transfer to humans (Marcaccini *et al.*, 2008).

Malignant catarrhal fever (MCF), which is associated with the infection of certain animal species with specific gammaherpesviruses, is one of the viral diseases for which researchers have yet to find a way to prevent outbreaks. The first reports of MCF being recognised as a distinct entity came from France in the late 1700s, with subsequent records of the disease scattered in the literature throughout the 1800s (Plowright, 1965; Metzler, 1991). Experimental studies on MCF began to appear in the first third of the twentieth century.

MCF is an invariably infectious lymphoproliferative, multi-systemic and frequently lethal viral disease which affects a wide range of ungulates (members of the family *Artiodactyla*), which are generally ruminants belonging to the subfamily *Bovinae* and

include cattle, bison (*Bison bison*), water buffalo (*Bubalus bubalis*), African buffalo (*Syncerus caffer*) and exotic ruminants such as antelope, guar and banteng. The disease can also affect animals of the family *Cervidae*, such as deer, reindeer and moose, and other wild living ruminants. It also occasionally affects domestic pigs (family *Suidae*) and giraffes (family *Giraffidae*) (Moore *et al.*, 2010). MCF has variously been known as African malignant catarrhal fever, bovine malignant catarrhal fever (BMCF), wildebeest disease, and even snotsiekte, a collective term for the clinical and pathological signs described in cattle and other susceptible ungulates (Costa *et al.*, 2009; Headley *et al.*, 2012). MCF has been described based on the host in which the virus was originally carried, e.g. ovine herpesvirus 2 from domestic sheep, caprine herpesvirus 2 from goats, and alcelaphine herpesvirus 1 and 2 from members of the subfamily *Alcelaphinae*, which includes wildebeest and hartebeest (Vikøren *et al.*, 2006).

Worldwide, MCF usually occurs as sporadic cases (the most common form); however, a few epizootic outbreaks have been reported (O'Toole and Li, 2014). MCF has been recognised as a particularly serious problem in different parts of the world, including Indonesia, North America, Eastern and Southern Africa and New Zealand (Simon *et al.*, 2003). Because MCF is a frequently lethal immunopathological viral disease, it has a significant negative impact on livestock, especially when an infection occurs where multiple species (reservoir and susceptible animals) are housed in close proximity, as in auctions and zoological collections. Reservoir animals are the species of animal which can carry the virus without present any symptomatic infection but can transmit to other susceptible animals and cause the fatal disease. Although reservoir species are not

adversely affected by the virus, they can be the source of infection for susceptible animals (Martucciello *et al.*, 2006).

### 1.2.1 The economic importance of MCF

MCF is important because of the economic losses resulting from significant and devastating outbreaks which cause the deaths of large numbers of animals (O'Toole and Li, 2014). The economic importance of an MCF outbreak differs depending on the source of the virus, the species affected and the circumstances in which the animals are kept; for example, Bali cattle, American bison and buffalo are more susceptible to MCF (Daniels *et al.*, 1988; Wiyono *et al.*, 1994), whereas European cattle are more resistant to it (Otter *et al.*, 2002). Over the last few years, in a number of countries, such as Switzerland, the farming of water buffaloes for milk production has risen in popularity (Li *et al.*, 2000; Keel *et al.*, 2003a; Swai *et al.*, 2013). Game farms in continents including Africa, Australia and Europe have also recently developed into a major industry, which has led to an increase in the incidence of MCF (Cleaveland *et al.*, 2001).

The course of the disease is characterised by low morbidity and an increasingly high mortality rate (Russell *et al.*, 2009). In some cases, losses of 40–50% of herds have been reported, and outbreaks can last for several months.

Economically, AlHV-1 is an important concern in Africa because it causes outbreaks of MCF where cattle share grazing with wildebeest (Bedelian *et al.*, 2007). Outbreaks have caused losses of between 5–10% in domestic cattle groups and farm game, although this percentage varies depending on the size of the herd and the wildebeest birthing season (Ababneh *et al.*, 2014). Sheep-associated MCF (SA-MCF) can occur in cattle when sheep are also farmed and this has economic importance worldwide, (Figure 1-5 panel A). It usually

presents as a sporadic outbreak in many domestic and wild ruminants and occasionally outbreaks will cause losses of about 50% within a herd (Heuschele, 1988). Overall, SA-MCF is a worldwide problem and can have a remarkable economic impact resulting from the death of a large number of animals on highly susceptible species such as American bison (Berezowski *et al.*, 2005), because it is usually fatal and a significant major public health problem for highly disease-susceptible species, (Figure 1-5 panel B)(Brown and Torres, 2008; Russell *et al.*, 2009; O'Toole and Li, 2014). The localized mass loss of livestock resources due to MCF may pose significant population bottlenecks and subsequent loss of valuable diversity of adapted cattle breeds, whose genetic conservation is critical (Mbole-Kariuki *et al.*, 2014).

Over the last decade or so, several large outbreaks of MCF have occurred, making it one of the most important viral infectious diseases in commercially farmed animals. A wide range of scientific, industrial and veterinary researchers are very interested in and making great efforts to control the disease (Moore *et al.*, 2010; Zemljic *et al.*, 2012).

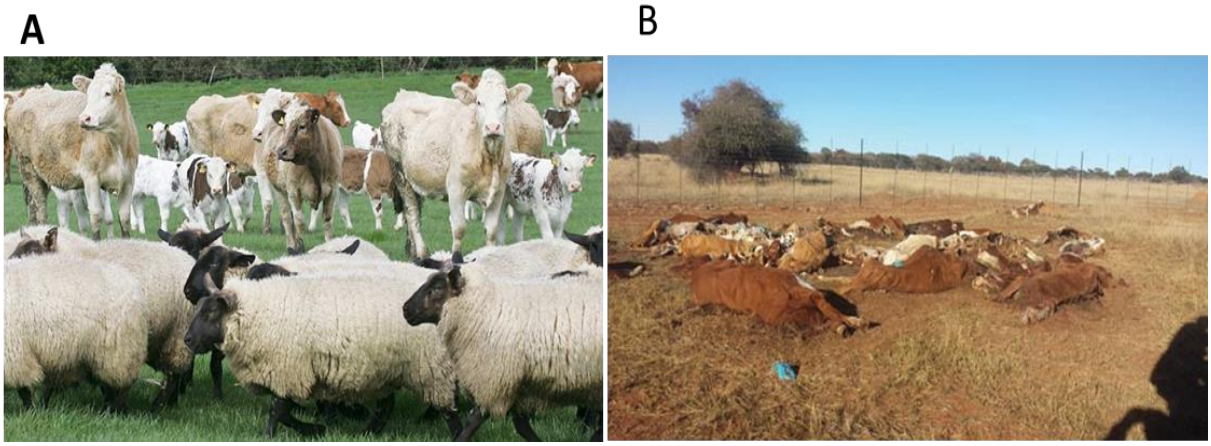


**Figure 1- 5. The economic importance of MCF.**
A: mixed animals on the farm. B: MCF infected dead animals.
https://www.fwi.co.uk/.../dorset-devon-farms-report-rare- cattle fever

### 1.2.2 The causative agents of MCF

MCF is caused by several gammaherpesviruses of the genus *Macavirus* (they were previously classified in the genus *Rhadinovirus*), which are found in nature as endemic subclinical infections in some ruminants (Russell *et al.*, 2009; O'Toole and Li, 2014). Malignant catarrhal fever viruses (MCFVs) infect T cells in particular as a part of their life cycle (Nelson *et al.*, 2010; O'Toole and Li, 2014) and establish one of two modes of infection: (a) latent infection, in which the viral genome persists in its host cell with restricted gene expression without cell destruction (Jarosinski, 2017), and (b) lytic infection, which produces virion progeny and destroys the host cell (Sarid *et al.*, 1998; Gelgor *et al.*, 2018).

The MCF viruses group comprises at least 10 known viruses (Crawford *et al.*, 2002; Li *et al.*, 2005a) which share the ability to propagate infectious viruses without causing clinical signs within their specific reservoir host species (Brown and Torres, 2008), as listed in Table 1-1. Three viruses of this family are not associated with MCF: gemsbok-MCFV, muskox-MCFV and aoudad-MCFV. A further member, hippotragine herpesvirus 1 (HipHV-1), has been described to cause MCF in experimental animals, but to date has not been reported to cause MCF under natural conditions (Taus *et al.*, 2014). The remaining six viruses of this family have been shown to be pathogenic under natural conditions: ovine herpesvirus-2 (OvHV-2), alcelaphine herpesvirus-1 (AlHV-1), alcelaphine herpesvirus-2 (AlHV-2) (Reid *et al.*, 1989; Bridgen and Reid, 1991; Davison *et al.*, 2009b), caprine herpesvirus2 (CpHV-2) (Li *et al.*, 2001c), ibex malignant catarrhal fever virus (Ibex-MCFV) (Okeson *et al.*, 2007) and caprine herpesvirus 3 (CpHV-3), a virus of unknown origin which causes MCF in white-tailed

deer, Table (1-2) (Teankam *et al.*, 2006; Li *et al.*, 2013a; Giangaspero *et al.*, 2013; Modesto *et al.*, 2015).

The two most widely prevalent and most important viruses causing MCF are AlHV-1 and OvHV-2. AlHV-1 is harboured by wildebeest (genus *Connochaetes*) and causes wildebeest-associated-MCF (WA-MCF) in Africa where the natural hosts live. OvHV-2, for which the natural host is sheep (*Ovis aries*), causes sheep-associated-MCF (SA-MCF), which occurs worldwide and is the major form of the disease (Ensser *et al.*, 1997; Nishimori *et al.*, 2004; Russell *et al.*, 2009; Sood *et al.*, 2013). The genome sequences of OvHV-2 and AIHV-1 are very similar, particularly in the presence of unique segments bounded by terminal repeats of 1.1 kbp in AlHV-1 (Ensser *et al.*, 1997) or 4.2 kbp in OvHV-2 (Hart *et al.*, 2007) (see Figure 1-6). Moreover, the OvHV-2 sequence showed that is shared co-linear with the other known rhadinoviruses. However, there are significant differences between OvHV-2 and AlHV-1 viruses, including infection and shedding from natural hosts, the requirements for *in vitro* propagation and the expression of viral genes responsible for lytic replication in affected hosts (Li *et al.*, 2008b; Cunha *et al.*, 2012; Palmeira *et al.*, 2013). Moreover, these viruses are related to other gammaherpesviruses such as KSHV, Epstein-Barr virus (EBV), murine herpesvirus 4 (MuHV-4) also called murine gammaherpesvirus (MHV-68).

MCF is also reported in common domestic pigs and has been produced experimentally in rabbits (Plowright *et al.*, 1960; Wessels *et al.*, 2011). More MCFV variants are likely to be identified in coming years.

| Causative agent | Reservoir host | Susceptible host | Economic importance | Reference |
|---|---|---|---|---|
| **Alcelaphine herpesvirus 1 AlHV-1** | African Wildebeest (*Connochaetes taurinus taurinus; Connochaetes taurinus albojubatus; Connochaetes albojubatus*) | Bison and Domestic cattle (*Bos taurus*) | Moderate | (Plowright *et al.*, 1960) |
| **Alcelaphine herpesvirus 2 AlHV-2** | Hartebeest(*Alcelaphus buselaphus*), topi (*Ammotragus lervia*) (*Damaliscus lunatus*) | Barbery red deer (*Cervus elaphus barbarous*) | Minimal | (Mackintosh, 1993) |
| **Ovine herpesvirus 2 OvHV-2** | Sheep(*Ovis aries*), /goat | Cattle( *B. Taurus*), water buffalo (*Bubalus bubalis*), bateng (*Bos javanicus*), antelopes, pigs (*Sus scrofa),* | Moderate | (Baxter *et al.*, 1993) |
| **Caprine herpesvirus 2 CpHV-2** | Goat (C. hircus) | Several ruminants, Domestic pig (*Sus scrofa domesticus*), sikka deer(*Cervus nippon*), white-tailed deer (*Odocoileus virginianus*), moose (*A. alces*), roe deer (*Capreolus capreolus*) | Minimal | (Li *et al.*, 2001b) |
| **White –tailed deer virus (Caprine herpesvirus 3)** | Domestic goat (*C. hircus*) | White-tailed deer (*O. virginianus*) and red brocket deer (*Mazama americana*) | Minimal | (Li *et al.*, 2000) |
| **Ibex-MCFV** | Nubian ibex (*Capra nubiana*) Bongo Minimal HipHV-1 Roan antelope (*Hippotragus equinus*) and Scimitar-horned oryx (*Oryx dammah*) | Bongo, anoa, pronghorn | Minimal | (Gasper *et al.*, 2012) |
| **Hippotragine herpesvirus 1 HipHV-1** | Roan antelope | Not documented | Non | (Reid and Bridgen, 1991) |
| **Gemsbok-MCFV** | Gemsbok (Oryx gazella) | Not documented | Non | (Shapshak *et al.*, 2015) |
| **MuskoxMCFV Muskox** | Muskox (Ovibos moschatus) | Not documented | Non | (Li *et al.*, 2003a) |
| **Audad AoudadMCFV** | Aoudad (Ammotragus lervia) | Not documented | Non | (Li *et al.*, 2003a) |

**Table 1- 2. List of MCF viruses that cause MCF naturally and their susceptible hosts (O'Toole and Li, 2014).**

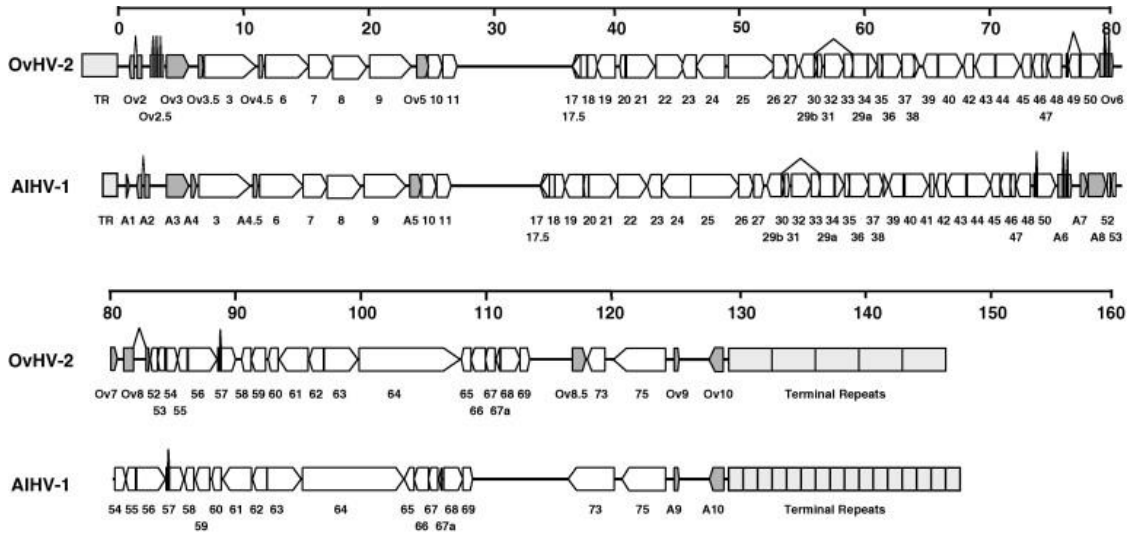


**Figure 1- 6. Genome organisation of AlHV-1 and OvHV-2.**
Schematic maps illustrate the relative organisation of genes in the OvHV-2 and AlHV-1 genomes. The genes scale showed the position and direction of open reading frames (ORFs) as block arrows and the terminal repeat (TR) sequences shaded in a pale grey (Russell *et al.*, 2009).

### 1.2.2.1 Alcelaphine herpesvirus 1 (AlHV-1)

AlHV-1, the first identified MCF virus, is carried by African blue and black wildebeest (*Connochaetes taurinus* and *Connochaetes gnou,* respectively) and causes wildebeest-associated MCF (WA-MCF) in cattle in Africa. The earliest reports from Plowright *et al*. (1960) found that WA-MCF caused by AlHV-1 was the prevalent disease in sub-Saharan Africa and that blue and black wildebeest were the natural hosts for the virus in East Africa. AlHV-1 is the most prevalent form of MCFV in Africa and persists as a subclinical infection (asymptomatically endemic) in wildebeest. The AlHV-1 name was determined according to the taxonomy of its reservoir hosts, wildebeest, hartebeest and topi, which belong to the subfamily *Alcelaphinae* (Mushi and Rurangirwa, 1981).

AlHV-1 can be transmitted horizontally and vertically, so a high proportion of wildebeest are reported carriers from a young age (Wambua *et al.*, 2016). The incidence of WA-MCF infection in horizontal transmission increases after three months of age, because maternal antibodies (IgG) provide protection up to that point. By six months of age, animals tend to shed viral particles through nasal and ocular secretions rather than the virus itself, except for shedding when under stressful conditions (Bartley *et al.*, 2014b; Wambua *et al.*, 2016). The calving season is characterised by the migration of large numbers of wildebeest herds to their favourite areas where green grass is found. This migration increases the chances of meeting and coming into close contact with cattle, possibly exposing the latter to placental matter and contaminated tissues left in rangelands after the birth of wildebeest calves. Plowright (1965) showed that the AIHV-1 virus was recovered from a splenic cell culture of a wildebeest foetus and can be transmitted vertically. This intermingling of animals represents a real threat of infection to cattle and is compounded by stressful conditions such as captivity or starvation (Honiball *et al.*, 2008; Lankester *et al.*, 2015a). Vertical transmission, which occurs via utero has also been found in 50% of parturient wildebeest, as they carry viral DNA in their placental tissue (Lankester *et al.*, 2015b).

Animals can become infected with AlHV-1 in the form of the cell-free virus, which is shed in nasal and ocular secretions and saliva for a short period. While this may be a main source of infection in wildebeest, the cell-free virus has also been reported to survive for more than 13 days in moist environments (Pagamjav *et al.*, 2005; Mlilo *et al.*, 2015). AIHV-1 can be propagated *in vitro* by using T-lymphoblastoid cell lines known as large granular lymphocytes (LGLs) which originate from hosts affected with MCF. These cell lines have

enabled researchers to understand the genome sequence of AIHV-1. Russell *et al.* (2009) showed the genome sequence of AIHV-1 contains about 131,000 bp surrounded by terminal repeats of 1100 bp. The genome sequence of AIHV-1 contains at least 70 ORFs, of which 10 genes are unique and are known as A1-A10. Eight of these unique genes are similar to those found in OvHV-2; most of the non-unique ORFs (60) are conserved across homologous γ-herpesviruses.

This disease is seen in cattle in Kenya, Tanzania and other areas of the African sub-continent and in a variety of ruminant species in zoological collections worldwide where susceptible cattle interact with wildebeest. WA-MCF disease annually causes a catastrophic loss of cattle affecting the livelihoods of nomadic pastoralist communities in eastern and southern Africa (Mlilo *et al.*, 2015).

### 1.2.2.2 Ovine herpesvirus 2 (OvHV-2)

OvHV-2 is the origin of sheep-associated MCF (SA-MCF) in several ruminant species and is carried asymptomatically in all breeds of sheep (subfamily *Caprinae*, which includes sheep and goats) wherever sheep husbandry is practised (Li *et al.*, 2006; Bastawecy and El-Samee, 2012). OvHV-2 has a double-stranded DNA genome: it can be divided into a long fragment of about 130 kbp and multiple copies of about 4 kbp repetitive terminal elements (Sood *et al.*, 2013). OvHV-2 causes sheep-associated MCF in animals belonging to the *Bovidae* and *Cervidae* families, including cattle (*Bos taurus*), bison, water buffalos (*Bubalus bubalis*), various species of deer, swine (*Sus scrofa domesticus*), farmed sika deer (Sieber *et al.*, 2010) and a wide variety of wild animals in captivity (Foyle *et al.*, 2009). OvHV-2 has also been found in other species such as pigs, where a polymerase chain reaction (PCR) detected a positive OvHV-2 DNA signal in males and the virus was shown to be transmitted

sexually to sows via semen (Alcaraz *et al.*, 2009; Azevedo Costa *et al.*, 2010). Goats can also be infected asymptomatically with OvHV-2 (Taus *et al.*, 2005). Viral shedding occurs intermittently, with higher shedding in adolescent sheep which may result in higher rates of transmission to susceptible species.

In general the paucity of research on OvHV-2 is due to the lack of a cell culture system to propagate the virus *in vitro*, limiting the work which could be done to study the basic biological features of the virus and resulting in difficulties in the study of the molecular epidemiology, diagnosis and pathogenesis of OvHV-2 (Russell *et al.*, 2009). However, the propagation of LGLs which carry OvHV-2 or AIHV-1 originating from tissues of animals affected with MCF has provided a better understanding of MCF pathogenesis (Schock and Reid, 1996; Russell *et al.*, 2009). These T-lymphoblastoid cell lines have cytotoxic activity. Thonur *et al.* (2006); Hart *et al.* (2007) described the genomic DNA of OvHV-2, explaining that the DNA genome appears as linear and circular conformations inside the LGLs originating from hosts affected with MCF (cattle and rabbits), indicating latent and lytic viral transcripts. In comparison, the genomic sequence in peripheral blood mononuclear cells (PBMNCs) obtained from the reservoir host (sheep affected with MCF), appears as a circular internal conformation with ORF73 transcription, indicating a latency phase inside these cells. ORF73 is homologous with the Latency-associated nuclear antigen (LANA) of KSHV and other gammaherpesviruses. It is likely therefore that the OvHV-2 ORF73 encodes a LANA protein that is a genome maintenance protein (Hart *et al.*, 2007; Russell *et al.*, 2009). Several attempts to recognise the viral particles inside the cytoplasm of LGLs using electron microscopy were efficient in the case of AIHV-1 but not OvHV-2 (Rosbottom *et al.*, 2002). Taus *et al.* (2007) found that LANA encode ORF73s are highly variable in length.

In 2008, (Jayawardane *et al.*) analysed a unique ORF in the OvHV-2 genome, which was annotated as Ov2.5. This ORF encodes a protein similar to ovine interleukin (IL)-10, which may modify the immunity of the host by stimulating mast cell proliferation and suppress the production of macrophage inflammatory chemokines. OvHV-2 is similar to AIHV-1 in a number of microRNA genomes, including ORF9 (DNA polymerase), ORF25 (major capsid protein), ORF50 (R-transactivator, inducing a latent to productive cycle switch) and the episome maintenance protein, which is encoded by ORF73.

In 2009, Russell *et al*. showed that OvHV-2 has four completely unique genes, Ov2.5, Ov3.5, Ov4.5 and Ov8 (Russell *et al.*, 2009), and confirmed high variability in ORF73, which could be a useful tool for informing epidemiological studies between different isolates. Both OvHV-2 and AIHV-1 can form a latent infection by expressing a LANA protein encoded by ORF73 in both viruses (Taus *et al.*, 2015).

### 1.2.2.3 Caprine herpesvirus 2 (CpHV-2)

Goats are natural hosts of CpHV-2, another causative agent of MCF disease. DNA sequence alignment analysis revealed that CpHV-2 virus is highly similar to OvHV-2 and AlHV-1, can spread between goats when housed together and causes a chronic disease in both domestic and wild goats (Li *et al.*, 2005b). To date, this virus has been reported to cause disease in two cervid species, white-tailed deer and Sika deer (*C. Nippon*), as well as in moose, water buffalo (*B. bubalis*) and pronghorns (*Antilocapra americana*) (Li *et al.*, 2013a). There is little information about the possibility that CpHV-2 virus can cause MCF disease in other ruminant species (Keel *et al.*, 2003b; Li *et al.*, 2003b; Li *et al.*, 2005a).

Most domestic goats are infected with CpHV-2 under natural herd conditions (Chmielewicz *et al.*, 2001; Li *et al.*, 2001b). Both CpHV-2 and OvHV-2 infection can occur

when goats interact with an OvHV-2 infected animal (Li *et al.*, 2001a); goats do not manifest any symptoms of infection and can spread the virus to other susceptible hosts. The clinical signs of MCF cases caused by CpHV-2 differ from those induced by OvHV-2 and AlHV-1, as the disease tends to be more chronic and dominated by skin conditions such as dermatitis and alopecia. Furthermore, histopathological examination would reveal systemic lymphoproliferative vasculitis (Suavet *et al.*, 2016).

Goats can be infected with OvHV-2 and can therefore be a source of infection for SA-MCF, as OvHV-2 is asymptomatic. While an MCF-like syndrome has been reported in goats, at present it is not clear whether this is because of challenge with OvHV-2 and response to infection or if OvHV-2 DNA is unrelated to the presence of the infection (Li *et al.*, 2005a).

### 1.2.2.4 Malignant catarrhal fever virus white-tailed deer (MCFV-WTD or caprine herpesvirus 3)

MCFV-WTD, recently named caprine herpesvirus 3, was first described in 2000 and recognised as a distinct new pathogenic MCFV (Li *et al.*, 2000) which causes MCF in white-tailed deer in North America, New Zealand, Scotland and elsewhere. It has become important due to its high morbidity and cumulative mortality (Palmer *et al.*, 2013). The host species of caprine herpesvirus 3 is the domestic sheep and goats according to phylogenetic analysis (Brown and Torres, 2008). The susceptibility of deer species to MCF varies from mild or low in some species, such as fallow deer, to extremely high in others, such as white-tailed, axis, and Pere David's deer. Because the reservoir host is to date unknown, the transmission method of the virus has not yet been identified (Li *et al.*, 2003b).

In a recent study, it was proposed that goats are a possible reservoir host of caprine herpesvirus 3 because deer developed MCF after exposure to goats (Li *et al.*, 2013a). Deer infected with caprine herpesvirus 3 show the classical symptoms of MCF, similar to those in cattle but without corneal involvement (Li *et al.*, 2000).

### 1.2.3 MCF pathogenesis, infection and transmission

#### 1.2.3.1 Pathogenesis of MCF

The pathogenesis of MCF is characterised by lymphoproliferation, vasculitis and epithelial inflammation (Russell *et al.*, 2009; Russell *et al.*, 2012). Overall, studies suggest that different MCFVs may have different pathogenic mechanisms; however, MCF pathogenesis is still not fully clear. Plowright (1968) was the first person to suggest that immune mechanisms play a role in the pathogenesis, as the infection occurs in LGLs, which have cytolytic or natural killer (NK) activity, and consequently the immune functions of these cells are deregulated prior to the development of clinical symptoms. Studies of MCF disease suggest that the autoimmune-like pathogenesis is caused by the cytotoxic activity of uninfected cells under the regulatory influence of small numbers of infected cells—that is, initially, the very few cells infected with the MCF virus interfere with the surrounding uninfected T cells, resulting in the auto-destruction of tissues by indiscriminately cytotoxic lymphocytes (Schock and Reid, 1996; Swa *et al.*, 2001).

The pathogenesis of MCF induced experimentally in sheep by nasal OvHV-2 aerosol nebulisation indicated lytic replication in the turbinates, trachea and lungs in the respiratory tract of infected animals (Taus *et al.*, 2005), indicating that sheep play a role as reservoir host in OvHV-2 transmission (Cunha *et al.*, 2008): localisation of the virus in alveolar epithelial cells was detected, and was also found in the nasal secretions of

naturally infected sheep (Taus *et al.*, 2010). Moreover, Anderson et al. (2007) demonstrated differences in the pathogenic mechanisms between SA-MCF and WA-MCF in rabbits—namely, infection with OvHV-2 was shown to cause more tissue necrosis and less lymphoid hyperplasia. Furthermore, Anderson *et al*. (2007) also suggested that predominantly cytotoxic CD8+ T cells were involved in lymphoid hyperplasia associated with vasculitis. Another study on laboratory rabbits suggested that the viral infection in lymphocytes or possibly in antigen-presenting cells changed the lymphocyte function by altering a T cell activator, such as interleukin-2 (IL-2) (Schock *et al.*, 1998). Thus far one other study has demonstrated a generalised lymphocytic arteritis in lambs infected with OvHV-2 DNA virus (Gaudy *et al.*, 2012).

*In vitro* cell cultures from MCF-case lymph nodes have been established to show the morphology of LGLs, indicating that LGLs share features of activated NK cells in reacting to a host's own cells as a response to cytokines from infected lymphocytes (Swa *et al.*, 2001).

On the other hand, a study of the pathogenesis of AlHV-1 infection in laboratory rabbits showed that the virus in latent infection was associated with proliferating CD8+ T and that these cells were detectable as early as two weeks after inoculation (Dewals *et al.*, 2008). Another study showed that the virus has its own role in pathogenicity: the lesions are positively associated with the abundance of virus ORF25 in experimentally infected rabbits with OvHV-2, while cattle with AlHV-1 showed an association with ORF73 latent transcripts detected in T cells (Palmeira *et al.*, 2013).

In goats the infected signs appeared as clinical neurological signs with digestive and corneal involvement and tissue damage was seen in several organs, including kidney,

spleen, lung, brain and liver, with vascular lesions which appeared as lympho-histiocytic with fibrinoid necrosis, especially in medium-sized arteries (Jacobsen *et al.*, 2007).

### 1.2.3.2 MCF transmission

MCF viruses are present anywhere and are usually asymptomatically carried by their reservoir hosts, causing infection in susceptible hosts. Viral transmission of any MCFV or the several closely related gammaherpesviruses (Russell *et al.*, 2012) occurs by numerous methods, including direct and indirect contact with the reservoir infected animals (Münz, 2016) (Figure 1-7). In the asymptomatic carrier (reservoir), infection is persistent as subclinical; whilst completely susceptible to other viral infections, such reservoir hosts do not succumb to MCF (Wambua *et al.*, 2016). Therefore, the virus can circulate freely among them without causing harm, having evolved strategies to persist in their reservoir hosts and enter to lytic infection later. During the lytic stage, the viruses manipulate the host's gene expression to optimise the cellular environment for viral replication and to evade the immune response (Slater *et al.*, 2017). In contrast, MCFVs can cause severe, striking and fatal diseases in susceptible species. In this situation, the virus is not shed either to other animals or the environment; infected animals will die and are considered dead-end hosts "a host from which infectious agents are not transmitted to other susceptible hosts" (Russell *et al.*, 2009; Parameswaran *et al.*, 2014; Mlilo *et al.*, 2015). One of the key issues in the transmission of MCF includes the uncontrolled multiplication of lymphocytes in various tissues, which may act as a growth factor for the host's lymphocytes depending on the species of animal infected (Arnold *et al.*, 2006). MCFVs are highly variable in their distribution due to the widespread of the reservoir ruminant species; however, environmental conditions such as moisture levels, (cool) temperatures and the absence of

ultraviolet light provide opportunities for transmission over longer distances (Brown and Torres, 2008). The natural transmission of MCFVs generally occurs either via inhalation or ingestion of infectious cell-free virus shed in the mucous secretions of reservoir hosts (Li *et al.*, 2005a). It is commonly thought that inhalation might be the primary method of transmission for all MCF viruses: the respiratory tract remains the common route for both entry and shedding of many herpesviruses in animals. Kim *et al*. (2003) and Taus *et al*. (2005) both proved that the nasal secretions of sheep suffering from MCF contain infectious OvHV-2 virions. Direct nose-to-nose contact appears to be the most efficient way to transmit MCFVs between animals, while indirect transmission may also take place via aerosol, be vector-borne or carried in fomites such as pastures, tools, water and contaminated travel or shipping vehicles (Brenner and David, 2005). No studies have been conducted on how long the MCF virus may survive in contaminated environments such as transport vehicles; however, the virus does not live freely outside the host cell. If inappropriate moisture and temperature conditions are prevalent, the virus is unlikely to survive more than 24 to 48 hr (Wambua *et al.*, 2016). It is also known that MCF viruses can be carried by wind, but it is unknown how this works (Li *et al.*, 2008b). Although intra-uterine infections sometimes occur in sheep (Li *et al.*, 1999), the majority of lambs are not infected until they reach two to two and a half months of age under natural herd conditions (Li *et al.*, 1999).

The other factor which affects the transmission of MCF between animal's herds and flocks is the minimum distance between them. It is not possible to specify exactly what minimum distance is effective; this may vary depending on factors such as temperature, relative humidity and the direction, the virus load of infected animals and speed of the

wind (Li *et al.*, 2008b). Therefore, maintaining the maximum possible distance between adjacent herds and flocks within the limitations of existing facilities will help minimise the risk of transmitting MCF viruses.

AIHV-1 virus in wildebeest is transmitted to calves, which become infected within the first few months of life either *in utero*, via direct contact or through respiratory tract secretions (Reid *et al.*, 1989). Infected calves subsequently demonstrate neutralising antibodies to the virus in their blood continuously for several weeks or months and shed the virus for a prolonged time during their first few months of life. When the animals reach 13 to 14 months of age, the shedding declines; however, the calves remain latently infected for the rest of their lives. They are considered a major source of infection and play an important role in transmitting MCF, as they excrete non-cell-associated viruses in their nasal and ocular secretions (Lankester *et al.*, 2015a; Lankester *et al.*, 2015b).

The transmission of OvHV-2 overall is similar to that which occurs with AlHV-1, and takes place mainly through respiratory (nasal) and ocular secretions; it is probably also spread via aerosol transmission, mainly from lambs less than a year old (Kim *et al.*, 2003; Taus *et al.*, 2005). It seems that the age of lambs is particularly important in transmission: lambs about 6 to 9 months old are chiefly responsible for spreading the virus, with adolescents posing the highest risk. Li *et al.* showed that lambs who get the virus from ewes can spread it to other lambs and the rest of the flock very soon after birth (Li *et al.*, 2008b). Some lambs are infected *in utero* or become infected during the perinatal period, while other cases may not occur till after three months of age (Li *et al.*, 2004). However, the shedding patterns of OvHV-2 are different from AlHV-1. OvHV-2 infection is mostly sporadic and short-lived: the virus is shed intermittently for a short time from the nasal

secretions of latently infected sheep. Therefore, in contrast to most new born wildebeest, which are considered the source of infection of WA-MCF, the majority of new born lambs are not considered a source of infection because the virus-shedding period is short in sheep, although it is more intensive than in wildebeest and the transmission of OvHV-2 between sheep during the perinatal period is minimal (Li *et al.*, 2004). Similarly to AIHV-1, direct contact between infected sheep and susceptible species may spread MCF, but in some cases susceptible species (cattle) have been reported to get the infection while separated from the infected sheep by 70 kilometres (Li *et al.*, 2013a). However, transmission of the OvHV-2 from sheep to cattle or bison or between cattle and bison was reported (Nelson *et al.*, 2013). Similarly to AIHV-1 and OvHV-2, CpHV-2 transmission occurs in the same way between goats and domestic sheep (Li *et al.*, 1998; Li *et al.*, 2000; Li *et al.*, 2002). Thus, goat kids may be affected between 3 and 9 months of age and they can shed the virus to other goats in the herd. In the case of MCF in pigs, large amounts of OvHV-2 DNA have been found in the semen of asymptomatic boars and in the nasal mucosa and skin of sick animals (Li *et al.*, 2012).

The main remaining issue in MCF transmission is the distance over which the disease is transmitted. In wild animals in particular, it is difficult to recommend a typical separation distance between reservoir hosts and susceptible host species. In special cases, such as in islands, a separation zone between the reservoir and susceptible species is a reasonable approach. This distance would vary depending on factors such as viral load, temperature (climate conditions), relative humidity, the number of animals involved, wind direction, and wind speed (Brown and Torres, 2008). The potential impact of herpesvirus on other

species is unknown; there is no evidence that MCF viruses can be transmitted to human and no cases have been reported (Li *et al.*, 2001a).

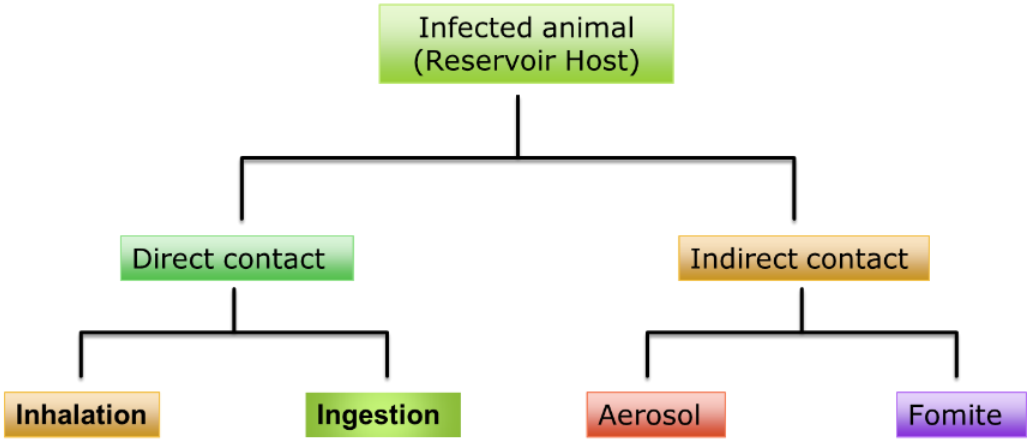


**Figure 1- 7. General transmission ways of MCF viruses in reservoir host.**

### 1.2.4 Experimental MCF

The issue of using large ruminants for the study of transmission and pathogenesis of MCF is considered a critical factor in research due to the high costs of caring for these animals, the small size of test groups and the range of available immunological reagents. Laboratory animals such as rabbits (*Oryctolagus cuniculus*), mice, rats and hamsters are thus invaluable tools for investigating the various aspects of virus-host interactions, which would otherwise be difficult or impossible to study (Myers and Connelly, 1992). Rabbits have been used for experimental studies with OvHV-2 and AIHV-1 due to the similarity of the lesions produced to those in naturally affected ruminant species (Li *et al.*, 2011; Cunha *et al.*, 2013). Rabbits can develop an MCF-like disease following experimental infection with either OvHV-2 or AlHV-1, which is very similar to the MCF seen in naturally susceptible animals (Anderson *et al.*, 2007), either by inoculation of lymphoblastoid cells derived from

infected animals, cell suspension from lymph nodes of infected animals or from other tissues such as spleens or corneas from infected ruminants (Buxton and Reid, 1980; Dewals and Vanderplasschen, 2011). The observed lesions in the rabbits subjected to induce MCF were indistinguishable from those described in MCF-susceptible species. These animals can also be used as a model to study natural infections of AlHV-1 and OvHV-2 by nebulisation (Dewals *et al.*, 2008; Gailbreath *et al.*, 2008).

Another successful model is infected laboratory hamsters (Reid *et al.*, 1986). Both rabbits and hamsters developed histological lesions related to MCF, including multisystemic interstitial and perivascular lymphoproliferation with less vasculitis (Buxton *et al.*, 1984).

OvHV-2 virus from SA-MCF-affected animals has been found in hyperplastic T cells (Bridgen and Reid, 1991; Baxter *et al.*, 1993). Subsequently, these T cells can be cultured into lines and will transmit MCF disease back into cattle as well as to experimental animals such as rabbits, rats and hamsters (Buxton *et al.*, 1988; Burrells and Reid, 1991).

### 1.2.5 Morbidity of MCF

The morbidity of MCF disease varies from sporadic cases to outbreaks. Differences depend on the virus type and the infected species—for example, reports document morbidity rates of 65% in deer, 20% in Bali cattle and 28% in water buffalo (Wambua *et al.*, 2016). In Africa, the approximate rate in domestic cattle infected with WD-MCF can be 6–7%, but in some cases as high as 50%, while in domestic cattle infected with OVHV-2 the morbidity is less than 1%. However, there are reports of higher morbidity rates in cattle from different countries, ranging from 8.3–50% in Ireland and South Africa and some U.S. states such as Wyoming, California, Colorado and Michigan. While the collected data on

bison refer to morbidity rates approaching 50%, especially when they are in close contact with sheep flocks, herd losses may reach to 90–94%, and in some cases 5% of the infected bison die within a few hours or days of infection.

### 1.2.6 Clinical signs of MCF

MCF disease in susceptible animals tends to appear sporadically, although occasionally, relatively large numbers of animals may be affected (Løken *et al.*, 2009). The clinical signs of MCF are highly variable in individual animals and different species, depending on the virulence of the virus infection, affected species and their susceptibility, as well as which organ is most affected and the rapidity of progression. MCF is usually fatal in susceptible species; however, cases of animals which recovered from the disease have been recorded (O'Toole and Li, 2014). In general, lymph nodes are one of the main sites for MCF diagnosis and lymphocytes are the main carriers of OvHV-2 DNA and AIHV-1; however, death or euthanasia is the most common final outcome after 2 to 18 days in all cases, depending on the animal species (Meier-Trummer *et al.*, 2009).

The incubation period of herpesviruses, particularly MCFVs, is uncertain and varies based on the virus strain, but it can vary between two to three weeks to as long as seven to 10 months or even longer. This differentiation is based on the viral dose, host immunity, host health and other factors (Bedelian, 2004; Russell *et al.*, 2009). Examples from the literature demonstrating different incubation periods include Mushi and Wafula (1983), who reported a mean incubation period of 14 days in rabbits infected with AlHV-1, while, in contrast, Jacoby *et al.* (1988) reported 21–90 days in rodent models of AlHV-1 and Kalunda *et al.* (1981) found a mean incubation period of 16–29 days was achieved experimentally in cattle with AlHV-1. Furthermore, an experimental investigation by Haig

*et al.* (2008) found that the incubation period ranged between 21 and 68 days depending on the host species and the virus. MCF infection can occur any time throughout the year but seems to be more common during the birthing season (Zemljic *et al.*, 2012; O'Toole and Li, 2014).

Several characteristic forms of the clinical disease in cattle have been described for MCF, ranging from per acute, acute (head and eye), alimentary and chronic (Berezowski *et al.*, 2005; Li *et al.*, 2006; Li *et al.*, 2008a). However, the clinical signs are often not clearly related to one of the clinical forms and it is difficult to clinically differentiate MCF infection from several other common viral diseases. There are no significant clinical differences in MCF caused by OvHV-2 from that caused by AlHV-1 (Commission and Committee, 2008).

In its peracute form (rapid onset), which occurs in highly susceptible animals, the clinical signs progress very rapidly within 12–24 hr, through depression followed by diarrhoea and dysentery then death. Sometimes no clinical signs may be noted and sudden death may occur (Russell *et al.*, 2009). In contrast, the acute form (head and eye) is the most common expression of the disease in cattle: in this form, MCF caused by OvHV-2 is indistinguishable from that caused by AlHV-1 (O'Toole *et al.*, 2002). The disease usually begins with severe depression and a sudden onset of high and severe fever (40–42°C) lasting for the initial first to third days of the disease, but the temperatures can vary widely. Head down, the animal separates from the herd, tachycardia of 100–120 beats per minute develops, accompanied by anorexia and agalactia (Blood and Radostits, 1989). The acute form is characterised by bilateral corneal opacity and nasal discharges which are initially serous then become more profuse and mucopurulent in all cases. Ocular signs range from corneal oedema to severe lacrimation and severe conjunctivitis (Zemljic *et al.*, 2012)

(Figure 1-8). The eye becomes cloudy and bulging, and slightly grey to totally white; one or both eyes may be affected and they may even rupture (Figure 1-9). Later, signs of necrosis, erosion, ulceration and/or crusting of the muzzle are seen. Open mouth breathing, dyspnoea and cough may develop as the disease progresses (Mlilo *et al.*, 2015). Superficial lymphoma and muscle tremor can be observed by clinical examination. Diarrhoea, dehydration, hard faeces or sometimes not passing faeces have been reported as alimentary signs related to MCF (Traul *et al.*, 2007). Neurological signs such as hypersensitivity, aggressiveness, convulsions, hyperaesthesia, lack of coordination, ataxia, inability to walk and eventually paralysis may also appear as the disease progresses (Mitchell and Scholes, 2009). Skin lesions may develop in some cases, such as crusting and exudation on the skin of the neck, shoulder, axillae, back, udder, vulva or scrotum, and sometimes patchy excessive sweating (Dry *et al.*, 2016).

The symptoms seen in bison and deer are slightly different from those in cattle and include dehydration, severe depression, weight loss, haematuria, diarrhoea, melena and haemorrhagic enteritis (which is more common in these species than in cattle) developing to dysentery; affected animals may die within 12 hr. However, the corneal opacity is less than in cattle (Anderson *et al.*, 2007). Other possible signs which may appear on the animals are swollen limb joints, possibly leading to lameness, which may be seen after 10 to 12 days, prior to onset of any other symptoms. Difficult and painful urination or bloody urine (haematuria) and terminal signs of involvement such as impaired vision or total blindness have been reported in the neurological form (O'Toole and Li, 2014). Studies of OvHV-2 show that when MCF is induced in bison it is usually fatal once clinical signs appear (O'Toole and Li, 2014; Slater *et al.*, 2017).

The mild clinical form may occur, with almost no clinical signs but resulting in multiple organ failure. Unwell yearling cattle have been reported with a mild form of MCF: these animals are seropositive for MCF, but this is a very uncommon form (Zemljic *et al.*, 2012).

The chronic form of MCF disease can appear in cattle which have recovered from acute and subclinical infections (Moore *et al.*, 2010). Infected animals usually die, but some cases may survive for a short time and usually remain chronically infected with symptoms such as arteriopathy, dermal lesions, emaciation, proliferative arteriopathy present in vascular lesions and anterior or posterior iris adhesion and fibrosis in corneal substantia (Keel *et al.*, 2003a). The clinical signs in bison and deer are slightly different from those in domestic cattle, which manifest severe depression, weight loss, haematuria and bloody diarrhoea but are less often affected by corneal opacity (O'Toole *et al.*, 2002; Li *et al.*, 2014).

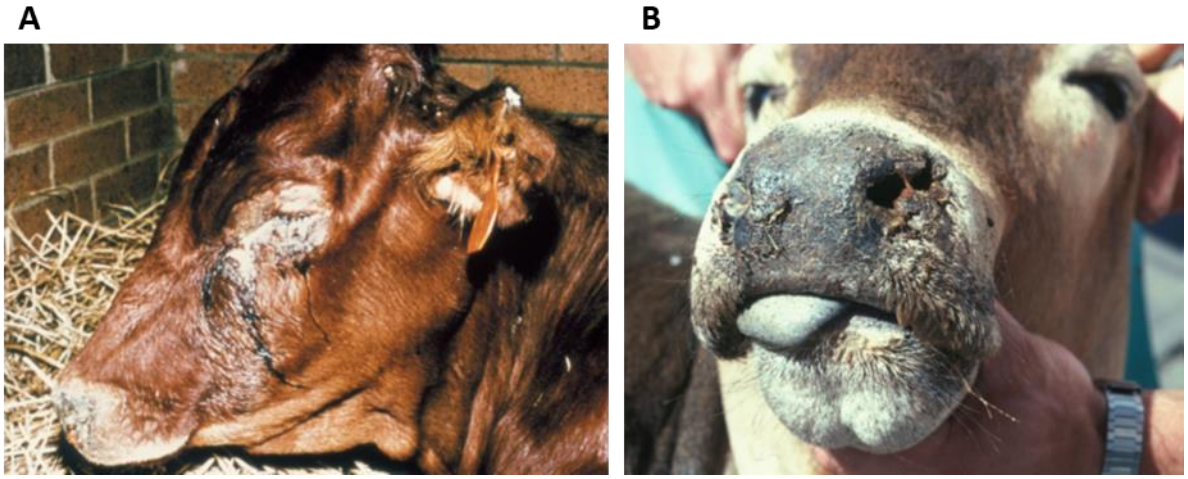


**Figure 1- 8. Lachrymation and a serous nasal exudate in cattle infected with MCF.**
**A.** Profuse and mucopurulent discharges from the eyes and nasal cavities. B. Blockage of the nares as a result of nasal exudate (van Vuuren, 2004)

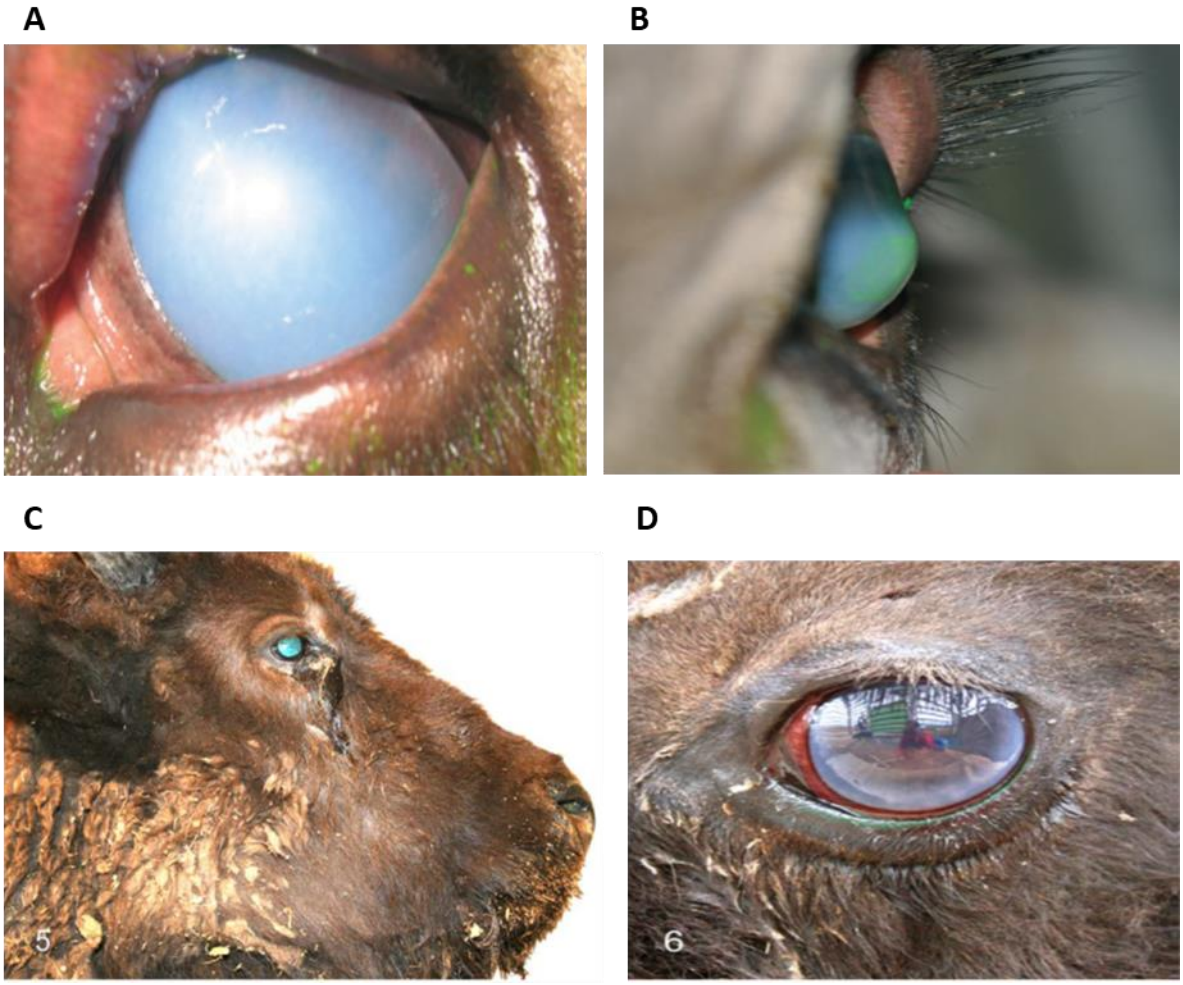


**Figure 1- 9. Photos demonstrated severe corneal oedema in cattle and bison sequentially.**

**A.** MCF corneal oedema in cattle that showed difficult to observe the intraocular structures. **B.** MCF case in cattle showing severe corneal oedema (Zemljič *et al.*, 2012). **C.** MCF case in bison showing severe corneal oedema with oculonasal discharge. **D.** Cornea from experimental of MCF in bison showing the clear and severe oedema (O'Toole and Li, 2014).

## 1.2.7 Pathological findings

Despite the severe pathological changes which occur in animals affected with MCF, the presence of lesions based on the severity and the course of the disease, viral genomic transcription and replication (which is subsequently associated with clinical signs and the severity of the lesions) (Cunha *et al.*, 2012), infection is widespread and may include most

organs of the body. Pathological features depend on the duration of disease and the affected species rather than the infecting virus, but generally the hallmark of MCF pathology includes lymphoproliferative inflammatory infiltrates, systemic vasculitis, and epithelial necrosis (Phillips *et al.*, 2018). The main issue of MCF disease is that the disease is systemic and the lesions may present throughout the body, including the brain, retina, uvea, cornea, synovia and skin. Replication of the virus occurs initially in the lung but latterly is propagated throughout multiple tissues (Slater *et al.*, 2017). The common lesions in cattle dying from the peracute form are extensive inflammation of the mucosal linings with less obvious corneal opacity (Wambua *et al.*, 2016); cattle also exhibit emaciation and dehydration.

On the other hand, in many acute cases, multisystemic ulcerations and erosions related to haemorrhages and hypertrophy of lymphoid organs are noted (O'Toole and Li, 2014). Multifocal petechial haemorrhage and heavy congestion of the alimentary tract, erosions and ulcers in the oesophagus and occasionally the small and large intestines are features, (erosion and haemorrhages have been also found in the gastrointestinal tract); in severe cases, the contents of the intestines may be haemorrhagic (Sood *et al.*, 2013). However, it may be difficult to identify lesions in the gastrointestinal tract, especially when the carcass is autolysed. Enlargement of the liver, oedema, petechiae, ecchymosis of the spleen, intestines, heart, liver, gallbladder and other organs and extensive haemorrhages in the musculature and subcutaneous tissue above the epicardium have also been seen (Zachary, 2012) (Figure 1-10). Multifocal haemorrhage in the urinary bladder and bloody urine are also seen, and frequently the kidneys are slightly swollen and reveal multiple

small white foci of lymphoid infiltration in the cortex, appearing grossly as separate white lines within the cortex (Li *et al.*, 2004).

In chronic cases, the small arteries in many different organs may be very prominent and sinuous with thickened walls; necrosis of the mucous membrane, accumulation of lymphocytes in small and medium arteries and veins (O'Toole *et al.*, 2007). Fibrinoid necrosis of the muscular walls (tunica media) of affected arteries has also been found. Ulceration of the cornea is also present in some cases. The muzzle is usually found to be cold, hard and showing small focal erosions or ulcers on the nasal mucosa (Li *et al.*, 2011). There may difficulty in differentiating lesions of MCF from those accompanying bovine virus diarrhoea/mucosal disease, infectious bovine rhinotracheitis and epizootic haemorrhagic disease (Taus *et al.*, 2006).

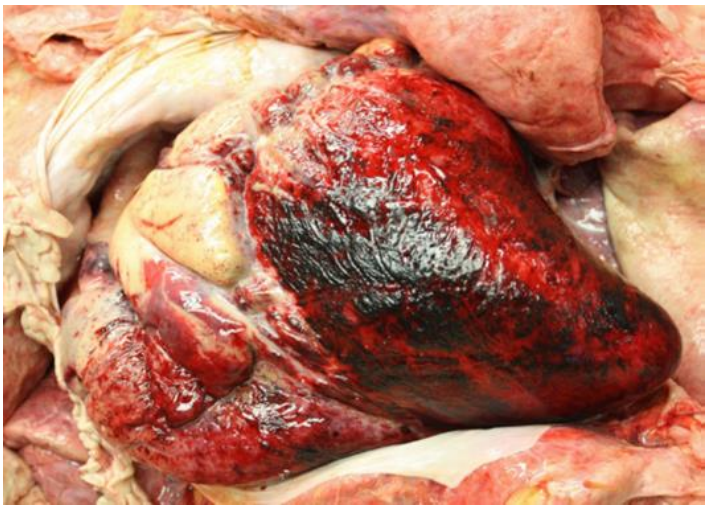

**Figure 1- 10. Epicardial haemorrhages. Severe multifocal haemorrhages in epicardium in the water buffalo cow with MCF.**
The pericardium contained 1.5 litres of serous fluid (evacuated) (Dettwiler *et al.*, 2011).

### 1.2.8 Histopathological findings

The histopathological findings for the WA-MCF and SA-MCF forms are similar to those of other MCFVs, which usually occur in cattle or farmed wild ungulates. The severity of lesions varies according to the course of the disease but the main target of the virus is the lymphocytes (Li *et al.*, 2005c).

Histological lesions are mainly lymphocytic infiltrations in multiple tissues in infected animals and are principally characterised by extensive vasculitis, necrosis of the epithelial cells and the infiltration and accumulation of large numbers of mononuclear cells. This infiltration predominantly consists of lymphoid cells (small and large T cells), macrophages, plasma cells, neutrophils and a few B cells, leading to T lymphocyte hyperplasia in lymphoid organs (hypertrophy), accumulation of these cells in non-lymphoid tissues and necrosis of the tunica media in medium-calibre arteries and veins, with a particular orientation to vascular structures and beneath inflamed mucous membranes (Plowright *et al.*, 1960; Swa *et al.*, 2001; Palmer *et al.*, 2013), (Figures 1-11 and 1-12). Inflammation and fibrinoid necrosis of small muscular arteries is a classical lesion, but in some cases of rapid death it can be difficult to see (O'Toole *et al.*, 2002). An infiltrate of mononuclear cells, which demonstrate a high mitotic index, is seen surrounding arteries and veins in almost all organs. Other histopathological signs which may be present include haemorrhagic intestinal mucosa, pulmonary congestion, inflammatory secretion and erosion in the upper respiratory tract and diphtheria (O'Toole *et al.*, 2002; O'Toole *et al.*, 2007) (Figure 1-11). Haemorrhages may be present in many parenchymatous organs, particularly lymph nodes and serosanguinous to fibrinous effusion in some cavities (Slater *et al.*, 2017). Detection of very low levels of infected cells in lesions accounts for the hypothesis that MCF could be

caused by very few infected cells interacting with the surrounding uninfected T cells, resulting in their deregulation.

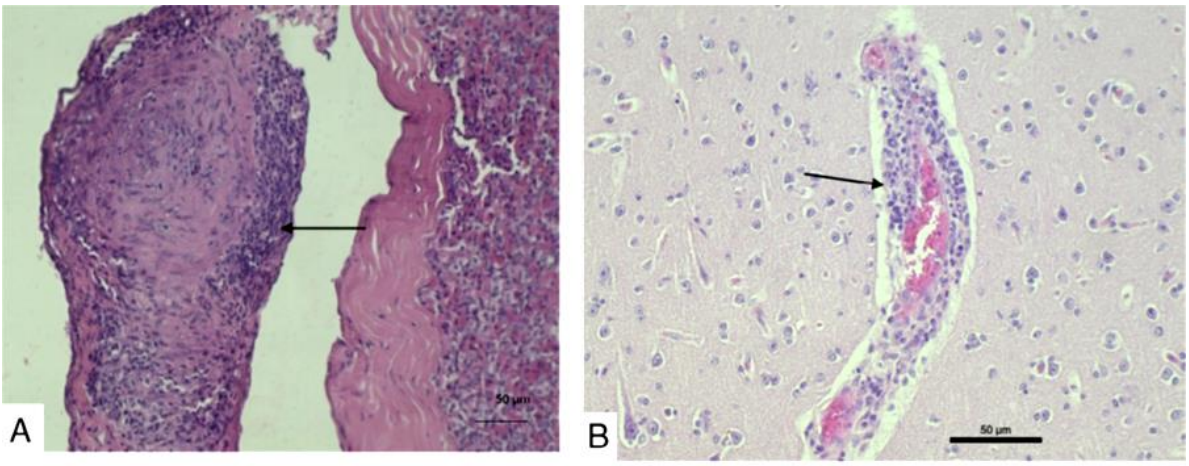


**Figure 1- 11. Histopathological changes observed in MCF in tissues of the animal.**
**A.** Carotid rete mirabile of MCF case that showed mild infiltration of mononuclear inflammatory and hyalinization of the parietal gland (200× magnification). **B.** The renal cortex of the kidney illustrating the intensive infiltration of mononuclear inflammatory cells and hyalinization in both the tunica and adventitia of blood vessels (100× magnification) (Martins *et al.*, 2017)

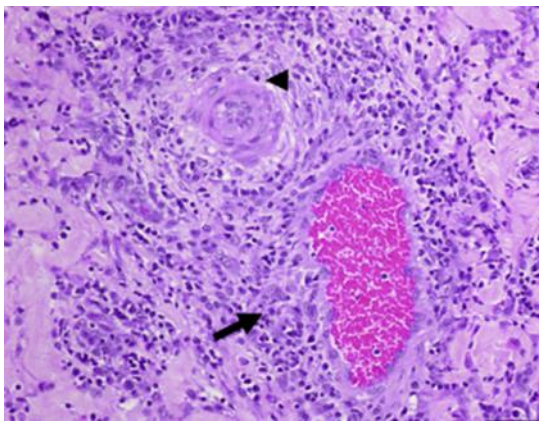

**Figure 1- 12. Histological section of the urinary bladder obtained from bison with SA-MCF.**
The section shows the primary infiltration of lymphocytes on the tunica adventitia (arrow) and tunica muscularis (arrowhead) of small to medium-calibre vessels (Nelson *et al.*, 2010)

Phillips *et al.* (2018) demonstrated that lymphocytic vasculitis with a few lymphoblasts and segmental fibrinoid necrosis was present in the vascular wall of some organs, such as tongue, lung, oesophagus and the liver, (Figure 1-13).

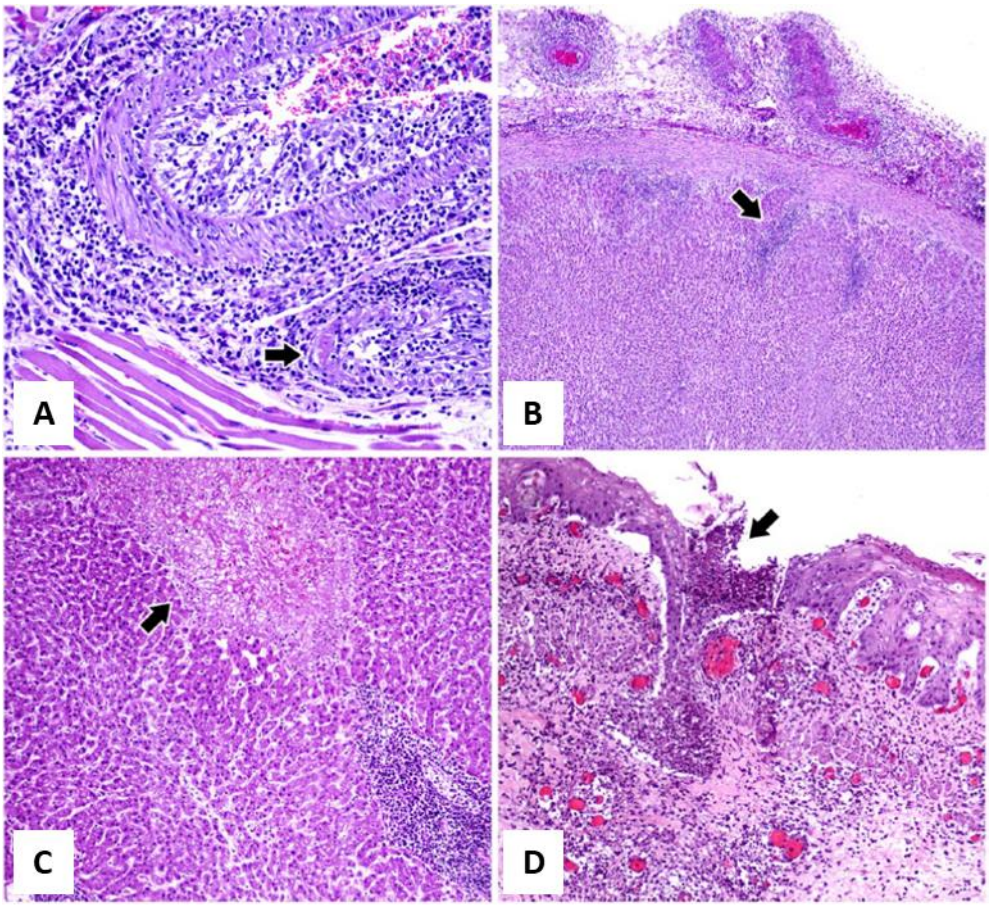


**Figure 1- 13. Different tissue sections from lamb affected with MCF.**
**A.** The artery section in a tongue showed the various sizes of lymphocytes, as well as fibrinoid necrosis, is observed in the small artery (arrow).**B.** The arrows refer to the extracapsular lymphocytic vasculitis with lymphocytic infiltrates which extending into the surrounding adipose tissue and adrenal cortex. **C.** hepatic coagulative necrosis (arrow) and adjacent perportal lymphocytic aggregates. **D.** Focal ulceration (arrow) and subtending lymphocytic vasculitis in the oesophagus (Phillips *et al.*, 2018)

## 1.2.9 MCF pathogenesis

The pathogenesis remains to be fully clarified and at present is poorly understood. However, in general, both host immune responses and viral gene expression play a role in the pathogenesis of MCF in animals (Brown, 2007). Lymphocytes are the predominate host

cells for OvHV-2 in sheep Baxter et al. (1997). Another study showed that cyclosporine-A mediated suppression of the T cells but failed to inhibit the development of MCF lesions (Buxton *et al.*, 1984). Research has consistently shown that the pathogenesis of MCF may be related in the first place to direct virus-cell interactions or immune-mediated responses (as lymphoproliferative and vascular lesions are considered indicators of immunologically mediated disease) to infected cells in which the virus causes dysregulation of cell function, leading to uncontrolled proliferation and cytotoxicity at the site of a lesion (Simon *et al.*, 2003). More recently, other researchers have shown that the pathology of MCF is initiated by interactions between the virus and host cell, which is affected by the glycoproteins in the virus membrane, which are in turn responsible for interacting with the cell-surface receptors on target cell types and facilitate or enable the fusion of the virus with cell membranes (Cunha *et al.*, 2015). Thus, both the virus entry and lymphoproliferation are responsible for vascular and epithelial destruction. Other studies (Ohteki, 2002; Waldmann, 2006) have shown that IL-15, a pleiotropic cytokine, plays a role in the pathogenesis of MCF and that overexpression of IL-15 is part of an inflammatory response which kills T cell. However, the main pathological changes noted in the disease, including lymphoproliferation, vascular and epithelial lesions, are well described (O'Toole and Li, 2014).

The mechanism by which OvHV-2 and AIHV-1 induce MCF is unknown; it is thought that virus-induced cytopathology is not involved in lesion development and it has been proposed that tissue damage arises from non-antigen-specific major histocompatibility complex (MHC) unrestricted cytotoxicity of the LGLs, as LGL cells play an integral role in the

immune system by circulating throughout the blood in search of infected cells (Russell *et al.*, 2009).

MCF viruses are predominate for at least two cell types—CD8+ T cells, which have a natural killer phenotype through destroy cells infected by intracellular viruses and cancer cells using programmed cell death in the infected cell, and epithelial cells. Interestingly, 10% of aggregated CD8+ T cells contain viral genes, while the majority do not. Thus, these cells may be responsible for mediating the tissue damage caused by MCF (Hart *et al.*, 2007; Dewals and Vanderplasschen, 2011) (see Figure 1-14).

The study of experimental MCF infection in rabbits has further enhanced the understanding of the disease's pathogenesis and differences between SA- and WA-MCF (Anderson *et al.*, 2007), particularly by showing that OvHV-2-induced additional tissue necrosis and less lymphoid hyperplasia of predominantly CD8+ and fewer CD4+ T cells than AIHV-1. Furthermore, the study of MCF in cattle has shown that cytotoxic CD8+ T cells are predominantly involved in the lymphoid hyperplasia associated with vasculitis (Simon *et al.*, 2003). To further understand MCF, cell cultures from proliferating lymphocytes were established to study their features *in vitro*; it was found that they responded to cytokines from other virus-infected lymphocytes and started to react against the host's own LGLs, which are non-MHC (major histocompatibility). The host's LGLs restrict cytotoxic activity and activate NK cells (such as expressing CD4 or CD8, but always CD2, and not transcribing IL-1ß or IL-2) (Burrells and Reid, 1991; Swa *et al.*, 2001).

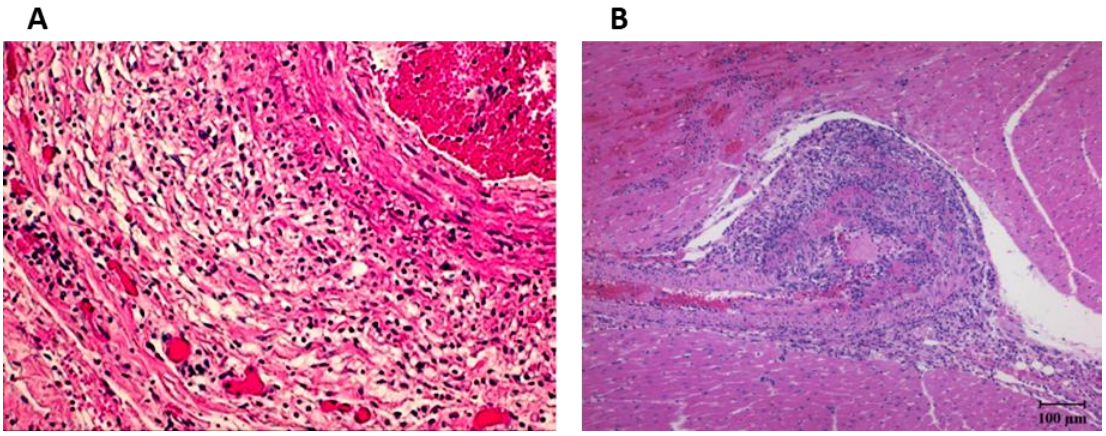


**Figure 1- 14. MCF lesions in bison and deer.**
**A.** Urinary bladder of bison affected with MCF, mononuclear cells infiltration of adventitia of the arteritis of a submucosal and medium-sized vessel, endothelial swelling of the intima, and a thrombus in the lumen. (Campolo *et al.*, 2008). **B:** Myocardium section from a white-tailed deer spleen that exhibited clinical signs of SA-MCF expanded tunica media of the artery and tunica adventitia due to infiltrate of lymphocytes and fibrinoid necrosis. (Palmer *et al.*, 2013)

## 1.2.10 Large granular lymphocytes in MCF

MCF disease is characterised by degenerative changes in multiple organs, with infiltration of enormous numbers of lymphocytes which leads to hyperplasia of lymphoid organs (Thonur *et al.*, 2006). LGLs can be cultured from different tissues of MCF-affected animals infected with OvHV-2 or AlHV-1, such as lymph nodes, spleen, corneas and other tissues (Wilkinson *et al.*, 1992). LGLs exhibited cytotoxicity characteristic of T cell or natural killer cells (NK) and can kill various target tissues in a major histocompatibility complex (MHC) unrestricted manner (Russell *et al.*, 2009). These cell lines can be maintained *in vitro*, by the addition of exogenous interleukin-2 (IL-2). Researchers found that cultured LGL cells infected with the OvHV-2 virus contained viral gene transcripts and antigens (Rosbottom *et al.*, 2002). These cultured LGL cells from OvHV-2 or AlHV-1 infected cattle may transmit MCF when injected into rabbits or other susceptible experimental species (Swa *et al.*,

2001). Uninfected T lymphocytes proliferated on the exposure of concanavalin A (ConA) whereas LGL cell lines were found to be unresponsive to ConA stimulated proliferation.

The major features of cultured LGLs include: (1) constitutive and indiscriminate cytotoxicity (2) failure to respond to stimulation by mitogens; and (3) LGLs derived from cattle infected with OvHV-2 which failed to express IL-2 mRNA and protein, although they can express pro-inflammatory cytokines (e.g. TNF-α and IL-1 β) and interferon- γ (IFN-γ) (Schock *et al.*, 1998; Swa *et al.*, 2001). LGLs are usually grown in a medium containing IL-2 but can also be implanted in the absence of IL-2 and other external added cytokines (Swa *et al.*, 2001).

LGL cell lines from cattle infected with OvHV-2 had viral genomes that were mainly circular in form, which is suggestive of latency (Rosbottom *et al.*, 2002). On the other hand, another study showed that these cell lines contained a mixture of circular and linear genome configurations, which indicated that LGLs may be comprised of a mixture of latently and productively infected cells (Thonur *et al.*, 2006).

## 1.2.11 Diagnosis of MCF

### 1.2.11.1 Clinical signs and differential diagnosis

MCF is one of the most widely spread viral diseases in ruminants and is difficult to differentiate from other viral diseases which cause similar indistinguishable clinical signs. These include foot and mouth disease viruses, vesicular stomatitis virus, infectious bovine rhinotracheitis virus, bovine viral diarrhoea virus, rinderpest virus, bovine papillar stomatitis, bluetongue viruses and MCF-associated viruses (Musser, 2004). The sporadic incidence with typical signs and lesions of MCF and contact with infected animals is

sufficient to reach a hypothetical diagnosis, but diagnosis of MCF generally is based on the combination of a history of exposure, epidemiological data, clinical signs and histopathologic findings (Williams and Barker, 2008). However, such a diagnosis is not reliable because, as noted above, it is difficult to differentiate MCF from some other similar viral diseases. Therefore, recourse to laboratory confirmation such as PCR is generally required to reach a definitive diagnosis (Holliman, 2005; Traul *et al.*, 2007). Rapid definitive diagnosis distinguishing MCF from other pathogens, especially those which cause similar clinical diseases, is very important in programs for eradicating and controlling epidemics.

### 1.2.11.2 Histopathologic analysis of post-mortem samples

The World Organisation for Animal Health recognises histopathological analysis as an useful test in the diagnosis of MCF because it allows clear a diagnosis in combination with the laboratory approaches (Gelaye *et al.*, 2013). Post-mortem examinations are performed and tissue samples are taken for histopathological examination to observe vasculitis and epithelial necrosis in various organs, especially in the brain (Li *et al.*, 2014).

### 1.2.11.3 Serology

Laboratory serological tests have been developed to detect antibodies against viruses in MCF cases, including immunoblotting (Herring *et al.*, 1989), enzyme-linked immunosorbent assay (ELISA) (Fraser *et al.*, 2006), competitive inhibition (CI)-ELISA (Li *et al.*, 1994; Li *et al.*, 2001c; Powers *et al.*, 2005), indirect immunofluorescence, immunoperoxidase assay (Rossiter, 1981b) and complement fixation test (Sentsui *et al.*, 1996).

### 1.2.11.4 Polymerase chain reaction (PCR)

Several PCR-based assays have been developed over the years to improve the diagnosis options of MCF cases. PCR assays allow the use of organs and fluid (uncoagulated blood, ocular and nasal swabs, and tissues) to obtain a highly specific diagnosis of MCF in acute and chronic cases (Traul *et al.*, 2005; Lung *et al.*, 2017). Such approaches, however, can also be used in the examination of fresh fixed organs from dead cases. The main advantages of a PCR assay compared to traditional laboratory methods is that PCR can be quickly performed and is highly productive; furthermore, the results are specific and sensitive, quantitative information is produced over a large dynamic range and measures are available to reduce the potential for cross-contamination (Burggraf and Olgemoller, 2004).

## 1.2.12 Treatment and control

To date, no effective treatment or vaccine is available for this disease to provide any consistent benefit. The treatment is limited to supportive care and to reduce subclinical or mild infection in affected animals with drugs such as nonsteroidal anti-inflammatory drugs (NSAIDs) which may allow for prolonged survival in some cases (Milne and Reid, 1990). On the other hand, the spontaneous recovery of cattle from MCF has been reported, which was confirmed by serology and PCR tests (O'Toole *et al.*, 2002).

In general drugs that are effective against herpesviruses interfere with DNA replication. There are two types of inhibitors for herpesvirus; nucleoside analogs and Non-nucleoside inhibitors. The nucleoside analogs (acyclovir and ganciclovir) mimic the normal nucleoside and block the viral DNA polymerase enzyme, which is important in the formation of DNA. All the nucleoside analogs before they have antiviral activity, they were

activated by addition of a phosphate group. Some of the agents (acyclovir) are activated by a viral enzyme, so they are specific for the cells that contain viral particles. While other agents (idoxuridine) are activated by cellular enzymes, so these have less specificity. Non-nucleoside inhibitors of herpesvirus replication include foscarnet, which directly inhibits the viral DNA polymerase and thus blocks formation of new viral DNA (Bartley *et al.*, 2014a).

There is no reliable way to control MCF; however, important strategies to mitigate the risk of MCF are to avoid direct contact between susceptible species and carriers, to breed virus-free reservoir hosts and to separate grazing areas under natural flock conditions (Cleaveland *et al.*, 2001). However, this is not always achievable in places such as zoos. Other risk factors which may affect the protection against MCF include the concentration of animals (size of flocks/herds), the animals' ages and stress levels, environmental conditions such as climate, wind, temperature and extreme weather, and factors such as the weaning and migration seasons. Clearly, there is no one-size-fits-all strategy for managing the risk of MCF (Lankester *et al.*, 2015a). One of the main obstacles in MCF disease control is livestock management, which involves keeping cattle away from wildebeest during the critical calving period.

### 1.2.13 A predictable vaccine for MCF

No vaccine is currently available to prevent MCF; many research attempts to develop a vaccine have been unsuccessful (O'Toole *et al.*, 2002; Martins *et al.*, 2017). It is important to find an effective vaccine to limit the infection of cattle, bison and exotic animals with MCF (Li *et al.*, 2014). In 1981, (Rossiter) showed that there are antigenic relationships between AIHV-1 and OvHV-2, as the reservoir and susceptible hosts infected with OvHV-2

can produce antibodies which can cross-react with AIHV-1 antigens. However, Taus *et al*. (2015) showed that the possibility for a vaccine based on AlHV-1 to provide cross-protective immunity against SA-MCF is likely to be slight.

In the case of OvHV-2, a limited number of studies of vaccines have been done due to the lack of a cell-free virus cultured *in vitro*. However, Li *et al*. (2013b) showed that the antibodies from cases infected *in vivo* with OvHV-2 can block OvHV-2 entry and help limit the infection. Previously, two vaccine models using attenuated AIHV1 either live or inactivated were used in rabbits, but these approaches did not prevent MCF (Rossiter, 1982).

The different approach to produce a possible vaccine against MCF was to develop a recombinant viral vaccine consisting of either an entire or partial virus genome cloned in a bacterial artificial chromosome which would allow the propagation of OvHV-2 (Dewals *et al.*, 2006; Stear, 2005). Most successful attempts to design and test a vaccine effective against MCF have used an attenuated version of the AlHV-1 virus, which protects against intra-nasal challenge with virulent AIHV-1 using cell-free virus. These attempts showed that a two-dose inoculation of AlHV-1 administered via injection into the cranial musculature of the neck on day zero and boosted at day 28 protected cattle when they faced an intranasal challenge with a virulent AlHV-1 isolate obtained from low-pass filter tissue culture (Haig *et al.*, 2008).

## 1.3 Latency-associated nuclear antigen (LANA)

LANA is a multifunctional protein that has a homologue present in all *Rhadinovirus* and *Macavirus* subfamilies of the gammaherpesviruses. The KSHV LANA was the first to be

discovered and most is known about this protein. KSHV LANA is a large (222- to 234-kDa) nuclear protein approximately 1162 amino acids in length, is encoded by the open reading frame 73 gene (ORF73). It is the major antigen expressed during latent infection and forms nuclear speckles or puncta in infected cells. LANA tethers virus circular episomes to host chromosomes during interphase and mitosis, which allows for efficient segregation of virus episomes to daughter cells (Piolot *et al.*, 2001; Ye *et al.*, 2011). KSHV LANA binds to the viral latent origin of replication located at the terminal repeat (TR) sequence of the KSHV genome, and is highly expressed in all KSHV-associated disorders (Kedes *et al.*, 1997; Hu *et al.*, 2002). It modulates viral and cellular gene expression affecting both transcription and regulation of both cellular and viral genes (Verma and Robertson, 2003). Furthermore, LANA contributes to a number of cellular processes, including cell growth, regulation of cellular angiogenesis and immune modulation (Cloutier and Flamand, 2010; Zhang *et al.*, 2016b). For instance, KSHV-LANA can modulate a host's adaptive immunity by inhibiting antigen presentation of both major histocompatibility complex class I (MHC I) and class II (MHC II) (Kwun *et al.*, 2011).

LANA can be subdivided into three major distinct protein domains (Figure 1-15): N-terminal, central and C-terminal. The N-terminal domain contains a nuclear localisation sequence (NLS), a chromosome binding sequence and a proline-rich region which has been shown to be important for tethering the protein to the host chromatin (Cotter and Robertson, 1999; Krithivas *et al.*, 2002). The central domain region is a large acidic repetitive region of which is rich in glutamine (Q), glutamic acid (E) and proline residues, which are reported to have variable lengths from different isolates; this may account for its slow electrophoretic migration (Ballestas and Kaye, 2011; Vázquez *et al.*, 2013). LANAs

vary greatly in size because of variations in the length of the large internal acidic domain (Zhang *et al.*, 2000). As shown in (Figure 1-15), LANA interacts with a variety of cellular proteins (Gao *et al.*, 1999; Garber *et al.*, 2002). Cotter II and Robertson (1999) showed that KSHV LANA binds to histone H1 but not to core histones and tethers virus episomes to the host's chromatin. The C-terminal domain contains a unique leucine zipper motif which is important for interaction with various cellular proteins such as p53 and histone H1 (Lim *et al.*, 2000). By interacting with the tumour suppressor protein p53 KSHV LANA is also thought to suppress lytic viral replication to promote cell survival and prevent apoptosis (DeWire and Damania, 2005; Wen *et al.*, 2009). The C-terminal domain also has a nuclear localisation signal sequence, which may be important for the characteristic nuclear speckling of LANA (Schwam *et al.*, 2000). KSHV LANA binds to the viral latent origin of replication located at the terminal repeat (TR) sequence of the KSHV genome (Kedes *et al.*, 1997; Hu *et al.*, 2002), which is crucial for tethering the viral genome to the host chromosome (Shinohara *et al.*, 2002b; Ye *et al.*, 2004) . Thus, it was supposed that LANA may act as a 'bridge' between nuclear heterochromatin and viral episomal DNA (Cotter *et al.*, 2001); specifically, LANA associates with host-cell mitotic chromosomes via chromosome-binding domains within its N- and C-terminal regions (Ballestas *et al.*, 1999; Piolot *et al.*, 2001). LANA plays a critical role in the maintenance and persistence of the viral genome in new daughter cells by preventing the loss of viral DNA after the cell divides, which is a crucial step in establishing the latent form of MCF. Therefore, the presence of LANA has been shown to be essential for the long-term maintenance of the disease (Ye *et al.*, 2004). Interestingly, LANA can autoactivate its promoter during latent infection, thereby ensuring that the different levels of LANA are sufficient to maintain latency (Groves *et al.*, 2001; An *et al.*, 2005).

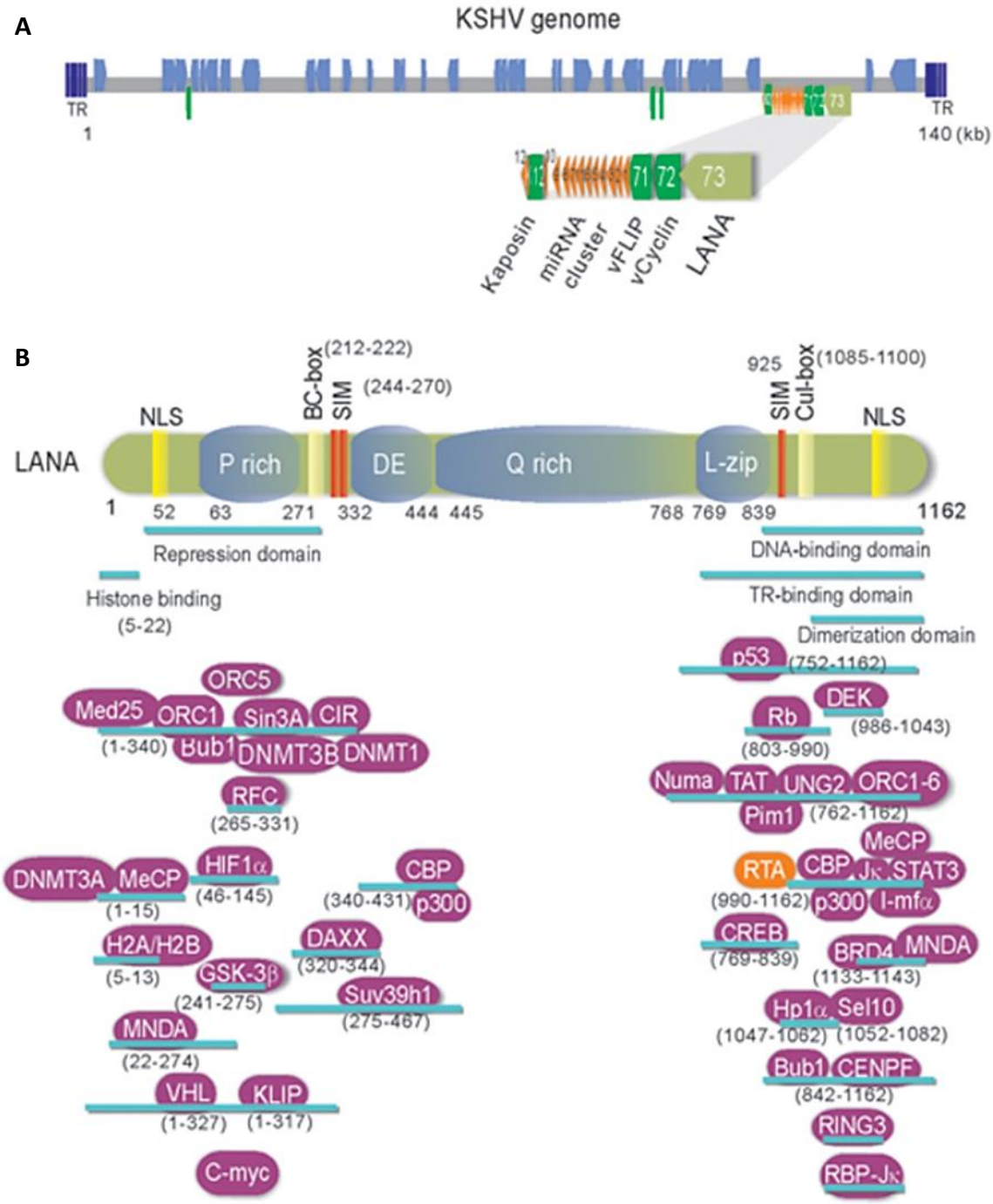


**Figure 1- 15. Latency-associated nuclear antigen protein.**

**A:** Schematic and location of the KSHV latent genes including miRNA cluster. Bottom: The major latency locus (ORF73/LANA, ORF72/v-Cyclin, ORF71/vFLIP, and K12/Kaposin) of KSHV is shown in an enlarged view. Position of 12 pre-miRNA cluster is shown in red triangle. **B:** The structure and functional motifs of Latency-associated nuclear antigen (LANA). LANA consists of 1162 amino acids. Numbers indicate the amino acids (aa). Repetitive regions and key motif of LANA are noted. P, Proline; DE, Aspartic acid and Glutamic acid; Q, Glutamine; L, Leucine; NLS, nuclear localized sequence; BC, Elongin B and C; Cul: Cullin5; SIM, SUMO-interacting motif. The binding regions of LANA-associated cellular and viral proteins are listed at the bottom panel (Wei *et al.*, 2016).

# 1.4 OvHV-2 LANA (oLANA)

All gammaherpesviruses have a conserved set of genes that show homology between each other. One of these, OFR73, is known to encode the latency-associated nuclear antigen (LANA). Unlike most gammaherpesvirus genes (and proteins), the degree of sequence similarity between LANA proteins is very low (< 20%) and they vary in length considerably. In spite of this, they all have a conserved domain structure (short N-terminal domain, longer C-terminal domain interspersed by a repetitive domain.), conserved nuclear localisation signal and also conserved functions and binding partners. For example the MHV-68 LANA, although sharing <20% amino-acid identity with KSHV LANA, still binds to viral genome and tethers it to chromatin, binds to similar cellular proteins as KSHV LANA and has a similar structure (Hellert J,. PLOS Pathogens 9(10): e1003640. https://doi.org/10.1371/journal.ppat.1003640). Very little is known about the OvHV-2 LANA (oLANA). It is 495 aa in length and, like all other LANAs, is divided into a short N-terminal domain, a long repetitive domain that mostly composed of glycine, glutamic acid and proline and an C-terminal domain. (See Figure 1-16)

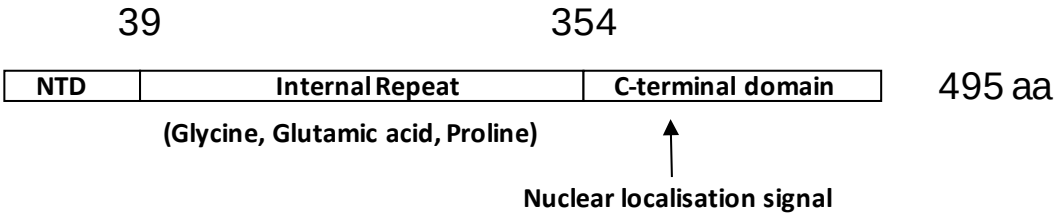


**Figure 1- 16. Schematic diagram of oLANA showing the three domains and the nuclear localisation signal.**

It has a predicted molecular weight of 49 KDa and a pI of 3.75. It has low DNA or protein (aa) sequence homology with other LANA proteins including KSHV (<20% sequence identity) although there are patches of sequence identity/similarity that indicate that oLANA may conserved some function with other LANA proteins (Figure 1-17). Analysis of the sequence shows that the internal repetitive domain is composed of 44% glutaminc acid, 42% glycine and 12% proline and is largely composed of blocks of the element PGGEEEG. Like other LANA proteins there is a conserved nuclear localisation signal. Work by a previous PhD student led to the development of an antibody to oLANA (Al-Saadi, 2018). This demonstrated that the native protein migrates on SDS-PAGE gels with an apparent Mr of 37 KDa and is predominantly localised to the nucleus of infected cells in puncta (Al-Saadi, 2018).

```
MHV-68       1 ------------------------------------------------------------
EquinEHV2    1 ------------------------------------------------------------
RRV          1 ------------------------------------------------------------
KSHV         1 ------------------------------------------------------------
HVS          1 ------------------------------------------------------------
OvHV-2       1 ------------------------------------------------------------
AlHV-1       1 MVLLRSGLGTRPGEEDCDGGPSTRTRGHGPLGPNIKSAAGIGGKFPPSPQGRKRKKGPKK

MHV-68       1 ------------------------------------------------------------
EquinEHV2    1 ------------------------------------------------------------
RRV          1 ------------------------------------------------------------
KSHV         1 ----------------------------------------------MAPPGMRLRS--
HVS          1 ------------------------------------------------------------
OvHV-2       1 ------------------------------------------------------------
AlHV-1      61 SGGKKKKRKVTGEGPGGGEGPGGGEGPGGGEGPGGGEGPGGGEGPGGGEVPGGGEVPGGG

MHV-68       1 ------------------------------------------------------------
EquinEHV2    1 ------------------------------------------------------------
RRV          1 ------------------------------------------------------------
KSHV        11 -----------GRST-GAPLTRGSCRKRNRSPERCDLGDDLHLQPRRKHVADSIDGR-EC
HVS          1 ------------------------------------------------------------
OvHV-2       1 ------------------------------------------------------------
AlHV-1     121 EGPGGGEGPGGGEGPGGGEGPGGNSRKRKRGDGSKKHGG-----KKKK--KTTVTGEGGS

MHV-68       1 ------------------------------------------------------------
EquinEHV2    1 ------------------------------------------------------------
RRV          1 ------------------------------------------------------------
KSHV        58 GPHTLPIPGSPTVFTSGLPAFVSSPTLPVAPIPSPAPATPLPPP-----ALLPPVTT-SS
HVS          1 ------------------------------------------------------------
OvHV-2       1 ------------------------------------------------------------
AlHV-1     174 GPEG------PERDDPDGPGSQEGPKREEGPLGPDGPEGPEGPEGEGPEGLEGPKGEGPE

MHV-68       1 ------------------------------------------------------------
EquinEHV2    1 ------------------------------------------------------------
RRV          1 ------------------------------------------------------------
KSHV       112 SPIPPS--HPVSPGTTDT----HS-------PSPALPPTQSPESSQRPPLSSPTGRPDSS
```

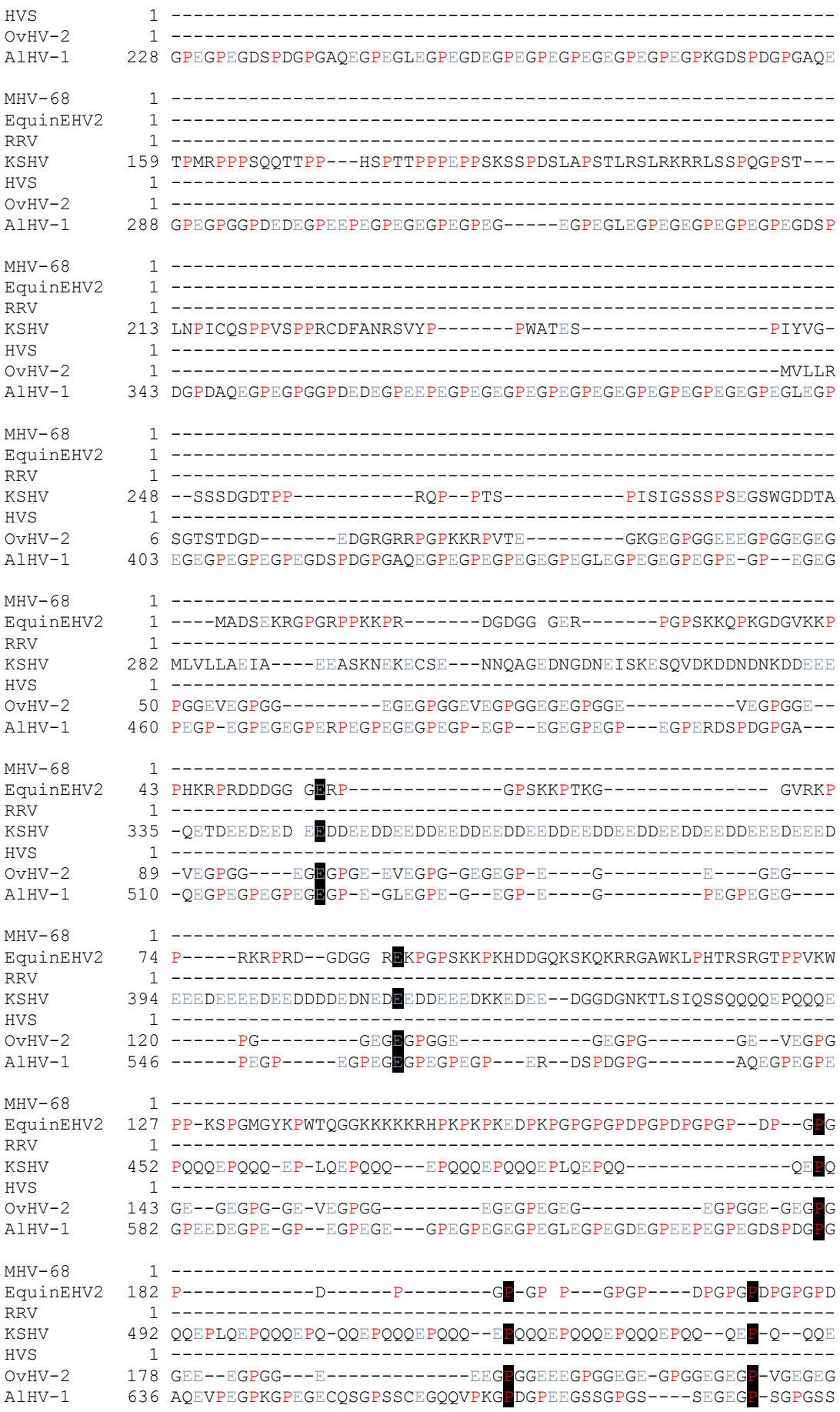
HVS 1 ----------
OvHV-2 1 ----------
AlHV-1 228 GPEGPEGDSPDGPGAQEGPEGLEGPEGDEGPEGPEGPEGEGPEGPEGPKGDSPDGPGAQE
MHV-68 1 ----------
EquinEHV2 1 ----------
RRV 1 ----------
KSHV 159 TPMRPPPSQQTTPP---HSPTTPPPEPPSKSSPDSLAPSTLRSLRKRRLSSPQGPST---
HVS 1 ----------
OvHV-2 1 ----------
AlHV-1 288 GPEGPGGPDEDEGPEEPEGPEGEGPEGPEG-----EGPEGLEGPEGEGPEGPEGPEGDSP
MHV-68 1 ----------
EquinEHV2 1 ----------
RRV 1 ----------
KSHV 213 LNPICQSPPVSPPRCDFANRSVYP-------PWATES----------PIYVG-
HVS 1 ----------
OvHV-2 1 ----------MVLLR
AlHV-1 343 DGPDAQEGPEGPGGPDEDEGPEEPEGPEGEGPEGPEGPEGEGPEGPEGPEGEGPEGLEGP
MHV-68 1 ----------
EquinEHV2 1 ----------
RRV 1 ----------
KSHV 248 --SSSDGDTPP----------RQP--PTS----------PISIGSSSPSEGSWGDDTA
HVS 1 ----------
OvHV-2 6 SGTSTDGD-------EDGRGRRPGPKKRPVTE---------GKGEGPGGEEEGPGGEGEG
AlHV-1 403 EGEGPEGPEGPEGDSPDGPGAQEGPEGPEGPEGEGPEGLEGPEGEGPEGPE-GP--EGEG
MHV-68 1 ----------
EquinEHV2 1 ----MADSEKRGPGRPPKKPR-------DGDGG GER-------PGPSKKQPKGDGVKKP
RRV 1 ----------
KSHV 282 MLVLLAEIA----EEASKNEKECSE---NNQAGEDNGDNEISKESQVDKDDNDNKDDEEE
HVS 1 ----------
OvHV-2 50 PGGEVEGPGG---------EGEGPGGEVEGPGGEGEGPGGE----------VEGPGGE--
AlHV-1 460 PEGP-EGPEGEGPERPEGPEGEGPEGP-EGP--EGEGPEGP---EGPERDSPDGPGA---
MHV-68 1 ----------
EquinEHV2 43 PHKRPRDDDGG GERP--------------GPSKKPTKG--------------- GVRKP
RRV 1 ----------
KSHV 335 -QETDEEDEED EEDDEEDDEEDDEEDDEEDDEEDDEEDDEEDDEEDDEEDDEEEDEEED
HVS 1 ----------
OvHV-2 89 -VEGPGG----EGEGPGE-EVEGPG-GEGEGP-E----G---------E----GEG----
AlHV-1 510 -QEGPEGPEGPEGEGP-E-GLEGPE-G--EGP-E----G---------PEGPEGEG----
MHV-68 1 ----------
EquinEHV2 74 P-----RKRPRD--GDGG REKPGPSKKPKHDDGQKSKQKRRGAWKLPHTRSRGTPPVKW
RRV 1 ----------
KSHV 394 EEEDEEEEDEEDDDDEDNEDEEDDEEEDKKEDEE--DGGDGNKTLSIQSSQQQQEPQQQE
HVS 1 ----------
OvHV-2 120 ------PG---------GEGEGPGGE----------GEGPG--------GE--VEGPG
AlHV-1 546 ------PEGP-----EGPEGEGPEGPEGP---ER--DSPDGPG--------AQEGPEGPE
MHV-68 1 ----------
EquinEHV2 127 PP-KSPGMGYKPWTQGGKKKKKRHPKPKPKEDPKPGPGPGPDPGPDPGPGP--DP--GPG
RRV 1 ----------
KSHV 452 PQQQEPQQQ-EP-LQEPQQQ---EPQQQEPQQQEPLQEPQQ--------------QEPQ
HVS 1 ----------
OvHV-2 143 GE--GEGPG-GE-VEGPGG---------EGEGPEGEG----------EGPGGE-GEGPG
AlHV-1 582 GPEEDEGPE-GP--EGPEGE---GPEGPEGEGPEGLEGPEGDEGPEEPEGPEGDSPDGPG
MHV-68 1 ----------
EquinEHV2 182 P----------D------P--------GP-GP P---GPGP----DPGPGPDPGPGPD
RRV 1 ----------
KSHV 492 QQEPLQEPQQQEPQ-QQEPQQQEPQQQ--EPQQQEPQQQEPQQQEPQQ--QEP-Q--QQE
HVS 1 ----------
OvHV-2 178 GEE--EGPGG---E----------EEGPGGEEEGPGGEGE-GPGGEGEGP-VGEGEG
AlHV-1 636 AQEVPEGPKGPEGECQSGPSSCEGQQVPKGPDGPEEGSSGPGS----SEGEGP-SGPGSS

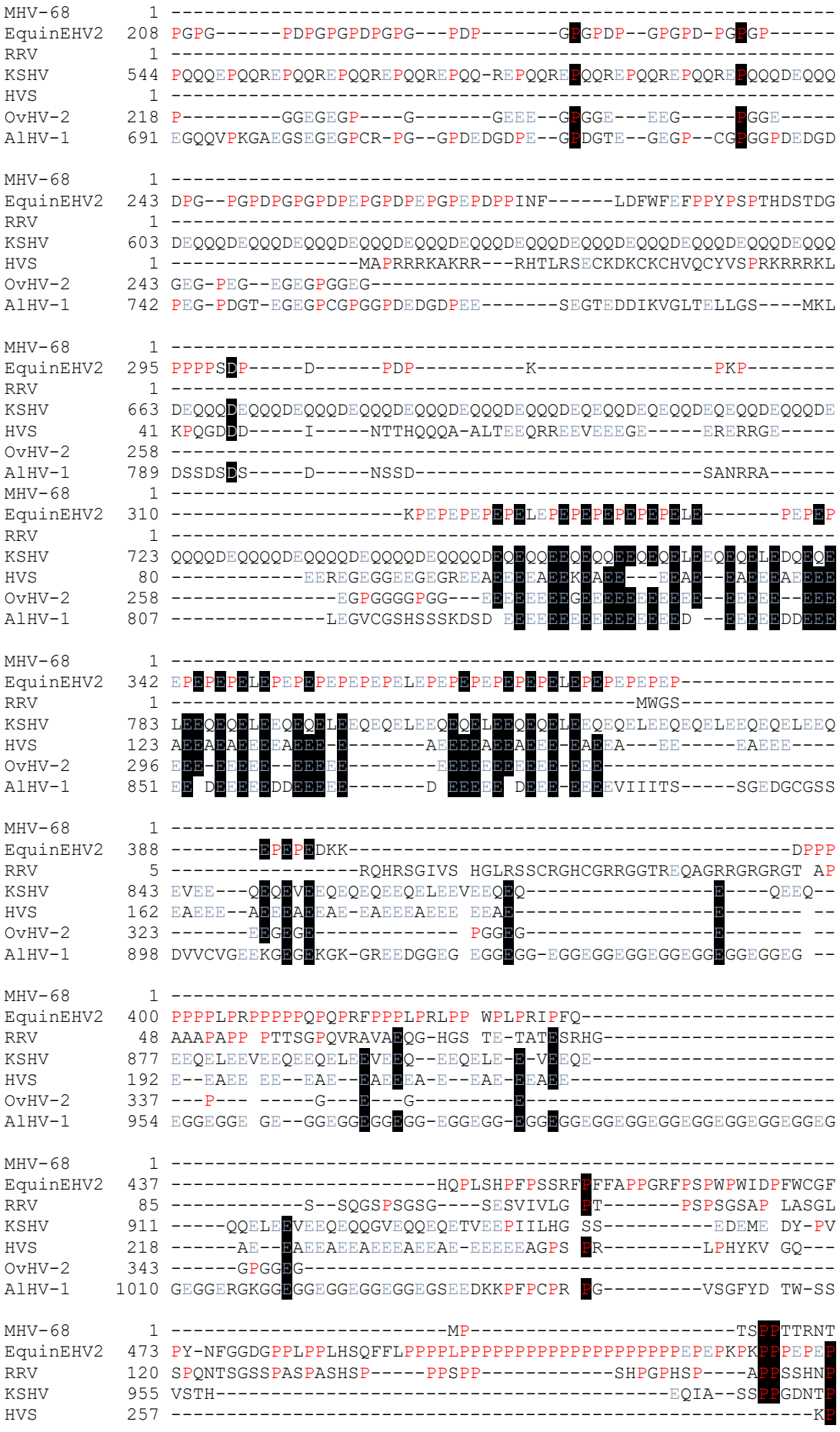
MHV-68 1
EquinEHV2 208
RRV 1
KSHV 544
HVS 1
OvHV-2 218
AlHV-1 691
MHV-68 1
EquinEHV2 243
RRV 1
KSHV 603
HVS 1
OvHV-2 243
AlHV-1 742
MHV-68 1
EquinEHV2 295
RRV 1
KSHV 663
HVS 41
OvHV-2 258
AlHV-1 789
MHV-68 1
EquinEHV2 310
RRV 1
KSHV 723
HVS 80
OvHV-2 258
AlHV-1 807
MHV-68 1
EquinEHV2 342
RRV 1
KSHV 783
HVS 123
OvHV-2 296
AlHV-1 851
MHV-68 1
EquinEHV2 388
RRV 5
KSHV 843
HVS 162
OvHV-2 323
AlHV-1 898
MHV-68 1
EquinEHV2 400
RRV 48
KSHV 877
HVS 192
OvHV-2 337
AlHV-1 954
MHV-68 1
EquinEHV2 437
RRV 85
KSHV 911
HVS 218
OvHV-2 343
AlHV-1 1010
MHV-68 1
EquinEHV2 473
RRV 120
KSHV 955
HVS 257

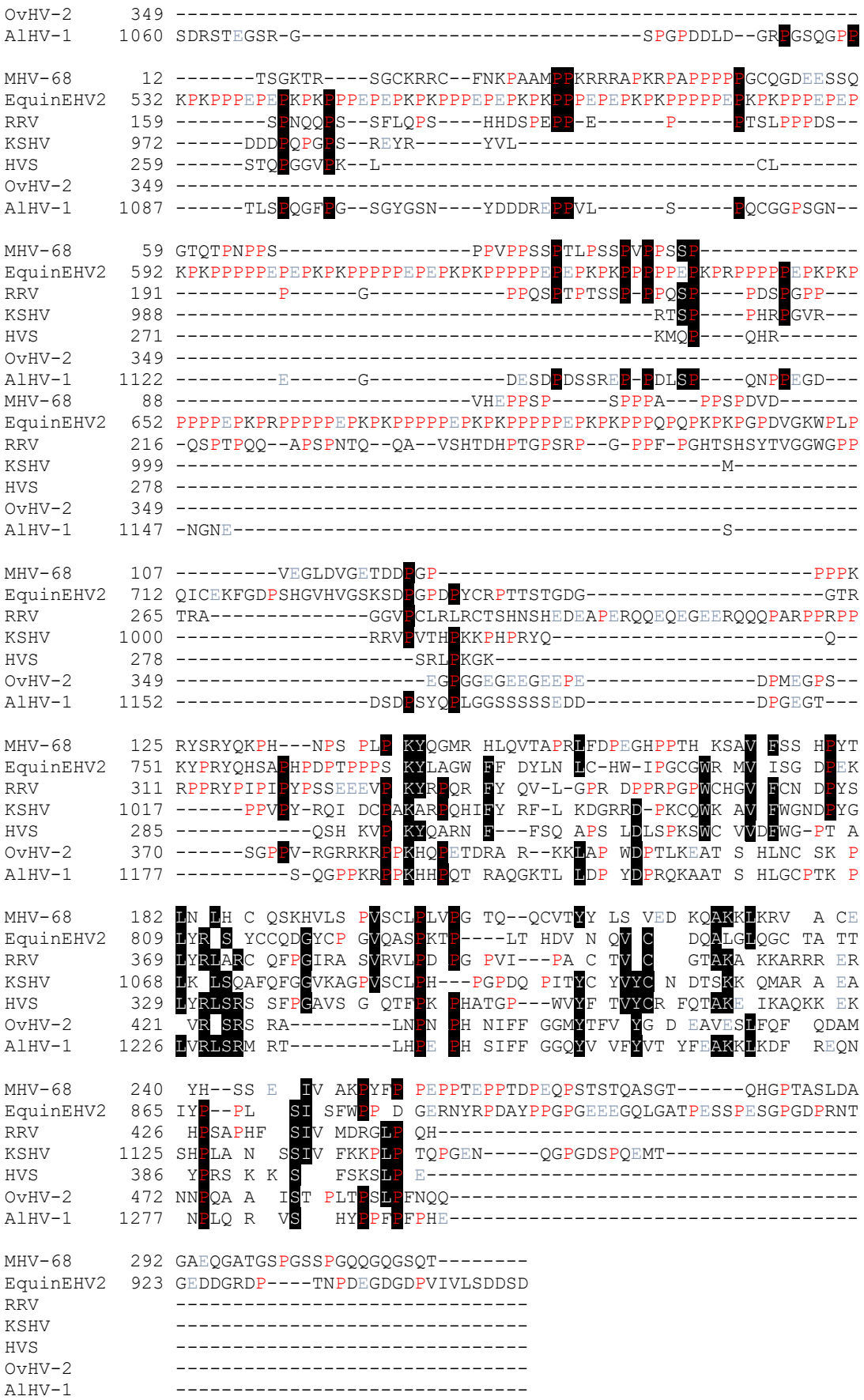
OvHV-2 349
AlHV-1 1060
MHV-68 12
EquinEHV2 532
RRV 159
KSHV 972
HVS 259
OvHV-2 349
AlHV-1 1087
MHV-68 59
EquinEHV2 592
RRV 191
KSHV 988
HVS 271
OvHV-2 349
AlHV-1 1122
MHV-68 88
EquinEHV2 652
RRV 216
KSHV 999
HVS 278
OvHV-2 349
AlHV-1 1147
MHV-68 107
EquinEHV2 712
RRV 265
KSHV 1000
HVS 278
OvHV-2 349
AlHV-1 1152
MHV-68 125
EquinEHV2 751
RRV 311
KSHV 1017
HVS 285
OvHV-2 370
AlHV-1 1177
MHV-68 182
EquinEHV2 809
RRV 369
KSHV 1068
HVS 329
OvHV-2 421
AlHV-1 1226
MHV-68 240
EquinEHV2 865
RRV 426
KSHV 1125
HVS 386
OvHV-2 472
AlHV-1 1277
MHV-68 292
EquinEHV2 923
RRV
KSHV
HVS
OvHV-2
AlHV-1

**Figure 1- 17. Alignment analysis of LANA amino acids homologue of different γ-herpesviruses including: MHV-68, Equid HV2, RRV, KSHV, HVS, OvHV-2, and A1HV-1) corresponded with GenBank accession numbers (NP_044913, AIU39518, NP_570820, ACY00477, NP_040275, AAL05844, and NP_065570) respectively.**

This was performed using "Clustal Omega" program and displayed by the "BOXSHADE" server. This highlights sequence diversity of LANA in which the highly identical residues (can be seen predominantly within C terminal homologue) are depicted in black. Similar residues are depicted in grey (appear mostly within N terminal homologue). Dashes represent sequence gaps. The predominant tandem repeats appear within the central domain of LANA. The Glutamic acid is coloured in blue while the Proline are highlighted red. (Al-Saadi, 2018)

## 1.5 The Aim

MCF is a frequently lethal, immunopathological, viral disease, which can be caused by several distinct gammaherpesviruses, it is a worldwide disease which occurs in many ruminants, including domestic cattle, bison, deer and others. The most frequent causative agent of MCF is OvHV-2 which cannot be propagated *in vitro.* There is no vaccine and there are no effective drugs to treat animals that are affected by MCF. The ultimate aim is to understand the mechanism of disease pathogenesis and to develop possible drug interventions that might be useful in combatting disease. I hypothesised that, by homology with other gammaherpesviruses, the LANA protein plays an important role in the maintenance of virus and establishment of the disease. Other LANA proteins are known to function by binding/association with proteins involved in cell replication and the innate immune response. The specific aim of this project was to work out which cellular proteins OvHV-2 LANA interacts with to start determining its exact function. Using the information of LANA-interacting proteins it may be possible to be able to use known drug inhibitors of these cellular proteins to treat MCF.

# Chapter two: Materials and Methods

# 2. Materials and Methods

In this section, we intend to determine the cellular protein interact with oLANA through three different approach; first, three-plasmid production system was used to generate a recombinant retrovirus to deliver oLANA into bovine T cells. Second approach was to insert GFP-oLANA template which lack the internal domain into a pMSCV-IRES-GFP vector using EcoRI and NOTI restriction enzymes. The success insertion of the protein was transfected into HEK 293T cells followed by co-immunoprecipitation of the transfected cells which then proceed for proteomics. Third and final approach was to confirm these interactions using immunofluorescence and localisation assays.

## 2.1 Generation of recombinant retrovirus

A key aspect in the generation of recombinant retrovirus as tools is the introduction of appropriate DNA vectors into a cell line which is able to produce the viral proteins needed for encapsidation of the required recombinant. One of the most important steps in gene transfer applications is the generation of pure stocks of recombinant virus free of replication-competent helper (Coffin *et al.*, 1997).

The three major proteins encoded within the retroviral genome are gag, pol and env, each of which plays a specific role in the retrovirus structure. Gag, an acronym for Group Antigens (Ag), is a polyprotein which acts as the core structure of the virus. It is the major component of the herpesvirus viral capsid and the major protein comprising the nucleoprotein core particle. Pol, a reverse transcriptase, is the essential enzyme which carries out the reverse transcription process which transforms the RNA genome to a double-stranded DNA pre-integrate form. Env, the envelope protein, determines the viral

tropism and plays a role in the association and entry of virions into the host cell; it also allows the retrovirus to bind to its target host cell using specific cell-surface receptors (Coffin *et al.*, 1997).

### 2.1.1 Purification of three plasmids

To express oLANA, a three-plasmid production system was used based on the murine stem cell retrovirus (pMSCV) (Plasmid 20672, Addgene). These vectors will then be used to transfect mammalian cells and make recombinant retrovirus expressing the gene of interest. For recombinant retroviral work we will use three vectors containing LTRs and packaging signal (pMSCV-IRES-GFP) gag and pol (pEQpAM3) (The Pol-coding region conserved regions of reverse transcriptase) and the vesicular stomatitis virus G protein (pSRG), these plasmids were kindly provided by friend to this study. The recombinant retrovirus is replication defective the three plasmids were expressed using transfection assay into HEK293 T cells (Graham *et al.*, 1977). The VSV G molecule will confer a broad host and cell type range to the recombinant virus (Finkelshtein *et al.*, 2013).

### 2.1.2 Plasmid Purification (Maxi prep technique)

### 2.1.2.1 Agar plate and cell culture preparation

Agar plates were prepared by diluting the appropriate weight of LB agar (Luria-Bretani agar) (LB 1 % w/v tryptone, 0.5 % w/v yeast extract, 1 % w/v NaCl) (22700025, Invitrogen) in distilled water and then autoclaved. After cooling the agar to be below 60°C, 0.5 µl /ml ampicillin (Ampicillin, sodium salt 100mg/ml, A5354, Sigma) was added, then the agar was poured into Petri dishes (150318, ThermoFisher) and left to solidify. A volume of 10-20 µl of glycerol stock for each plasmid was add to the surface of separate plates and spread over using disposable loops, then plates were incubated overnight at 37 °C. On the

following day, single colonies were picked and inoculated in 10 ml LB broth (LB Broth Powder microbial growth medium (Lennox), 10 g/L Tryptone, 5 g/L Yeast Extract, 5 g/L NaCl, L3022, Sigma), containing 0.5 µl/ml ampicillin (minipreparation), then incubated 16 - 18 hr at 37 °C in individual universal tubes on orbital incubator (Sanyo) at 200 rpm to prepare sufficient cells for plasmid purification.

### 2.1.2.2 Plasmid Purification

For large-scale propagation of the three plasmids in *E. coli* and to produce a large amount of plasmid DNA suitable for transfection into cell lines, Endo Free Plasmid Maxi Kit (10) (12362, QIAGEN) was used following the manufacturer's instructions. Single colonies were picked up from previously cultured plates (one for each plasmid) and used in to inoculate 10 ml LB broth starter supplemented with 0.5 µl/ ml ampicillin, and incubated overnight at 37 °C with shaking at 200 rpm in an orbital incubator (Sanyo). On the following day and in order to yield enough culture for plasmid expression, the starter culture was used to inoculate a further overnight culture of 100 mL LB broth containing 0.5 µl/ml ampicillin in a 1 L conical flask. The flask was placed in orbital incubator (SANYO) with shaking and incubated overnight using the same parameters mentioned before for culture. On the following day, the large-scale bacterial cultures were centrifuged at 6000 x g for 15 minutes at 4 °C. The resulting bacterial cell pellet was resuspended in 10 ml buffer P1 (50 mM Tris.Cl, 10 mM EDTA, 100 µg/ml RNase A, pH 8.0), then the bacteria were lysed by adding 10 ml buffer P2 (200mM NaOH, 1 w/v SDS) and inverting 4–6 times to mix and incubated for 5 minutes at room temperature (RT). The next step neutralised the lysate by addition of 10 ml chilled buffer P3 (3 M potassium acetate, pH 5.5). The solution was mixed thoroughly by inverting 4–6 times until the solution became completely colourless, and

then the cell lysate was poured into the barrel of the QIAfilter Cartridge (Qiagen) and Incubated at room temperature for 30 minutes. The cleared cell lysate was collected in a clean 50 ml tube (430829, Corning) by inserting the plunger gently into the QIAfilter Cartridge. 2.5 ml Buffer ER was added to the filtered lysate and mixed by inverting the tube approximately 10 times, followed by incubation for 30 minutes on ice. The lysate was decanted into Qiagen tip 500 (Qiagen) which had been pre-equilibrated by washing with 10 ml equilibration buffer QBT (750 mM NaCl, 50 mM MOPS, 15% isopropanol v/v, 0.15% Triton X-100 v/v) that was allowed to drain by gravity flow. The lysate was applied into the QIAGEN-tip and allowed to enter the tip. The tips were then washed twice with 30 ml Buffer QC (1.0 M NaCl, 50 mM MOPS, 15% isopropanol v/v, PH 7.0) and left to pass through by gravity flow. The DNA was then eluted with 15 ml QN buffer (1.6 M NaCl, 50 mM MOPS, 15% isopropanol v/v, PH 7.0). The eluted DNA was precipitated with 10.5 ml isopropanol (2-propanol BioReagent, 19516, Sigma) and pelleted by centrifugation at ≥15,000 x g for 30 minutes at 4 °C. Pellets were further washed with 5 ml 70% molecular grade ethanol (E7023, Sigma), and spun at 15000 x g for 10 minutes, air dried for 5-10 minutes and the DNA resuspended in 1 ml of endotoxin-free Buffer TE (10 M Tris, PH 8.0; 1 mM EDTA). Concentration and purity of the DNA was measured as mentioned in section (2.1.3) and DNA was stored at 4 °C.

### 2.1.3 Measuring the deoxyribonucleic acid (DNA)

The concentration of each DNA samples was measured using the Qubit® dsDNA BR Assay kit, (Q32850, Invitrogen) following the manufacture's instruction. Initially, Qubit working solution was prepared in a ratio of1:200 by mixing Qubit dsDNA reagent with Qubit dsDNA buffer in a clean 1.5 ml sterile tube (S1615-5500, STARLA). The assay was performed

using 0.5 ml tubes (Axygen™ PCR Tubes with 0.5mL Flat Cap, 11331974, AXYGEN) with a final volume in each tube of 200 µL, 190 µL of working solution was pipetted into two individual tubes followed by 10 µL of Qubit standard 1 and 2 respectively to prepare the standards for the assay. 199 µL working solution was pipetted into a clean tube for each sample to be assayed followed by 1 µL of each DNA separately, then mixed by vortexing 2–3 s, the tubes then were incubated at room temperature (RT) for 2 minutes (to allow the DNA to stabilize with the reagent) and measured by Qubit® 2.0 Fluorometer, Invitrogen. The DNA was either used directly or stored at 4 °C until further use.

DNA concentration was calculated using the following equation:

**Concentration of the DNA = QF value × (200)/x**

QF value = the value given by the Qubit® 2.0 Fluorometer.

x = the number of microliters of the sample that was added to the assay tube.

## 2.1.4 Endotoxin free Plasmid Samples

Endotoxin-free preparations of plasmid DNA and high molecular weight genomic DNA is required in many molecular biology applications. As *E. coli* and Gram-negative eubacteria are common hosts for plasmid production, and the outer membrane contains lipopolysaccharides (endotoxin) which can cause inflammatory reactions, fever and endotoxic shock *in vivo* and decrease transfection efficiencies *in vitro.* Thus, Endotoxin Removal Kits were used to remove the endotoxin preparations (Petsch and Anspach, 2000). Some cells respond strongly even to very low endotoxin concentrations in plasmid DNA, resulting in significantly reduced transfection efficiencies in these so called endotoxin-sensitive cell lines.

The three plasmids were cleaned to remove harmful endotoxins that could cause decreased transfection efficiencies using a Mira CLEAN® Endotoxin Removal Kit (Mirus Bio LLC, MIR 5910) which based on a rapid phase extraction that efficiently and conveniently removes endotoxin contamination from DNA according to the manufacturer's instructions. The EndoGO Extraction Reagent was warmed to room temperature and vortexed before use. The DNA samples were diluted to 0.5 - 1.0 mg/ml using TE buffer (10 M Tris, PH 8.0; 1 mM EDTA), Table (2-1).

| DNA | Volume µL | TE µL | Total Volume mL |
|---|---|---|---|
| **pEQpAM3** | 960 | 40 | 1 |
| **PMSC-IRES-GFP** | 920 | 80 | 1 |
| **pSRG** | 577 | 423 | 1 |

**Table 2- 1. Dilution volumes used for endotoxin removal assay**

Volumes of 0.1 of MiraCLEAN® Buffer were added to the DNA, which was then mixed by vortexing, Table (2-2). The samples were incubated on ice for 5 minutes, then vortexed, the DNA was extracted by adding 0.03 volumes of the EndoGO Extraction Reagent to each tube, Table (2-3), the reaction's colour changed to pink. Samples were vortexed briefly and incubated in the ice box for 5 minutes with intermittent vortexing (at least 2 times), followed by incubation for 5 minutes in a pre-warmed water bath at 50°C, which is required for complete separation of phases.

| DNA | Volume µL | MiraCLEAN buffer µL |
|---|---|---|
| **pEQpAM3** | 960 | 96 |
| **pMSC-IRES-GFP** | 920 | 92 |
| **pSRG** | 577 | 57.7 |

**Table 2- 2. Volumes of MiraCLEAN® Buffer used in endotoxin removal assay**

| DNA | Volume | EndoGO Extraction Reagent µL |
|---|---|---|
| **pEQpAM3** | 1096 | 32.88 |
| **pMSC-IRES-GFP** | 1092 | 32.76 |
| **Psrg** | 1057.7 | 31.73 |

**Table 2- 3. EndoGO Extraction Reagent volumes used in endotoxin removal assay**

Samples were centrifuged for approximately 20 seconds at 14000 x g or faster at room temperature, the tubes were removed gently from the centrifuge and tilted carefully. The upper colourless aqueous phase (containing the DNA) was transferred slowly to new sterile tubes to avoid the collapse of the interface between the two phases, the lower pink phase which contained the extracted endotoxin was discarded, then the tubes were placed on ice. To get a high quality and quantity of purified DNA, an extra 2/3 rounds of extraction were performed by repeating the steps but 0.03 volumes of the EndoGO Extraction Reagent were added to each tube to take in account the changes in volume, Table (2-4).

This repetition is sufficient to remove (or reduce to undetectable levels) endotoxin from contaminated plasmid DNA preparations.

| DNA | Volume µL | EndoGO Extraction Reagent µL |
|---|---|---|
| **pEQpAM3** | 1000 | 30 |
| **pMSC-IRES-GFP** | 900 | 27 |
| **pSRG** | 1000 | 30 |

**Table 2- 4. EndoGO Extraction Reagent volumes used in second round of endotoxin removal assay**

DNA samples were precipitated with 2 volumes of cold 100% ethanol, Table (2-5), then incubated at -20 °C or colder for 30 minutes. Samples were centrifuged at 14000 x g at 4°C for 20 minutes. The pellet was washed with 1 ml of 100 % ethanol and the supernatant was discarded. Followed by centrifugation at 14000 x g at 4°C for 20 minutes, the supernatant was discarded. Pellet was air dried for 5-10 minutes, then pellet was resuspended in 1 ml of TE buffer.

| DNA | Volume µL | 100 %ethanol µL |
|---|---|---|
| **pEQpAM3** | 500 | 1000 |
| **pMSC-IRES-GFP** | 750 | 1500 |
| **Psrg** | 800 | 1600 |

**Table 2- 5. Ethanol concentration used per DNA sample in endotoxin removal assay**

## 2.1.5 Cell line culture maintenance

Cells were thawed in a 37 °C water bath for about 1-2 minutes then added into 10 ml tissue culture media containing foetal calf serum (F6178, Sigma). After 2-4 days, cells were passaged when they reached a cell density of approximately 90% confluent. All cell lines except the LGL cell line (suspension), as described in section (2.1.5.3) were split and harvested into a new flasks once they covered ~80% of the bottom of the flask, as assessed by eye and seeded at a density of 10,000 cells per $cm^2$. The media was removed and the cells were washed three times with 10 mL of sterile 1 x PBS (Phosphate Buffered Saline, D8662 Sigma). Monolayer cells were then detached from the plastic flask using 5 mL pre-warmed trypsin-EDTA (Trypsin-EDTA (0.25%), 25200072, Life Technologies) and incubated a 37 °C for 1 minute. To inhibit the activate trypsin, 5 ml of fresh media containing 10 % foetal calf serum was add to the trypsinised cells and gently pipetted to break up the clumps and ensure the homogeneity. The cells were pelleted by centrifuged for 5 minutes at 1500 rpm (Eppendorf Centrifuge 5810 R, Eppendorf) to obtain the cell pellet and remove the trypsin residue, the supernantant was discard and the cells were resuspended in 10 ml fresh media. Cells were then counted by haemocytometer to about 1 x $10^6$ cell/ ml ( 0.5-2.5 ml depending on the cell number of the cell suspension) and seeded into new T175 $cm^2$ tissue culture flasks (431080,Corning) which contained 30 mL of fresh media. This procedure was repeated twice a week.

### 2.1.5.1 Human embryonic cells (HEK 293T) cell line culture

Adherent HEK 293T cell line was established from human embryonic kidney (Graham *et al.*, 1977), cells were maintained at 37 °C in a humidified atmosphere at 5% $CO_2$ in DMEM (Dulbecco's modified Eagle's medium, D6429 Sigma) supplemented with 1% L-glutamine

(350 µg/ml) (G7513, Sigma), penicillin (100 U/ml)/ streptomycin (100 µg/ ml) (P0781, Sigma), and 10% heat-inactivated foetal bovine serum (FBS) (F6178 Sigma).

### 2.1.5.2 Mouse embryonic fibroblast cells lines (NIH 3T3)

NIH 3T3 mouse embryonic fibroblast cells (originally derived from Swiss albino mouse embryo tissue) (ATCC® CRL1658™) were maintained in DMEM media (Dulbecco's Modified Eagle's Medium-high glucose, D6429, Sigma) supplemented with 10% FBS, 100 µg/ml of penicillin/ streptomycin (100 µg/ ml) (P0781, Sigma), and 350 µg/ml of glutamine. The cells were grown and maintained as described in section (2.1.5).

### 2.1.5.3 Large granulocyte lymphocyte (LGL)

The large granulocyte lymphocyte cell line known as (BJ1035) contains OvHV-2 and was propagated from infected cattle *in vitro,* this line was kindly provided for this study by (George Russell, Moredun institute). The LGL cell line was maintained in Iscove's Modified Dulbecco's Medium (IMDM) (13390, Sigma) supplement with 10 % foetal calf serum (F6178, Sigma), penicillin (100 U/ml) / streptomycin (100 µg/ ml), and 350 IU/ ml of IL-2 (Chiron), the LGL cell was incubated at 37 °C and 5 % CO2 as recommended by (Schock *et al.*, 1998).

### 2.1.5.4 Preparation of cell Lines for long term storage

For long term storage, cells which were 70-80% confluent were detached from the flask, as described in section (2.1.5), at a concentration of 2-10 x $10^6$ cells per ml were transfered to 15 ml tubes and pelleted by centrifuge at 1300 rpm for 5 minutes. The supernatant was discarded and the pellet were incubated on ice for 10-30 minutes. Meanwhile, freezing medium was prepared by mixing 1.5 ml of dimethylsulphoxide

(DMSO) (D8418 Sigma-Aldrich), 4ml of FBS and 4.5 ml of required media and incubated on ice for 10 minutes. One- three ml of the freezing medium was then added to the cell pellet, 1 ml of suspension was aliquoted in a cryovial and slowly frozen overnight at -80°C. The vials were then transferred to liquid nitrogen for long term storage.

### 2.1.5.5 Growing cell lines from frozen stock

Frozen cells were removed from liquid nitrogen and immediately thawed at 37 °C. The thawed sample was transferred to 15 ml tubes, pre-warmed media was added gradually to the thawed cells to prevent disruption of the cell membrane. Then complete medium add to 10 ml. Cells were pelleted at 1300 rpm for 5 min, re-suspended in 10 ml of the pre-warmed complete medium and added to a T25 cm2 flask. Cells were then placed in an incubator at 37°C with 5% CO2 in air.

## 2.1.6 *In vitro* transfection of pMSCV-IRES, pSRG and pEQpAM3 in HEK 293T cells

### 2.1.6.1 Calcium phosphate Transfection

Transfection is a powerful scientific technique widely used in the study of the action of genes, gene products, gene expression and protein functions in cells. The transfection technique was developed to deliver foreign nucleic acids into certain cellular regions of cells to produce genetically modified cells (Recillas-Targa, 2006). The classical calcium phosphate transfection method was developed by Graham and van der Eb from 1973 (Graham and van der Eb, 1973). It has become one of the major methods for DNA transfer into mammalian cells.

For transfections, HEK 293T cells were plated the night prior to transfection in sterile 6-well tissue culture plates (Corning® Costar® TC-Treated Multiple Well Plates, CLS3516,

Sigma) at 2 x$10^5$/well with DMEM containing 10% FBS and incubated overnight at 37°C with 5% $CO_2$ in air to give 80 to 90% confluence next day. Cells were counted for seeding by viable cell number per ml using a haemocytometer by mixing Trypan blue (Trypan Blue solution 0.4%, liquid, Sigma, T8154) with the cultured cell suspension in a 1:1 v/v ratio then added to the haemocytometer chambers. Basically, the number of cells was multiplied by total cell suspension volume (10 ml) to estimate total viable cell numbers. All transfections were done with freshly prepared 2 M $CaCl_2$ (Calcium chloride dehydrate, C7902, Sigma) with the desired amount of plasmid DNA (2-30 µg).

Firstly, the pMSCV-IRES-GFP plasmid was transfected in HEK 293T cells as it is tagged with GFP and can express the green fluorescent protein. The transfection mixes were prepared by mixing an equal volume of 2xHEPES solution (274 mM NaCl (S7653, Sigma), 1.5 mM Na2HPO4 (71643, Sigma), 50 mM HEPES (54457, Sigma), 4·7 H2O, pH 7.0) and DNA/CaCl2 precipitation, the volumes are shown in Table (2-6), the two solutions (tube A and tube B) were mixed dropwise to give a final volume 344 µl (172 µl/ well), and added to the cell culture medium after the time frame indicate below. For each transfection experiment, one well was transfected with pEGFP-C1 as a control which expressing the green fluorescent protein (GFP) alone to allow comparison of transfection efficiency with the pMSCV-IRES-GFP plasmid.

| DNA | Tube A | Tube B | | | |
|---|---|---|---|---|---|
| | 2XHEPES | 2M $CaCl_2$ | DNA | nuclease-free Water | Total Volume of tube B |
| **pEGFP-C1** | 172 | 21 | 2 (1.6 µg/ml) | 149 | 172 |
| **pMSCV-IRES-GFP** | 172 | 21 | 6 (1 µg/ml) | 145 | 172 |

**Table 2- 6. Volumes of DNA plasmids, 2XHEPES, $CaCl_2$ and nuclease-free water for the transfection assay**

To make the transfection solutions, 2 sterile Eppendorf tubes each containing 172 µl 2XHEPES (Tube A) were prepared, a further 2 sterile Eppendorf tubes were then prepared (Tube B) containing the nuclease-free water which was added first, and then 21 µl of 2M CaCl2, finally 6 µg of DNA was added. The contents of tube B were added to the 2XHEPES in tube A dropwise and incubated for 30 minutes at room temperature to allow the DNA complexes to form. 172 µl media from each well in the plates was discarded and then 172 µl from the mixture was added drop by drop to each of two wells, cells were incubated for 24 hr in a humidified incubator at 37°C and then processed for subsequent assays.

Secondly, and after confirmed the green fluorescent expression of pMSCV-IRES-GFP, transfection was performed for the three plasmids (pEQPMA3, pSRG and pMSCV-IRES-GFP) together in order to produce the recombinant retrovirus in same procedure above with different DNA concentrations, Table (2-7).

| | Tube A | Tube B | | | |
|---|---|---|---|---|---|
| **DNA** | **2XHEPES** | **2M $CaCl_2$** | **DNA** | **nuclease-free Water** | **Total Volume of tube B** |
| **pEGFP-C1** | 172 | 21 | 2 (1.6 µg/ml) | 149 | 172 |
| **pMSCV-IRES-GFP, pSRG and pEQpAM3** | 172 | 21 | 3.42,5.42,5.7 (1, 1.71 and 1.83 µg/ml) | 136.46 | 172 |

**Table 2- 7. Volumes of DNA plasmids pEQPAM3, pSRG and pMSCV-IRES-GFP, 2XHEPES, $CaCl_2$ and nuclease-free water for the transfection assay**

### 2.1.6.2 *In vitro* transfection of three plasmids using Polyethlenimine PEI

PEI reagent was used in order to increase the efficiency of transfection in consider the insufficiency using calcium phosphate. To express the plasmids in HEK 293T cells, the plasmids were transfected in to the seeded cells using Polyethlenimine PEI reagent[1] (Polysciences, Germany, cat no 23966) according to manufacturer's instructions. The transfection was prepared by diluting Polyethlenimine PEI reagent (4 µl) in 46 µl of OptiMEM medium per well (Opti-MEM™ Reduced Serum Medium, 31985070, Thermofisher). An appropriate amount of each vector (pMSCV-IRES-GFP, pSRG, pEQpAM3) (0.35, 0.52, 0.58 µg/ well of each vector sequentially) was added to the diluted PEI reagent, Table (2-8) and then mixed by pipetting up and down 4-6 times, then the components were centrifuged for 2 seconds. This was followed by incubation for 30 minutes at room temperature. The old media was discarded from each well and 1 ml of OptiMEM medium was added taking care not to disturb the cells, then 120 µl of PEI and DNA mixture was

[1] 0.1g Polyethlenimine dissolve in 150mM NaCl, Once all PEI has dissolved, pH adjust to 7.0 with 6M HCL then filter with 0.2 filter

added drop by drop spread over the plates(because we used 2 plats so we mix 56 µl of PE and 644 µl of OptiMEM, 14 wells). Then the plates were incubated for 6 hr at 37 °C with 5% $CO_2$ in air. Subsequently, the medium was replaced with 2.5 ml fresh MDEM medium supplemented with 10% FBS, glutamine (350 µg/ml) and penicillin (100 µg/ml). The plates were then incubated at 37°C, 5% CO2 in air for 72 hr.

The transfected cells were prepared on ice by collecting the supernatants 72 hr post transfection in new sterile Eppendorfs and centrifuged at 150 xg for 10 minutes to pellet and collect any cell debris. Replace supernatant carefully using a pipette into a new Eppendorfs, discarding the pellet (Virus is stable at 4 °C no longer then 3-4 weeks).

| **Volume per well (µl)** | | | | | **Total** | **OptiMEM** | **Final** |
|---|---|---|---|---|---|---|---|
| **1** | **GFP** | 0.56 (1.6 µg/ml) | | | | 1 | GFP |
| **2** | **pMSCV-IRES-GFP,pEQpAM3 and pSRG** | 0.35 (1µg/ml) | 0.58 (1.83µg/ml) | 0.52 (1.71µg/ml) | 1.45 | 48.00 | 59.45 |
| **Volume per 2 plates (x5) (µl)** | | | | | **Total** | **OptiMEM** | **Final** |
| **1** | **GFP** | 0.56 (1.6 µg/ml) | / | / | 0.56 | 48.00 | 48.56 |
| **2** | **pMSCV-IRES-GFP, pEQpAM3 and pSRG** | 1.75 (1µg/ml) | 2.9 (1.83µg/ml) | 2.60 (1.71µg/ml) | 7.25 | 48.00 | 55.26 |

**Table 2- 8. The volumes of pSMCV-pEQpAM 3-pSRG plasmids and GFP**

## 2.1.7 Determination of Viral Titres

### 2.1.7.1 Cell culture maintenance

NIH 3T3 fibroblast cells were maintained in DMEM media and seeded into 6 well plates as $1.2x10^6$/plate, cells were 60-70% confluent or less the next day, as described in section (2.1.5.2).

### 2.1.7.2 Virus titre determination

Virus titre was determined as the average number of fluorescence-activated cell (the infected cells will appear green fluorescent under the fluorescent microscope) take in consider the plate size, and dilution of the infectious stock. Initially, the virus stocks were filtered through a 0.45 m filter, then diluted (on ice) with different volumes; 1 ml, 200 µl, 100 µl, 40 µl and 20 µl crude supernatant made up to 1 ml with fresh DMEM media (without serum), (Figure 2-1). These virus dilutions from transfected HEK293T cells were used to infect NIH 3T3 cells by replacing the old media with 1 ml virus dilution and incubated for 1-3 hr at 37°C with 5% $CO_2$ in air, the plate was agitatied every 10-15 minutes or so, then a further 4 ml DMEM media plus 10 % serum was added, then the plates were incubated for 5 days at 37°C with 5% $CO_2$ in air. Cells were visualized under an inverted fluorescence microscope for a green signal of transduction over the course of 5 days.

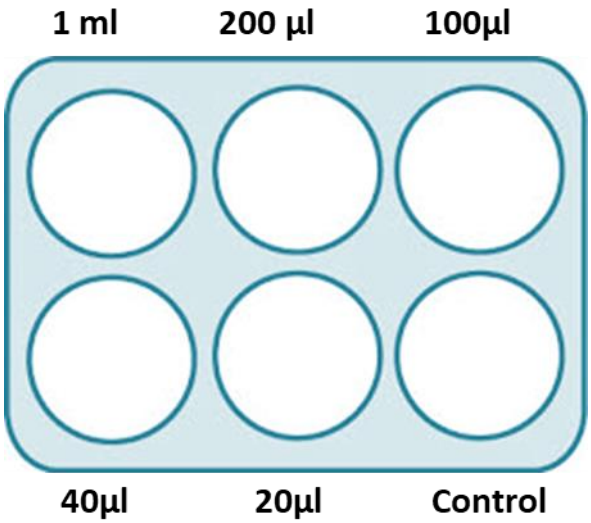


**Figure 2- 1. Dilutions of virus used in measurement the viral titre**

### 2.1.8 Isolation mononuclear cells from healthy cattle blood (MINCs)

Blood contains different types of cells such as red blood cells (RBC) and white blood cells (WBC). Peripheral blood mononuclear cells (PBMCs), comprising lymphocytes (B-cells, T-cells, and NK-cells), monocytes, and dendritic cells, are frequently used for the evaluation of immune responses (Grievink *et al.*, 2016).

Isolation of MINCs from peripheral blood was performed using bovine blood which was acquired from healthy cattle from the abattoir in Liverpool city. The mononuclear cells were separated from peripheral blood leukocyte (PEL) using Lymphoprep™ density gradient medium (07801, STEMCELL Technologies) according to the manufacturer's instructions. Fifteen ml of Lymphoprep density medium was add to the SepMate™-50 (IVD) (85450, STEMCELL Technologies) by pipetting it through the central hole of the tube insert, then the blood samples were diluted with an equal volume of PBS with 2%FBS which will help to dispose the red blood cells later. The diluted blood then was pipetted slowly down to the side of the tube. The SepMate tubes were centrifuged at 1300 xg for 10 minutes at

room temperature, then the top layer which contains the enriched MINCs was poured into a new sterile tube. Ten ml of sterile water was add immediately to cells to remove the RBC, and centrifuged at 300 xg for 8 minutes at room temperature. Cells were washed twice with PBS with 2%FBS and then centrifuged at 300 xg for 8 minutes at room temperature. The pellet was resuspended with 10 ml of RPMI 1640 (Roswell Park Memorial Institute, R8758, Sigma) supplement with 10% FBS and 100 U/ml of penicillin. Then, 500 µl of Concanavalin A Jack bean (Con A to final concentration 500 µl) (C5275/ Sigma) was add to stimulate the cell growth. Cells were seeded into 24 well plates (3524, Costar) and incubated at 37°C.

## 2.2 oLANA cloning into pMSCV-IRES-GFP vector

Cloning is a molecular biology technique producing genetically identical individuals of an organism either naturally or artificially. On the other hand, in biological research the clone (molecular cloning) is generated by using recombinant DNA molecules which are inserted into a cloning vector, then incorporated into cultured host cells through a set of experimental methods (Lodish and Matsudaira, 2000). Many of The common cloning vectors that are used in molecular biology contain a green fluorescence protein (GFP) gene which is extremely useful as a reporter in eukaryotic cells studies since it was discovered in the jellyfish Aequorea victoria in the 1990s (Dai *et al.*, 2007). GFP-oLANA template which was synthesised by Invitrogen (Amp 2016AB3JIP, Kozak-eGFP-oLANA del, 2053282, Invitrogen), was amplified using PCR, then inserted into pMSCV-IRES-GFP vector (Plasmid 20672, Addgene) (Figure 2-3) using EcoRI and NotI enzymes and then cloned to produce a new construct oLANA DNA (Figure 2-2). We clone full-length oLANA protein which is encodes open reading frame 73 of OvHV-2 viruses by cloning approach and generated an

oLANA protein deletion mutant which lacked the internal domain. To date, only a small number of protein interactions have been reported for OvHV-2. To further confirm the quality of our construct results and generate a set of high-confidence interactions, we tested all positive DNA interactions in parallel by western immunoblotting and immunoprecipitation assays (IP) (Figure 2-2). About 50% of the protein interactions could be confirmed by IP, however, those which could not confirmed have previously been identified in studies focusing on other herpesviruses. However, some of the interactions not confirmed by IP may be nonphysiological and, for example, caused by auto activation (false positive results). We indicated that protein interactions occurred predominantly between proteins expressed at the same time point after infection.

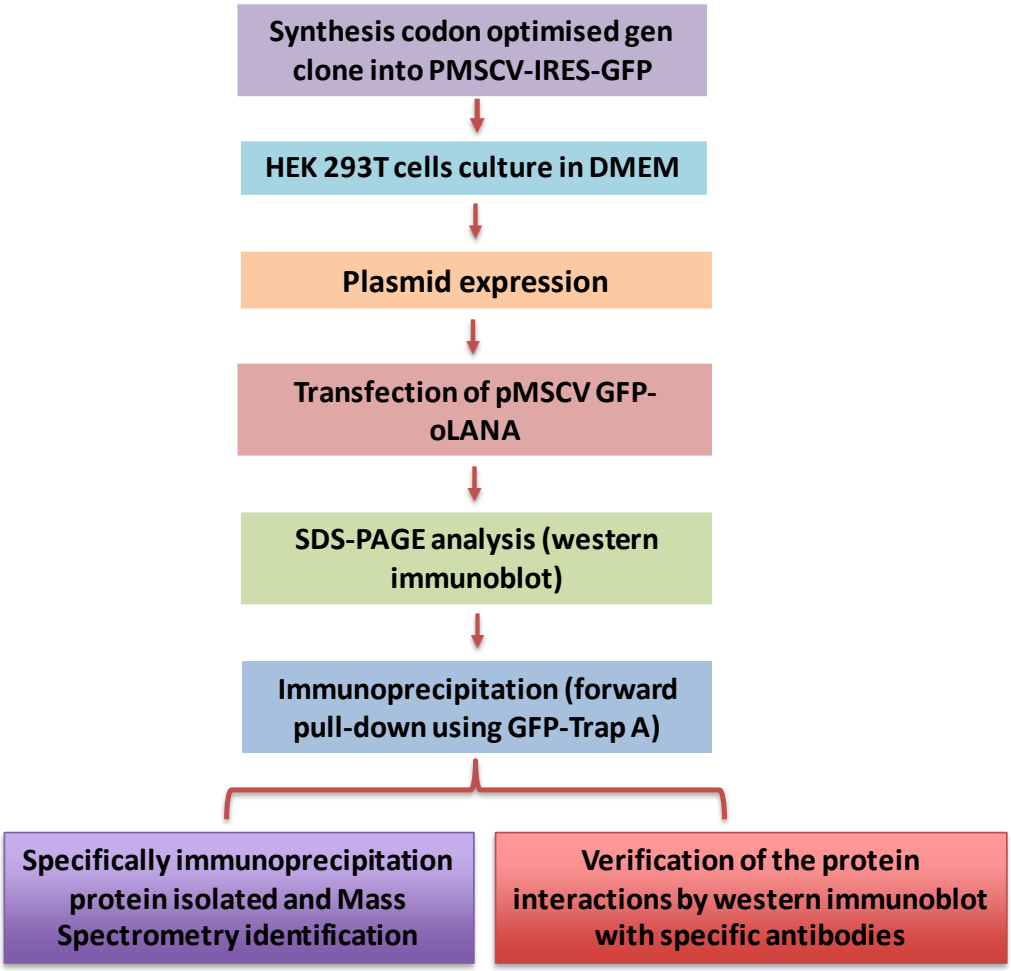


**Figure 2- 2. Schematic representation of oLANA construct generation**
HEK 293T cells stably expressing LANA Δ140–419 were obtained from OvHV-2 herpesvirus virus. OLANA-FL: oLANA-Full length, NTD: N-terminal domain. Constructs were utilised for immunoprecipitation and MS analysis.

## 2.2.1 Conventional Polymerase Chain Reaction (PCR).

PCR is one of the revolutionary molecular biology method developed by (Mullis, 1990) which is used to make many copies (millions or billions) of a particular region of DNA. PCR is one an important, basic and valuable methods used in molecular biology field for DNA analysis, not only because the ability to run quickly with highly specific and sensitive

quantitative production, but also to reduce the potential of cross-contamination (Burggraf and Olgemoller, 2004).

Conventional PCR was employed to confirm the successful oLANA construct. PCR reactions were performed in a 20 µl volume in a thin-walled 200 µl PCR tube (PCR Tubes with Individual Attached Caps, Star Lab) following the manufacturer's instructions for KODX kit (71087-3, Merck, Novagen). The reaction mix was prepared in a clean hood (Captair® Biohood, Erlab) treated by UV exposure for 20 min prior and after use. The reaction mix consisted of 2 µl of 10x KODX1 buffer (50 mM KCl, 50 mM Tris-HCl pH 8.0, 1 mM DTT, 0.1 mM EDTA, 50% glycerol, 0.1% Nonidet P–40, 0.1% Tween® 20,); Merck (Novagen), 71087-3), 0.62 µl of PCR Grade Water (Nuclease-Free Water, AM9937, Thermofisher (Ambion)), 2 µl of 2 mM dNTPs (71154, Novagen), 0.8 µl of each primer (working concentration 10 pmol/µl) (Eurofins Genomic), primer sequences are shown in Table (2-9), 0.4 µl of KOD XL polymerase (2.5 U/µL) ( Novagen, 71157) to which was added 100 ng/ml of template DNA (Invitrogen) predicted to encode a protein of 495 amino acids, Table (2-10), The appropriate annealing temperature (52.9°C) was determined and confirmed using a BIO-RAD T100™ Thermal Cycler machine through using 8 samples from the same template with different temperatures to optimize the appropriate temperature. The PCR thermal cycle programme was composed of an initial denaturation step consisting of a 30 second incubation at 94 °C, an additional incubation for 5 seconds at 52.9 °C and extension step of 74 °C for 60 second, then these amplification cycles were repeated for 30 cycles, followed by a final extension at 74 °C for 10 min.

| Oligonucleotide | Sequence (5'→3') | Volume for 100pmol/µl |
|---|---|---|
| **Forward primer** | **5' ATGAATTCCGCCGCCACCATGGTGAGCAAGGGCGAG 3'** | **234** |
| **Reverse primer** | **5' TAGCGGCCGCCTATTGTTGGTTAAAAGGTAAAGATG 3'** | **322** |

**Table 2- 9. Primer sequences and p moles used in PCR assay to add restriction enzymes sites to synthetic gene.**

Restriction sites are underlined EcoRI in forward primer sequence and NotI in reverse primer sequence. These primer used in conventional PCR assay to produce construct DNA

| Reagents | Volume per reaction (µl) |
|---|---|
| 10X Buffer KODX1 | 2 |
| nuclease -free water | 0.62 |
| (0.5 mM) dNTPs | 2 |
| Primer F | 0.8 |
| Primer R | 0.8 |
| KOD polymerase | 0.4 |
| DNA | 13.37 |
| Total | 20 |

**Table 2- 10. Reagents, primers and DNA used in PCR Assay**

## 2.2.2 Agarose gel electrophoresis

Agarose gel electrophoresis is a process used to identify and separate the DNA based on size/ molecular weight and rate of movement through the gel under the electric field. A 1% w/v agarose gel was made by mixing 1 g of agarose (Agarose Molecular grade, BIO-

41025, Bioline) with 100 ml of 1x TAE buffer (40 mM Tris-base, 20 mM glacial acetic acid, 1 mM EDTA pH 8.0). The mixture was heated in a microwave oven until all agarose had melted, then the solution was left to cool (to approximately 65 °C). Followed by adding 10 µl of fluorescent nucleic acid SYBR Safe gel stain (S 33102, Invitrogen) and gently mixed into the agarose. Then, gel was poured slowly into a gel tray, the comb was set at one side of the gel, and any bubbles in the solution were removed. The gel was allowed to set 20 - 30 minutes to solidify, then the comb was removed and the gel placed into a gel tank (BioRad) filled with 1X TAE running buffer. PCR reactions were mixed 3:1 with loading dye (0.4% orange G, 0.03% bromophenol blue, 0.03% xylene cyanol FF, 15% Ficoll® 400, 10mM Tris-HCl (pH 7.5) and 50mM EDTA (pH 8.0) Blue/Orange 6x loading Dye, Promega) in order to visualize the DNA samples. Then 10-20 µl of amplified products were electrophoresed through 1 % w/v agarose gels and run at 100 V for the appropriate time. Gels were then documented under ultraviolet (UV) light (Ultraviolet Transilluminator, BioRad), images taken and target DNA bands sizes compared with 1 kb (CSL-MDNA-1KB DNA ladder, 1x500ul vial, Cleaver) or 100 bp DNA ladders (green cleaver CSL- MDNA 100BP, lot 15D10).

### 2.2.3 Extraction of DNA from agarose gels

Initially, and after confirming the expected DNA fragments size, each gene sample visualized from agarose gel under UV light was excised from the gel using a clean sharp scalpel (Disposable Scalpels – Sterile, Swann Morton, 0501), and placed in a clean 1.5 ml Eppendorf tube; then purified using The PureLink™ Quick Gel Extraction Kit (Quick Gel Extraction Kit, K210012, Invitrogen) according to the manufacturer's instructions. The DNA fragments of interest were dissolved in 500 µl Buffer L3 and then incubated for 10 minutes in a 50°C heat block which was preheated to 50°C before starting. The tube was inverted

every 3 minutes to mix and dissolve the gel and then incubated for a further 5 minutes. One gel volume of isopropanol was added to the dissolved gel slice and mixed well. This was followed by transfer of the DNA onto a Quick Gel Extraction Column which was placed inside a wash tube, and the column was centrifuged at >12,000 × g for 1 minute to allow the DNA to bind to the column. Then the DNA was washed with 500 µl wash buffer (W1) which contained ethanol and the flow-through was discarded. The column was centrifuged at >12,000 × g for 1 minute. Further centrifugation of the column for an extra 2 minutes was done to completely remove the wash buffer and the flow through was discarded. The column then was placed in a new 1.5 ml Eppendorf tube and 25-50 µl elution buffer (E5) was added and left for 1 minute at room temperature to elute the DNA. The column was centrifuged at >12,000 × g for 1 minute to get the elution which contains the purified DNA and stored at 4°C for immediate use or at −20°C for long-term storage.

### 2.2.4 Restriction digest reaction of the DNA

The PCR product containing the pMSCV-GFP-oLANA DNA sequence was cloned into the effector plasmid pMSCV-IRES-GFP vector, (Figure 2-3) (Plasmid 20672, Addgene), which was used for expression studies. The vector and purified PCR product were both cleaved using two restriction enzymes NotI which used to cut the 5'..GCˇGGCCGC..3' sequence site (R0189s, 10U/ml, Biolabs) and *Eco*RI which was used to cut the 5'..GˇAATTC..3' sequence site (R0101s, 20,000U/ml, Biolabs); in 1x reaction buffer 3.1 (NEB buffer 10x concentrate, B7203s, 1.25 ml, Biolab), Table (2-11), by incubation for 2 hr at 37°C, reactions contained 10U and 20 units of NoTI and *Eco*RI enzyme sequentially in a total volume of 20 µl. This released the IRES-GFP fragment from the pMSCV-IRES-GFP vector. Then the vector only was processed with calf intestinal alkaline phosphatase (CIAP) (18009-027, Invitrogen) to

remove the terminal 5'-phosphate groups from the plasmid backbone and the IRES-GFP fragment, reactions were in a total volume of 20 µl and contained 1µl of CIAP and 2 µl of 10X dephosphorylation buffer (Y 01371, Invitrogen), this procedure suppresses re-ligation of vector molecules with the IRES-GFP fragment in the ligation reaction. This step will favour the intact 5'-terminal phosphate residues of our PCR product ligating into the dephosphorylated plasmid vector by reducing the efficiency of the relegation of the IRES-GFP reaction.

| Buffers | pMSCV-IRES-GFP Vector | pMSCV-GFP-oLANA |
|---|---|---|
| nuclease -free water | 11 µl | - |
| Buffer3.1 | 2 µl | 2 µl |
| DNA | 5 µl | 16 µl |
| NoTI Enzyme (10000U/ml) | 1 µl | 1 µl |
| *Eco*RI Enzyme (20,000U/ml) | 1 µl | 1 µl |

**Table 2- 11. Restriction enzymes and buffers used in restriction digests of pMSCV-GFP-oLANA PCR product and the plasmid vector**

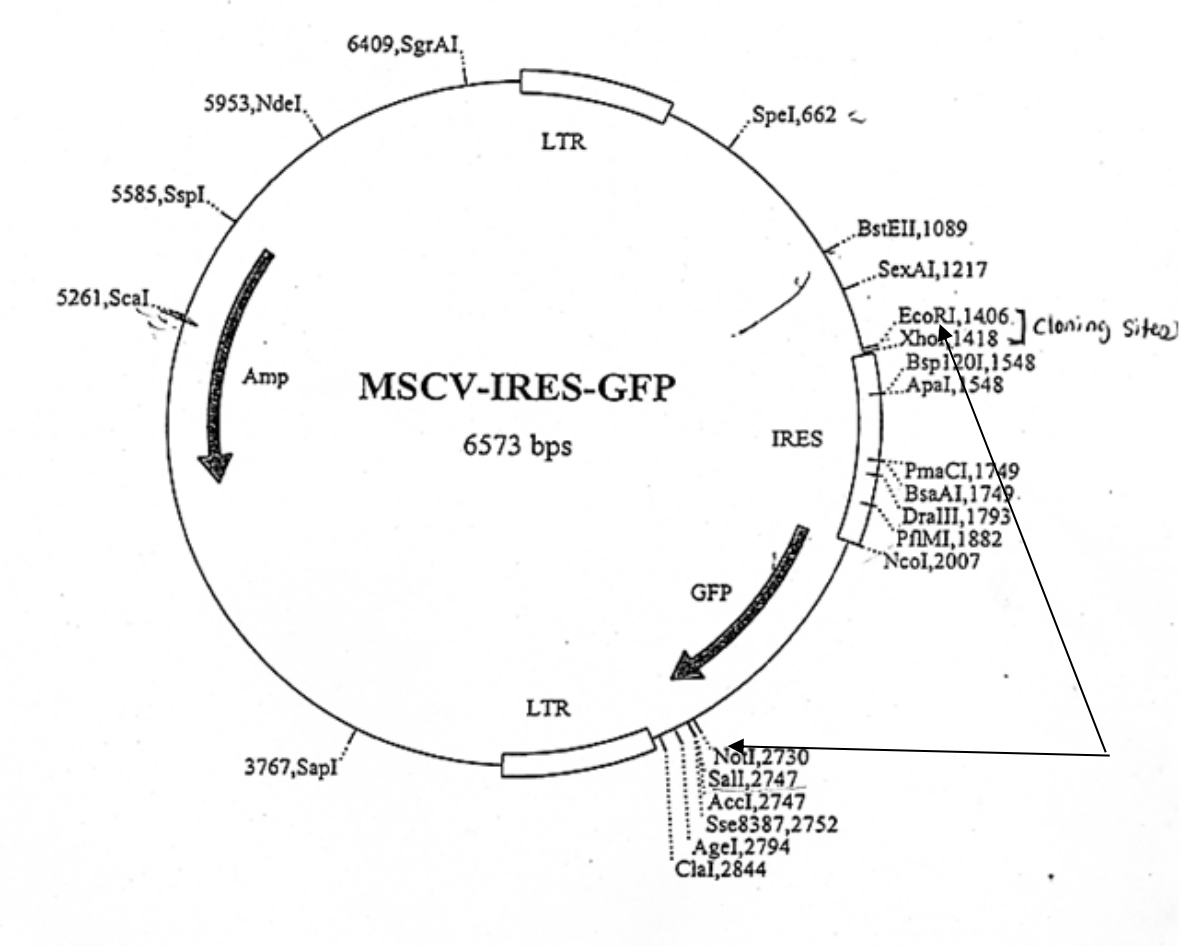


**Figure 2- 3. MSCV-IRES-GFP map indicating the EcoRI and NotI restriction sites**
Other restriction sites are shown alongside the location of restriction. Long terminal repeat (LTR) regions are shown, as in the ampicillin (Amp) and green fluorescent protein (GFP) genes. The internal ribosome entry site (IRES) is shown downstream of the GFP gene. Direction of translation is represented via arrows.

## 2.2.5 PCR product purification

The PCR product was purified (to remove the unwanted fragment ends after restriction enzyme digestion) using (QlAquick PCR purification kit, 28104, Qiagen). Initially, 5 volumes of Buffer PB were added to 1 volume of the PCR sample and mixed thoroughly. The DNA was transferred to the QIAquick column which placed in 1.5 ml microcentrifuge tube to bind to the column membrane and centrifuged for 30–60 seconds, the column was

washed with 750 µl of Buffer PE and centrifuged for 30–60 seconds and the flow-through was discarded. The QIAquick column was centrifuged once more for 1 minute after discarding the flow-through to remove residual wash buffer. The DNA was eluted by adding 20-50 µl of EB Buffer (10 mM Tris-Cl, pH 8.5) and centrifuged for 1 minute, then the purified DNA was analysed on a 1% agarose gel as in (2.2.2).

## 2.2.6 DNA ligation

Ligation is a method by which a DNA insert is joined to a vector through a covalent bond called a phosphodiester bond. T4 DNA ligase is an enzyme that catalyses the end-to-end joining of the DNA by forming a phosphodiester bond between the 3'hydroxyl and the 5'phosphate ends of nucleic acid molecules (Sambrook *et al.*, 2001).

For ligation step in a microfuge tube to ligation mixture was set up by mixing 1 µl (5 ng) of linearised vector and 4 µl (5-50 ng) of digested PCR product was set up, then 1 µl of T4 DNA ligase (1U/ul) (15224-017, Invitrogen), and 4 µl of 1x T4 buffer (5x T4 ligase buffer 250 mM Tris-HCl (pH 7.6), 50 mM MgCl2, 5 mM ATP, 5 mM DTT, 25% (w/v) polyethylene glycol-8000) (1253689, Invitrogen) were added to a final volume of 10 µl, the Ligation reaction was mixed gently and incubated at 4°C, overnight.

## 2.2.7 Plasmid transformation into chemical competent cells

Transformation is the ability of bacteria to directly uptake, incorporate and express exogenous genetic material from its surrounding. It might occur in nature as a response to environmental conditions such as starvation and cell density, and can also be induced in a laboratory (Johnston *et al.*, 2014).

To transform the pMSCV-GFP-oLANA DNA, clone reaction was prepared by mixing 4 µl of the ligation reaction with 1 µl supplied salt solution (1.2 M NaCl, 0.06 M $MgCl_2$, 1718889, Invitrogen). For transformation, a volume of 2 µl (5-50 ng DNA) of the cloning reaction was mixed gently with 50 µl vial of Chemically Competent *Escherichia coli* (*E.coli*) (Mach1™ One Shot®, C404003, Invitrogen), and incubated on ice for 30 minutes, the bacterial mixture was heat- shocked for 30 seconds at 50 °C in a water bath (Heat water bath, Grant Instruments) which opens the pores of the cell membrane allowing entry of the plasmid. The vial was then transferred back to ice immediately and 250 µl of supplied S.O.C medium (Super Optimal broth with Catabolite repression) ( 15544034, Invitrogen) (2 % tryptone, 0.5 % yeast extract, 10 mM NaCl, 2.5 mM KCl, 10 mM MgCl2, 10 mM MgSO4, and 20 mM glucose) was added into the transformed *E.coli*, then capped tightly and incubated horizontally with rotation for 1 hr at 37 °C in an orbital incubator (Sanyo) at 200 rpm to allow the bacteria to recover from the heat shock and to express the antibiotic resistance gene present on the plasmid DNA. This was followed by streaking the transformed bacteria on pre-warmed LB agar plates supplemented with 0.5 µl/ml ampicillin, as mentioned in section (2.1.2.1), then the plates were incubated inverted, overnight at 37 °C.

## 2.2.8 Plasmid purification (mini preparation)

Purification of the plasmid DNA from transformed bacteria was carried out using a mini preparation using Qiagen plasmid purification kit (QIAprep Spin Miniprep Kit (50), 27104, Qiagen) following the manufacturer's instructions. A single colony was picked from the freshly streaked LB agar plate, and inoculated in 5 ml LB broth (LB Broth Powder microbial growth medium (Lennox), 10 g/L Tryptone, 5 g/L Yeast Extract, 5 g/L NaCl, L3022,

Sigma), supplement with 0.5 µl/ml ampicillin (minipreparation), and incubated 18-24 hr at 37 °C in individual universal tubes in orbital incubator (Sanyo) at 200 rpm to prepare sufficient cells for plasmid mini purification. The overnight saturated growth cultures from an inoculating individual-single colony were harvested by spinning at 6800 x g (› 8000 rpm) for 3 minutes at room temperature using microfuge centrifuge (Backman Coulter). The supernatant was discarded and the bacterial pellet was resuspended in 250 µl resuspension buffer P1, when there were no visible cell clumps, 250 µl lysis buffer P2 was added after transfer to a micro centrifuge tube, the reaction was mixed thoroughly by inverting the tube 4-6 times until the colour turned blue, 350 µl of Buffer N3 (3 M potassium acetate, pH 5.0) was added to neutralized the reaction by mixed thoroughly until the solution became colourless. The lysate was centrifuged at 13,000 rpm (~17,900 x g) for 10 minutes. 800 µl of the supernatant which contained the plasmid DNA was carefully applied into the QIAprep 2.0 spin column and centrifuged for 30-60 s. The flow-through was discarded, 500 µl of PB buffer was added to the column and centrifuged for 30-60 s. at 13,000 rpm (~17,900 x g) and the flow-through was discarded, the column was washed with 750 µl Buffer PE and centrifuged for 30-60 s. and the flow-through was discarded, then the column was placed in a clean 1.5 ml microcentrifuge tube and further centrifuged for 30-60 s at 13,000 rpm to completely remove the residual ethanol. The DNA was eluted from the column 1.5 ml microcentrifuge by apply 50 µl of Buffer EB (10 mM TrisCl, pH 8.5), then incubated for 1 minute at room temperature, followed by centrifuge for 1 minute, the purified plasmid DNA was stored at 4 °C.

### 2.2.9 Restriction digestion mini prep DNA and agarose gel electrophoresis

To confirm the identity the insertion, the mini prep DNA was cut with restriction enzymes NotI and *Eco*RI as described in section (2.2.4.) Table (2-11), then the DNA electrophoresed through 1 % w/v agarose gel as described in section (2.2.2).

### 2.2.10 Measuring the deoxyribonucleic acid (DNA)

To measure the concentration of the DNA plasmid, Qubit® dsDNA BR Assay kit from ThermoFisher (Q32850) was used according to the manufacturer instructions, as mentioned in section (2.1.3).

### 2.2.11 DNA sequencing

The resulting plasmids (10-20 ng) were sequenced at Source Bioscience (Rochdale, UK) to confirm the identity and orientation of the inserts after being confirmed by restriction enzyme digestion by using 3' sequencing primer: pCDH-rev (GCATTCCTTTGGCGAGAG), and 5' sequence primer: pBABE 5' (CTTTATCCAGCCCTCAC) (Weinberg Lab) Psi packaging signal, these primers central M to the vector sequences adjacent to the insert, facilitating sequencing of the entire insert. The derived sequence data were aligned using Basic Local Alignment Search Tool programme (BLAST) via the National Centre for Biotechnology Information website (http://www.ncbi.nlm.nih.gov/) to confirm the sequence of the cloned targets and compared to other available sequences on Genbank (http://blast.ncbi.nlm.nih.gov/Blast.cgi).

### 2.2.12 Plasmid purification (maxi preparation)

For large-scale propagation of the plasmid from transformed bacteria in order to produce a large amount of plasmid DNA suitable for transfection into mammalian cells, the

Endo Free Plasmid Maxi Kit (10) (12362, QIAGEN) was used following the manufacturer's instructions. Single colonies were picked up from a freshly streaked LB agar plate previously confirmed to contain the correct insert by mini preparation analysis as described in section (2.2.8), inoculated into 10 ml LB broth supplemented with 0.5 µl/ ml ampicillin, and incubated overnight at 37 °C with shaking at 200 rpm in an orbital incubator (Sanyo). On the following day and in order to yield enough cells culture for plasmid expression, this starter culture was inoculated into 100 ml LB supplement with 0.5 µl/ml ampicillin in a 1 L conical flask. The flask was placed in an orbital incubator (SANYO) with shaking and incubated overnight using the same parameters mentioned before for culture. Bacterial cells were harvested by centrifugation at 6000 x g for 15 minutes at 4 °C. The resulting bacterial cell pellet was resuspended in 10 ml buffer P1 (50 mM Tris.Cl, 10 mM EDTA, 100 µg/ml RNase A, pH 8.0), 10 ml of buffer P2 (200mM NaOH, 1 w/v SDS) in order to lyses them, and incubated for 5 minutes at RT. next and to neutralise the lysate 10 ml of chilled buffer P3 (3 M potassium acetate, pH 5.5) was added and the solution mixed thoroughly until the solution became completely colourless. Then, the cell lysate was poured into the barrel of the QIAfilter Cartridge (Qiagen) and Incubated at room temperature for 30 minutes. The cleared cell lysate was collected in a clean 50 ml tube by inserting the plunger gently into the QIAfilter Cartridge. 2.5 ml Buffer ER was added to the filtered lysate and mixed, followed by incubation for 30 minutes on ice. The lysate was decanted into a Qiagen tip 500 (Qiagen) which had been pre-equilibrated by washing with 10 ml equilibration buffer QBT (750 mM NaCl, 50 mM MOPS, 15% isopropanol v/v, 0.15% Triton X-100 v/v) that was allowed to drain by gravity flow. The lysate was applied into the QIAGEN-tip and allowed to enter the tip, the tips were then washed with 2 x 30 ml Buffer QC (1.0 M NaCl, 50 mM MOPS, 15% isopropanol v/v, PH 7.0) and left to pass through by gravity flow. The

DNA was then eluted with 15 ml QN buffer (1.6 M NaCl, 50 mM MOPS, 15% isopropanol v/v, PH 7.0). The eluted DNA was precipitated with 10.5 ml isopropanol (2-propanol BioReagent, 19516, Sigma) and pelleted by centrifugation at ≥15,000 x g for 30 minutes at 4 °C. Pellets were further washed with 5 ml 70% molecular grade ethanol (E7023, Sigma), spun at 15000 x g for 10 minutes, air dried for 5-10 minutes and the DNA resuspended in 1 ml of endotoxin-free Buffer TE (10 M Tris, PH 8.0; 1 mM EDTA). Concentration and purity of the DNA was measured (section 2.1.3) and DNA was stored at 4 °C.

### 2.2.13 Preparation of bacterial stocks for long term storage

To store bacterial clones, 750 µl of sub-confluent bacterial culture was mixed with 250 µl of sterile glycerol (60 %) and immediately snap frozen in dry ice and kept at -80 °C as a glycerol stock (Ferrer-Miralles *et al.*, 2015) .

### 2.2.14 *In vitro* calcium phosphate Transfection of pMSCV–GFP-oLANA in HEK 293T cells:

#### 2.2.14.1 HEK 293T cell culture maintenance

HEK 293T cell line was maintained at 37 °C in a humidified atmosphere at 5% $CO_2$ in DMEM as described in section (2.1.5.1)

#### 2.2.14.2 *In vitro* calcium phosphate Transfection

For transfections, HEK 293T cells were seeded the day before transfection, and the transfection was done with freshly prepared 2 M $CaCl_2$ with the desired amount of plasmid DNA, as described in section (2.1.6.1) take in consider the different DNA concentration, as shown in Table (2-12).

| | Tube A | Tube B | | | |
|---|---|---|---|---|---|
| **DNA** | **2XHEPS** | **2M $CaCl_2$** | **DNA** | **nuclease -free Water** | **Total Volume Tube B** |
| **pEGFP-C1** | 172 | 21 | 2 (1.6 µg/ml) | 149 | 172 |
| **pMSCV-IRES-GFP** | 172 | 21 | 6 (1 µg/ml) | 145 | 172 |
| **pMSCV-GFP-oLANA** | 172 | 21 | 6.44 (1.86 µg/ml) | 144.56 | 172 |

**Table 2- 12. Volumes of DNA, 2XHEPES, $CaCl_2$ and nuclease-free water for the transfection assay**

Successful transfection of pEGFP-C1 and pMSCV-GFP-oLANA was confirmed by visualizing the expression of GFP by fluorescent microscope 24 hr after the transfection procedure. Cells were harvested in 500 µl PBS (Dulbecco's Phosphate Buffered Saline, D8662, Sigma), by scraping from the surface of the substrate using a cell scraper (CytoOne® Cell Scrapers, CC7600-0250, Star lab) after removal of the media from the cells, and then pelleted by centrifugation at 2,500 rpm for 5 minutes at 4°C. The supernatant was discarded and the cell pellet was lysed in 50 µl of 2x SDS sample buffer (1M Tris PH 6.8, 1% v/v of 20% SDS (sodium dodecyl sulphate), 20% glycerol, 90 mM 2-mercaptoethanol, 0.05% bromophenol blue) followed by sonication with Ultrasonic Processor for Small Volume Applications (VCX130, Sonic) for 5 seconds, followed by heating for 10 minutes at 95 °C, then quick centrifugation and stored at -20°C for immunoblot analysis.

## 2.2.15 western Immunoblotting (WB)

Western blotting or Sodium- dodecyl sulphate polyacrylamide gel electrophoresis (SDS-PAGE) is an important technique used in cell and molecular biology which was introduced by Towbin *et al.* (1979). Western blotting technique is a technique used for protein analysis because it uses a specific antibody to identify target proteins that have

been separated based on size by gel electrophoresis. The technique uses three elements to accomplish this task: (1) separation by size, (2) transfer to a solid support, and (3) marking target protein using a primary antibody for detection and a secondary antibody to visualize. In general, the primary antibody that recognizes the target protein in a western blot is not directly detectable. Therefore, tagged secondary antibodies are used as the means of ultimately detecting the target antigen (indirect detection).

### 2.2.15.1 Sample preparation

Monolayer cells were harvested by adding 500 µl PBS (Dulbecco's Phosphate Buffered Saline, D8662, Sigma), and scraping the cells from the surface of the substrate using cell scraper (CytoOne® Cell Scrapers, CC7600-0250, Star lab) after discarded the old media from the cells, then transferred into Eppendorf tube and centrifuged at 2,500 rpm for 5 minutes at 4°C. The supernatant was discarded and pellets were resuspended in equal amount of sample loading buffer (2 x) (62.5 mM Tris–HCl pH 6.8, 3 % (w/v) SDS, 5 % β– mercapto-ethanol, 10 % glycerol and 0.01 % bromophenol blue) (about 20-50 µl) for protein extraction. Cell lysate were sonicated with Ultrasonic Processor for Small Volume Applications (VCX130, Sonic) for 5 seconds, followed by heating for 10 minutes at 95 °C to denature the protein, then centrifugation and use directly or stored at -20°C for later immunoblot analysis.

### 2.2.15.2 SDS-Polyacrylamide gel electrophoresis preparation (SDS-PAGE)

The glass plates (90 mm-wide x 83 mm-high x 1 mm-thick) (ATTO, AE6530 mPAGE, Japan) were thoroughly cleaned and then dried and assembled according to the manufacturer's instruction. The resolving gel stocks of 15% and 12% concentration (15 ml/ 2 gels) were prepared freshly with $dH_2O$, see Table (2-13). After pouring the resolving gel

into the plates, it was overlaid by adding 1 ml of $dH_2O$ then permitted to polymerize for 30 min. Then 5% stacking gel (5 ml/ 2 gels) was prepared (0.62 ml of 0.5 M Tris pH 6.8, 0.833 ml of 30 % acrylamide, 25 µl of 20 % SDS, 50 µl of 10 % (w/v) APS, 5 µl TEMD) and added after removing the $H_2O$, to fill the space above the resolving gel; the comb was then inserted immediately without forming air bubbles and left for 30 minutes to polymerise. The comb was removed gently, when the gel was completely polymerized. After removing comb the wells were washed with 1 x running buffer to remove any un-polymerised acrylamide.

| Buffers | 12%Resolving Gel | 15%Resolving Gel | Stacking Gel |
|---|---|---|---|
| Acrylamide/bisacrylamide | 6 ml | 7.5 ml | 833 µl |
| Resolving gel buffer (1.5M Tris pH 8.8) | 5 ml | 5 ml | ------ |
| Stacking gel buffer (0.5M Tris pH 6.8) | | ----- | 820 µL |
| dH2O | 3.9 ml | 2.4 ml | 3.817 ml |
| 20% SDS | 75µl | 75µl | 25 µl |
| 10% APS | 75 µl | 75 µl | 50 Ml |
| TEMED | 25 µl | 25 µl | 5 Ml |

**Table 2- 13. The recipe for 12% and 15% SDS-PAGE gels for western blot assay**

### 2.2.15.3 Western blotting

Equivalent amounts of denatured protein samples (10 µg-20 µg) were loaded onto the gel alongside one well loaded with 8-10 µl of protein marker sample (Spectra™ Multicolour Broad Range Protein Ladder, 26634, thermos scientific, Lithuania) for protein size estimation. Electrophoresis was performed in 1X running buffer (50 mM Tris, 192 mM glycine, 0.1 % (w/v) SDS pH 8.3) using a vertical gel apparatus (ATTO, Japan) at 220 V for 60

min at room temperature (or at 60 Volts (V) for 90 minutes), then at 200 V for 1 hr or until the dye front had migrated to the bottom of the gel to separate the proteins (Kurien, 2012). Wet transfer method was used to transfer the separated proteins onto a polyvinylidene fluoride (PVDF) membrane (IVPH00010, Merck). To assemble the transfer sandwich, double Whatman filter paper and the sponges were saturated in cold transfer buffer (120 mM Tris, 192 mM glycine and 20 % (v/v) methanol), and the membrane soaked in 100 % methanol for 1 min followed by washing in freshly prepared transfer buffer for 1 min at RT. This was followed by assembly of the gel sandwich without trapping air bubbles by placing the gel and membrane between the double filter papers and sponges which were saturated with transfer buffer (any trapped air bubbles were carefully squeezed out by gently rolling a pipette over the top blotting paper). The membrane was always placed between the gel and the positive electrode in a vertical electrophoresis tank that was filled with cold transfer buffer and frozen cool block. The tank was kept cold during the electrophoresis by placing in an ice tray. The electro- blotting was performed at 200V and 350mA for 60:15 min. Then and to identify the transferred protein the membrane was carefully removed after transfer and blocked in blocking buffer (5% (w/v) skimmed milk powder ( Marvel,Uk) in 1x Tris buffered saline-tween 20 (TBS-T) (20 mM Tris-HCl, pH 7.5, 150 mM NaCl and 0.1 % (v/v) Tween 20) overnight at 4 °C with gentle shaking.

Subsequently, the membrane was incubated with required concentration of primary antibody diluted in blocking buffer for 2hr at RT with gentle shaking, Table (2-14), then the membrane was washed three times with 1x Tris buffered saline-tween 20 (TBS-T) (20 mM Tris-HCl, pH 7.5, 150 mM NaCl, 0.1 % (v/v) Tween20) for 10 minutes each with shaking. Bound primary antibody was incubated with an appropriate secondary (HRP) (referred in

the following relevant following sections) diluted appropriately in blocking buffer for 1 hr at RT with gentle agitation. The membranes were further washed 3X with 1x TBS-T for 10 minutes each with shaking at room temperature, and then the membrane was developed for detection the protein band by freshly prepared substrate working solution (chemiluminescence (ECL)) (ECL substrate, 1705060, BioRad) by mixing both substrate components 1:1 (0.1 mL/ cm2) to identify the target proteins and visualised by using ChemiDoc™ touch Imaging Systems (Bio-Rad, 1708370) according to manufacturer's instructions (Kurien and Scofield, 2015).

### 2.2.15.4 Antibodies used in western blot assay.

Western blot assays were performed to analyse pMSCV-GFP-oLANA protein samples and to determine the molecular size of the target protein using a number of primary antibodies with different host origins combined with appropriate secondary antibodies. The primary antibodies were diluted to the appropriate concentration with blocking buffer (5% skimmed milk/ TBS-T) and incubated for 2 hr at room temperature with shaking. The secondary antibodies were diluted in the same buffer but incubated for 1 hr at room temperature with shaking. Following Table (2-14) showed the antibodies with their dilution and host origin.

| Antibody | Dilution | Manufacturer | Host |
|---|---|---|---|
| **Primary Antibody** | | | |
| GFP-SC | 1:500 | Santa Cruz Biotechnology, sc-9996 | Mouse |
| Anti-Rad50 | 1:2000 | Merck, 05-525 | Mouse |
| Anti-p53 | 1:5000 | Sigma, PLA0072 | Rabbit |
| Anti-cGAS | 1:10000 | Merck, ABF124 | Rabbit |
| Anti-SDF2L1 | 1:1000 | ThermoFisher,PA5-71817 | Rabbit |
| Anti-CCDC12 | 1:1000 | Sigma,SAB1412929 | Rabbit |
| Anti-histone | 1:500 | Abcam, 71594 | Mouse |
| **Secondary Antibody** | | | |
| Anti-mouse IgG (whole molecule) Peroxidase | 1:10000 | Sigma, A4416 | Mouse |
| HPR Goat Anti-Rabbit IgG | 1:10000 | Vector Laboratories, PI-1000 | Rabbit |

**Table 2- 14. List of primary and secondary antibodies used for western blot assay.**
**GFP:** green fluorescent protein, **Rad50:** DNA repair protein, **p53:** tumour protein, **CGAS:** Cyclic GMP-AMP synthase, **SDF2L1:** Stromal Cell Derived Factor 2 Like 1, **CCDC12:** Cell division control protein 12, **HPR:** horseradish peroxidase

## 2.2.16 Immunoprecipitation of pMSCV-GFP-oLANA from HEK 293T mammalian cell

### 2.2.16.1 *In vitro* calcium phosphate transfection of pMSCV-GFP- oLANA in HEK 293T cells

For immunoprecipitations, the HEK 293T cell line was seeded into large 25 cm Cell Culture/Petri Dishes (168381, ThermoFisher) at 4.5 x$10^6$/dish and cultured in DMEM media without penicillin, so that cells were more than 70-80% confluent after 24 hr incubation at 37°C with $CO_2$ in air. The cells were transfected by calcium phosphate transfection method

using 2 M $CaCl_2$ reagent (Calcium chloride dehydrate, C7902, SIGMA), mixed with 2XHEPES in a total volume of 2560 µl, Table (2-15) see section (2.1.6.1).

| | Tube A | Tube B | | | |
|---|---|---|---|---|---|
| **DNA** | **2XHEPES** | **CaCl2** | **DNA** | **Nuclease-Free Water** | **Total Volume** |
| **pEGFP-C1** | 1280 | 156.16 | 32 (1.6 µg/ml) | 1091.84 | 1280 |
| **pMSCV-GFP-oLANA** | 1280 | 156.16 | 96.6 (1.86 µg/ml) | 1027.24 | 1280 |
| **pMSCV-GFP-oLANA** | 1280 | 156.16 | 41.4 (1.28 µg/ml) | 1082.44 | 1280 |

**Table 2- 15. The volumes of DNA, 2XHEBES, CaCl2 and dH2O for calcium chloride transfection assay**

The tube B contents were added to tube A dropwise and incubated for 30 minutes at room temperature as described in section (2.1.6.1), 2560 µl media were discarded from each plate and the transfection mixture was added in a dropwise manner (very slowly) and the plates then were incubated overnight at 37°C in $CO_2$ incubator.

### 2.2.16.2 Immunoprecipitation using GFP-Trap A

### 2.2.16.2.1 Immunoprecipitation using lysis buffer without sodium deoxycholate

GFP-Trap A beads (Chromotek) were used for immunoprecipitation of GFP-fusion proteins according to the manufacturer's instructions. The growth media was aspirated and the adherent cells were harvested by adding 1 ml ice-cold PBS (Dulbecco's Phosphate Buffered Saline, D8662, Sigma) to the cells and the cells were scraped from the dishes. The

cells were transferred to a pre-cooled tube (Protein LoBind Tubes, Eppendorf, 022431081) and spun at 500 xg for 3 minutes at 4°C to pellet them, the supernatant was discarded. The cell pellet was washed twice with ice-cold PBS. Cells were lysed by resuspending and pipetting up and down in 200 µl ice-cold lysis buffer (10 mM Tris/Cl pH 7.5; 150 mM NaCl; 0.5 mM EDTA; 0.5% NP-40) which contained proteinase inhibitor cocktail at 1:100 (Halt™ Protease Inhibitor Cocktail (100X), 78429, Thermo Scientific™). The tubes were placed on ice for 30 minutes with extensive pipetting every 10 minutes. The cell lysate was centrifuged at 20,000 x g for 10 minutes at 4°C, the supernatant was transferred to a pre-cooled tube and the pellet was discarded, 300 µl dilution buffer (10 mM Tris/Cl pH 7.5; 150 mM NaCl; 0.5 mM EDTA) containing proteinase inhibitor at 1:100 was added. GFP-Trap®_A beads (Chromotek) were vortexed to ensure they were in suspension and 25 µl beads slurry were pipetted into 500 µl ice-cold dilution buffer, then centrifuged at 2500x g for 2 minutes at 4°C. This wash was repeated twice, the diluted lysate was then added to the equilibrated GFP-Trap®_A beads, and 50 µl of diluted lysate was saved for immunoblot analysis. The lysate and beads mix was incubated overnight at 4°C with end-over-end tumbling. After 24 hr incubation, the lysate and beads mix was resuspended in 500 µl ice-cold dilution buffer (wash buffer). The beads with bound complexes were then centrifuged at 2.500 x g for 2 minutes at 4°C and the pellet was washed twice with 500 µl dilution buffer and the supernatant discarded.

For western blot analysis, the GFP-Trap®_A beads and lysate mixes were resuspended in 100 µl 2x SDS-sample buffer and heated for 10 minutes at 95°C to dissociate immunocomplexes from GFP-Trap®_A beads. The beads were pelleted by centrifugation at

2.500 xg for 2 minutes at 4°C and SDS-PAGE gels were performed with the supernatant, section (2.2.15.2), and the bead pellet discarded.

### 2.2.16.2.2 Immunoprecipitation using lysis buffer with sodium deoxycholate

Basically, the same procedure as that described in the above section (2.2.16.2.1) was repeated for same target protein with similar conditions. The only different step was to use 200 µl ice-cold lysis buffer that contains sodium deoxycholate (10 mM Tris/Cl pH 7.5; 150 mM NaCl; 0.5 mM EDTA; 0.5% NP-40; 0.5 Mm sodium deoxycholate) to better extract the proteins from the nucleus, which also contained proteinase inhibitor cocktail at 1:100.

## 2.2.17 Proteomic analysis

Recently, developments in the field of genome sequencing, transcriptomic and proteomic approaches have been crucial for identifying the interactions of proteins expressed in host cells. The field of proteomics is the large-scale study of proteins, it involves many techniques; including; LC-MS/MS, immunoassays and two-dimensional differential gel electrophoresis (Wilson, 2013). Proteomics involves the study of peptides and proteins within a biological system and it is intended to quantify changes in protein abundance.

More recently, advances in mass spectrometry (MS) have allowed the development of methods which are more sensitive and are not hindered by modifications to or a blocked N-terminus. MS-based proteomics is now the most commonly used technology for identifying proteins in a single spot or gel band slice from a simple experiment and is increasingly being used to identify as many proteins in a single experiment as possible. The

technique is not always completely successful and requires a high level of expertise (Steen and Mann, 2004).

In order to identify proteins, they can be enzymatically cleaved using proteases and the resulting peptides are analysed by MS. Proteins are commonly digested using trypsin which cleaves proteins at the C-terminal side of arginine and lysine residues. Other proteases used include Lys-C and Glu-C which cleave at the C-terminus of lysine and glutamate residues respectively and Asp-N which cleaves at the N-terminus of aspartate residues.

Furthermore, the importance of proteomic analysis is its ability to study post-transcriptional control as well as post-translational modifications (PTMs) of proteins. The challenge with proteomics is to establish effective connections between protein level and nucleic-acid level information about genes and gene networks which is important for understanding the mechanism of pMSCV-GFP-oLANA replication and interaction.

### 2.2.17.1 Sample preparation for proteomic analysis

Samples were prepared by using calcium phosphate transfection process, as described in section (2.2.14), followed by immunoprecipitation with GFP-Trap A beads, as described in section (2.2.16), but instead of using SDS sample buffer to resuspend the bound proteins, the bound proteins from the lysate were eluted from the washed beads by adding 25 µl 0.2 M glycine pH 2.5 to give a final concentration 200 mM glycine pH 2.5 and incubated for 30 s under constant mixing at room temperature, followed by centrifugation to pellet the beads. The supernatant was transferred to a new tube and 2.5 µl 1M Tris base pH 10.4 added for neutralization. The elution step was repeated 3 times to increase elution efficiency.

### 2.2.17.2 Proteomic analysis

Samples were prepared for proteomics by Dr Stuart Armstrong using the following protocol. The eluted samples were diluted two-fold with 25mM ammonium bicarbonate to normalize the protein content between the samples, then the proteins were reduced with 3 mM dithiothreitol (Sigma) at 60 °C for 10 minutes to reduce and blocked cytesines and allows more complete denaturation and allows trypsin to cleave more completely, followed by alkylation with 9 mM iodoacetamide (Sigma) at room temperature for 30 minutes in the dark, 0.2 µg of Proteomic grade trypsin (Sigma) at ratio 50:1 protein: trypsin was added and samples incubated at 37°C overnight. The resulting peptide samples were then acidified by adding trifluoroacetic acid (TFA) to a final concentration of 1% (v/v). The peptides were concentrated and desalted using C18 Stage tips (ThermoFisher Scientific) and then the samples were dried using a centrifugal vacuum concentrator (Eppendorf). Peptides were resuspended in 0.1% (v/v) trifluoroacetic acid and 5% (v/v) acetonitrile.

All peptide mixtures within this thesis were run through the mass spectrometer by Dr Stuart Armstrong. Protein data was generated using the following protocol which was essentially described by (Dong *et al.*, 2017).

Peptide mixtures (2µl) were separated by nanoflow reverse phase HPLC (Ultimate 3000 nano system, Dionex/Thermo Fisher Scientific) coupled to a Q-Exactive mass spectrometer (Thermo Fisher Scientific) that measured both the peptide mass and obtained the peptide sequence. Samples were loaded on a 50cm Easy-Spray column with an internal diameter of 75 µm, then packed with 2 µm $C_{18}$ particles, samples then fused to a silica nano-electrospray emitter (Thermo Fisher Scientific). The analytical column (nanoACQUITY UPLCTM BEH130 C18 15cm x 75µm, 1.7µm capillary column) was operated

at a constant temperature of 35 °C. Chromatography was performed with a buffer system consisting of 0.1 % formic acid (buffer A) and 80 % acetonitrile in 0.1 % formic acid (buffer B). The peptides were separated by a linear gradient of 3.8 – 50 % buffer B over 30 minutes at a flow rate of 300 nl/min. The survey scans were acquired by the Q-Exactive mass spectrometer at a resolution of 70,000. And the analysis was performed in data-dependent mode.

Up to the top 10 most abundant isotope patterns with charge states +2, +3 and/or +4 from the survey scan were selected with an isolation window of 2.0Th and fragmented by higher energy collisional induced dissociation (CID) with normalized collision energies of 30. The maximum ion injection times for the survey scan and the MS/MS scans were 250 and 100ms, respectively, and the ion target value was set to 1E6 for survey scans and 1E4 for the MS/MS scans. Repetitive sequencing of peptides was minimized through the dynamic exclusion of the sequenced peptides for 20 second.

### 2.2.17.3 Label free analysis

Label-free quantitation of proteins was performed using MaxQuant (MQ) software (version 1.6.1.0) with its internal search engine Andromeda as described in (García-Dorival *et al.*, 2014). Precursor mass (the mass of the intact peptide) and fragment mass (the mass of the associated fragments from the peptide) were searched with the mass tolerance of 6 ppm and 0.01 Da respectively. All other settings were defaulted. The search included variable modifications of methionine oxidation and N-terminal acetylation and fixed modification of carbamidomethyl cysteine. Enzyme specificity was set to trypsin, minimal peptide length was set to 7 amino acids and a maximum of two mis-cleavages was allowed. The false discovery rate (FDR) is a statistical measure to ensure the reliability of protein identification in a given dataset. It uses a decoy database (usually a reverse of the database

used) concatenated with the target database to estimate how many identifications will be false by chance alone (a hit to a decoy peptide). It is usually set at 1%for peptide and protein identifications. The Andromeda search engine was configured for a database containing human proteins (UniProt release-2018_03) and oLANA constructs. The MQ software further includes a decoy database as well as common contaminants database to determine the false discovery rate and to exclude false positive hits due to contamination by proteins from different species. For LFQ analysis, "multiplicity" was set to one. Feature matching between raw files was enabled; using a retention time window of 2 min. "Discard unmodified counterpart peptides" was unchecked. Only unmodified and unique peptides were utilized. Averaged LFQ intensity values were used to calculate protein ratios.

### 2.2.17.4 Bioinformatics Analysis

Label-free mass spectrometry results were processed and analyzed using the Perseus software (version 1.6.1.1) which contains several statistical and visualization tools for the analysis of proteomic data (Tyanova *et al.*, 2016); this software was used to perform the statistical analysis and to differentiate background proteins (those cellular proteins that interacted with EGFP alone) from interacting proteins (those cellular proteins that interacted with pMSCV-GFP-oLANA). LFQ intensity values were analyzed using a t-test. A volcano plot graphic and a table were generated showing the statistical significant proteins, those proteins that had a high probability of interacting with pMSCV-GFP-oLANA.

## 2.3 Indirect immunofluorescence assay (IF)

Immunofluorescence (IF) is a common laboratory technique which is used primarily on biological samples, and it is based on the use of specific antibodies which have been

chemically conjugated to fluorescent dye detect antigens in cellular contexts. The technique has a number of different biological applications including evaluation of cells in suspension, cultured cells, tissue, beads and in microarrays (Odell and Cook, 2013) (Figure 2-4).

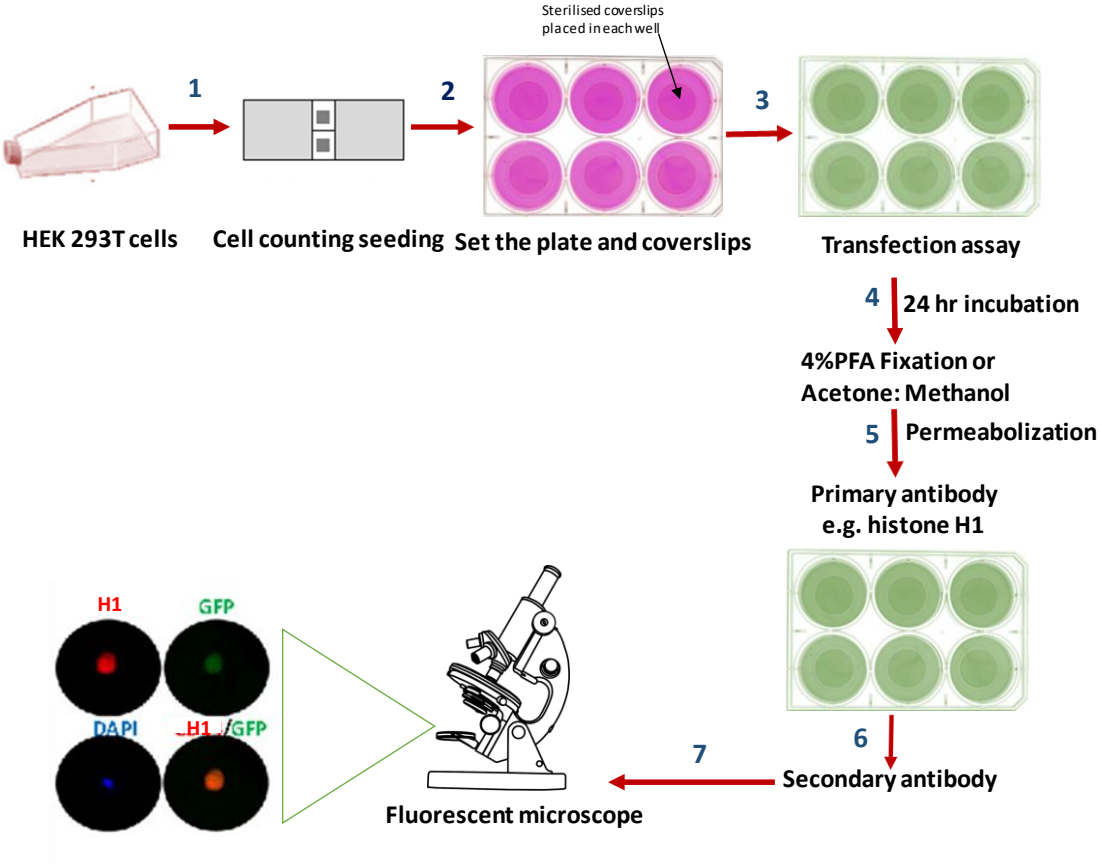


**Figure 2- 4. Flowchart of indirect immunofluorescence**

## 2.3.1 Transfected Cell Fixation, Antibody Staining and Confocal Imaging for HEK 293T cells

To study the localization of expressed proteins utilising the GFP tag, $2\times10^5$ HEK 293T cells were seeded on 13mm glass coverslips (round, No1.5, VWR) inside 6 well tissue culture plates with DMEM 10% FBS and incubated overnight at 37 °C 5% $CO_2$ in air. HEK

293T cells were transfected with 1-10 µg of pMSCV-GFP-oLANA using the calcium phosphate method, as mentioned in section (2.1.6.1), 24 hr post-transfection, cells were washed 3X with 1X PBS after discard the media. Cells were fixed in 500 µl-1 ml of 40:60 methanol/acetone mixture and incubated for 10 minutes at 4-8°C. The cells were washed with 1X PBS three times, followed by permeabilisation by adding 0.5-1 ml of permeabilization buffer (1X PBS, 0.1 % (v/v) Triton x-100) for 10 minutes at RT to induce cell membrane permeability . After 3 rounds of rinsing with washing buffer (1 X PBS-0.5 % tween-20), cells were incubated with primary antibody that had been diluted in blocking buffer (1X PBS, 2% donkey serum (D9663, Sigma), 1% Triton X-100) for 1 hr, see Table (2-16). After three rounds of rinsing of coverslips with washing buffer ( 1X PBS with 0.5% Tween 20) to remove unbounded antibody, cells then were incubated with either Alexa Fluor 594-conjugated goat anti-mouse IgG (115-585-062, Jackson ImmunoResaerch Laboratories, Startech), or Alexa Fluor 594-conjugated goat anti-rabbit (111-585-144, Jackson ImmunoResaerch Laboratories, Startech) conjugated antibodies for 1 hr at RT in dark (The IgG secondary antibodies diluted 1:100/ 1:800 in blocking buffer, according to the manufacturer's recommendations). The cells were washed 3 X in washing buffer. Meanwhile, a drop of either ProLong® Gold Antifade Reagent with DAPI (P36941, Invitrogen) or Vectorshiled (Vector, H-1500) was put on each clean glass slides to stain the cells and to maintain them in good condition, either for a short period or for long-term storage and preservation. The coverslips were then semi-dried and placed upside down onto the drop of mountant on the glass slides, and then left for 24 hr at room temperature in dark to allow hardening followed by imaging under the fluorescent microscope (Carl Zeiss, Axio Imager 2) and analysis by ZEN 2 Pro software.

The immersion oil lens (63X) was used for studying the localization of expressed proteins inside cells. The images were linearized and formatted to automated best fit using blue (DAPI) and green (GFP) imaging filters forming either mono or double colour merge images.

| Antibody | Dilution | Manufacturer | Host |
|---|---|---|---|
| **Primary Antibody** | | | |
| GFP-SC | 1:500 | Santa Cruz Biotechnology, sc-9996 | Mouse |
| Anti-Rad50 | 1:500 | Sigma, 05-525 | Mouse |
| Rabbit anti-p53 | 1:500 | Sigma, PLA0072 | Rabbit |
| Anti-Histone H1 | 1:1000 | Abcam, 71594 | Mouse |
| Anti-CCDC12 | 1:1000 | Sigma,SAB1412929 | Mouse |
| SDF2L1 | 1:1000 | ThermoFisher,PA5-71817 | Rabbit |
| Anti-cGAS | 1:1000 | Merck,AB124 | Rabbit |
| **Secondary Antibody** | | | |
| Goat Anti-Mouse IgG Alexa Fluor 594 | 1:100 | Jackson ImmunoResearch /Startech | Mouse |
| Goat Anti-Rabbit IgG Alexa Fluor 594 | 1:100 | Jackson ImmunoResearch /Startech | Rabbit |

**Table 2- 16. List of primary and secondary antibodies used in the indirect Immunofluorescence assay with HEK 293T cells.**
**GFP:** green fluorescent protein, **Rad50:** DNA repair protein, **p53:** tumour protein, **CGAS:** Cyclic GMP-AMP synthase, **SDF2L1:** Stromal Cell Derived Factor 2 Like 1, **CCDC12:** Cell division control protein 12

All images reported were acquired in the Centre for Cell Imaging within the Institute of Integrative Biology, University of Liverpool. Confocal images were acquired using Zen Black software (Zeiss) on a Zeiss LSM880 upright confocal microscope with laser lines Diode (405), Argon (488), DPSS-5610 (561) and HeNe633 (633) and W-Plan Apochromat 40x/1.0

Dic (water immersion) objective (Zeiss) or Plan-Apochromat 63x/1.0 oil DIC M27 (oil immersion) objective (Zeiss) lenses (Marchisio and Trusolino, 1999).

### 2.3.2. Indirect immunofluorescence assay of LGL cells (Double-labeling antibodies)

The LGL cells were splotch onto a coverslips using CytoSpin 4 centrifuge (A78300003, ThermoFisher). About 100-150 µl of the suspension cells were loaded through the Shandon cytofunnel (5991040, ThermoFisher) after placed with Shandon cytoslide (5991056, ThermoFisher) into Cytoclip Slide Clip (59910052, ThermoFisher).

Initially, the cells were fixed for 15 min with 4 % paraformaldehyde (PFA) PH 7 (16% Formaldehyde, 28906, ThermoFisher) diluted in PBS (D8537 Sigma-Aldrich), then the slides were washed 3X in PBS buffer. The slides were then incubated in permeabilization buffer (1X PBS 0.1 % (v/v) Triton x-100) for 10 minutes at RT to induce cell membrane permeability, followed by 3X washing with washing buffer. Then nonspecific binding sites were blocked in blocking buffer containing (1x PBS, 2 % donkey serum, 1 % Triton X-100). Then, slides were incubated with the mixture of two primary antibodies diluted in blocking buffer (to limit cross-reactivity and non-specific binding with high sensitivity for many targets at the same time give the ability to use conjugated secondary, which are usually offered with a wide selection of fluorophores and other probes ), Table (2-17) for 1h at Rt, the slides were washed 3 X in washing buffer (1 X PBS-0.5 % tween-20) for 30 min to remove unbounded antibody followed by adding the mixture of two Alexa Flour antibodies for 1h in dark at RT . The cells were washed 3 X in washing buffer then one drop of Prolong Gold® anti-fade reagent (P36941, Invitrogen) were applied on each slides and incubated

overnight in dark. The slides were examined under fluorescent microscopy (Carl Zeiss, Axio Imager 2).

All images reported were acquired in the Centre for Cell Imaging within the Institute of Integrative Biology, University of Liverpool. Confocal images were acquired using Zen Black software (Zeiss) on a Zeiss LSM880 upright confocal microscope with laser lines Diode (405), Argon (488), DPSS-5610 (561) and HeNe633 (633) and W-Plan Apochromat 40x/1.0 Dic (water immersion) objective (Zeiss) or Plan-Apochromat 63x/1.0 oil DIC M27 (oil immersion) objective (Zeiss) lenses (Marchisio and Trusolino, 1999).

| Antibody | Dilution | Manufacturer | Host |
|---|---|---|---|
| **Primary Antibody** | | | |
| Anti-oLANA + Anti-Rad50 | 1:500/1:500 | Al-Saadi /Sigma, 05-525 | Rabbit/ Mouse |
| Anti-oLANA + Anti-Histone H1 | 1:500/1:1000 | Al-Saadi / Abcam, 71594 | Rabbit /Mouse |
| Anti-oLANA + Anti-CCDC12 | 1:500/1:1000 | Al-Saadi /Sigma,SAB1412929 | Rabbit /Mouse |
| **Secondary Antibody** | | | |
| Donkey anti-rabbit IGg FITIC Alexa Fluor 488 + Goat Anti-Mouse IGg Alexa Fluor 594 | 1:200/1:100 | Startech Scientific/ Jackson ImmunoResearch | Rabbit/ Mouse |

**Table 2- 17. List of primary and secondary antibodies used in the indirect Immunofluorescence assay with LGLs**

## 2.3.3 Quantification analysis of Confocal Images

The colocalisation can be readily observed using images obtained with confocal microscopes but significantly more important information can be obtained when

estimating colocalisation quantitatively. Colocalisation quantification allows to extend the applicability of qualitative observations (Zinchuk *et al.*, 2005).

All images quantified for characterisation were processed using Imaris x64 v9.0.1 image analysis software (BitPlane), then detection the fluorescent signals from any chosen source channel to quantify nuclear staining by detecting DAPI fluorescence. To identify the total number of localised cells within an image, the spots function was used to quantify nuclear staining by detecting DAPI fluorescence. Using the default settings (minimum diameter: 4.15µm), followed by manually adjusting the detection threshold, it was possible to generate an overlay of "surfaces" that was representative of the cells within the image and quantified the cells using "surfaces" functions in Imaris. Within this surface, it was possible to detect overlapping AF594 fluorescence of oLANA generate a duplicated channel which was allocated the colour yellow. There are some factors impact on the level of resolution and image quality must take in consider; oversaturation, noisy images and human factor such as; parameter settings and colocalisation method.

### 2.3.4 Colocalisation Analysis

Colocalisation analysis of the fluorescent signal in paired images is based commonly on superimposition of images ("merging") and visual inspection (Zinchuk *et al.*, 2007). Colocalisation analysis was performed of three images to show the fluorescence for red and green channels, as well as a third merged image where the channels are combined and overlapping pixels turn yellow. The degree of colocalisation was quantified using ImagePro using the Pearson's correlation coefficient. This quantitative analysis is based on the assessment the colour components of a pair of selected channels. Quantitative colocalisation analysis depend on a number of coefficients to estimate the degree of

colocalisation, which enables to observe the actual areas of colocalisation on the images (BOLTE and CORDELIÈRES, 2006; Dunn *et al.*, 2011).

# Chapter Three: Results

# Section one: Generation of recombinant retrovirus

The aim of this project was to determine interactions between the OvHV-2 oLANA protein and cellular proteins. This will give information on the function of oLANA in terms of virus biology and also identify potential druggable targets for the treatment of MCF. The approach taken to identify oLANA interactions was to express a recombinant oLANA-GFP fusion protein in cells and then identify interacting partners by mass spectroscopy in complexes pulled down using GFP-trap technology (Min *et al.*, 2013). In MCF there is a proliferation of T cells that are infected by OvHV-2. It was therefore surmised that the most relevant cell type to study oLANA interactions was bovine T cells. However, GFP trap experiments require high expression levels in a high proportion of cells. T cells are largely refractory to transfection but can be transduced by retroviruses (Ebert *et al.*, 1997). It was therefore decided to attempt the use of recombinant retroviruses to deliver oLANA-GFP to bovine T cells.

## 3.1. Production of T cell blasts from peripheral blood

Generation of recombinant retrovirus (MSCV) was performed using three plasmids which contain; gag, pol and a variety of env molecules in order to deliver the construct protein in bovine T cells which isolated from cattle. The generation of MSCV was successful but and unfortunately, the infection was not achieved.

Bovine blood treated with EDTA was obtained from healthy cattle from the abattoir in Liverpool. Mononuclear cells were isolated from peripheral blood (PBMCs), the primary source of lymphoid cells for investigation of the human and animal immune system, using Lymphoprep density gradient cell separation medium (07801, STEMCELL Technologies)

according to the manufacturer's instructions, as described in section (2.1.8). Isolated cells were plated into 24 well plates after mixing with Con A for first plant and incubated O/N at 37 °C (Figure 3-1 panel A and B), however few cells were successfully cultured. Therefore after 24 hr incubation, IL-2 ($10^6$ U/µl) was added and the cells incubated for a further 24 hr (Figure 3-1 panel C and D). After this modification PBMCs were successfully cultured. Con A blasts were then generated using ConA and IL-2 to maintain the PBMCs.

ConA blasts were therefore successfully generated from bovine PBMCs as a source of activated bovine T cells *in vitro* that will be transduced with recombinant retroviruses expressing GFP-oLANAΔ.

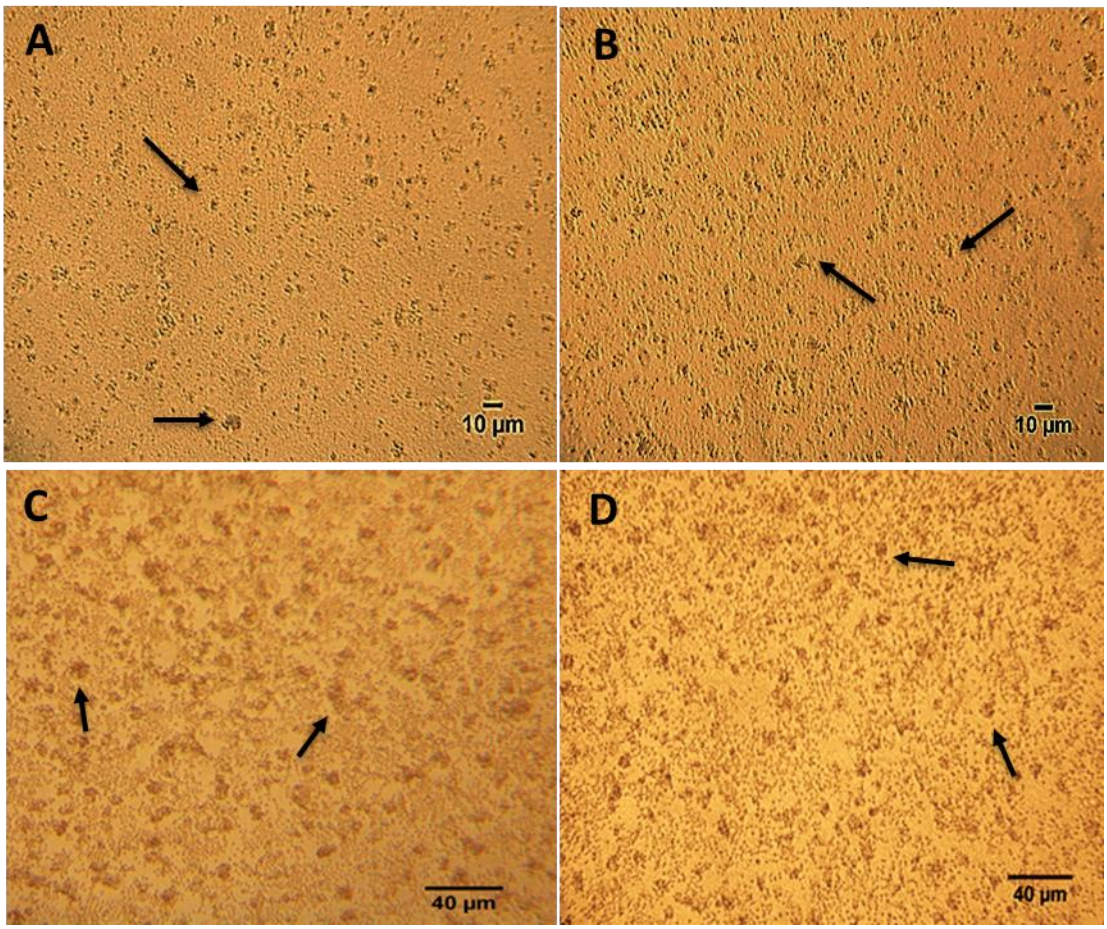


**Figure 3- 1. Isolation of PBMCs from peripheral blood, using Lymphoprep™ as density gradient medium.**
**A** and **B**: The arrows show the Con A blasts of PBMCs 24 h after being plated. The images were taken at 10x magnification. **C** and **D**: The arrows show the Con A blasts of PBMCs cells after adding IL-2. 48 h after plating. The images were taken at 40x magnification

### 3.1.1 Generation of recombinant retrovirus

Generation of recombinant retrovirus is a technological approach that enables gene transfer. Retroviruses can acquired an envelope gene (env) from a distantly related retrovirus or other viruses such as vesicular stomatitis virus (VSV), which is useful since env is the main factor in host range determination. A key aspect in the generation of recombinant retrovirus as tools is the introduction of appropriate DNA vectors in to a cell

line that is able to produce the viral proteins needed for encapsidation of the required recombinant retrovirus. It is also important in gene transfer applications to generate pure stocks of recombinant virus free of replication-competent helper (Coffin *et al.*, 1997). Recombinants are generated by providing gag, pol and env in *trans* either by use of a packaging cell line or by co-transfection of plasmids (Coffin *et al.*, 1997).

### 3.1.2 Development of recombinant retroviruses

It was decided to use a recombinant retrovirus based on the murine stem cell retrovirus (MSCV) (Cherry *et al.*, 2000). This system has been used with great effect to drive high levels of recombinant gene expression in haematopoietic cells (including T cells) in a number of species (Stuhlmann *et al.*, 1984). Three plasmid vectors were used to produce recombinant MSCV. The vector backbone pMSCV–IRES-GFP (which drives expression of recombinant protein from the MSCV LTR) pEQpAM3 (which encodes MSCV gag and pol) and pSRG (which encodes the VSV G envelope protein) (Figure 3-2). The inclusion of the VSV G protein enables recombinant particles to enter multiple cells types from multiple species (xenotropic) (Gallardo *et al.*, 1997). The three plasmids were cultured, as described in section (2.1.2.1 and 2.1.2.2).

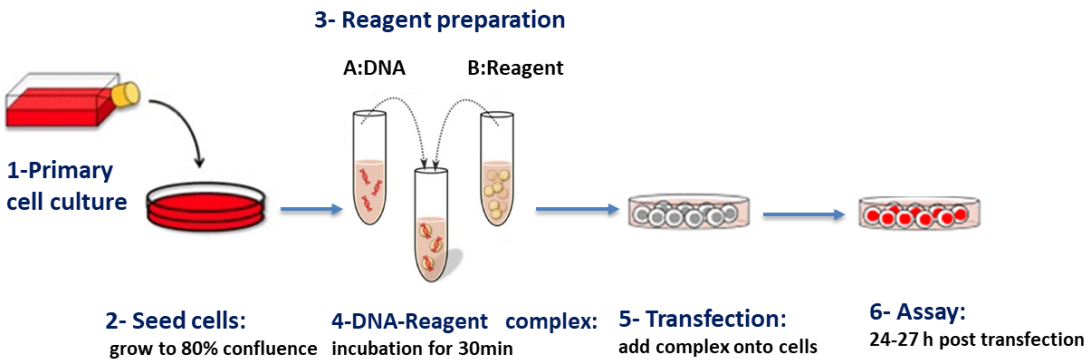


**Figure 3- 2. Flow diagram of transfection method**

### 3.1.3 Optimisation of Transfection Procedure using the three plasmid approach

The transfection optimisation was carried out using pMSCV-IRES-GFP plasmid and the pEGFP-C1 positive control plasmid (as it expresses the GFP protein) using calcium phosphate into HEK 293T mammalian cells seeded in 6 well tissue culture plate at 2x $10^5$ cells/well. The expression of transfected pMSCV-IRES-GFP was seen in approximately 70% of the cells, equivalent to the percentage of cells seen with the control pEGFP-C1 (Figure 3-3) when visualised using an inverted fluorescence microscope

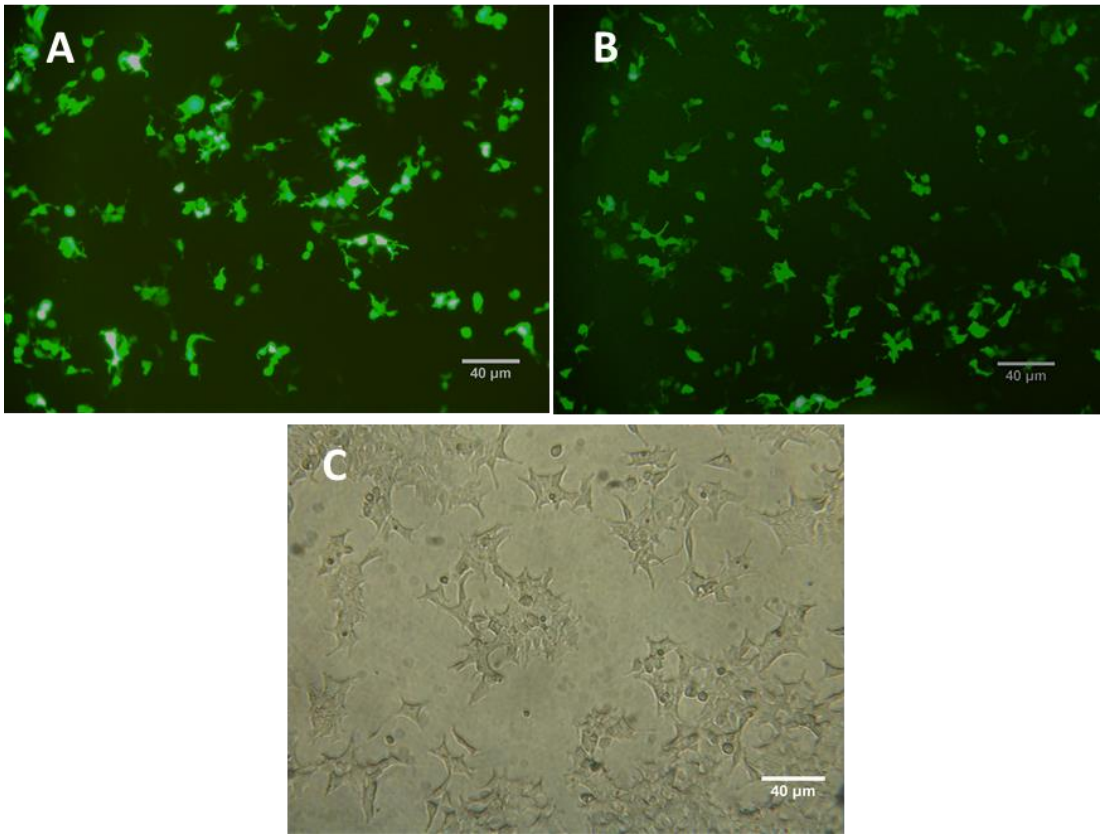


**Figure 3- 3. Transfection of pEGFP-C1 and pMSCV-IRES-GFP into HEK 293T cells demonstrating successful transfection by monitoring GFP expression**
Cells were transfected with plasmids using calcium phosphate and visualised after 24h using a fluorescence microscope. **A.** pEGFP-C1 **B.** pMSCV-IRES-GFP **C**. a bright field of cells shown in panel (B). The images were taken at 10x magnification

After confirmation of the expression of pMSCV-IRES-GFP plasmid in mammalian cells, pMSCV-IRES-GFP and the two other plasmids pSRG and pEQpAM3 were transfected together into HEK 293T cells in order to produce recombinant retrovirus. The transfection was performed using calcium phosphate, as described in section (2.1.6). As seen in (Figure 3-4) the expression of GFP in cells transfected with pEGFP-C1 (positive control) was strong in comparison with the expression of the cells transfected with three plasmids after observation using a fluorescence microscope. Thus, we hypothesised that endotoxins in the plasmid preparations may be causing a reduction in the transfection efficiency, so in the next section (3.1.4) we used an endotoxin free kit in order to clean our plasmids.

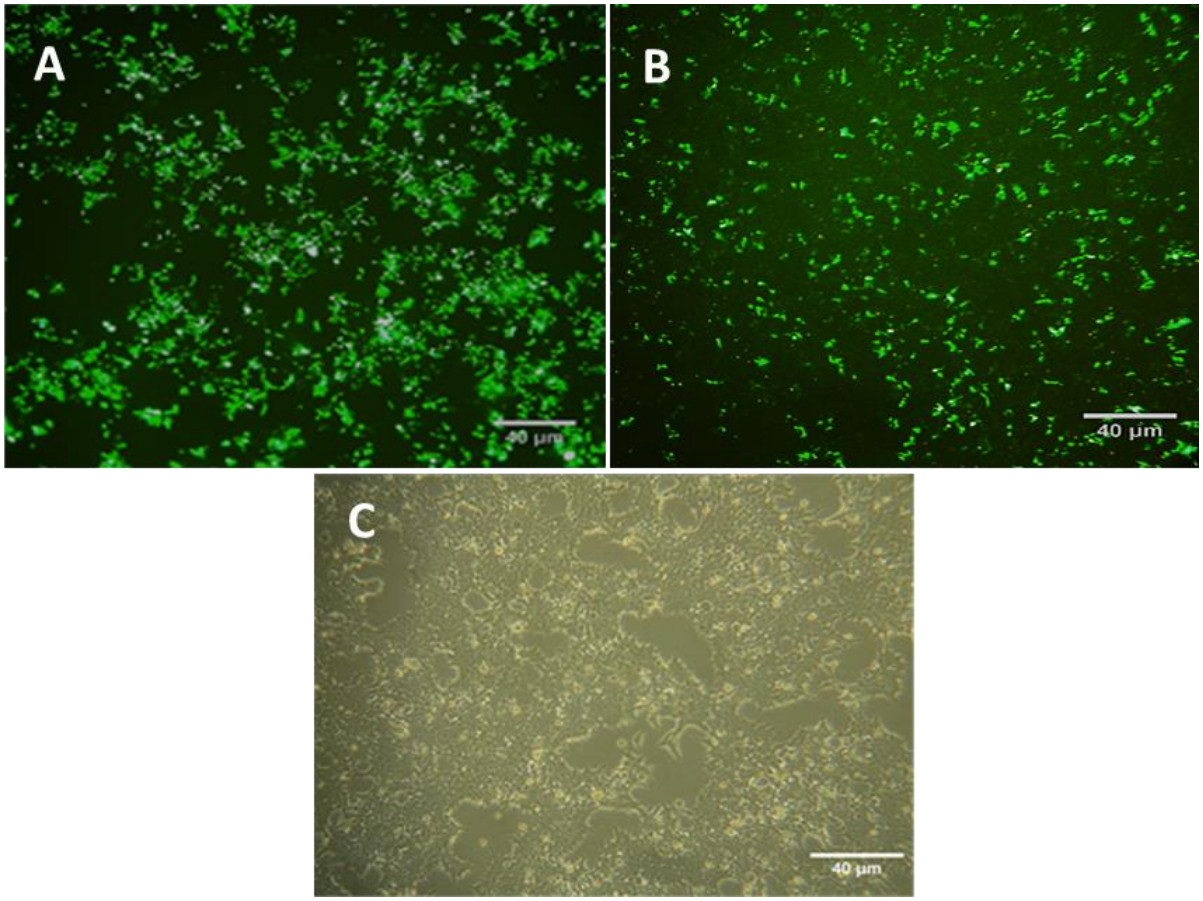


**Figure 3- 4. Comparison transfection of pEGFP-C1 (control) and the three plasmids (pMSCV-IRES-GFP, pSRG and pEQpAM3) into HEK 293 T cells using the calcium phosphate method.**

The images indicated the efficiency of transfection. Cells were imaged 24 hr after transfection with plasmids using calcium phosphate **A.** Fluorescence in pEGFP-C1 **B.** pMSCV-IRES- GFP, pSRG and pEQpAM3 (A). **C**. bright field of cells. The images were taken at 10x magnification

## 3.1.4 Preparation and transfection of Endotoxin free plasmids

Endotoxins are known to be frequent contaminants in plasmid DNA extracted from bacteria, they may serve as potent inhibitors in sensitive downstream applications such as the transfection of eukaryotic cells. Therefore, our aim was to remove any endotoxin contaminants from our plasmids hypothesising this would enhance the transfection, improve transfection efficiency and help to get pure and concentrated recombinant

retrovirus. Thus, Mira CLEAN® Endotoxin Removal Kit (5910, Mirus) was used to remove the endotoxin from the plasmids.

### 3.1.5 Optimisation of Transfection of endotoxin-free plasmids

Two transfection methods were compared, the calcium phosphate method and the PEI method. The transfection of both methods was repeated twice in order to confirm the results. Both methods demonstrated successful transfection but the efficiency varied between the two methods (Figure 3-5). PEI reagent showed a higher efficiency of transfection of three endotoxin-free plasmids together (recombinant retrovirus) when compared to the calcium phosphate method (Figure 3-6 B) (by comparing the number of fluorescent transfected cells). In calcium phosphate method cells were visualised 24 hr after transfection, while cells were visualised 72 hr after transfection in PEI method. The efficiency level of the calcium phosphate transfection lacked reproducibility (i.e calcium phosphate sometimes appeared to be toxic to the cells if did not added in appropriate way). Principally, using calcium phosphate transfection method need 24 h which could be not enough to generate the recombinant. In comparison, fluorescence intensity with PEI was higher, thus, the PEI method was chosen to generate recombinant retrovirus.

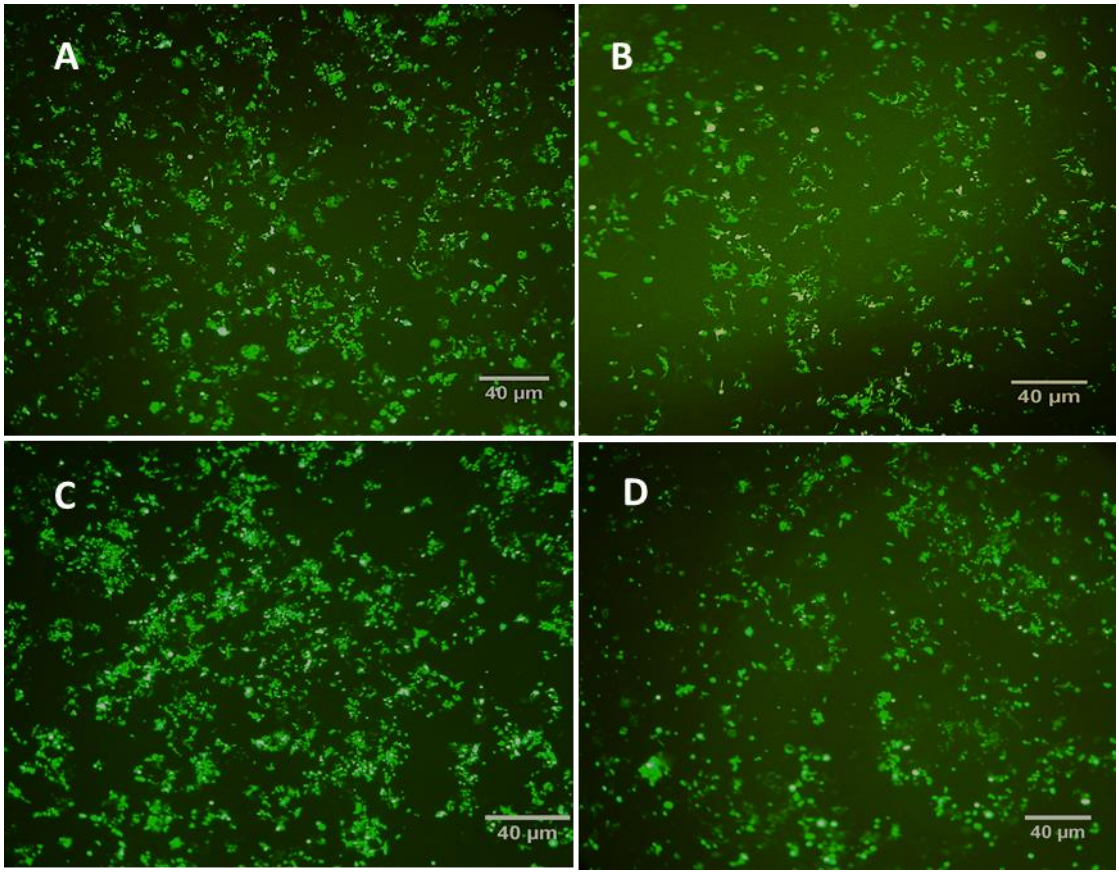


**Figure 3- 5. Transfection of pEGFP-C1 (control) and the three endotoxin-free plasmids (pMSCV-IRES-GFP, pSRG and pEQpAM3) into HEK 293 T cells using calcium phosphate method.**

HEK 293T cells were transfected with plasmids and then visualised by fluorescence microscopy 24h post-infection. Plasmids were as follows **A.** pEGFP-C1. **B.** pMSCV-IRES- GFP, pSRG and pEQpAM3 **C.** pEGFP-C1 (2nd experiment) **D.** pMSCV-IRES- GFP, pSRG and pEQpAM3 (2nd experiment). The images were taken at 10x magnification

PEI reagent was used to transfect the three endotoxin-free plasmids, as described in section (2.1.6.2). Interestingly, PEI reagent showed a higher efficiency of transfection (increase the number of transfected cells) when using three endotoxin-free plasmids together in comparison with calcium phosphate (Figure 3-6). The results indicated that endotoxin-free (EF) plasmids enable highest transfection efficiency in comparison with non-endotoxin-free plasmids.

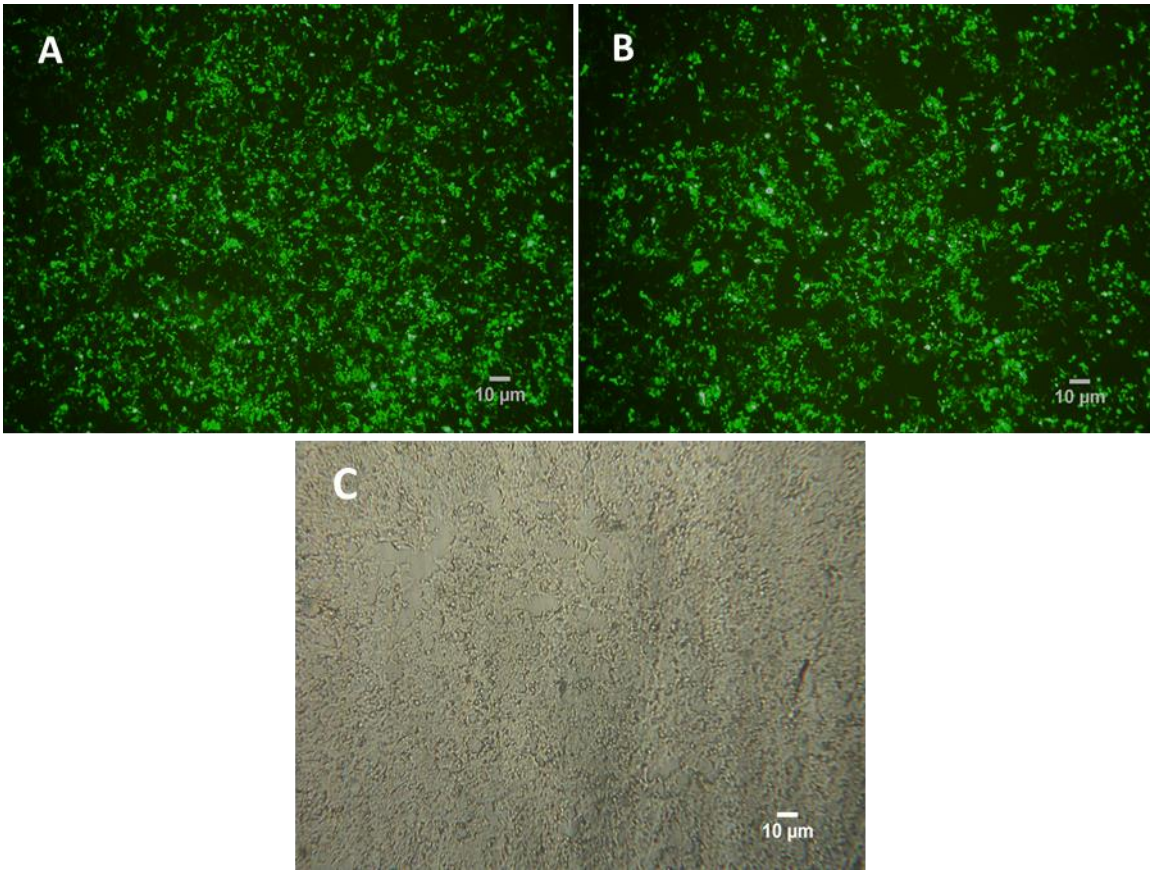


**Figure 3- 6. *In vitro* transfection of endotoxin-free DNA; pMSCV-IRES-GFP, pSRG and pEQpAM3 and pEGFP-C1 using PEI reagent.**
HEK 293T cells were transfected with endo-free plasmids using the PEI method and visualised using fluorescence microscopy 72 h post-transfection. Plasmids used were **A**. pEGFP-C1. **B.** pMSCV-IRES- GFP, pSRG and pEQpAM3. **C:** bright field of cells. The images were taken at 10x magnification

## 3.1.6 Production of recombinant retrovirus

Recombinant retrovirus was made by transfection of pMSCV-IRES-GFP, pSRG and pEQpAM3 into HEK 293T cells as above. After collection of the crude recombinant virus, the NIH3T3 cell line was used to determine the viral titre (described in section (2.1.7)). The titre of the crude stock of virus was analysed before and after endotoxin-free plasmid preparation to compare the role of endotoxin in virus production. Unfortunately with virus produced from cells transfected with plasmid DNA before endotoxin removal we found

that GFP signal was not apparent when the cells were visualized under an inverted fluorescence microscope over the course of 5 days. In comparison (Figure 3-7) shows a clear GFP signal indicating infection and transduction by recombinant MSCV.

Although production of recombinant MSCV was successful, unfortunately, production of high-titre retroviral stocks by transient transfection was not achieved. Thus this approach was not deemed suitable for the delivery of oLANA-GFP at levels that would be sufficient to perform the GFP-trap experiments.

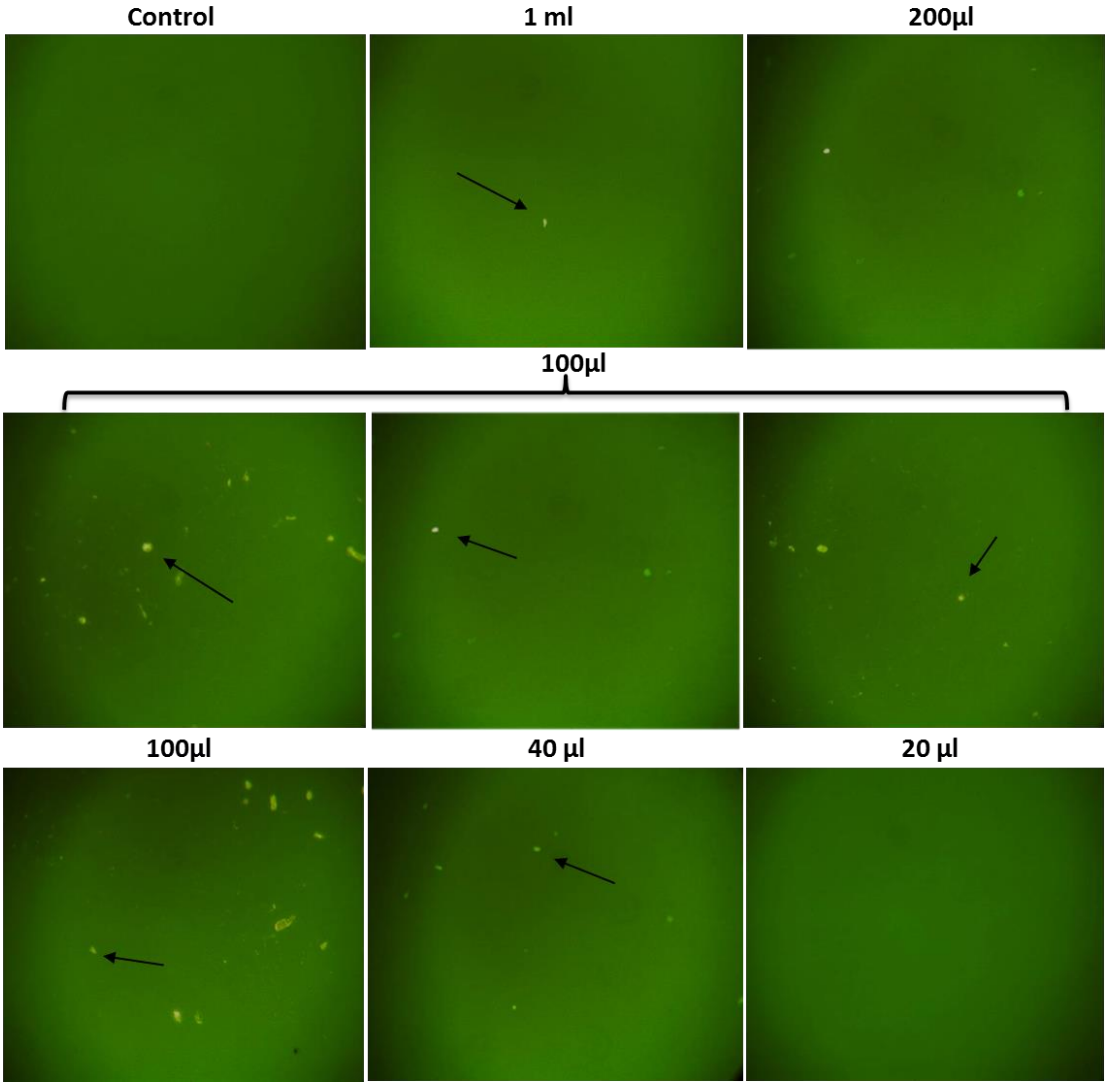


**Figure 3- 7. Titration of recombinant retrovirus in NIH3T3 cells after endotoxin-free plasmid DNA preparation.**

The images show the NIH3T3 cells after infection with different dilutions of virus stock: 1 ml, 200µl, 100µl, 40µl and 20µl respectively. The arrows indicate the infected cells

# Section two: Identification of oLANA binding partners

## 3.2 Construction of pMSCV-GFP-oLANAΔ

As the approach of introducing recombinant proteins into bovine T cells using retroviruses was not efficient enough to perform GFP-trap pull-down experiments, the more conventional approach of transfection into HEK293T cells was taken. Any interactions could then be confirmed in bovine T cells or OvHV-2-positive LGLs.

In this section of work we successfully insert the Kozak-eGFP-oLANA del in pMSCV-IRES-GFP vector expressing a fusion protein of GFP with LANA mutant lacking the internal repeat domain using DNA clone technique. Next, we showed significant transfection of the construct into HEK 293T cells using transfection assay. In addition, samples were co-immunoprecipitated using GFP Trap A to process for proteomics in order to identify the proteins interact with oLANA.

To identify novel cellular proteins interacting with oLANA, a clone which would express oLANA with eGFP fused to the N terminus was generated (Figure 3-8). The construct is also a mutant of oLANA lacking the internal repeats (glycine, glutamic acid and proline-rich). Previous studies on the homologous KSHV LANA have used this approach as: 1) The majority of the protein-protein interactions and DNA tethering domains are in the N-terminal and C-terminal domains and 2) There is a much higher level of protein expression and stability when the complex repetitive domain is removed (Figure 3-9) (Domsic *et al.*, 2013; Uppal *et al.*, 2014). The DNA sequence of this construct (GFP-oLANAΔ) was further codon-optimised for mammalian expression and a consensus 'Kozak' sequence

(translationial initiation) inserted at the 5'end. This construct was then synthesised and inserted into a generic cloning vector using the GeneArt service (ThermoFisher Scientific).

cgccgccaccatggtgagcaagggcgaggagctgttcaccggggtggtgcccatcctggtcgagctggacggcgacgtaaacggccacaagttc
agcgtgtccggcgagggcgagggcgatgccacctacggcaagctgaccctgaagttcatctgcaccaccggcaagctgcccgtgccctggccca
ccctcgtgaccaccctgacctacggcgtgcagtgcttcagccgctaccccgaccacatgaagcagcacgacttcttcaagtccgccatgcccgaag
gctacgtccaggagcgcaccatcttcttcaaggacgacggcaactacaagacccgcgccgaggtgaagttcgagggcgacaccctggtgaaccg
catcgagctgaagggcatcgacttcaaggaggacggcaacatcctggggcacaagctggagtacaactacaacagccacaacgtctatatcatg
gccgacaagcagaagaacggcatcaaggtgaacttcaagatccgccacaacatcgaggacggcagcgtgcagctcgccgaccactaccagcag
aacacccccatcggcgacggccccgtgctgctgcccgacaaccactacctgagcacccagtccgccctgagcaaagaccccaacgagaagcgc
gatcacatggtcctgctggagttcgtgaccgccgccgggatcactctcggcatggacgagctgtacaagatggtgctttacgaagtggcactagt
actgacggcgatgaagatggcaggggaagaagacctgggcccaagaaaagaccagtaactgaaggcaaaggagaaggtcctgggggagaag
gagaagagggagaggagccagaagaccctatggaaggcccttctagcgggcctccagtaagaggccggcgcaagcggccaccgaaacatcaa
ccagagactgacagggcaaaacgtaaaaagctagcacctatttggaaccctacattaaaggaagccacgtactctttacacttaaactgtacttc
aaaggatccagttgttagagtatctagatctgttcgagcgctcaatcctaacgctccacacagtaatattttctttacaggtggtatgtacacttttgt
aatttatggcaacgataaggaagctgtagaaagtttgttccaattcttgttgcaggatgcaatgaataatcctcaggcaggagcggttaacattag
tacaggtccacttactccatctttacctttaaccaacaatag

**Figure 3- 8. Sequence of synthetic gene Kozak-eGFP-oLANAΔ.**
The synthetic gene (1274 bp) consists of a Kozak consensus sequence (yellow) followed by the eGFP coding sequence (green) fused in frame to the oLANA coding sequence (blue) from which the internal repeats (glycine, glutamic acid and proline) have been deleted

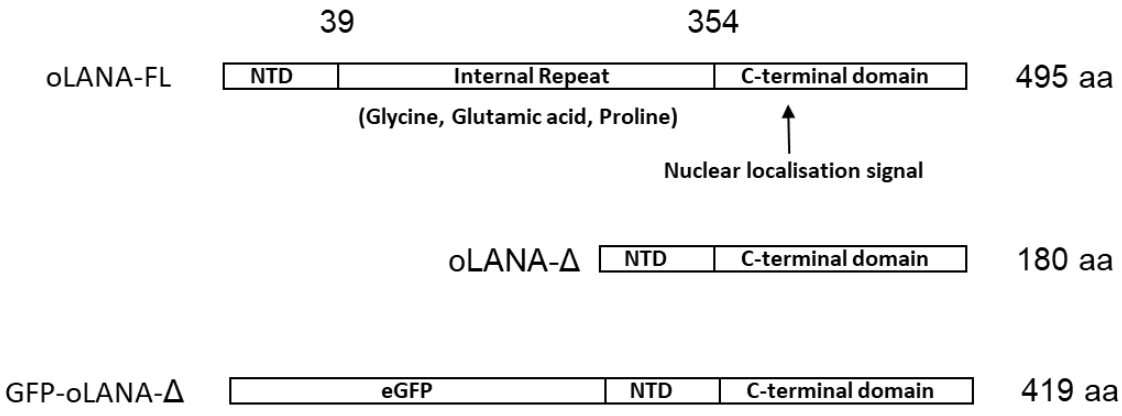


**Figure 3- 9. Schematic diagram of eGFP-oLANAΔ constructs.**
OLANA-FL: full-length oLANA showing the three domains and the nuclear localistaion signal. oLANAΔ: oLANA with the internal repeats deleted. GFP-oLANAΔ: Final construct with GFP fused in frame at the N-terminus.

### 3.2.1 Cloning GFP-oLANAΔ into pMSCV-IRES-GFP

The vector pMSCV-IRES-GFP is known to drive high level expression of recombinant protein in a variety of mammalian species and cell types, either using DNA transfection or when used to make a recombinant retrovirus. This vector was therefore used to drive GFP-oLANAΔ for the GFP-trap pulldown experiments.

The eGFP-oLANAΔ plasmid obtained from GeneArt synthesis was used as template to amplify the gene by conventional PCR using the proof-reading KOD polymerase (KODX kit, Novagen). Primers were used so as to generate an EcoRI site at the 5' end of the construct and a NotI site at the 3' end (see Materials and Methods). Cloning between the EcoRI and NotI sites of pMSCV-IRES-GFP (Figure 2-3) will replace IRES-GFP in the vector with GFP-oLANAΔ. The annealing temperature was optimised using gradient PCR and the correct size product was identified at 52 – 55 $^{o}$C (Figure 3-10).

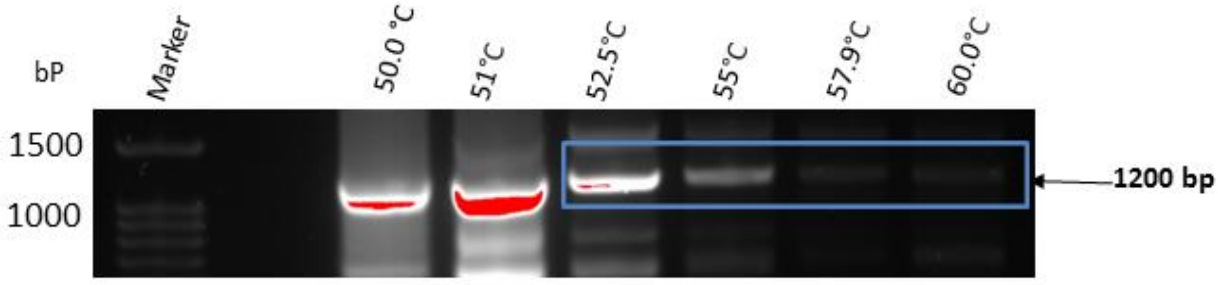


**Figure 3- 10. Amplification of GFP-oLANAΔ**
Plasmid containing GFP-oLANAΔ was amplified using forward and revers primers using different annealing temperatures as indicated. Samples were analysed using agarose gel electrophoresis (1% agarose) and visualised using BIO-RAD. DNA marker (100 bp, Cleaver Scientific).

The PCR product (52.9) was cut with *Eco*RI and NotI restriction endonucleases and inserted between the *Eco*RI and NotI sites of the pMSCV-IRES-GFP vector. Insertion was confirmed by restriction digest of mini-plasmid preparation using *Eco*RI and NotI l (Figure 3-11). All six clones tested showed positive bands at 1200 bp, as compared with 1500 bp in the parent vector.

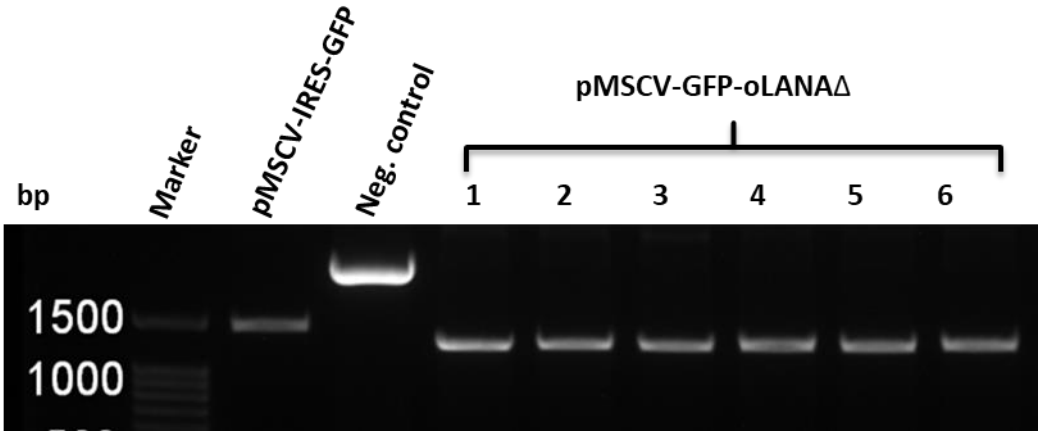


**Figure 3- 11. Analysis of pMSCV-IRES-GFP and pMSCV-GFP-oLANAΔ mini prep DNAs.**
DNA samples as indicated were cut using EcoRI and NotI and analysed using agarose gel electrophoresis (1% agarose). DNA marker (100 bp, Cleaver Scientific).

The DNA sequence of the insert was confirmed by sequencing using 3' sequencing primer: pCDH-rev and 5' sequence primer: pBABE as described in materials and methods. Sequencing confirmed that the selected clone was correct and that there were no mutations as a result of PCR and sub-cloning. Large plasmid preps of pMSCV-eGFP-oLANAΔ and pMSCV-IRES-GFP (control) were made using Qiagen endo-free DNA preparation kits for use in transfection experiments.

### 3.2.2 *In vitro* transfection and expression of GFP-oLANAΔ

The expression of GFP-oLANAΔ and GFP (used as a transfection Control) was confirmed by transfection into HEK293T cells using the calcium phosphate method. All the transfections were carried out in 6-well plates and were assayed for GFP expression 24 hr after transfection, as described in section (2.2.14). Highest transfection efficiencies were observed with precipitation mixtures 24 hr post-transfection. Representative images of expression 24 hr after transfection are shown (Figure 3-12). Strong GFP signal, which was in more than 80% of cells in the well comparison with the monolayer, was obtained with 6 and 6.44 µg (section 2.2.10) of unmodified pMSCV-IRES-GFP vector and pMSCV-GFP-oLANAΔ respectively. Three independent transfection experiments were performed in order to get cell lysate for western immunoblotting analysis.

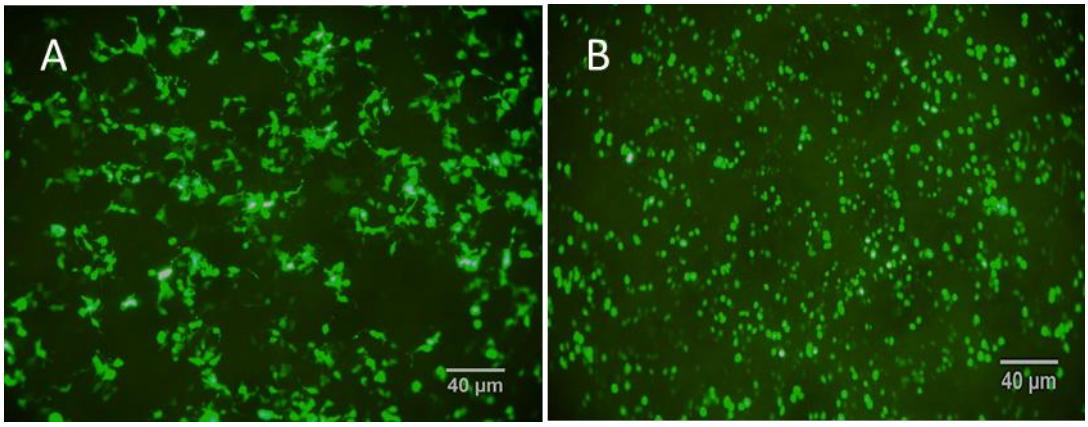


**Figure 3- 12. *In vitro* transfection in HEK 293T.**
HEK 293T cells were transfected with pMSCV-IRES-GFP and pMSCV-GFP-oLANAΔ and images taken 24 h post-transfection using a fluorescence microcope. **A.** pMSCV-IRES-GFP **B.** pMSCV-GFP-oLANAΔ. The magnification factor at 10x

### 3.2.3 Western immunoblotting analysis of pMSCV-GFP-oLANAΔ

Western immunoblotting was carried out for expressed protein in cell lysates. The cell lysates were analysed using SDS-PAGE and western blotting. The eGFP-oLANAΔ fusion protein has a molecular weight of approximately 47 kDa as predicted from the sequence using the ExPasy Comute pI/Mw algorithm. A band of this size was visible on the blot (Figure 3-13). With some smaller bands that are more than likely breakdown products. GFP has a molecular weight of 27 kDa and is shown expressed from pMSCV-IRES-GFP vector. No bands were observed to react with the GFP antibody in lysate from mock transfected cells. Furthermore the respective bands were not seen when probed with goat anti-rabbit IgG HRP conjugated antibody alone (negative control). This result confirms the expression of pMSCV-GFP-oLANAΔ and the experiment was repeated to confirm the positive finding.

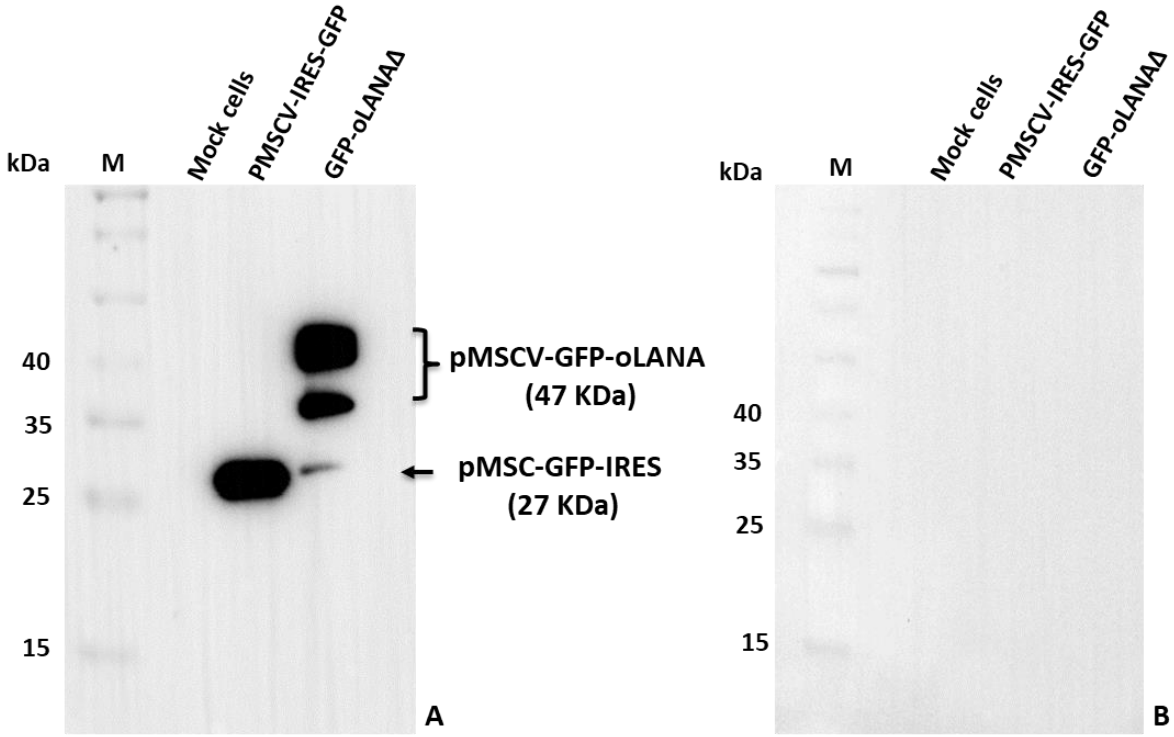


**Figure 3- 13. Western immunoblotting analysis of GFP-oLANAΔ**
HEK 293T cells were transfected with plasmids as indicated and lysates analysed by SDS-PAGE and western blotting. Panel **A:** blot probed using mouse monoclonal GFP-SC antibody at 1:500 dilution (Santa Cruz Technology) and goat anti-mouse HRP conjugate (A4416, Sigma). Panel **B:** blot probed with goat anti-mouse-HRP conjugate alone (A4416, Sigma). M: molecular weight marker (Spectra™ Multicolour Broad Range Protein Ladder, ThermoFisherScientific.

To confirm native oLANA expression for use in further analyses, OvHV-2 infected bovine large granulocyte lymphocytes (LGL; BJ1035) were also analysed by western immunoblotting using anti-oLANA antibody. These revealed a band at 37 kDa representing the full-length oLANA protein, with a second, smaller band at 17 kDa representing probable break down of protein (Figure 3-14). Additionally, the LGL lysates were probed with goat anti –rabbit IgG HRP conjugate alone as a negative control. The presence of immune reactivity in the bovine lymphocytes indicates that the OvHV-2- infected bovine LGLs

express detectable oLANA and demonstrate the instability of this protein. The size of the protein and the presence of the smaller 17 KDa band have been described previously (Al-Saadi, 2018). The high specificity of this antibody for oLANA has also been confirmed using a wide range of mammalian cell lines and viruses (Al-Saadi, 2018).

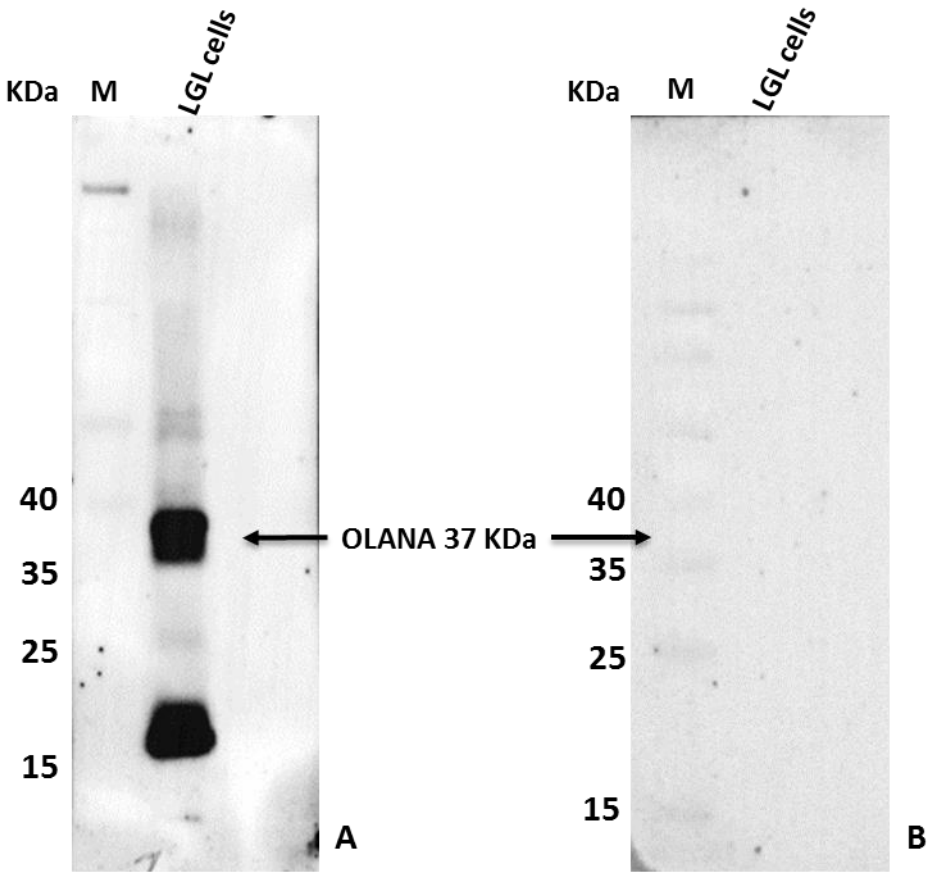


**Figure 3- 14. Western immunoblotting analysis of bovine large granulocyte lymphocytes. A:** blots of harvested BJ1035 LGL cells were probed using anti-oLANA polyclonal antibody diluted at 1/5000. Molecular weights of protein molecular weight markers run in parallel lanes are shown on the right and the location of expected bands for oLANA on the left. **B:** same protein lysate probed with secondary antibody alone goat anti- rabbit IgG conjugated to HRP (HRP P1-1000, Vector) as a negative control at dilution factor of 1:10000. M: molecular weight marker (Spectra™ Multicolour Broad Range Protein Ladder, Thermoscientific.

To further understand the function of oLANA, we used immunoprecipitation and mass spectrometry to identify oLANA-associated proteins in HEK 293T cells.

### 3.2.4 Optimisation of GFP-trap pull-down

Transfection using calcium phosphate was carried out to express the GFP-oLANAΔ fusion protein and GFP alone, as described in section (2.2.16.1). The expressed fusion protein GFP-oLANAΔ and unmodified GFP from the vector alone were immunoprecipitated using GFP-Trap A beads (chromotek) to obtain bound complexes, which were later dissociated for analysis. The transfection efficiency of the DNA construct in HEK 293T cells was confirmed as previously after transfection by fluorescence microscopy. Interestingly, the fusion protein expressed in HEK 293 cells was comparable with that seen from the unmodified vector when evaluated 24 hr post transfection. Cell lysates were obtained by lysing the cells with lysis buffer, as described in section (2.2.16.2).

In each experiment western immunoblot was performed to analyse for the presence of expressed proteins using both rabbit polyclonal and mouse monoclonal antibodies (explained in below section). The expression of the GFP-oLANAΔ fusion protein was high in all the independent experiments.

Lysates from HEK 293T cells were processed from successfully transfected cells using GFP-Trap A, as described in section (2.2.16.2). The whole lysates (input) and samples after pull-down and elution from pMSCV-GFP-oLANAΔ and pMSCV-IRES-GFP transfections were monitored by western immunoblotting using equal quantities of cell lysates and by probing with anti- GFP and detected with HRP conjugated antibody. As oLANA exists in both nuclear and cytoplasmic forms we tested using lysis buffers containing NP-40 (standard lysis buffer) or NP-40 plus sodium deoxycholate as previous studies have indicated that this may be better at extracting nuclear complexes for pull-down

experiments. The expected or predicted bands of GFP-oLANAΔ fusion with molecular weight of approximately 47 kDa were observed in both input and samples eluted from the GFP-trap beads when using the mouse monoclonal GFP-SC antibody, and there were several smaller breakdown products (Figure 3-15 A and B). While unmodified GFP was detected at approximately 27 kDa. Comparison of Figure 3-15 panel A and B shows that similar sized bands were extracted using both lysis buffers but that there appeared to be little difference in the intensities of bands between proteins extracted with lysis buffer either without or containing sodium deoxycholate. Identical blots were analysed with goat anti-mouse HRP conjugate alone which showed no reaction (Panel C).

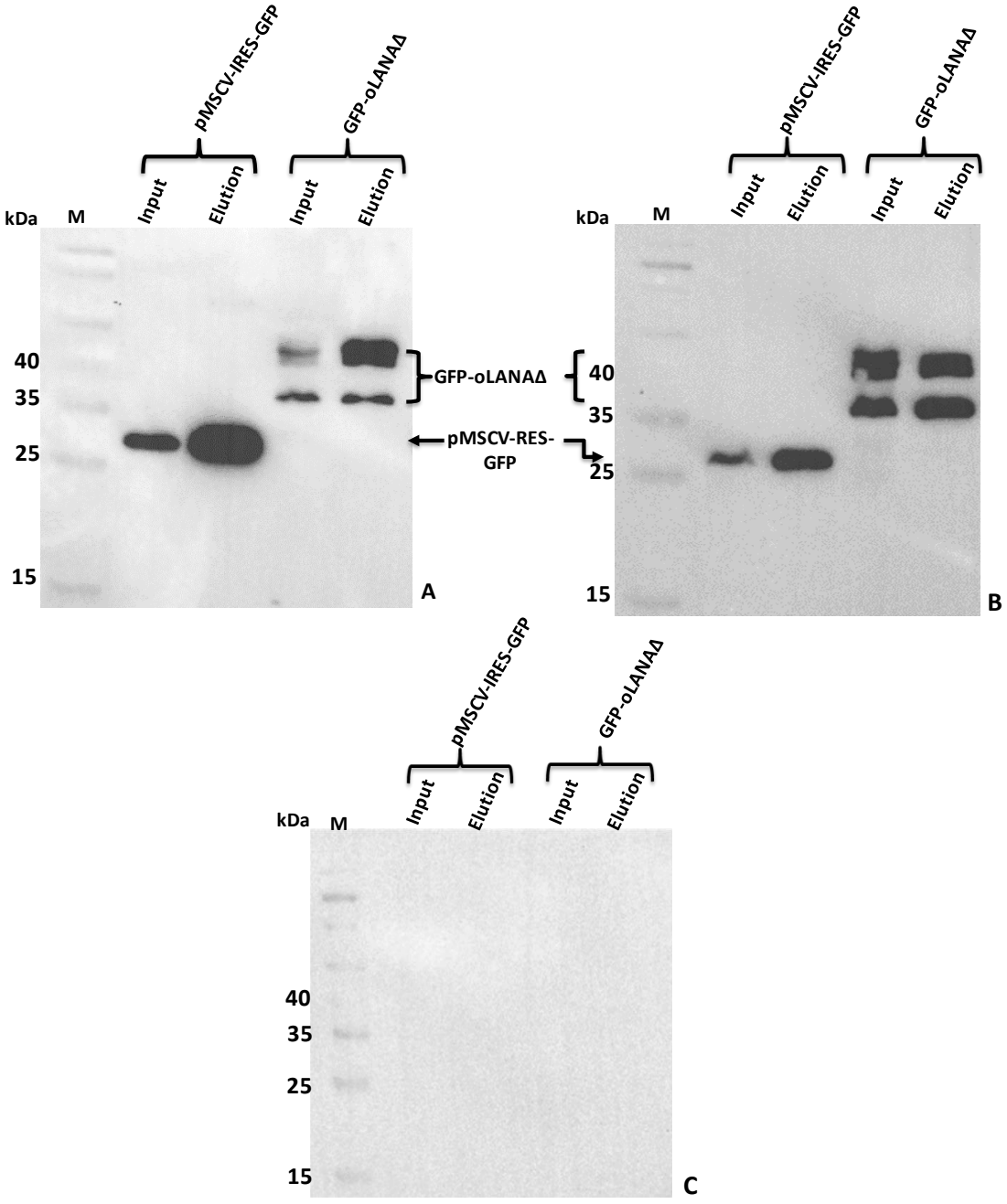


**Figure 3- 15. Western immunoblotting analysis of GFP-Trap pulldowns.**

Cell lysates were obtained 24 h post-transfection with the indicated plasmids and processed using GFP-trap and then subjected to SDS-PAGE and immunoblotting using mouse monoclonal GFP antibody at dilution 1:500. Samples were analysed after lysis (Input) and after elution from the GFP-trap beads (Elution) **A:** protein lysate of HEK 293T cells transfected with pMSCV- IRES-GFP- and pMSCV-GFP-oLANAΔ using lysis buffer with sodium deoxycholate. **B:** lysate of pMSCV-GFP-IRES and pMSCV- GFP-oLANAΔ using lysis buffer without sodium deoxycholate **C:** Similar to (A) but incubated with goat anti-mouse

as a negative control that shows no reaction. M: molecular weight marker (Spectra™ Multicolour Broad Range Protein Ladder, ThermoFisher Scientific.

### 3.2.5 Identification of oLANA interacting proteins by GFP-trap and Mass Spectrometry

To identify interacting proteins, HEK 293T cells were transfected with pMSCV-GFP-oLANAΔ and control GFP-expressing plasmid and then extracted using lysis buffer. The extract then was subjected to affinity purification mass spectrometry (APMS) analysis, as described in section (2.2.17). First, the complex formed by GFP-oLANAΔ was affinity purified via immunoprecipitation using GFP-Trap A beads. Secondly, western blot for GFP was performed to identify the presence of GFP-containing proteins. Samples eluted from GFP-Trap A beads were then processed for mass spectrometry as described in section (2.2.17.2) (Figure 3-16). Sequenced peptides were then identified using MaxQuant software using the Andromeda search engine against a database of human proteins and the oLANA construct. Label-free MS results were then analysed using Perseus software to quantify the data and identify significant peptides. The analysis procedure was repeated in triplicate to enable statistical evaluation of data. To identify significant interactions, exclusion criteria of; >2 unique peptides for quantification, log2 fold change > +/- 1 in abundance and p value < 0.05 was used. Two independent experiments were performed using lysis buffer with NP40 alone. Although both these runs identified approx. 600 unique peptides, none were significant interactions using the exclusion criteria. A third run was performed using NP40 plus sodium deoxycholate in the lysis buffer. This resulted in the identification of 355 proteins with > 2 unique peptides. Using the exclusion criteria, eight cellular proteins were identified as potential specific binding partners to the GFP-oLANAΔ. A 'volcano' plot showing the distribution of hits and those that are significant is shown in

Figure 3-17 and a list of the most abundantly associated proteins ranked according to the numbers of peptides identified is shown Table (3-1).

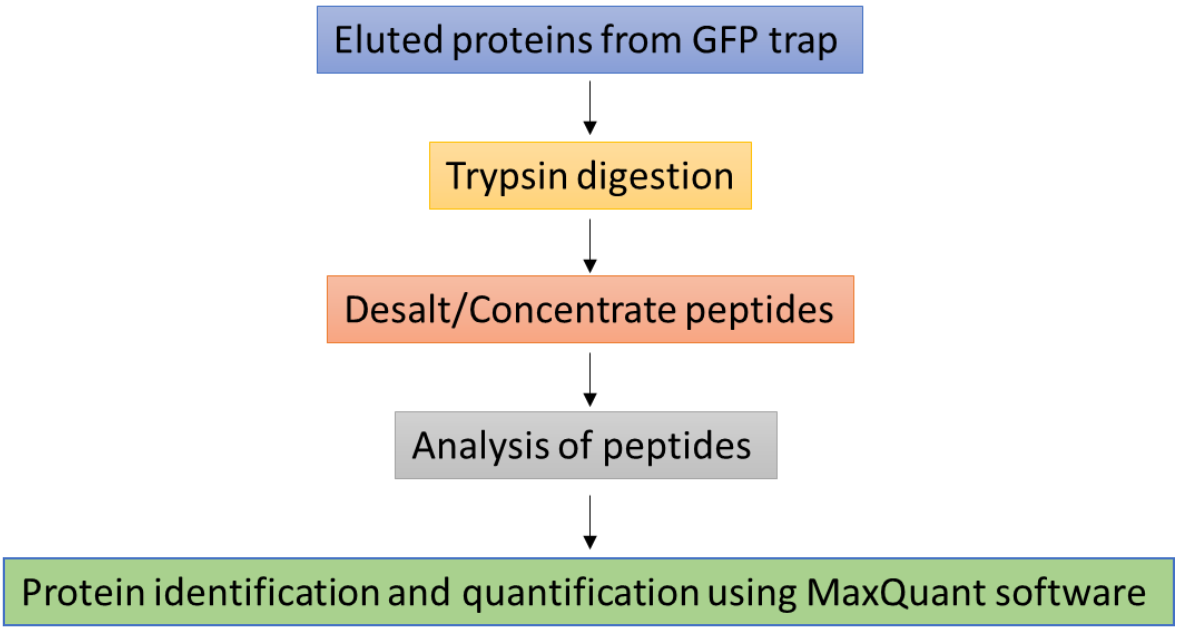


**Figure 3- 16. Simplified proteomic workflow of analysis of putative oLANA interacting proteins**

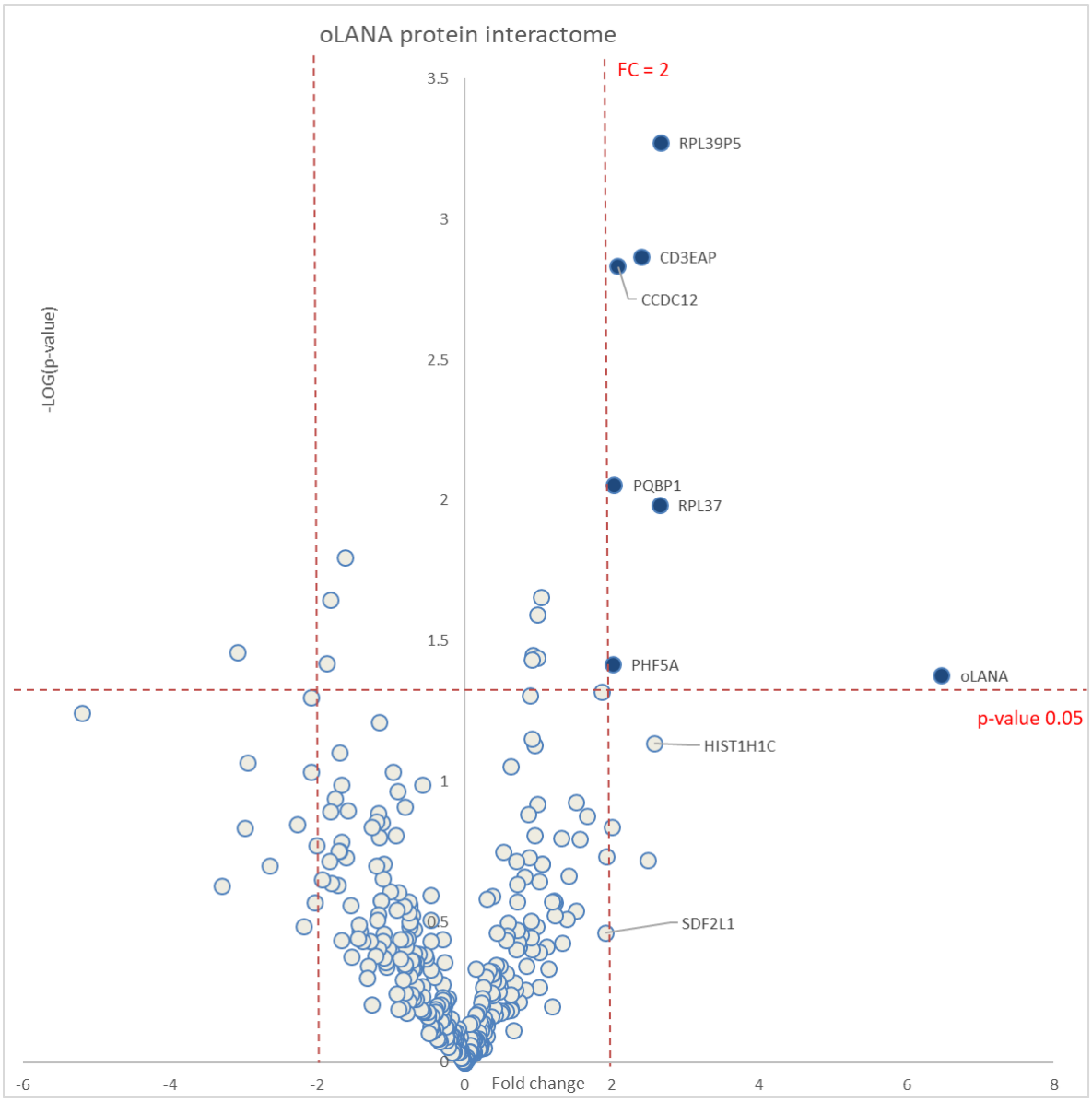


**Figure 3- 17. Quantitative label-free proteomics of GFP-trap pull-downs reveals specific oLANA interactions.**

The x-axis represents *log2* of gene expression fold change between samples transfected with pMSCV-GFP-oLANAΔ in comparison to unmodified pMSCV-IRES-GFP. The y-axis represents the p-value of differential levels in the pull-down complexes. The text in the two halves of the plot area provides information about the total number of proteins with differential expression P-value more significant than the cut off (0.05); and greater than 2-fold change (FC).Blue spots: significant ($p < 0.05$) and >2FC

| GFP-oLANAΔ - interacting Proteins | Proteins | GFP-oLANAΔ | |
|---|---|---|---|
| | | Fold change | No. of peptide |
| **HIST1H1C;HIST1H1A** | Histone H1.2; Histone H1.1 | 2.6 | 2 |
| **RPL39P5;RPL39** | Putative 60S ribosomal protein L39-like 5;60S ribosomal protein L39 | 2.6 | 2 |
| **PHF5A** | PHD finger-like domain-containing protein 5A | 2.0 | 2 |
| **RPL37** | 60S ribosomal protein L37 | 2.6 | 3 |
| **PQBP1** | Polyglutamine-binding protein 1 | 2.0 | 3 |
| **CCDC12** | Coiled-coil domain-containing protein 12 | 2.1 | 4 |
| **CD3EAP** | DNA-directed RNA polymerase I subunit RPA34 | 2.4 | 5 |
| **SDF2L1** | Stromal cell-derived factor 2-like protein 1 | 1.9 | 8 |

**Table 3- 1. Cellular proteins interacting with GFP-oLANAΔ were identified by MS.**

To confirm that the proteins identified by mass spectrometry did interact with GFP-oLANAΔ and to determine the binding interrelationship among all the associated proteins, we carried out western immunoblot of pull-downs with antibodies against selected proteins.

Stromal Cell-Derived Factor 2-Like 1 (SDF2L1) is a endoplasmic reticulum (ER)-resident protein that is involved in the ER-chaperone machinery and is highly expressed in haematopoietic cells (Fujimori *et al.*, 2017). Although this protein did not exactly match the inclusion criteria, it was deemed interesting enough to warrant further investigation.

CCDC12 is located within the nucleus. Its exact function is not known but CCDC12 is associated with erythroid differentiation and also susceptibility to Juvenile Idiopathic Arthritis (Fan *et al.*, 2012; McIntosh *et al.*, 2017).

Cell lysates of HEK 293T cells transfected with pMSCV-GFP-oLANAΔ and pMSCV-IRES-GFP and processed using GFP-trap were analysed by western immunoblotting using an SDF2L1 antibody (ThermoFisher) and anti-CCDC12 antibody (Sigma) (Figure 3-18). Unfortunately, neither antibody reacted with the protein in input cellular lysates or indeed with pulldown complexes. This could be because expression levels are below the sensitivity for this antibody. However, it does mean that we can neither confirm whether or not these proteins interact with oLANA.

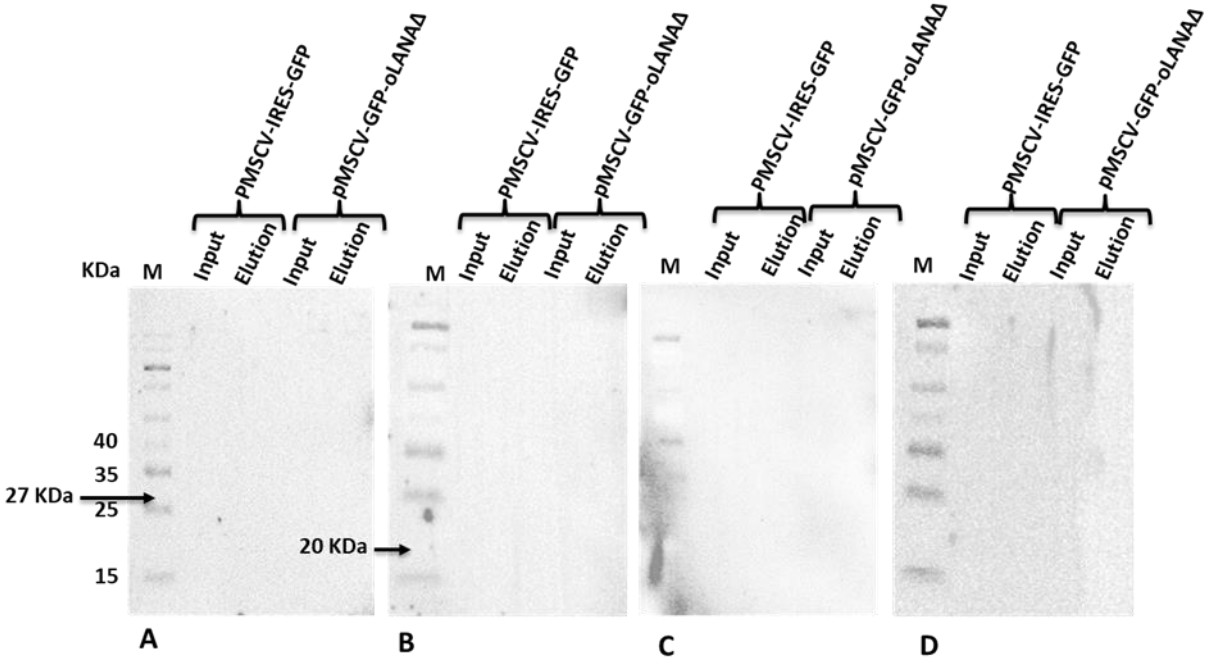


**Figure 3- 18. Western immunoblotting analysis of GFP-trap pull-downs probed with anti-SDF2L1 and anti-CCDC12**

Cell lysates were obtained 24 hr post-transfection using NP40 lysis buffer plus sodium deoxycholate with the indicated plasmids and pulled-down using GFP-Trap A beads. Samples were analysed by western blotting after lysis (Input) and after elution from the GFP-trap beads (Elution) **A**: SDF2L1 antibody (Apa5-71817) diluted 1/1000. **B**: anti-CCDC12 antibody (CB121-7B1, Sigma) diluted 1/1000. **C**: control negative blot probed with HRP goat anti-rabbit only. D: control negative blot probed with HRP goat anti-mouse only. M: molecular weight marker (Spectra™ Multicolour Broad Range Protein Ladder, ThermoFisher Scientific.

Histone H1 is one of the key components of chromatin and binds to the nucleosomal core particle around the DNA (Catez *et al.*, 2006). It has also been shown to interact with KSHV LANA and help tether latent genomes to chromatin (Verma and Armstrong-Altrin, 2013). To confirm oLANA- histone H1 interactions, proteins were immunoprecipitated by GFP Trap A beads, as described in section (2.2.16) and then western blots probed with an anti-histone- H1 antibody. The results, (Figure 3-19 A) showed that there was a band at 27-

29 kDa corresponding to histone-H1 and also a number of bands of other molecular weights. In contrast, no bands were present in both cells alone and vector-transfected cells. No reaction was seen in an identical blot probed with HRP goat anti-mouse (Figure 3-19 B). These data strongly suggest that histone-H1 associates with oLANA.

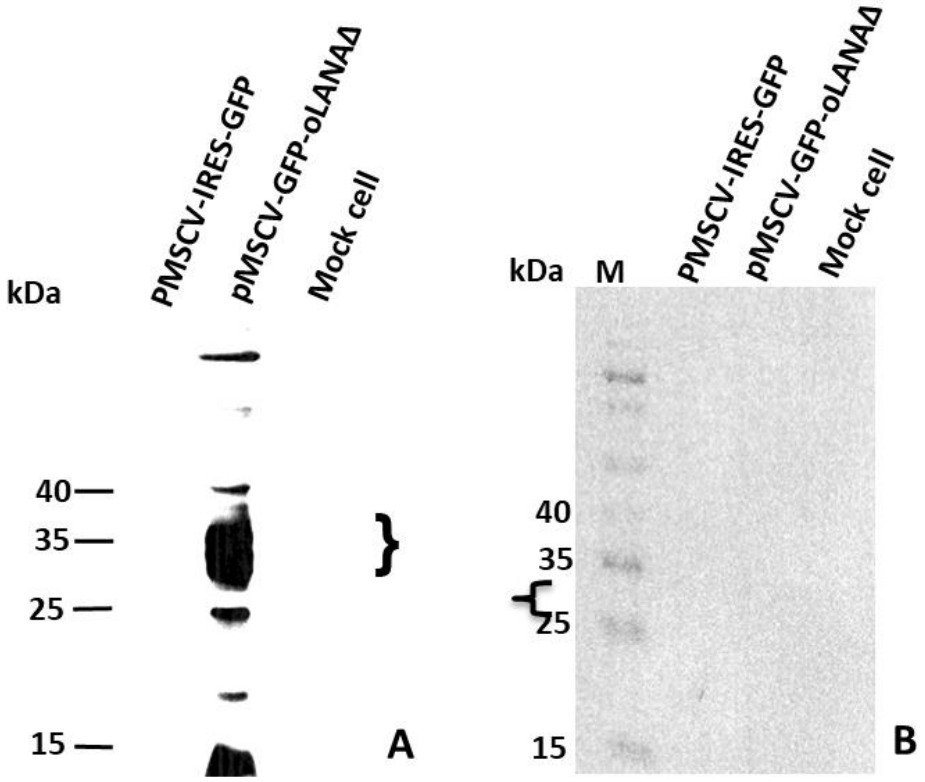


**Figure 3- 19. Western immunoblotting analysis of GFP-trap pull-downs probed with anti-H1.**

Cell lysates were obtained 24 hr post-transfection with the indicated plasmids and pulled-down using GFP-Trap A beads. **A:** protein expression was detected using an anti-histone H1 antibody (ab71594) diluted as 1/500 **B:** negative control blot using HRP goat anti-mouse only. M: molecular weight marker (Spectra™ Multicolour Broad Range Protein Ladder, ThermoFisher Scientific.

Recent data concerning the homologous KSHV LANA protein has shown that this protein can associate with a number of cellular molecules including cGAS, Rad50 and P53. Cyclic GMP-AMP synthase (cGAS) is a cellular sensor of foreign DNA that interacts with stimulator of interferon genes (STING) to initiate antiviral interferon responses. KSHV LANA has been shown to inhibit the cGAS-STING induction of interferon by binding to cGAS (Zhang *et al.*, 2016a). Rad50 is a DNA damage repair protein and is also involved in DNA sensing. KSHV LANA binds to Rad50 and modulates the IFN response after infection (Mariggiò *et al.*, 2017). Therefore, in addition to proteins identified by the GFP-trap and MS analysis proteins that co-immunoprecipitated with GFP-oLANAΔ were analysed by western immunoblotting using antibodies that recognise these proteins (Figure 3-20).

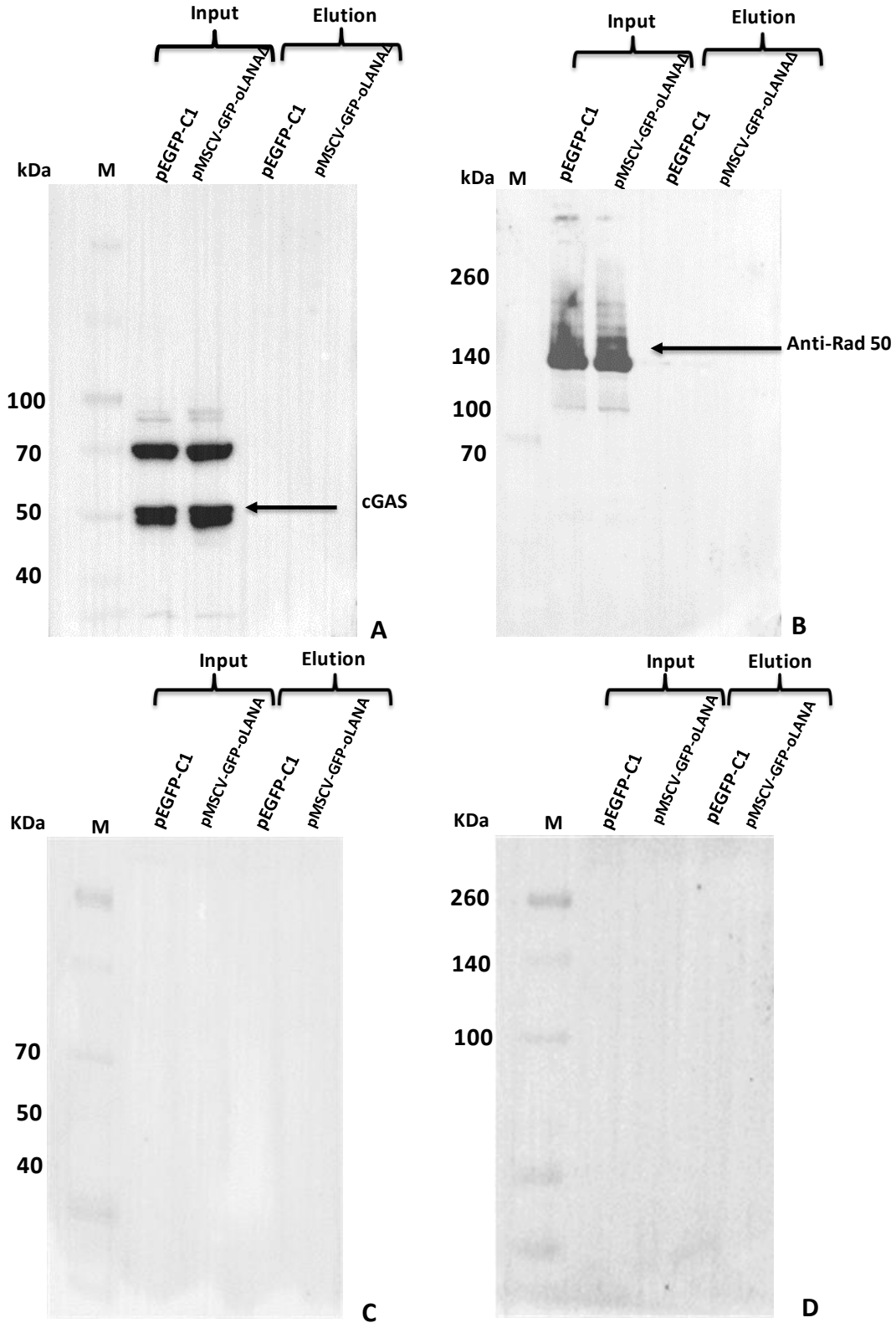


**Figure 3- 20. Western immunoblotting analysis of GFP-trap pull-downs probed with anti-cGAS and anti-Rad50.**

Cell lysates were obtained 24 hr post-transfection using lysis buffer contained sodium deoxychilate with the indicated plasmids and pulled-down using GFP-Trap A beads. Samples were analysed by western blotting after lysis (Input) and after elution from the GFP-trap beads (Elution) **A:** polyclonal anti-cGAS antibody (Millipore) **B:** anti-Rad 50 antibody (Sigma) **C:** secondary goat anti-mouse IgG (Sigma) as negative control. **D:** secondary antibody goat anti-rabbit. M: molecular weight marker (Spectra™ Multicolour Broad Range Protein Ladder, ThermoFisher Scientific.

The results (Figure 3-21) showed that while the respective bands were seen at 53 kDa for cGAS and 153 kDa for anti-Rad50 in the input samples, there were no bands in the elution samples indicating a lack of association between oLANA and these two proteins. The experiment was repeated with the same antibodies using cells lysed with and without sodium deoxycholate with a similar result (not shown).

It has been shown that KSHV LANA interactions with P53 are important for overcoming the P53-dependent cell cycle block induced by an activated DNA damage response (Chen *et al.*, 2010). GFP-oLANAΔ co-immunoprecipitating proteins were therefore analysed using an anti-p53 antibody. The results (Figure 3-21) showed that while the respective band was seen at 53 kDa for P53 in the input samples, there were no bands in the elution samples indicating a lack of association between oLANA and p53. The samples were blotted again and probed with goat anti-rabbit HRP conjugate only as a negative control

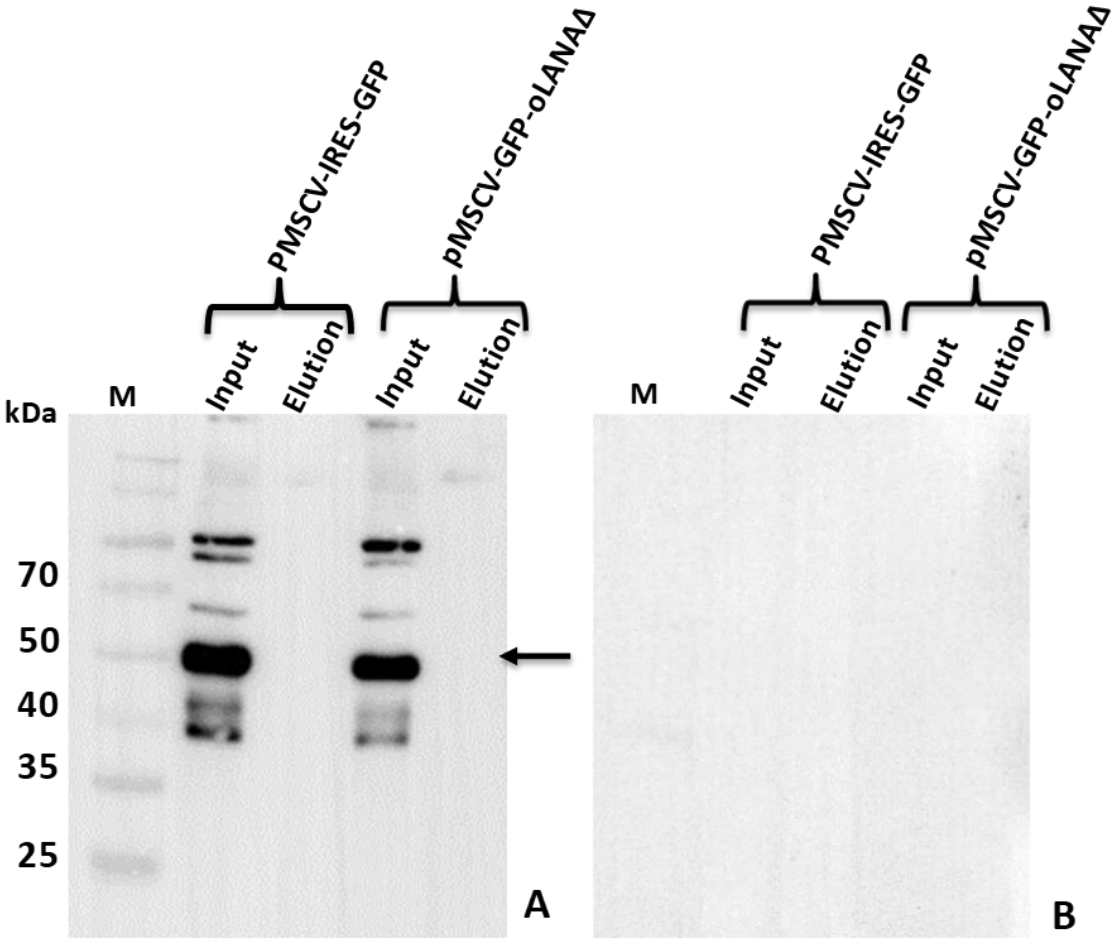


**Figure 3- 21. Western immunoblotting analysis of GFP-trap pull-downs probed with anti-P53.**

Cell lysates were obtained 24 hr post-transfection using lysis buffer contained sodium deoxycholate with the indicated plasmids and pulled-down using GFP-Trap A beads. Samples were analysed by western blotting after lysis (Input) and after elution from the GFP-trap beads (Elution) **A:** anti-P53 antibody (Sigma) diluted as 1/5000. **B:** control negative blot which detected with HRP goat anti-rabbit only. M: molecular weight marker (Spectra™ Multicolour Broad Range Protein Ladder, ThermoFisher Scientific.

# Section three: Validation of putative oLANA interacting proteins using co-localisation

Indirect and double immunofluorescence assay was carried out to define the subcellular location of GFP-oLANAΔ and full length oLANA within HEK 293T and LGL cells to determine localise of oLANA and interacts with cellular proteins using numerous of monoclonal and polyclonal antibodies which labelled later with Alexa flour 594 either mouse or rabbit antibodies and measure the quantification of coclocalisation using Pearson's Correlation.

The results in section 2 and previously published data identified proteins that potentially interacted with oLANA in HEK293s. Of these, only histone H1 was confirmed by co-immunoprecipitation analysis. This could be for a number of reasons. MS is extremely sensitive and the hits identified could either be low abundance/low affinity and thus not picked up by co-immunoprecipitation/western blot or they could be false hits. Co-localisation was therefore chosen as a means of identifying oLANA-protein interactions. Although it does not formally describe protein-protein interactions, colocalisation compares the subcellular distributions of two fluorescently labelled molecules by fluorescent confocal microscopy (Fay *et al.*, 1997; Lachmanovich *et al.*, 2003; Nicolas *et al.*, 2008; Zhang *et al.*, 2009).

The colocalisation of two probes can be determined individually by the appearance of structures whose colour reflects the combined contribution of both probes when the images of each probe are superimposed (or "merged"). For example, fluorescein and

rhodamine-labelled proteins can be colocalised by the appearance of yellow, due to combined fluorsecent contributions of green and red, respectively.

Channel overlap (overlap between two (or more) different fluorescent labels, each having a separate emission wavelength, to see if the different "targets" are located in the same area of the cell or very near to one another) can be quantified using cross-correlation algorithms like Pearson's correlation coefficient. Pearson's Correlation is a well defined and commonly accepted means for describing the extent of overlap between image pairs. It is a value computed to be between -1 and 1, with -1 being no overlap whatsoever between images and 1 being perfect image registration (van Steensel *et al.*, 1996; Zinchuk and Grossenbacher-Zinchuk, 2011). Pearson's correlation was calculated from confocal images using an inbuilt aglorithm in Image Pro Plus (Media Cybernetics).

### 3.3.1 Co-localisation analysis of oLANA and interacting proteins in HEK293T cells

Indirect immunofluorescence assays were carried out to detect the subcellular location of GFP-oLANAΔ protein in HEK 293T cells transfected with pMSCV-GFP-oLANAΔ. The native green fluorescence of GFP was used to mark GFP-oLANAΔ. Monoclonal and polyclonal antibodies to cellular proteins were then used as the primary antibodies which were then detected using Alexa flour 594-labelled secondary antibodies. After staining, the cells were imaged by confocal microscopy as described in section (section 2.3.1).

#### 3.3.1.1 GFP Control

First, as a positive control, anti-GFP was used to determine co-localisation with the GFP fluorescence. Figures (3-22 and 3-23) showed the expected cellular localisation of GFP-

oLANAΔ which was expressed predominantly in nuclei. There was excellent overlap between the GFP and anti-GFP signals as shown by yellow speckles in the nuclei (Panel D).

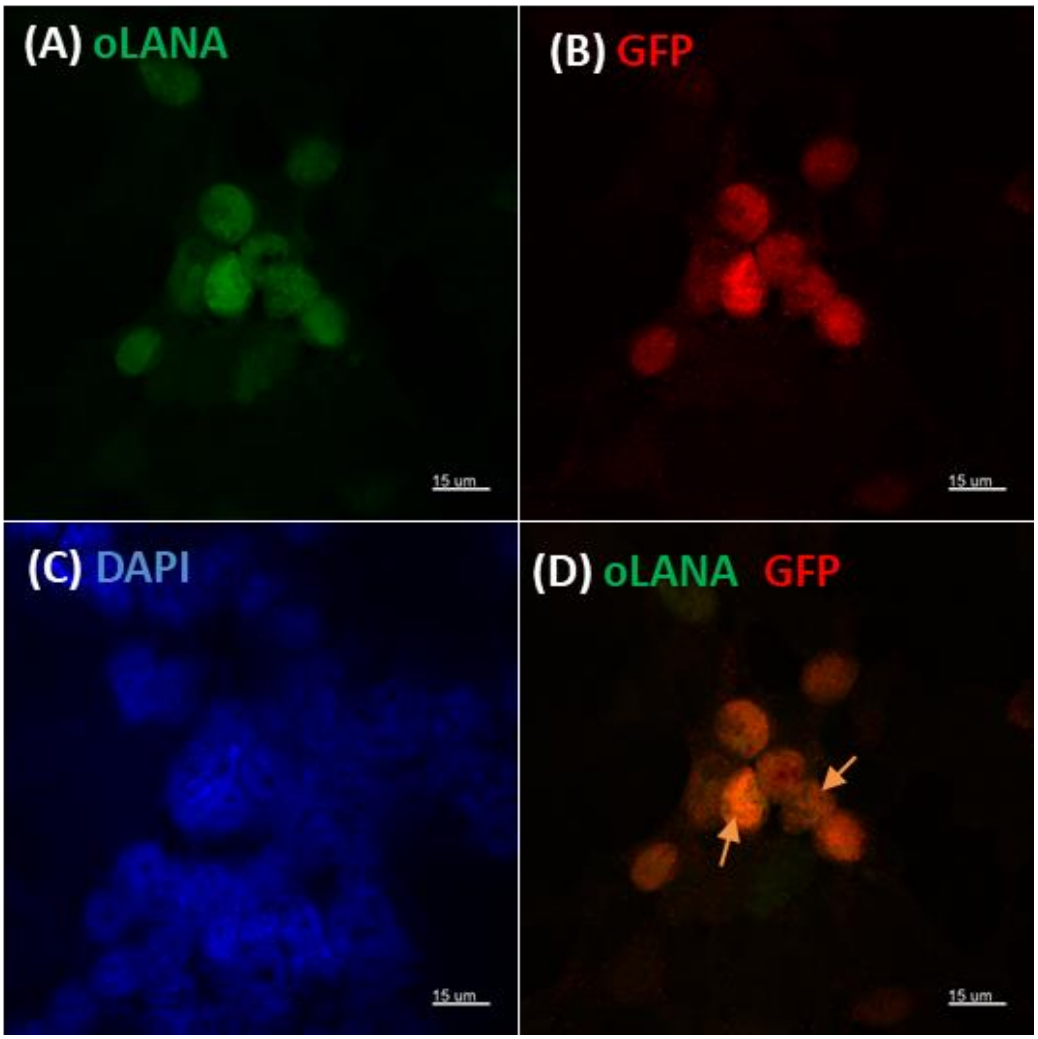


**Figure 3- 22. Colocalisation of GFP-oLANAΔ with anti-GFP.**
HEK 293 T cells were transfected with pMSCV-GFP-oLANAΔ using calicum phosphate. After 24 hr, cells were fixed, permeablised and immunostained using an anti-GFP antibody (Santa Cruz Biotechnology) and Alexa-fluor 594 anti-mouse. Nuclei were stained blue using DAPI and cells then visualised by confocal microscopy. **A:** Green channel **B:** Red channel **C:** Blue Channel **D:** Overlay of green and red pixel intensities. Images are representative of three experimental replicates. Scale bars represent 15µm. The arrows show the overlap areas

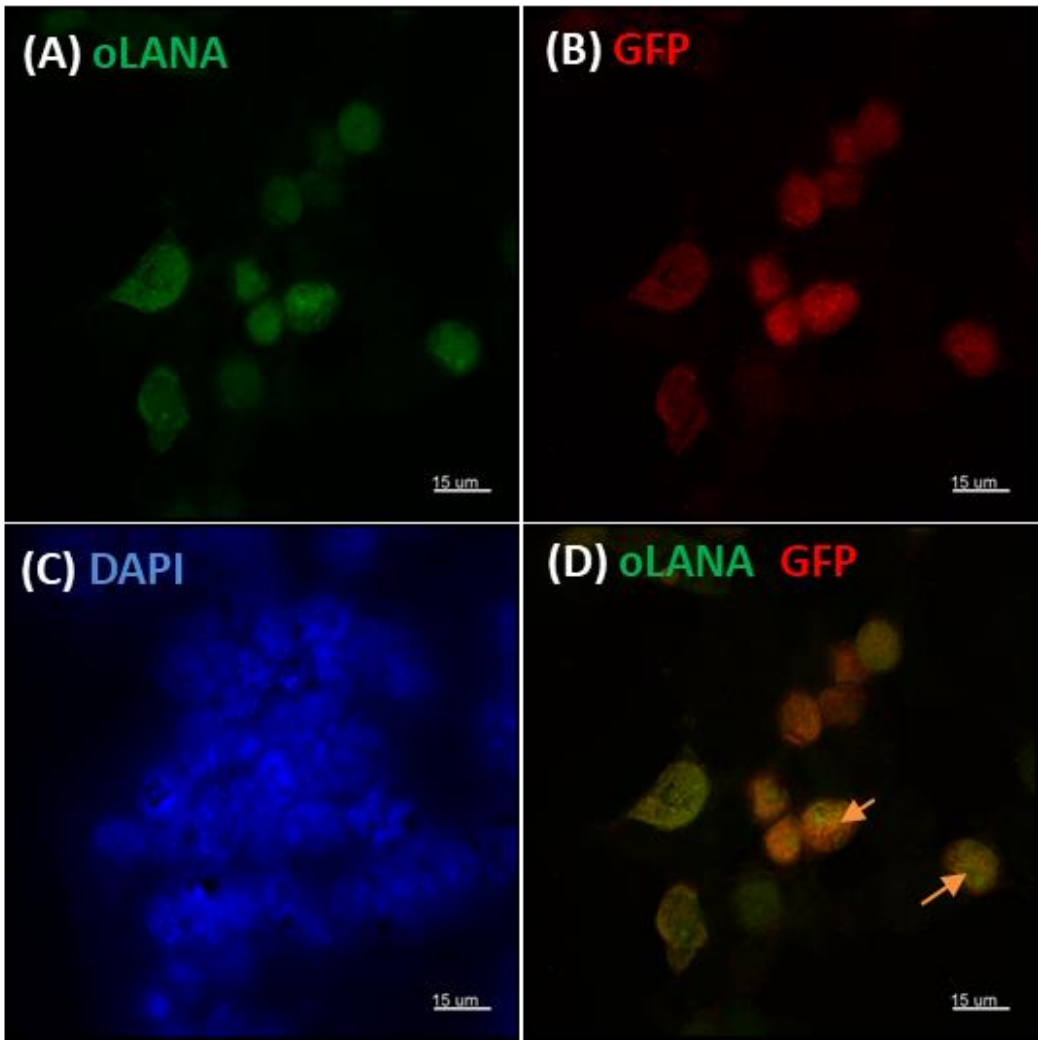


**Figure 3- 23. Colocalisation of GFP-oLANAΔ with anti-GFP.**
HEK 293 T cells were transfected with pMSCV-GFP-oLANAΔ using calicum phosphate. After 24 hr, cells were fixed, permeablised and immunostained using an anti-GFP antibody (Santa Cruz Biotechnology) and Alexa-fluor 594 anti-mouse. Nuclei were stained blue using DAPI and cells then visualised by confocal microscopy. **A:** Green channel **B:** Red channel **C:** Blue Channel **D:** Overlay of green and red pixel intensities. Images are representative of three experimental replicates. Scale bars represent 15µm. The arrows show the overlap areas

### 3.3.1.2 Rad50

As shown in Figure 3-24 and 3-25, Rad50 (Panel B) was diffusely distributed throughout the nucleus as well as present as clear speckles observed in the nuclei of many cells. This pattern was similar to the pattern of oLANA localisation as puncta in the nuclei

(Panel A). Panel D shows that there appeared to be some colocalisation (yellow) of GFP-oLANAΔ and Rad 50.

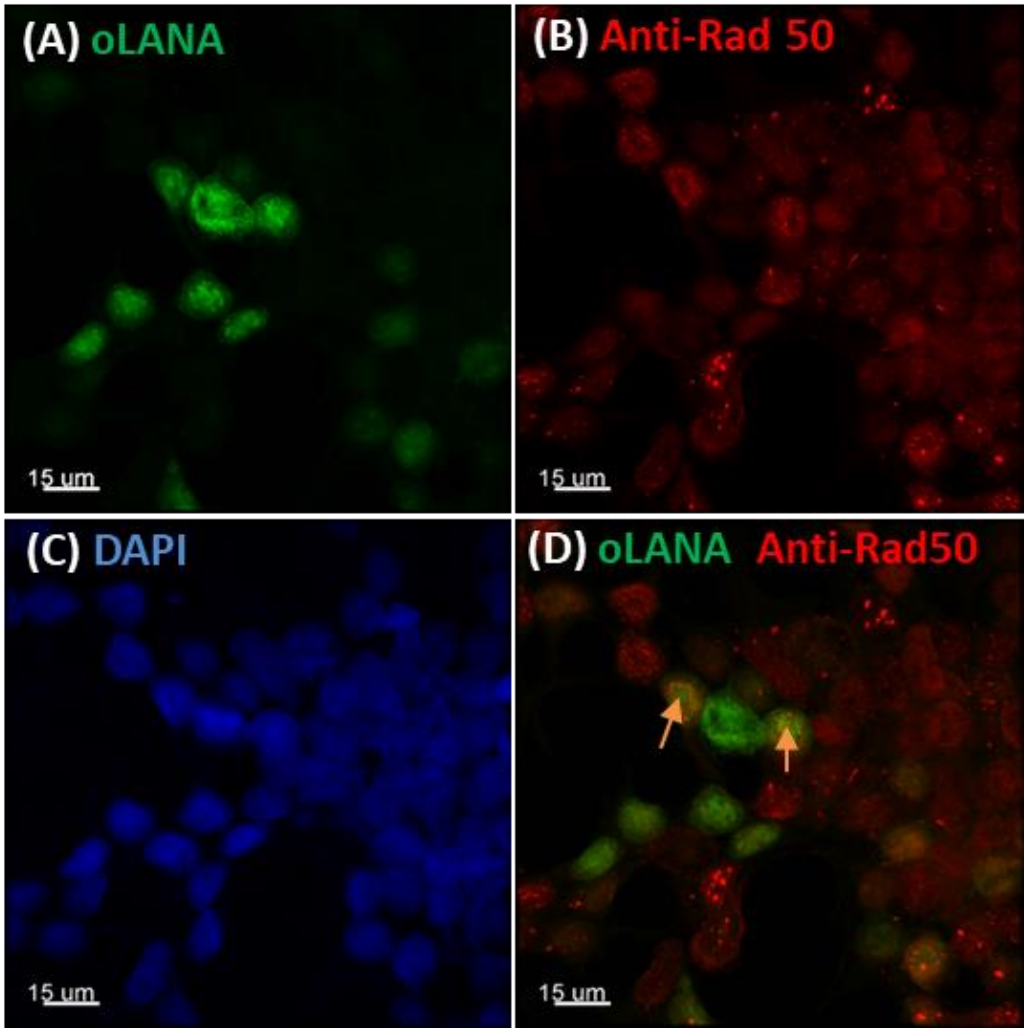


**Figure 3- 24. Colocalisation of GFP-oLANAΔ with Rad50.**
HEK 293 T cells were transfected with pMSCV-GFP-oLANAΔ using calicum phosphate. After 24 hr, cells were fixed, permeablised and immunostained using an anti-Rad50 antibody (Merck) and Alexa-fluor 594 labelled secondary. Nuclei were stained blue using DAPI and cells then visualised by confocal microscopy. **A:** Green channel **B:** Red channel **C:** Blue Channel **D:** Overlay of green and red pixel intensities. Images are representative of three experimental replicates. Scale bars represent 15µm. The arrows show the overlap areas

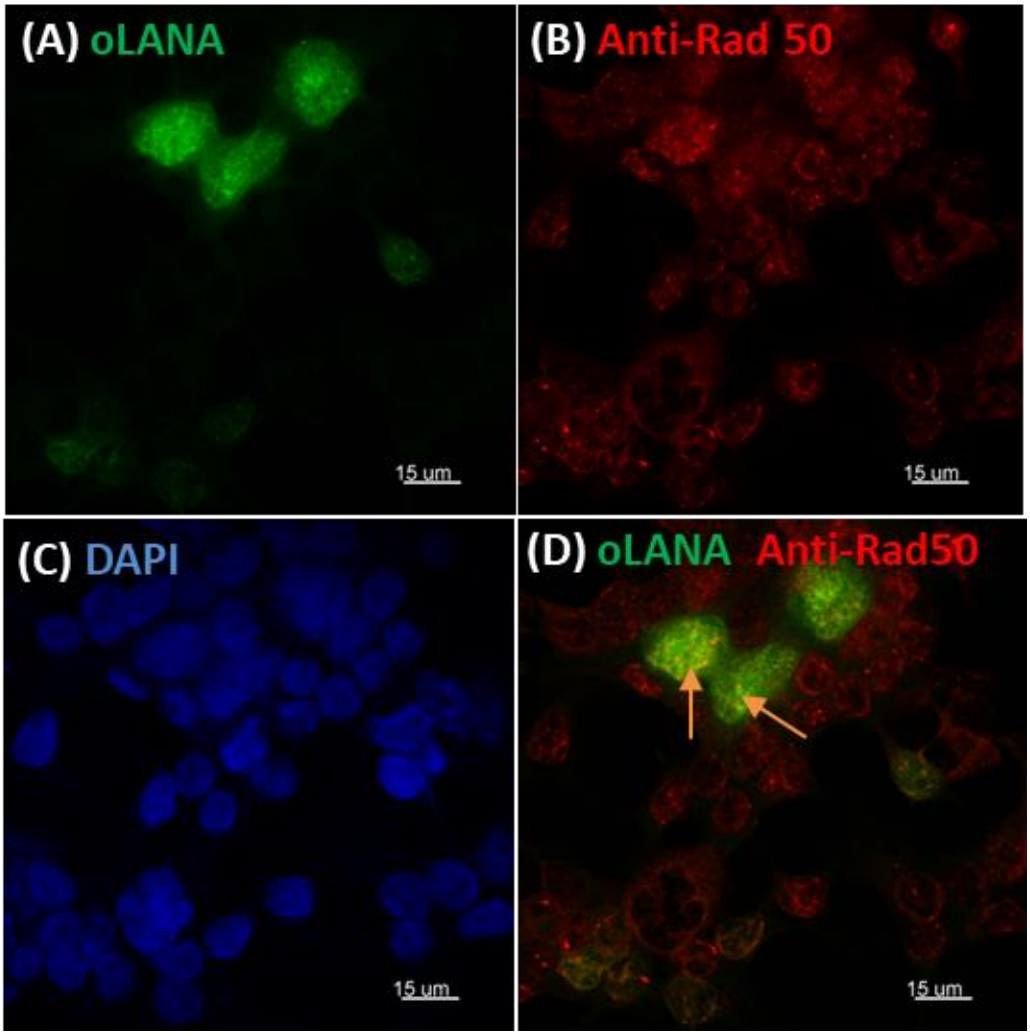


**Figure 3- 25. Colocalisation of GFP-oLANAΔ with Rad50.**
HEK 293 T cells were transfected with pMSCV-GFP-oLANAΔ using calicum phosphate. After 24 hr, cells were fixed, permeablised and immunostained using an anti-Rad50 antibody (Merck) and Alexa-fluor 594 labelled secondary. Nuclei were stained blue using DAPI and cells then visualised by confocal microscopy. **A:** Green channel **B:** Red channel **C:** Blue Channel **D:** Overlay of green and red pixel intensities. Images are representative of three experimental replicates. Scale bars represent 15µm. The arrows show the overlap areas

### 3.3.1.3 CCDC12

As shown in Figure 3-26 and 3-27, CCDC12 appeared to be localised as puncta in the cytoplasm with a much lower more diffuse pattern of staining in the nucleus (Panel B). As the GFP signal was far brighter than the Alexa Fluor 594 is hard to discern any overlap of signal.

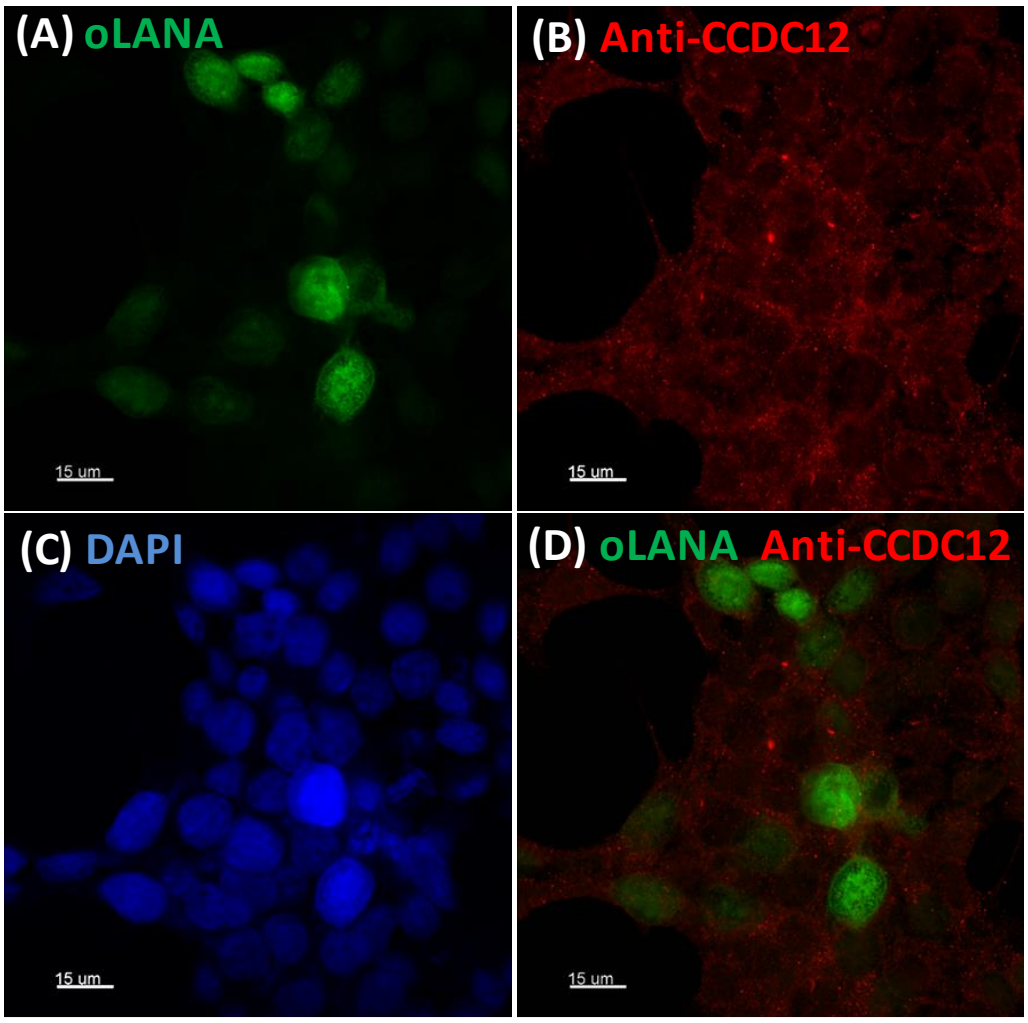


**Figure 3- 26. Colocalisation of GFP-oLANAΔ with CCDC12.**

HEK 293 T cells were transfected with pMSCV-GFP-oLANAΔ using calicum phosphate. After 24 hr, cells were fixed, permeablised and immunostained using an anti-CCDC12 antibody (Sigma) and Alexa-fluor 594 labelled secondary. Nuclei were stained blue using DAPI and cells then visualised by confocal microscopy. **A:** Green channel **B:** Red channel **C:** Blue Channel **D:** Overlay of green and red pixel intensities. Images are representative of three experimental replicates. Scale bars represent 15µm.

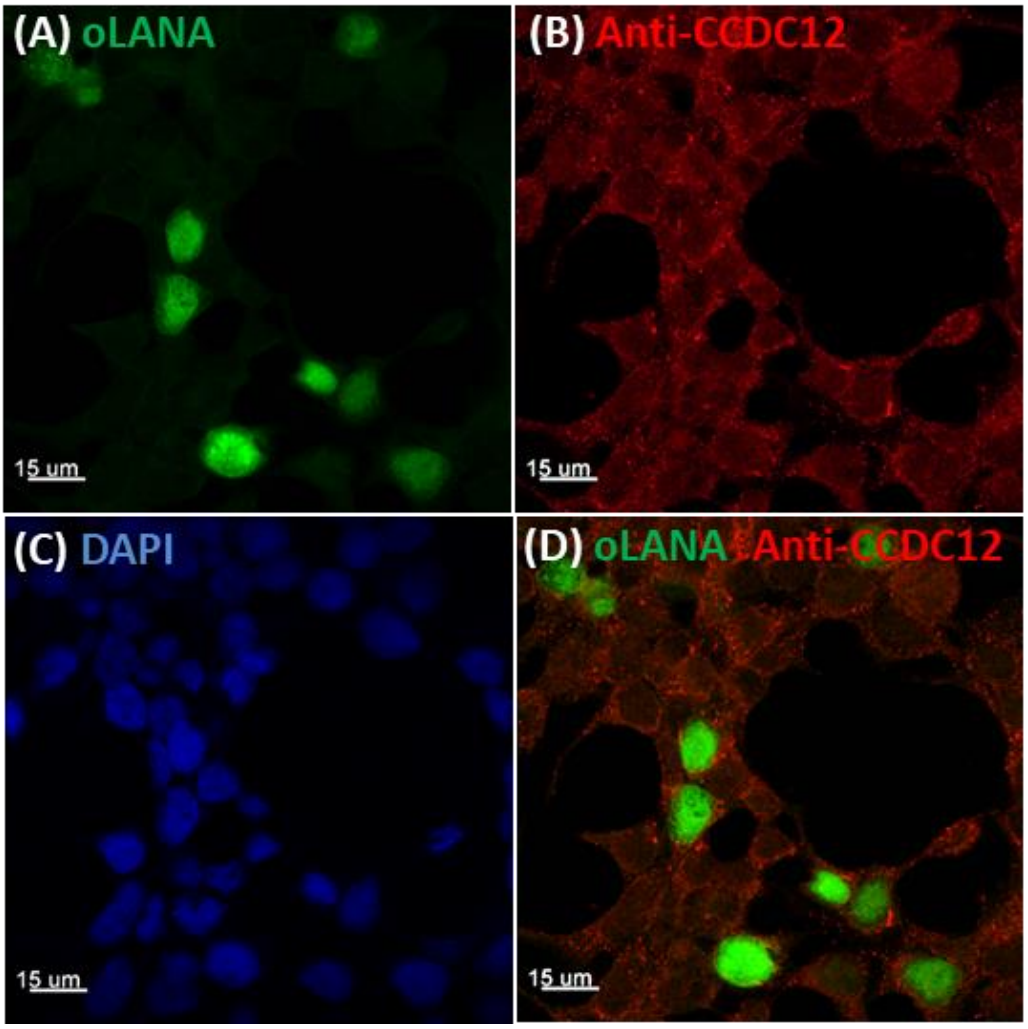


**Figure 3- 27. Colocalisation of GFP-oLANAΔ with CCDC12.**
HEK 293 T cells were transfected with pMSCV-GFP-oLANAΔ using calicum phosphate. After 24 hr, cells were fixed, permeablised and immunostained using an anti-CCDC12 antibody (Sigma) and Alexa-fluor 594 labelled secondary. Nuclei were stained blue using DAPI and cells then visualised by confocal microscopy. **A:** Green channel **B:** Red channel **C:** Blue Channel **D:** Overlay of green and red pixel intensities. Images are representative of three experimental replicates. Scale bars represent 15µm.

### 3.3.1.4 SDF2L1

Analysis of transfected cells using an SDF2L1 antibody (Figure 3-28 and 3-29) showed staining in the cytoplasm and to a lesser extent in nuclei. Although GFP signal from GFP-oLANAΔ was seen in nuclei it was hard to discern any yellow colour indicating overlap in these images by eye.

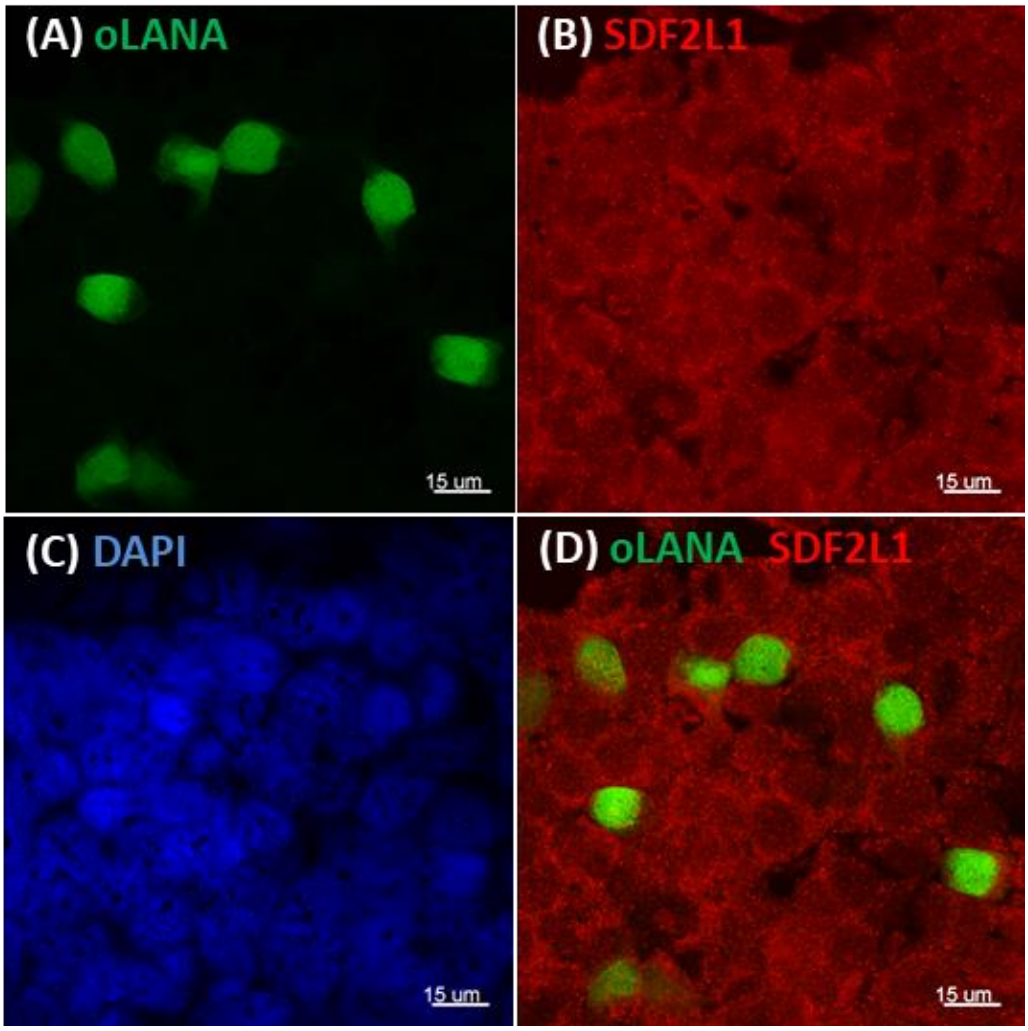


**Figure 3- 28. Colocalisation of GFP-oLANAΔ with SDF2L1.**
HEK 293 T cells were transfected with pMSCV-GFP-oLANAΔ using calicum phosphate. After 24 hr, cells were fixed, permeablised and immunostained using an anti-SDF2L1 antibody (ThermoFisher) and Alexa-fluor 594 labelled secondary. Nuclei were stained blue using DAPI and cells then visualised by confocal microscopy. **A:** Green channel **B:** Red channel **C:** Blue Channel **D:** Overlay of green and red pixel intensities. Images are representative of three experimental replicates. Scale bars represent 15µm.

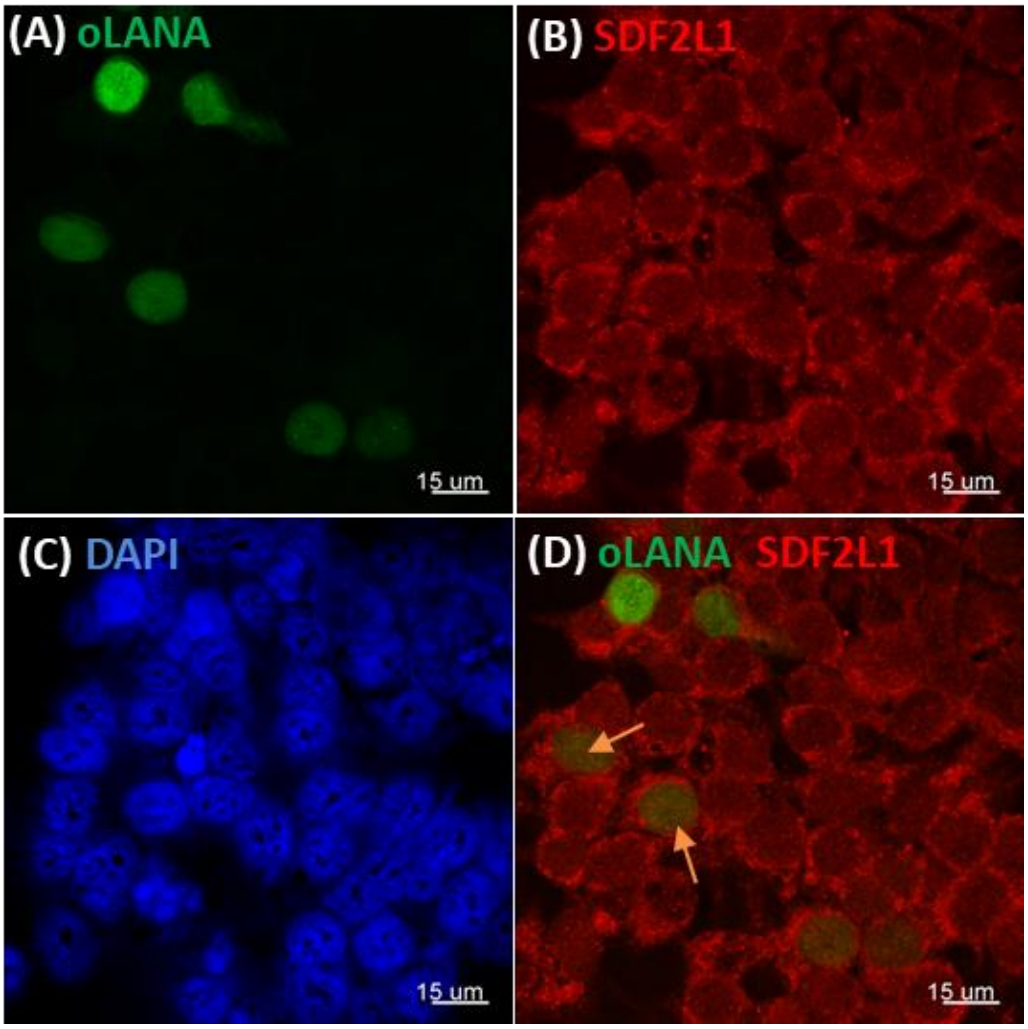


**Figure 3- 29. Colocalisation of GFP-oLANAΔ with SDF2L1.**
HEK 293 T cells were transfected with pMSCV-GFP-oLANAΔ using calicum phosphate. After 24 hr, cells were fixed, permeablised and immunostained using an anti-SDF2L1 antibody (ThermoFisher) and Alexa-fluor 594 labelled secondary. Nuclei were stained blue using DAPI and cells then visualised by confocal microscopy. **A:** Green channel **B:** Red channel **C:** Blue Channel **D:** Overlay of green and red pixel intensities. Images are representative of three experimental replicates. Scale bars represent 15µm. The arrows show the overlap areas

### 3.3.1.5 Histone H1

The results in Figures 3-30 and 3-31 demonstrated that histone H1 was observed in the nuclei of cells as puncta (Panel B). This is a typical distribution for histone H1. GFP-

oLANAΔ protein was localised in a similar pattern in nuclei and there appeared to be good evidence of colocalisation as yellow splecks (Figures 3-30 D and 3-31 D).

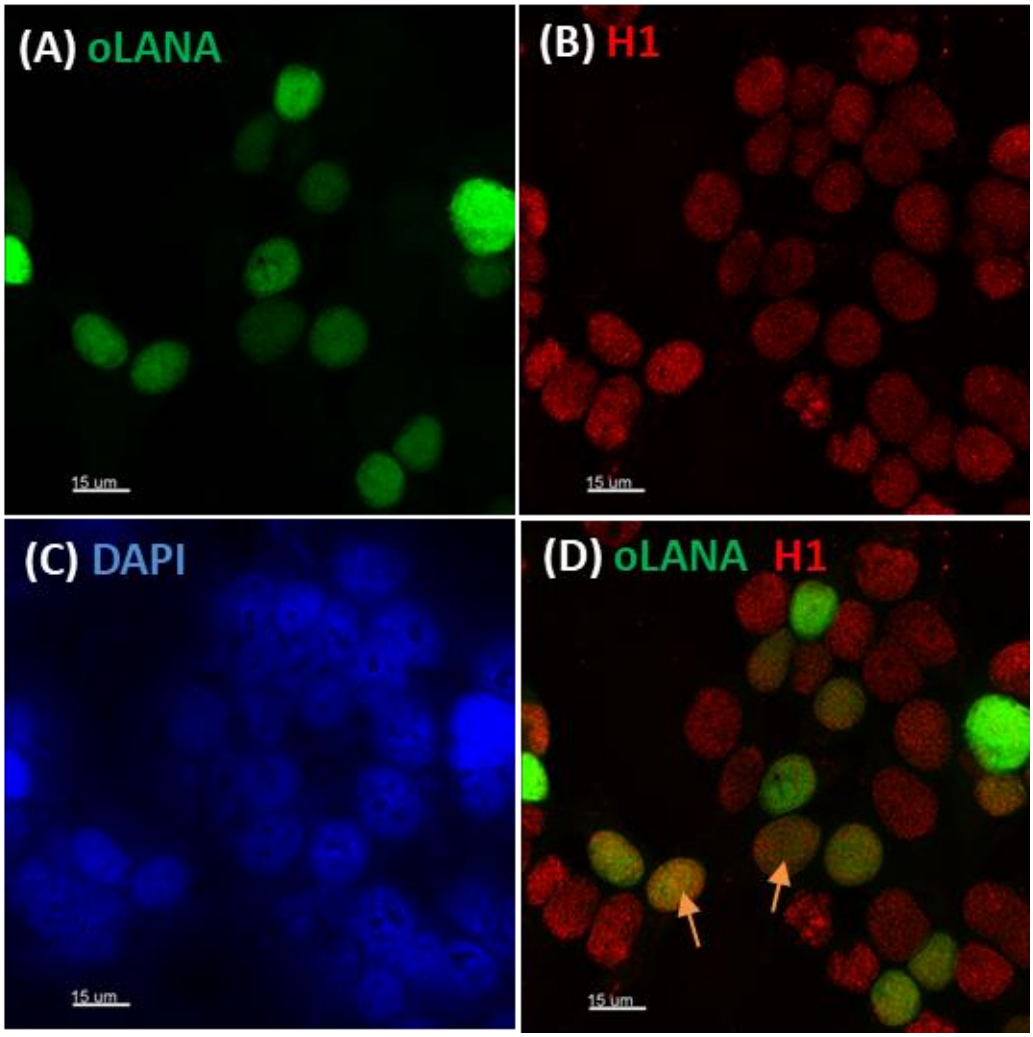


**Figure 3- 30. Colocalisation of GFP-oLANAΔ with Histone H1.**
HEK 293 T cells were transfected with pMSCV-GFP-oLANAΔ using calicum phosphate. After 24 hr, cells were fixed, permeablised and immunostained using an anti-histone H1 antibody (Abcam) and Alexa-fluor 594 labelled secondary. Nuclei were stained blue using DAPI and cells then visualised by confocal microscopy. **A:** Green channel **B:** Red channel **C:** Blue Channel **D:** Overlay of green and red pixel intensities. Images are representative of three experimental replicates. Scale bars represent 15µm. The arrows show the overlap areas

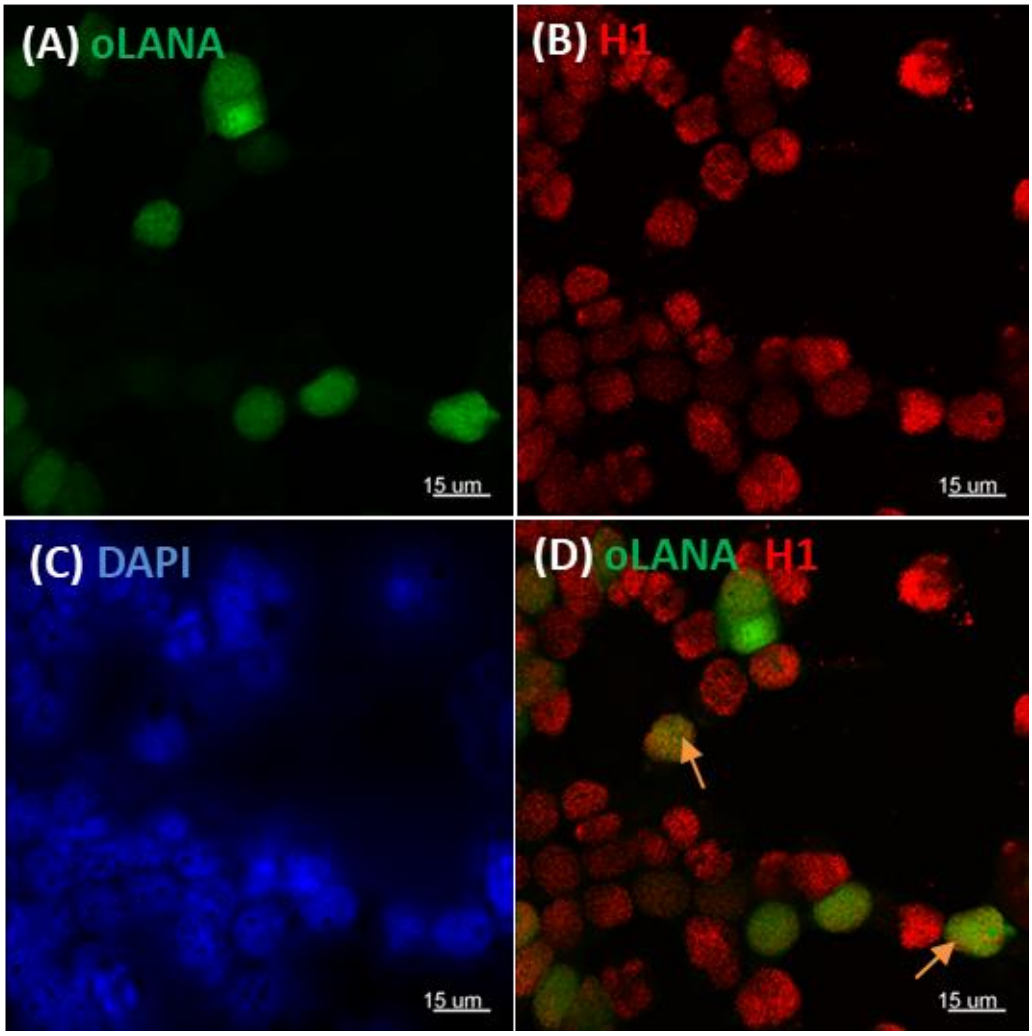


**Figure 3- 31. Colocalisation of GFP-oLANAΔ with Histone H1.**
HEK 293 T cells were transfected with pMSCV-GFP-oLANAΔ using calicum phosphate. After 24 hr, cells were fixed, permeablised and immunostained using an anti-histone H1 antibody (Abcam) and Alexa-fluor 594 labelled secondary. Nuclei were stained blue using DAPI and cells then visualised by confocal microscopy. **A:** Green channel **B:** Red channel **C:** Blue Channel **D:** Overlay of green and red pixel intensities. Images are representative of three experimental replicates. Scale bars represent 15µm. The arrows show the overlap areas

### 3.3.1.6 P53

As shown in Figure 3-32 and 3-33, p53 was localised in puncta in the cytoplasm and to a lesser extent in nuclei (Panel B). The pattern of staining was distinct from GFP-oLANAΔ and there appeared to be little colocalization (panel D).

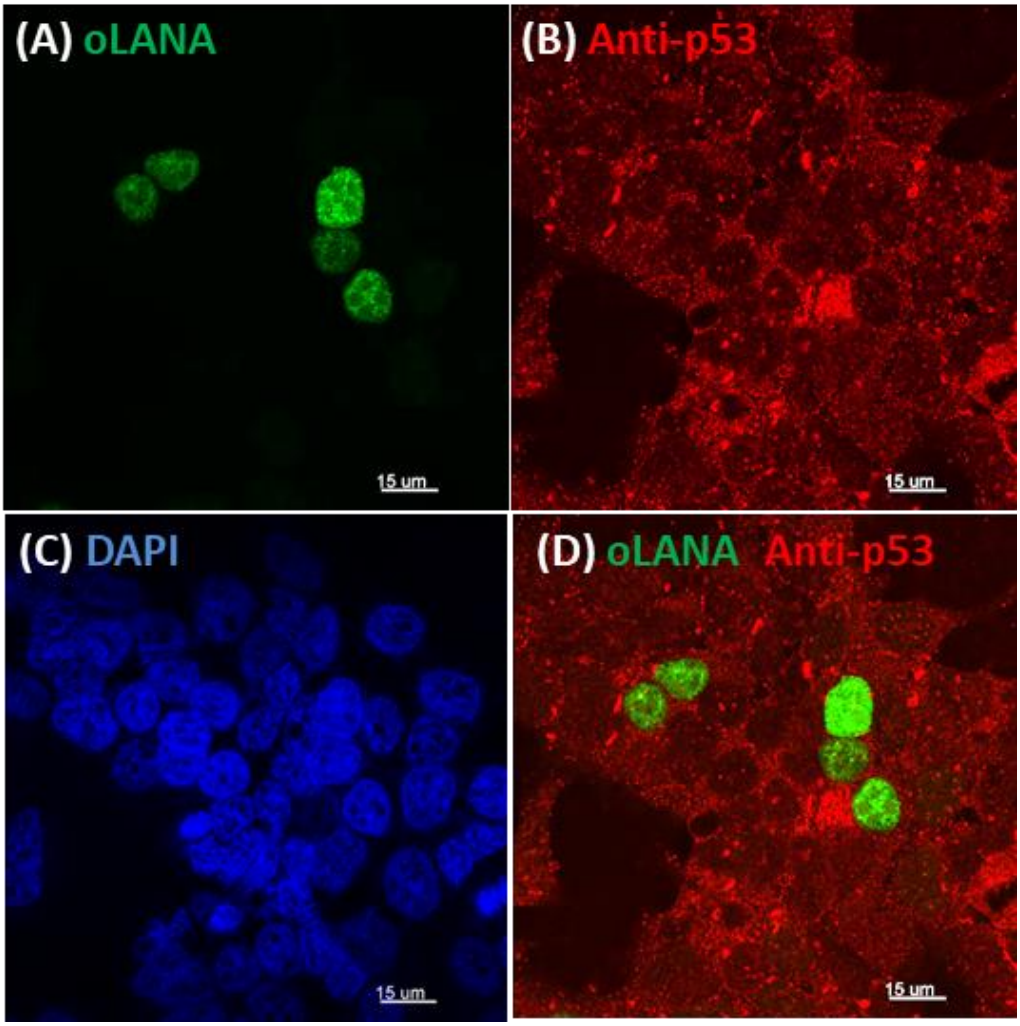


**Figure 3- 32. Colocalisation of GFP-oLANAΔ with P53.**
HEK 293 T cells were transfected with pMSCV-GFP-oLANAΔ using calicum phosphate. After 24 hr, cells were fixed, permeablised and immunostained using an anti-P53 antibody (Sigma) and Alexa-fluor 594 labelled secondary. Nuclei were stained blue using DAPI and cells then visualised by confocal microscopy. **A:** Green channel **B:** Red channel **C:** Blue Channel **D:** Overlay of green and red pixel intensities. Images are representative of three experimental replicates. Scale bars represent 15µm.

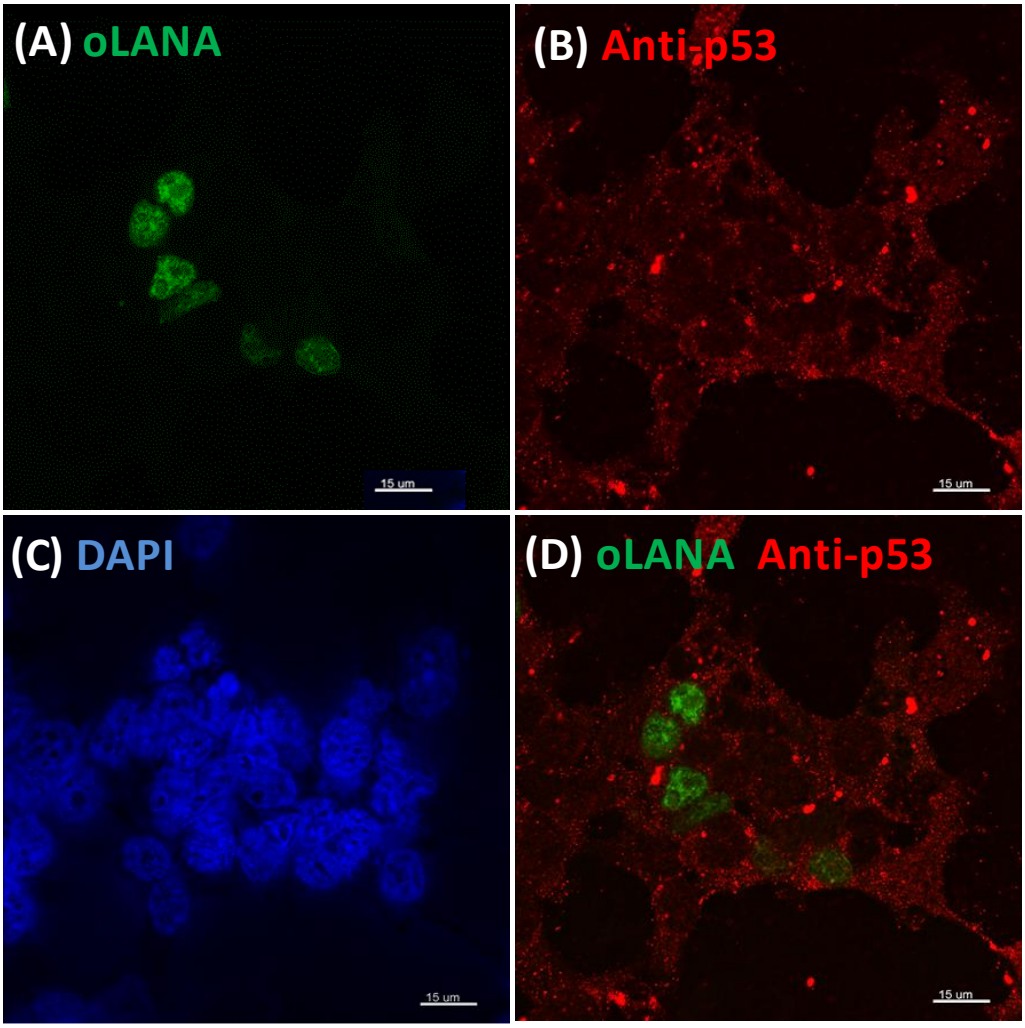


**Figure 3- 33. Colocalisation of GFP-oLANAΔ with P53.**

HEK 293 T cells were transfected with pMSCV-GFP-oLANAΔ using calicum phosphate. After 24 hr, cells were fixed, permeablised and immunostained using an anti-P53 antibody (Sigma) and Alexa-fluor 594 labelled secondary. Nuclei were stained blue using DAPI and cells then visualised by confocal microscopy. **A:** Green channel **B:** Red channel **C:** Blue Channel **D:** Overlay of green and red pixel intensities. Images are representative of three experimental replicates. Scale bars represent 15µm.

### 3.3.1.7 cGAS

As shown in Figure 3-34 and 3-35, cGAS was localised in puncta in the cytoplasm (Panel B). The pattern of staining was distinct from GFP-oLANAΔ and there appeared to be little colocalisation (panel D).

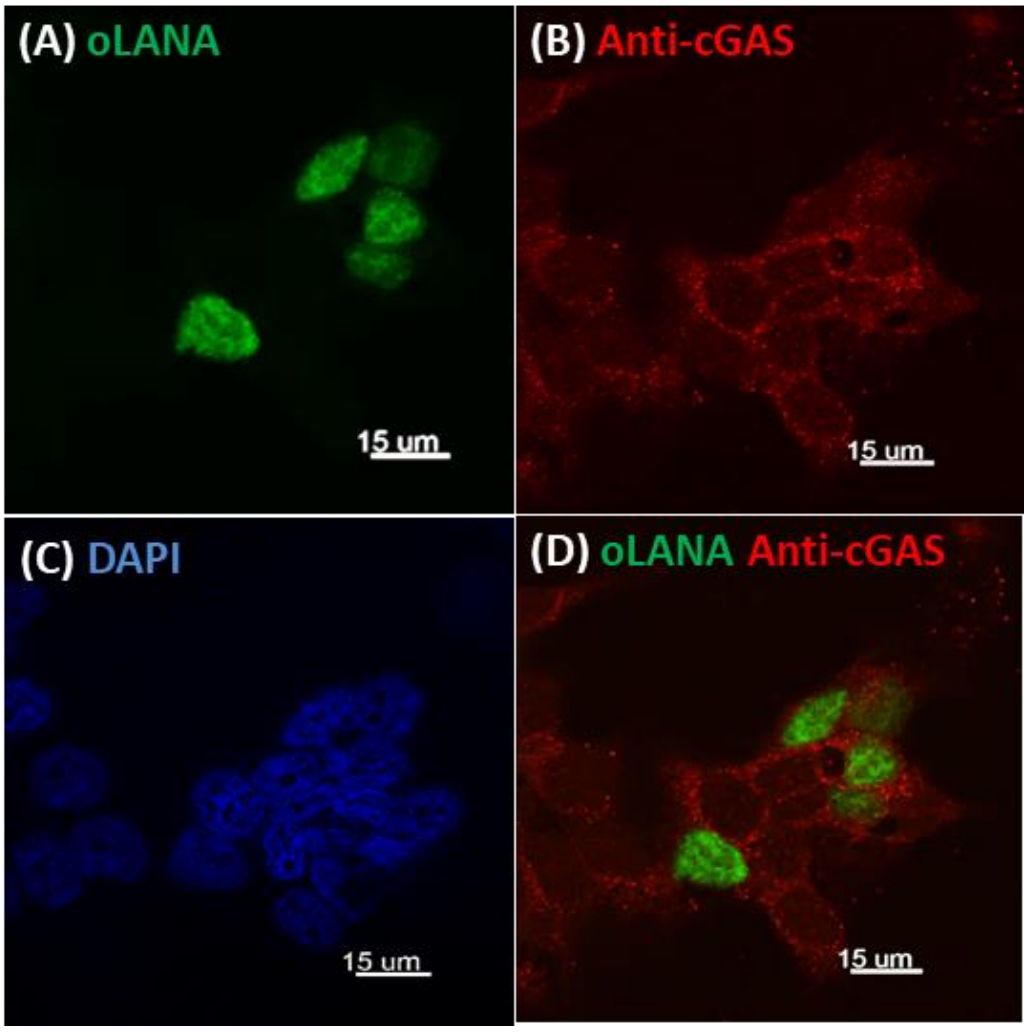


**Figure 3- 34. Colocalisation of GFP-oLANAΔ with cGAS.**
HEK 293 T cells were transfected with pMSCV-GFP-Olanaδ using calicum phosphate. After 24 hr, cells were fixed, permeablised and immunostained using an anti-cGAS antibody (Merk) and Alexa-fluor 594 labelled secondary. Nuclei were stained blue using DAPI and cells then visualised by confocal microscopy. **A:** Green channel **B:** Red channel **C:** Blue Channel **D:** Overlay of green and red pixel intensities. Images are representative of three experimental replicates. Scale bars represent 15µm.

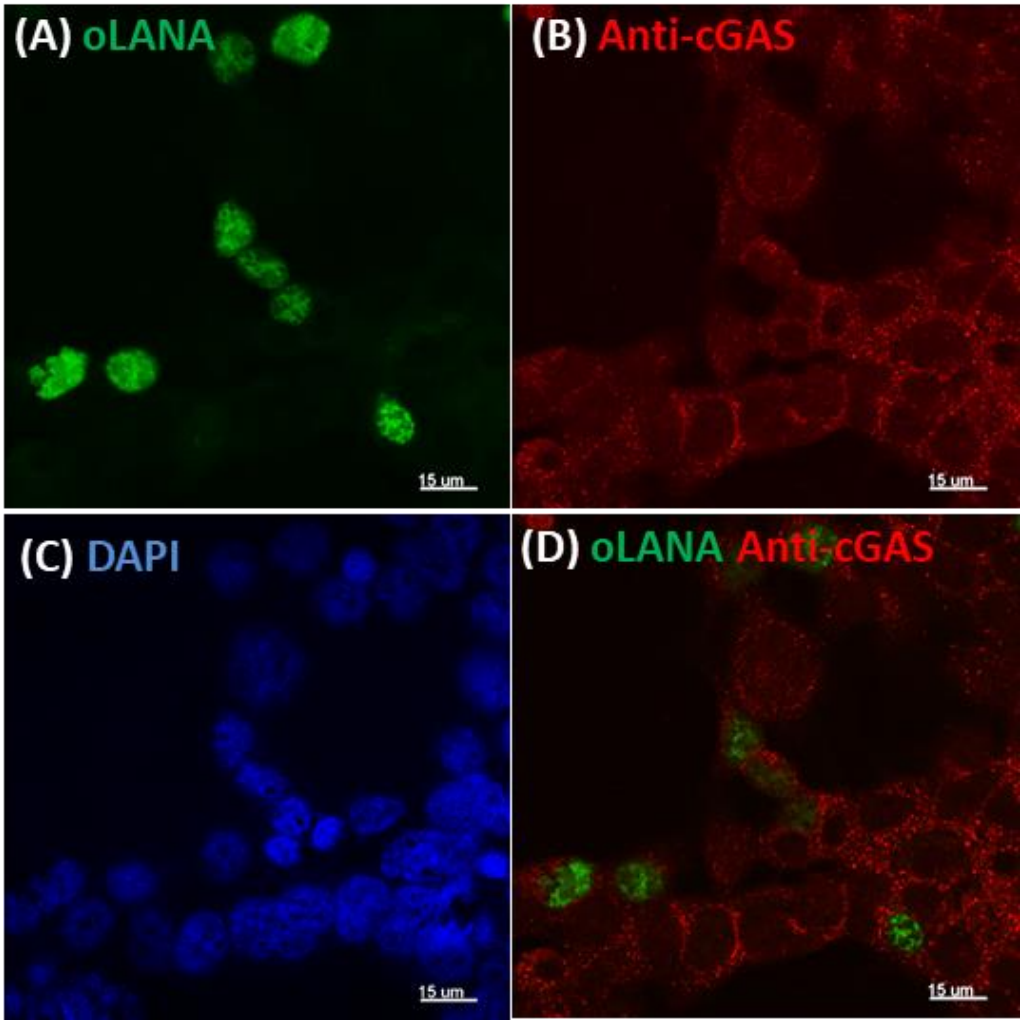


**Figure 3- 35. Colocalisation of GFP-oLANAΔ with cGAS.**
HEK 293 T cells were transfected with pMSCV-GFP-oLANAΔ using calicum phosphate. After 24 hr, cells were fixed, permeablised and immunostained using an anti-cGAS antibody (Merk) and Alexa-fluor 594 labelled secondary. Nuclei were stained blue using DAPI and cells then visualised by confocal microscopy. **A:** Green channel **B:** Red channel **C:** Blue Channel **D:** Overlay of green and red pixel intensities. Images are representative of three experimental replicates. Scale bars represent 15µm.

### 3.3.2 Quantification of coclocalisation of transfected GFP-oLANAΔ protein with cellular proteins

To quanifiy co-localisation between GFP-oLANAΔ and cellular proteins, images generated as in the section above were analysed using Image Pro Premier. The degree of pixel overlap between the green (GFP-oLANAΔ) and red (cellular protein) images was analysed and expressed using Pearson's Correlation. Separate images from three experimental replicates were analysed and the data expressed as a mean. The results (Figure 3-36), showed that the positive control (GFP antibody) as expected had a near perfect correlation between GFP and the antibody (0.8). Looking at cellular proteins, the data show very good coclocalisation of GFP-oLANAΔ and Rad 50 (0.75), CCDC12 (0.56) and histone (0.48). In contrast, there was a much lower level of colocalisation between GFP-oLANAΔ and p53, SDF2L1 and cGAS.

These quantification results generally correlate with the observations made by eye where good overlap was seen between GFP, histone H1 and Rad50. Overlap was not seen by eye for CCDC12 but was picked up by image analysis. Image analysis is far more sensitive and will pick up overlap even when one signal is far greater, as is the case with this antibody.

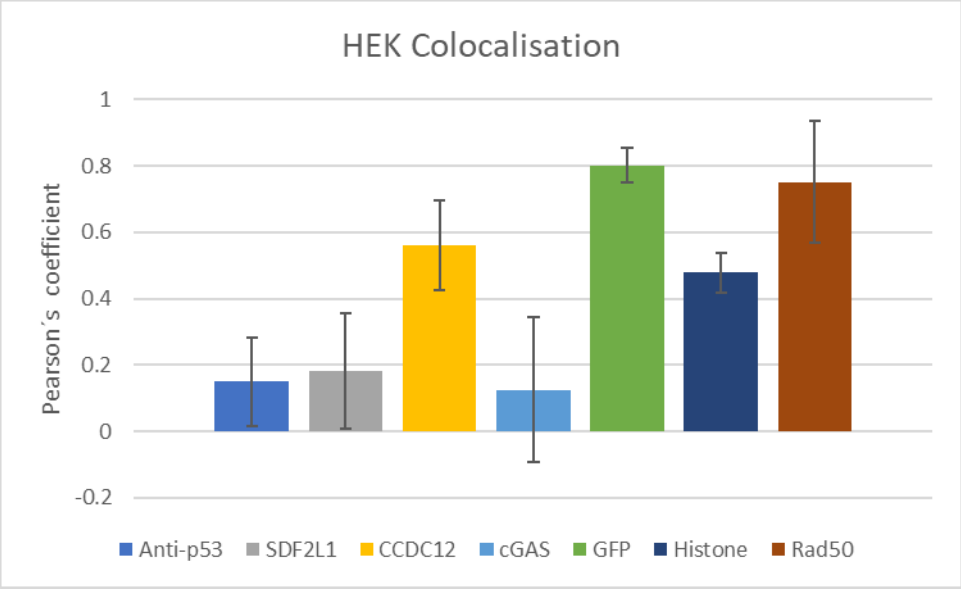


**Figure 3- 36. Quantification of colocalisation between GFP-OLANAΔ and cellular proteins.**
Immunofluorescence images of HEK 293T cells transfected with pMSCV-GFP-oLANAΔ and then stained with antibodies for cellular proteins were analysed using Image Pro Premier software and the Pearson's correlation coefficient was calculated. Y-axis represents the Pearson's correlation coefficient with values shown as the mean Pearson's correlation coefficient for three biological replicates for each antibody ± SD. Values close to 1 represent increased colocalisation.

### 3.3.3 Co-localisation analysis of oLANA and interacting proteins in bovine LGLs

The results above indicated co-localisation of oLANA with cellular proteins. However, this analysis was performed with an GFP-tagged expression construct that lacked the repetitive domain of oLANA. To confirm interactions of full-length oLANA in bovine cells, colocalisation analysis was performed in OvHV-2-infected bovine LGLs (T cells). In this analysis, oLANA was detected by using a polyclonal rabbit antibody to oLANA (Al-Saadi, 2018). This limited the double immunofluorescence to proteins where we either had or could source a mouse monoclonal antibody. These proteins were Rad 50, CCDC12 and anti-histone H1. These were detected using goat anti-mouse Alexa flour 594 (red) and anti-

rabbit-FITC (green)as described in section (2.3.2). The LGL cell line was obtained from infected cattle with SA-MCF which means that these cells carry an oLANA protein.

### 3.3.3.1 Rad50

Figures 3-37 A and 3-38 A showed oLANA distributed as nuclear puncta. Rad50 showed a similar pattern of staining to oLANA (panel B). Figures 3-37 D and 3-38 D showed the clear colocalisation of Rad 50 with the oLANA in the nuclei.

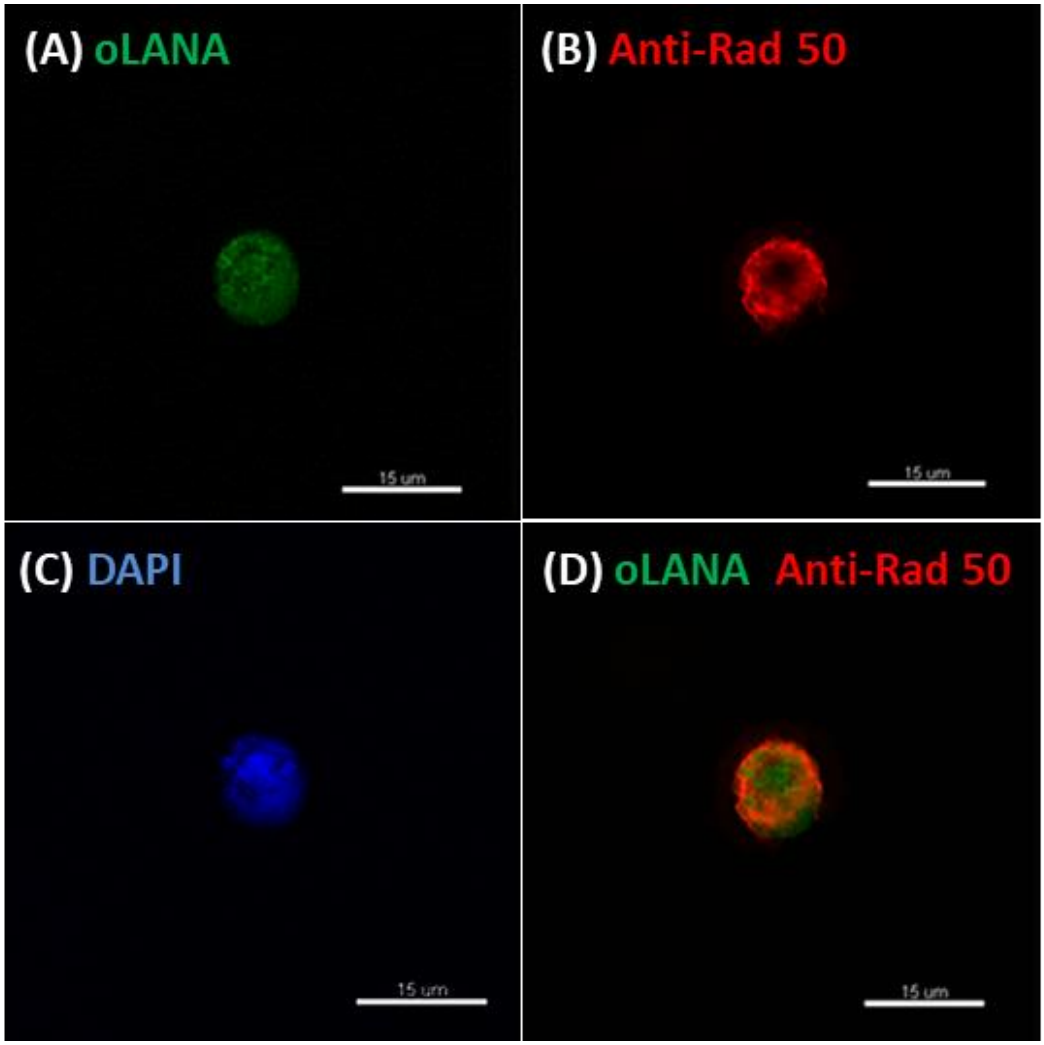


**Figure 3- 37. Colocalisation of oLANA with Rad50.**
LGL cells were fixed, permeablised and immunostained using rabbit anti-oLANA and anti-rabbit FITC as well as anti-Rad50 antibody (Merk) and Alexa-fluor 594 labelled secondary. Nuclei were stained blue using DAPI and cells then visualised by confocal microscopy. **A:** Green channel **B:** Red channel **C:** Blue Channel **D:** Overlay of green and red pixel intensities. Images are representative of three experimental replicates. Scale bars represent 15µm.

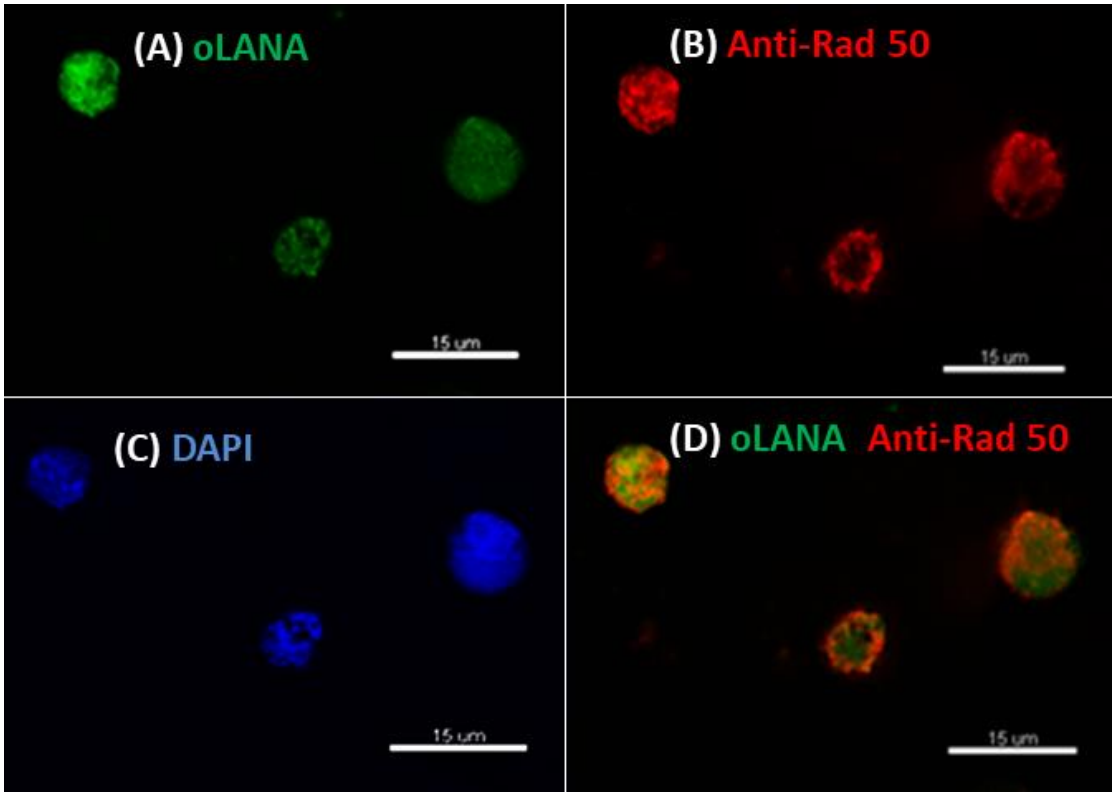


**Figure 3- 38. Colocalisation of oLANA with Rad50.**
LGL cells were fixed, permeablised and immunostained using rabbit anti-oLANA and anti-rabbit FITC as well as anti-Rad50 antibody (Merk) and Alexa-fluor 594 labelled secondary. Nuclei were stained blue using DAPI and cells then visualised by confocal microscopy. **A:** Green channel **B:** Red channel **C:** Blue Channel **D:** Overlay of green and red pixel intensities. Images are representative of three experimental replicates. Scale bars represent 15µm.

### 3.3.3.2 CCDC12

Further immmunoflurescence was performed to idenifiy colocalisation CCDC12 with oLANA in the nuclei of LGL cells. As shown in Figures 3-39 and 3-40, oLANA and CCDC12 discplay a similar pattern of staining in cells and there is also good overlap between the two molecules (Panel D).

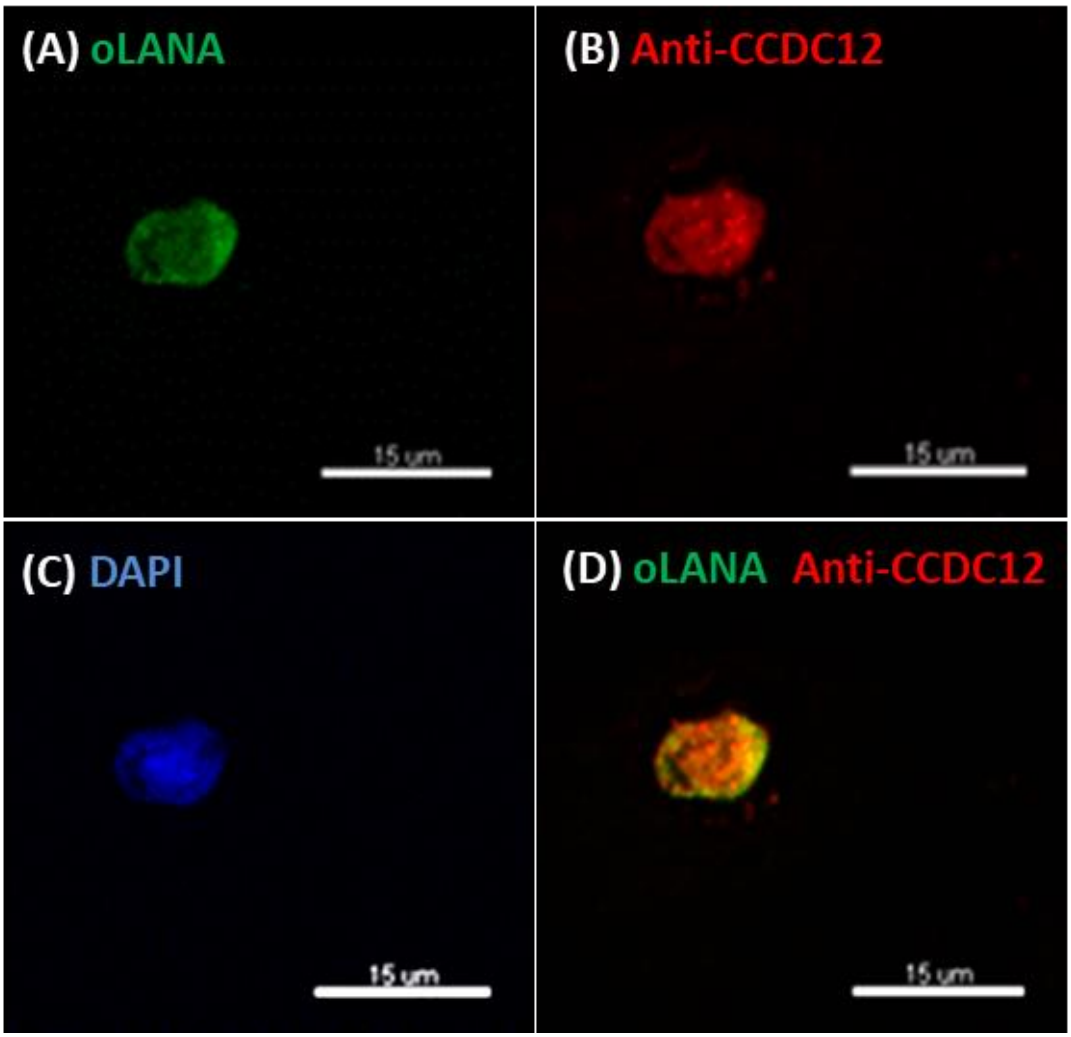


**Figure 3- 39. Colocalisation of oLANA with CCDC12.**

LGL cells were fixed, permeablised and immunostained using rabbit anti-oLANA and anti-rabbit FITC as well as anti-CCDC12 antibody (Sigma) and Alexa-fluor 594 labelled secondary. Nuclei were stained blue using DAPI and cells then visualised by confocal microscopy. **A:** Green channel **B:** Red channel **C:** Blue Channel **D:** Overlay of green and red pixel intensities. Images are representative of three experimental replicates. Scale bars represent 15µm.

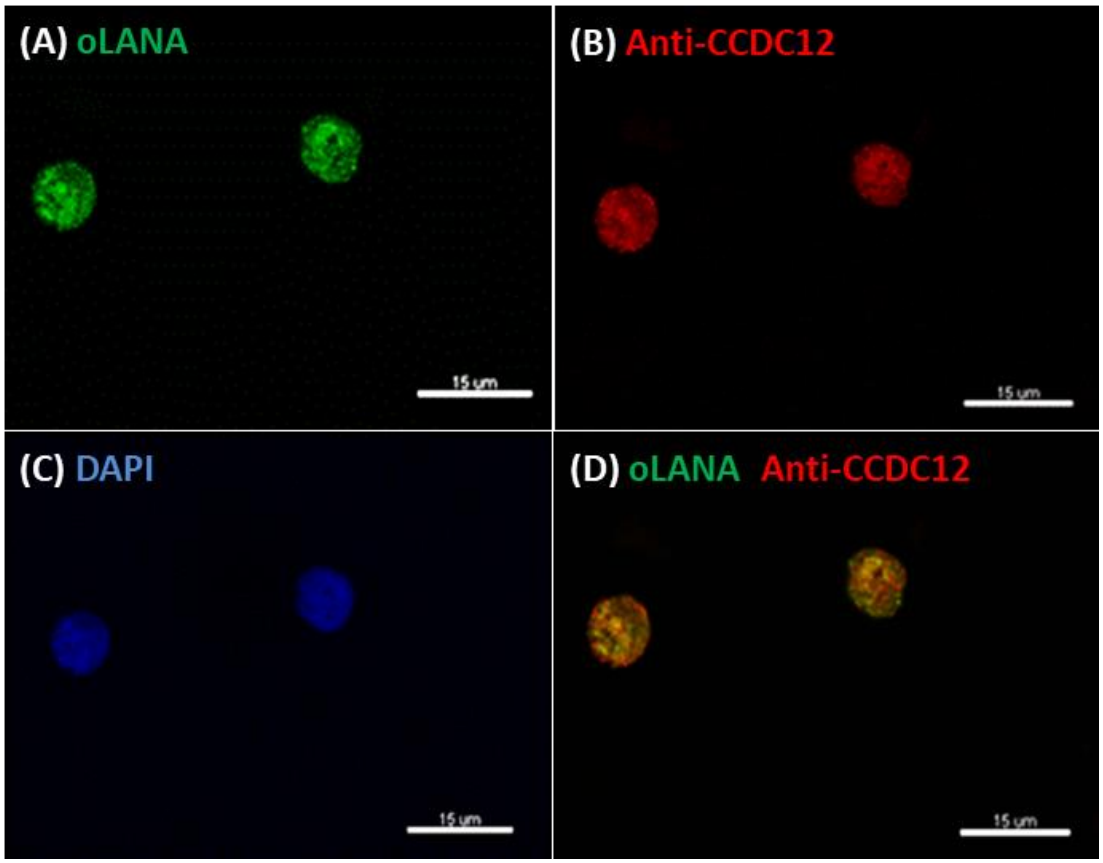


**Figure 3- 40. Colocalisation of oLANA with CCDC12.**
LGL cells were fixed, permeablised and immunostained using rabbit anti-oLANA and anti-rabbit FITC as well as anti-CCDC12 antibody (Sigma) and Alexa-fluor 594 labelled secondary. Nuclei were stained blue using DAPI and cells then visualised by confocal microscopy. **A:** Green channel **B:** Red channel **C:** Blue Channel **D:** Overlay of green and red pixel intensities. Images are representative of three experimental replicates. Scale bars represent 15µm.

### 3.3.3.3 Histone

Finally, as seen in Figures 3-41 and 3-42, we detected high level of nuclear localisation of histone H1 which was similar to the oLANA nuclear localisation in the LGL cells. A definite colocalisation was found between oLANA protein and histone H1 in the nucleus (Panel D).

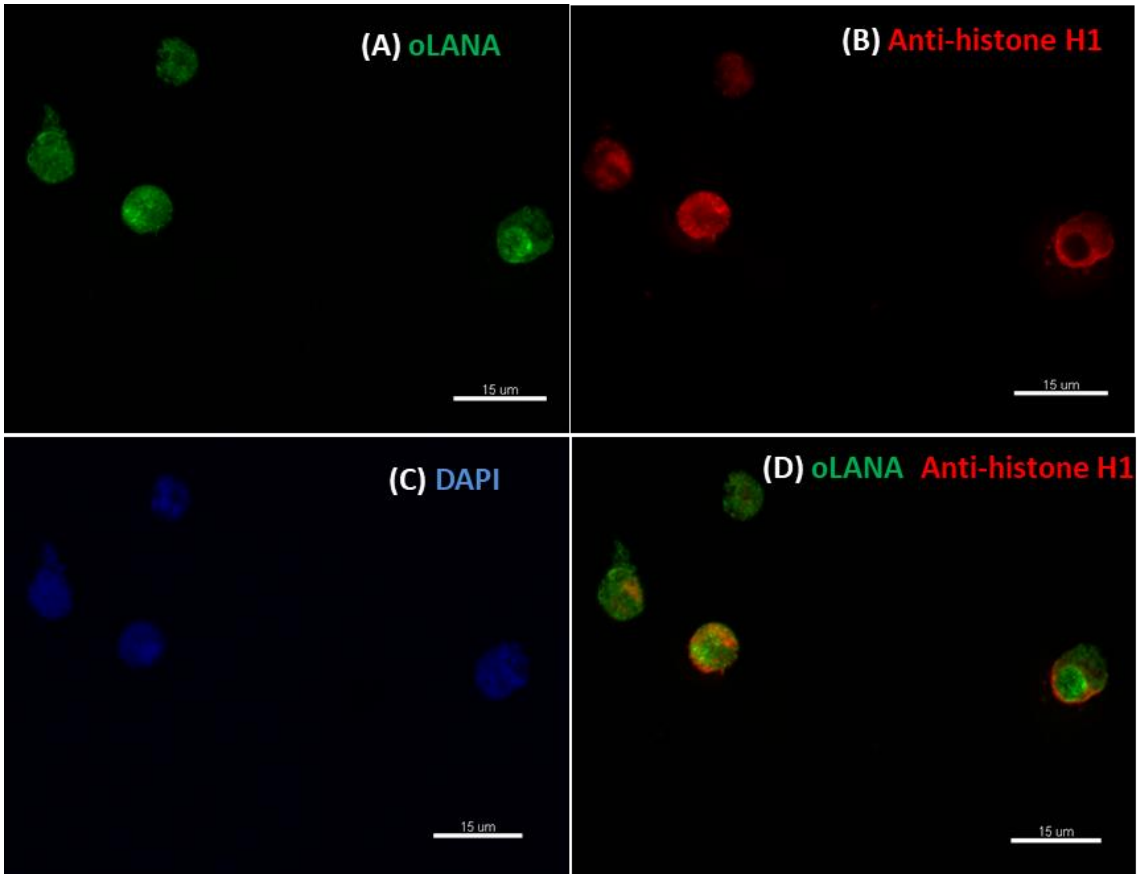


**Figure 3- 41. Colocalisation of oLANA with histone H1.**

LGL cells were fixed, permeablised and immunostained using rabbit anti-oLANA and anti-rabbit FITC as well as anti-histone H1 antibody (Abcam) and Alexa-fluor 594 labelled secondary. Nuclei were stained blue using DAPI and cells then visualised by confocal microscopy. **A:** Green channel **B:** Red channel **C:** Blue Channel **D:** Overlay of green and red pixel intensities. Images are representative of three experimental replicates. Scale bars represent 15µm.

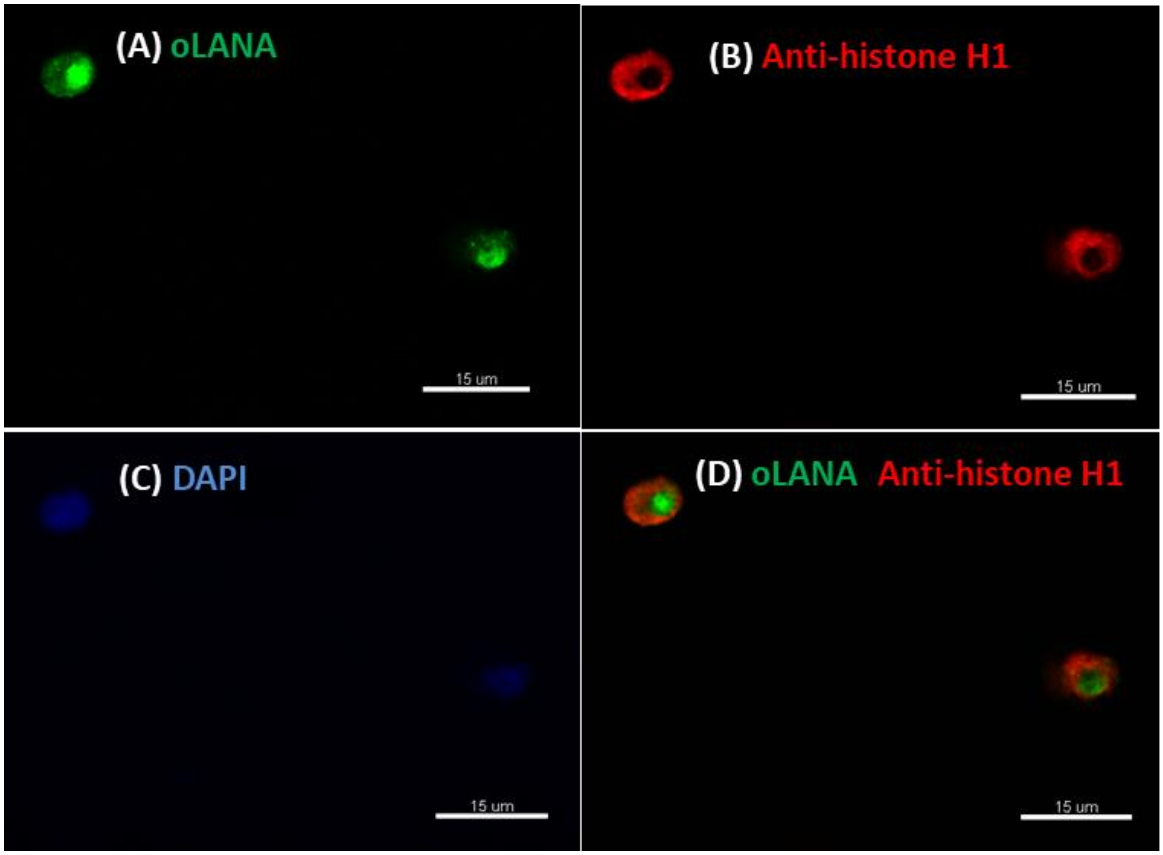


**Figure 3- 42. Colocalisation of oLANA with histone H1.**
LGL cells were fixed, permeablised and immunostained using rabbit anti-oLANA and anti-rabbit FITC as well as anti-histone H1 antibody (Abcam) and Alexa-fluor 594 labelled secondary. Nuclei were stained blue using DAPI and cells then visualised by confocal microscopy. **A:** Green channel **B:** Red channel **C:** Blue Channel **D:** Overlay of green and red pixel intensities. Images are representative of three experimental replicates. Scale bars represent 15µm.

## 3.3.4 Quantification of coclocalisation of oLANA protein with cellular proteins in bovine LGLs

To quanifiy co-localisation between oLANA and cellular proteins, images generated as in the section above were analysed using Image Pro Premier. The degree of pixel overlap between the green (oLANA) and red (cellular protein) images was analysed and expressed using Pearson's Correlation. Separate images from three experimental replicates were analysed and the data expressed as a mean. The results (Figure 3-43), showed that all

cellular proteins had a degree of overlap with oLANA and that this was greatest and least variable for CCDC12 (0.68) than for Rad50 and histone H1. These quantification results generally correlate with the observations made by eye. They also support the observations of colocalisation of GFP-oLANAΔ with all these molecules. CCDC12, Rad50 and H1 are all therefore strong candidates for oLANA interacting proteins and warrant future investigation.

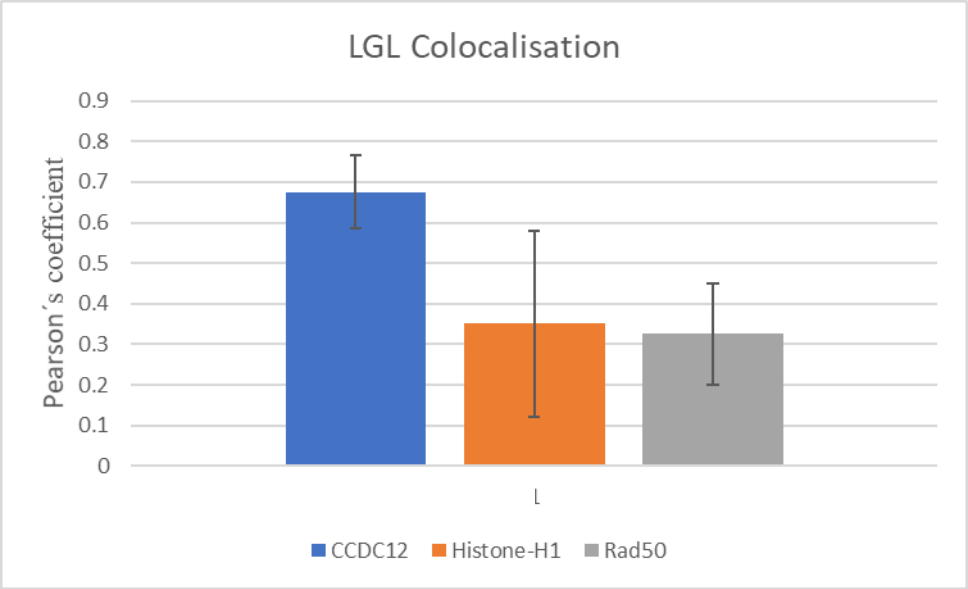


**Figure 3- 43. Quantification of colocalisation between oLANA and cellular proteins.** Immunofluorescence images of LGLs stained with antibodies for oLANA and cellular proteins were analysed using Image Pro Premier software and the Pearson's correlation coefficient was calculated. Y-axis represents the Pearson's correlation coefficient with values shown as the mean value coefficient for three biological replicates for each antibody ± SD. Values close to 1 represent increased colocalisation.

# Chapter Four: Discussion and Conclusion

# 4.1 Discussion

Malignant catarrhal fever (MCF) is a fatal disease, and the pathogenesis of MCF is not precisely understood. In spite of the importance of SA-MCF, until recently little research has been conducted with OvHV2 because there are no OvHV2 isolates available for research due to challenges with the virus isolation (Coulter *et al.*, 2001) and a lack of tools to study the virus (Ackermann, 2005b). However The availability of the complete genome sequence of OvHV-2, has made it possible more recently to initiate molecular studies of this virus (Hart *et al.*, 2007).

This project was undertaken to understand the pathogenesis of MCF further by evaluating the role of OvHV-2-oLANA and its interactions with cellular proteins. KSHV LANA is one of the major viral proteins expressed in virus latency, and it is essential for the replication and persistence of the viral episome during latent infection (Si *et al.*, 2008), particularly in proliferating cells. KSHV LANA recruits a number of molecules to regulate replication of cells, modulate the host response and it mediates the segregation of the newly synthesized genome copies to daughter nuclei during latency by tethering to the host chromosomes (Verma *et al.*, 2006). LANA has homologues in all gammaherpesviruses but their sequences are quite divergent and they are different sizes. In spite of this they all retain many of the functions that have been identified for KSHV LANA and they all contain a central highly repetitive domain (Domsic *et al.*, 2013; Uppal *et al.*, 2014). It was therefore assumed at the start of this project that the OvHV-2 oLANA protein also retained functions and similar cellular binding partners as the prototypic KSHV LANA. Indeed, work

in a previous PhD project has shown that, like all other LANA proteins studied to date, oLANA is localised in puncta in the nucleus of OvHV-2 infected cells (Al-Saadi, 2018).

In order to determine the potential role of oLANA protein in MCF pathogenesis, it was necessary to identify the presence of protein binding partners in cells. The approach taken was to express a recombinant oLANA fused to GFP, use this to pull down cellular partners using GFP-trap technology and then analyse co-precipitants by mass spectrometry. The central repetitive domain of KSHV LANA inhibits translation of the protein (Mariggiò *et al.*, 2017) and most of the interactions of KSHV are localised to the N- and C- terminal non-repetitive domains. So, an approach to studying KSHV LANA has been to utilise a deleted version of the protein lacking the central repetitive domain to maximise expression levels and hence the chances of identifying binding partners (Zhang *et al.*, 2016b). A codon-optimised GFP-oLANA lacking the central repetitive domain (GFP-oLANAΔ) was therefore used as bait in this project. Using this approach, eight oLANA-interacting proteins in HEK293T cells were identified by co-precipitiation and MS. Of these, only histone H1 was confirmed by co-immunoprecipitation and western blotting. Two others (CCDC12 and Rad50) were shown to co-localise with oLANA

## 4.1 Construction of recombinant retroviruses

The original aim was to use a recombinant retrovirus based on the murine stem cell retrovirus (MSCV) to deliver GFP-oLANAΔ- to bovine T cells and study interacting proteins. Retroviruses have many distinct advantages over other vectors, especially when permanent gene transfer is the preferred outcome. They can be 'pseudotyped' to contain alternative envelope glycoproteins and so efficiently infect a wide range of cells. However,

the use of retroviruses as a delivery tool for gene therapy is often limited by relatively low levels of virus production (Weber *et al.*, 2001).

The retrovirus chosen for these studies, MSCV has been used with great effect to deliver and express genes in a wide range of mammalian cells, in particular cells that are difficult to transfect such as T cells. The recombinant MSCV was generated using a three-plasmid system one containing the retroviral backbone (LTR, packaging signal and the GFP-oLANAΔ) one containing Gag and Pol and a third containing the VSV G protein to allow infection of most cell types. These were then transfected into HEK 293T cells to generate virus. HEK 293T cells are able to produce infectious retroviral stocks within 24 h after transfection and without selection. Retroviral stocks of high titres are necessary for efficient introduction of recombinant genetic material into target cells and ideally for the GFP-trap/MS technique to be successful >80% of the cells need to contain the bait protein. Unfortunately, the titre of the virus stocks generated on NIH3T3 cells was low and insufficient to efficiently infect the cells in a large target population. Improvements were made to the protocols by removing endotoxin from the plasmid DNA stocks and modifying the transfection protocols but the percentage of transduced cells was still too low. In the interests of time, this approach was not followed further. Future improvements might include testing different batches of HEK 293T cells from different sources as there may be variability in their ability to produce retrovirus. Also, an established protocol for transfection of the 3 plasmids was followed, but optimisation of the amounts of DNA of each plasmid may lead to improved yields. Finally large preparations of virus could be produced and then concentrated down to produce a more potent stock.

## 4.2 Transfection into HEK 293T cells

In the absence of an efficient method of delivery into bovine T cells, it was decided to use the more conventional method of transfection into HEK 293T cells. A codon-optimised GFP-oLANAΔ gene was cloned into the pMSCV-IRES-GFP vector as this would work well for expression in HEK 293T cells as well as possible future retroviral construction. Using this vector, GFP-oLANAΔ protein was strongly expressed in HEK 293T cells 24 h post transfection and was predominantly located in the nucleus of the cells. The nuclear localisation of GFP-oLANAΔ is not surprising as, like other LANA proteins, the sequence has two nuclear localisation signal sequences as predicted using the NucPred algorithm (Brameier *et al.*, 2007).

Western blotting was performed on lysates from transfected and immunoprecipitated samples. The fusion protein was apparent as a band at 47 kDa which corresponds to the predicted molecular weight, thus confirming the expression of GFP-oLANAΔ. The transfection efficiency is subjective and prone to many variable factors, such as cell cycle progression, the biological processes of gene expression activity, general activity of specific cell type and the reagent type. These factors can affect and inhibit the expression of the transfected DNA (Kim and Eberwine, 2010). The results presented here demonstrate that at 24 h post-transfection the fusion protein was present and abundant. However, the signal level was different between biological replicates. Nevertheless the overall signature of the response was similar and significant when observed by fluorescence microscope. Several important factors, such as the DNA quantity and quality, cell type, cell health, and transfection method (as stated above) affect transfection results also (Pfeifer and Verma, 2001).

## 4.3 GFP-trap and MS identification of oLANA-interacting proteins

Co-immunoprecipitation experiments using GFP-oLANAΔ and LC MS/MS identified 8 potential oLANA interacting proteins. Mass spectrometry is a primary tool for protein identification and is used to detect the multiple reaction of a peptide with greater sensitivity because the precursor ion is not detected in the full mass spectrum (Domon and Aebersold, 2006). The data gathered from proteomic analysis provides information on GFP-oLANAΔ relationships. A number of compromises were made in the proteomic study, including the number of replicates, quantitative nature of the mass spectrometry and cell line in which the immunoprecipitation was performed. In addition, the over-fitting due to detection of hundreds of proteins in small sample sizes which may easily lead to false correlations and over-interpretation of proteomic data (Borrebaeck, 2012). There were a large number of proteins identified that were present in immunoprecipitation samples. Although the protein score does approximately relate to the abundance of the protein such as number of peptides matching the protein are taken into consideration. In this analysis, there are a number of proteins that have a differential protein score of more than two-fold in the GFP-oLANAΔ sample compared to the control. There were also a large number of ribosomal proteins identified in GFP-oLANAΔ samples. Also, worth noting was the fact that GFP-oLANAΔ had a low protein score (The sum of the ion scores of all peptides that were identified).

Co-immunoprecipitation experiments using GFP-oLANAΔ identified 8 potential oLANA interacting proteins. Of these, only histone H1 is known to interact with other LANA proteins (Zhang *et al.*, 2016b). It was decided to follow up on a subset of these 8 proteins,

histone H1, CCDC12 and SDF2L1 as these has potentially interesting functions and there were antibodies readily available for further studies.

## 4.4 Confirmation of oLANA interactions

Interactions between oLANA and cellular proteins were tested by co-immunoprecipitation using GFP-oLANAΔ and western blotting using specific antibodies. Co-localisation of the proteins by confocal microscopy was also performed using GFP-oLANAΔ-transfected cells as well as OvHV-2 infected bovine LGLs. As well as the three interacting proteins identified by GFP-trap, we tested association between oLANA and p53, cGAS and Rad50 as these proteins have recently been identified as interacting with KSHV LANA and have functions critical for KSHV pathogenesis (Zhang *et al.*, 2016b).

Importantly, it was observed that the GFP-oLANAΔ fusion protein has affinity to some chromosomal proteins including histone-H1. Following the initial observation that GFP-oLANAΔ interacts with histone-H1 it was shown that histone H1 co-immunoprecipitated with oLANAΔ. GFP-oLANAΔ and native oLANA in LGL cells was also shown using confocal microscopy to co-localise with H1 in nuclear puncta. KSHV LANA was shown to bind to linker histone, H1 which was proposed to be required for tethering onto the host chromosome (Verma *et al.*, 2013). Further studies were carried out by Shinohara *et al.* (2002a) to determine whether a chimeric KS-LANA with histone H1 could be targeted to host chromosome and persist over multiple cell divisions. The results of the study showed that LANA deleted for aa 1–22 were unable to target to chromatin and replicate terminal repeat (TR) containing plasmids, whereas Δ1–22 aa LANA fused with histone H1 bound to chromosomes as well as supported replication.

The results presented here suggest that oLANA may have a similar function to other LANAs in associating with chromatin and tethering the viral genome. Further studies would be required to formally show this. In addition, chromatin immunoprecipitation assays with sequencing could be used to determine the binding sites for GFP-oLANAΔ in order to study OvHV-2 control of gene expression.

In this study the endo reticulum localised protein SDF2L1 was identified by GFP-trap as associating with oLANA. SDF2L1 is an ER-resident protein found in diverse cells and tissues, It has an N-terminal 28 amino acid residue hydrophobic signal sequence and a C-terminal HDEL sequence for ER-retention (Bies *et al.*, 2004). It could not be detected in co-IP/western blot assays as associating with oLANA and did not co-localise by immunofluorescence. Thus, the association between oLANA and SDF2L1 was not confirmed. Likewise, CCDC12 was identified by GFP-trap as associating with oLANA. A coiled coil is a motif constituted of α-helices that are coiled together like the strands of a rope, is found in many proteins, including transcription factors and signaling molecules. More recently, coiled coils have emerged as a unifying structural feature of several protein complexes that maintain spatial genome organization and DNA stability (Mason and Arndt, 2004). It could not be detected in co-IP/western blot assays as associating with oLANA but did co-localise with it by immunofluorescence in both GFP-oLANAΔ-transfected cells and LGLs. Thus, while oLANA-CCDC12 associations were not definitively confirmed by co-IP western, the co-localisation suggests that there may be some interactions that are potentially interesting and require further investigation. We suppose that CCDC12 maintains the stability and genome organization of the LANA protein during cell mitosis (Mason and Arndt, 2004).

KSHV LANA has been associated with many proteins (Radkov *et al.*, 2000). Several studies have shown that LANA in KSHV associates with tumour suppressor p53, and it inhibits p53-dependent transcription and apoptosis, and it has been demonstrated that LANA modulates p53-dependent pathways to prevent cell cycle arrest and apoptosis (Borah *et al.*, 2004; Si and Robertson, 2006; Petre *et al.*, 2007; Sarek *et al.*, 2007; Jia *et al.*, 2010). In contrast with these studies in KSHV it was found that GFP-oLANAΔ did not co-precipitate with p53 in western Immunoblot or co-localise in cells. A potential confounding factor is the status of the p53 gene in HEK 293T cells, which has a mutation in the amino acid sequences and may mean that GFP-oLANAΔ- p53 interactions are negated (Sarek *et al.*, 2007).

A further interacting protein with KSHV LANA is cGAS (Zhang *et al.*, 2016b). As shown in chapter three, cGAS protein was not detected in western blot for IP lysate cell or co-localising with oLANA. A subsequent literature search highlighted that Orzalli *et al.* (2015) were unable to detect a band corresponding to cGAS protein in HEK 293T cells when they examined the basal levels of cGAS protein in HEK293T cells in comparison with other different human cell lines by 'name technique'. Thus, it is still undetermined if oLANA can interact with cGAS in other more related cells and future work should investigate this further using cell lines in which the expression of cGAS has been confirmed. Further study by Zhang *et al.* (2016b) showed that the LANA-cGAS interaction occurs mainly in the cytoplasm of KSHV-infected cells and that cGAS immune-precipitated from the cytoplasm is associated with lower-molecular-weight forms of LANA.

Rad 50 has also been shown to associate with KSHV LANA. Rad50 belongs to the structural maintenance of chromosomes (SMC) protein family that control the higher-

order structure and dynamics of chromatin and displaying both sequence and structural homology (Lamarche *et al.*, 2010). Rad50 is involved in DNA replication, DNA repair, and checkpoint activation in KSHV (Dupré *et al.*, 2006). Cytoplasmic Rad50 sense cytoplasmic DNA and activate the NF-κB pathway, LANA isoforms recruit Rad50 in the cytosol and thereby interfere with the activation of the NF-κB cascade induced by transfected DNA, as well as KSHV reactivation from latency (Mariggiò *et al.*, 2017). It could not be detected in co-IP/western blot assays as associating with oLANA but did co-localise very well with it by immunofluorescence in both GFP-oLANAΔ-transfected cells and LGLs. Thus, while oLANA-Rad50 associations were not definitively confirmed by co-IP western, the co-localisation suggests that there may be some interactions that are potentially interesting and require further investigation. Rad50 is involved in DNA replication, DNA repair and often described as a 'first responder' to DNA damage. Similarly, in the case of KSHV, activation of Rad50 has been demonstrated following initial viral entry and during the lytic replication programme and appears to play a positive role in the viral lifecycle (Hollingworth *et al.*, 2015). Rad50 coiled coils also forms a metal-mediated bridging complex between two DNA-binding heads (Sohn and Hearing, 2012; Mariggiò *et al.*, 2017).

Some proteins identified by GFP-trap/MS did not show antibody binding (immune reactivity) in co-IP/western blot analysis, but did show clearly colocalisation in immunofluorescence with both HEK293T cells and LGLs. Some possible reasons for these findings might be based on many reasons include the protein interaction was not strong/stable which leads to total or partial protein loss during washing steps. Another possible reason for different detection between western immunoblot and immunofluorescence may be because the western immunoblotting is less sensitive than LC

MS/MS and there was an insufficient amount of GFP-oLANA protein present in the sample or the sample was too complex to detect the lowest abundance proteins. Future studies might include over-expression of target molecules to maximise the chances of seeing interactions, optimising the pull-down conditions to stabilise interactions and also adopting live-cell imaging techniques such as FRET and FRAP to study possible weaker protein-protein interactions.

Effective pharmacological intervention of MCF is an attractive option since no treatment or vaccine found which can reduce the progression of diseases by inhibiting the immune modulation. Pharmacological intervention relies greatly on the effective intervention of the interaction between LANA protein and cellular proteins to block the transmission of the virus from reservoir host to cattle. Such intervention would be highly desirable, as it would negate the need to separate cattle and other susceptible ungulates from reservoirs. However, further research is needed to elucidate the mechanisms underlying the interaction between LANA and cellular proteins so that they find a proper place in the pharmacological intervention.

Results obtained from this thesis present novel mechanisms of potential regulation of cellular processes by LANA protein. These may contribute to the differential outcomes observed in oLANA in cattle in compare with in sheep and MCF-susceptible species (previous others studies). The results also identify possible novel virus-cell interactions that could, if confirmed, provide druggable targets for intervention in SA-MCF disease. Although the story is incomplete, mainly due to restrictions in both time and the availability of appropriate systems for the study of OvHV-2, this thesis paves the way for future investigations into the role of LANA protein in OvHV-2 biology.

# References

## References


Ababneh, M. M., Hananeh, W. M. & Dalab, A. E. **2014**. Molecular and histopathological characterization of sheep-associated malignant catarrhal fever (SA-MCF) outbreak in beef cattle. *Transbound Emerg Dis,* 61**, 75-80**.

Ackermann, M. **2005a**. Virus in sheep's skin. *Schweizer Archiv fur Tierheilkunde,* 147**, 155-164**.

Ackermann, M. **2005b**. [Virus in sheep's skin]. *Schweiz Arch Tierheilkd,* 147**, 155-64**.

Ackermann, M. **2006**. Pathogenesis of gammaherpesvirus infections. *Vet Microbiol,* 113**, 211-22**.

Adler, B., Sattler, C. & Adler, H. **2017**. Herpesviruses and their host cells: a successful liaison. *Trends in microbiology,* 25**, 229-241**.

Al-Saadi, M. H. A. **2018**. Pathogenesis of Malignant Catarrhal Fever in Cattle.

Alcaraz, A., Warren, A., Jackson, C., Gold, J., McCoy, M., Cheong, S. H., Kimball, S., Sells, S., Taus, N. S., Divers, T. & Li, H. **2009**. Naturally occurring sheep-associated malignant catarrhal fever in North American pigs. *J Vet Diagn Invest,* 21**, 250-3**.

An, F.-Q., Compitello, N., Horwitz, E., Sramkoski, M., Knudsen, E. S. & Renne, R. **2005**. The latency-associated nuclear antigen of Kaposi's sarcoma-associated herpesvirus modulates cellular gene expression and protects lymphoid cells from p16 INK4A-induced cell cycle arrest. *Journal of Biological Chemistry,* 280**, 3862-3874**.

Anderson, I. E., Buxton, D., Campbell, I., Russell, G., Davis, W. C., Hamilton, M. J. & Haig, D. M. **2007**. Immunohistochemical study of experimental malignant catarrhal fever in rabbits. *J Comp Pathol,* 136**, 156-66**.

Arnold, R., Brenner, D., Becker, M., Frey, C. R. & Krammer, P. H. **2006**. How T lymphocytes switch between life and death. *European journal of immunology,* 36**, 1654-1658**.

Azevedo Costa, E., de Marco Viott, A., de Souza Machado, G., Quaresma Bomfim, M. R., Magalhaes Coelho, F., Portela Lobato, Z. I., Resende, M. & Carvalho Guedes, R. M. **2010**. Transmission of ovine herpesvirus 2 from asymptomatic boars to sows. *Emerg Infect Dis,* 16**, 2011-2**.

Ballestas, M. E., Chatis, P. A. & Kaye, K. M. **1999**. Efficient persistence of extrachromosomal KSHV DNA mediated by latency-associated nuclear antigen. *Science,* 284**, 641-4**.

Ballestas, M. E. & Kaye, K. M. **2011**. The latency-associated nuclear antigen, a multifunctional protein central to Kaposi's sarcoma-associated herpesvirus latency. *Future Microbiol,* 6**, 1399-413**.

Bartley, K., Deane, D., Percival, A., Dry, I. R., Grant, D. M., Inglis, N. F., Mclean, K., Manson, E. D., Imrie, L. H. & Haig, D. M. **2014a**. Identification of immuno-reactive capsid proteins of malignant catarrhal fever viruses. *Veterinary microbiology,* 173**, 17-26**.

Bartley, K., Deane, D., Percival, A., Dry, I. R., Grant, D. M., Inglis, N. F., McLean, K., Manson, E. D., Imrie, L. H., Haig, D. M., Lankester, F. & Russell, G. C. **2014b**. Identification of immuno-reactive capsid proteins of malignant catarrhal fever viruses. *Vet Microbiol,* 173**, 17-26**.

Barton, E., Mandal, P. & Speck, S. H. **2011**. Pathogenesis and host control of gammaherpesviruses: lessons from the mouse. *Annu Rev Immunol,* 29**, 351-97**.

Bastawecy, I. M. & El-Samee, A. A. **2012**. First isolation and identification of ovine herpesvirus 2 causing malignant catarrhal fever outbreak in Egypt. *Life science journal,* 9**, 798-804**.

Baxter, S. I., Pow, I., Bridgen, A. & Reid, H. W. **1993**. PCR detection of the sheep-associated agent of malignant catarrhal fever. *Arch Virol,* 132**, 145-59**.
Baxter, S. I. F., Wiyono, A., Pow, I. & Reid, H. W. **1997**. Identification of ovine herpesvirus-2 infection in sheep. *Archives of Virology,* 142**, 823-831**.
Bedelian, C. **2004**. *The impact of malignant catarrhal fever on Maasai pastoral communities in Kitengela Wildlife Dispersal Area, Kenya.* University of Edinburgh.
Bedelian, C., Nkedianye, D. & Herrero, M. **2007**. Maasai perception of the impact and incidence of malignant catarrhal fever (MCF) in southern Kenya. *Preventive veterinary medicine,* 78**, 296-316**.
Berezowski, J. A., Appleyard, G. D., Crawford, T. B., Haigh, J., Li, H., Middleton, D. M., O'Connor, B. P., West, K. & Woodbury, M. **2005**. An outbreak of sheep-associated malignant catarrhal fever in bison (Bison bison) after exposure to sheep at a public auction sale. *J Vet Diagn Invest,* 17**, 55-8**.
Bies, C., Blum, R., Dudek, J., Nastainczyk, W., Oberhauser, S., Jung, M. & Zimmermann, R. **2004**. Characterization of pancreatic ERj3p, ahomolog of yeast DnaJ-like protein Scj1p. *Biological chemistry,* 385**, 389-395**.
Blood, D. C. & Radostits, O. M. **1989**. *Veterinary medicine : a textbook of the diseases of cattle, sheep, pigs, goats and horses,* London, ELBS / Baillierre Tindall.
BOLTE, S. & CORDELIÈRES, F. P. **2006**. A guided tour into subcellular colocalization analysis in light microscopy. *Journal of Microscopy,* 224**, 213-232**.
Borah, S., Verma, S. C. & Robertson, E. S. **2004**. ORF73 of herpesvirus saimiri, a viral homolog of Kaposi's sarcoma-associated herpesvirus, modulates the two cellular tumor suppressor proteins p53 and pRb. *J Virol,* 78**, 10336-47**.
Borrebaeck, C. A. **2012**. Viewpoints in clinical proteomics: When will proteomics deliver clinically useful information? *PROTEOMICS–Clinical Applications,* 6**, 343-345**.
Brameier, M., Krings, A. & MacCallum, R. M. **2007**. NucPred—predicting nuclear localization of proteins. *Bioinformatics,* 23**, 1159-1160**.
Brenner, J. & David, D. **2005**. Sheep-associated malignant catarrhal fever in cattle (SA-MCF). Recent clinical and epidemiological aspects in Israel. *Isr J Vet Med,* 60**, 19-22**.
Bridgen, A. & Reid, H. W. **1991**. Derivation of a DNA clone corresponding to the viral agent of sheep-associated malignant catarrhal fever. *Res Vet Sci,* 50**, 38-44**.
Brown, C. & Torres, A. **2008**. USAHA Foreign Animal Diseases, Committee of Foreign and Emerging Diseases of the US Animal Health Association. Boca Publications Group, Inc.
Brown, C. C. **2007**. Alimentary system. *Pathology of Domestic Animals*.
Burggraf, S. & Olgemoller, B. **2004**. Simple technique for internal control of real-time amplification assays. *Clin Chem,* 50**, 819-25**.
Burrells, C. & Reid, H. W. **1991**. Phenotypic analysis of lymphoblastoid cell lines derived from cattle and deer affected with "sheep-associated" malignant catarrhal fever. *Vet Immunol Immunopathol,* 29**, 151-61**.
Buxton, D., Jacoby, R. O., Reid, H. W. & Goodall, P. A. **1988**. The pathology of "sheep-associated" malignant catarrhal fever in the hamster. *J Comp Pathol,* 98**, 155-66**.
Buxton, D. & Reid, H. W. **1980**. Transmission of malignant catarrhal fever to rabbits. *Vet Rec,* 106**, 243-5**.
Buxton, D., Reid, H. W., Finlayson, J. & Pow, I. **1984**. Pathogenesis of 'sheep-associated' malignant catarrhal fever in rabbits. *Res Vet Sci,* 36**, 205-11**.

Campolo, M., Lucente, M. S., Mari, V., Elia, G., Tinelli, A., Laricchiuta, P., Caramelli, M., Nava, D., Buonavoglia, C. & Decaro, N. **2008**. Malignant catarrhal fever in a captive American bison (Bison bison) in Italy. *J Vet Diagn Invest,* 20**, 843-6**.

Catez, F., Ueda, T. & Bustin, M. **2006**. Determinants of histone H1 mobility and chromatin binding in living cells. *Nat Struct Mol Biol,* 13**, 305-10**.

Chen, W., Hilton, I. B., Staudt, M. R., Burd, C. E. & Dittmer, D. P. **2010**. Distinct p53, p53:LANA, and LANA Complexes in Kaposi's Sarcoma-Associated Herpesvirus Lymphomas. *Journal of Virology,* 84**, 3898-3908**.

Cherry, S. R., Biniszkiewicz, D., van Parijs, L., Baltimore, D. & Jaenisch, R. **2000**. Retroviral expression in embryonic stem cells and hematopoietic stem cells. *Molecular and cellular biology,* 20**, 7419-7426**.

Chmielewicz, B., Goltz, M. & Ehlers, B. **2001**. Detection and multigenic characterization of a novel gammaherpesvirus in goats. *Virus research,* 75**, 87-94**.

Christian, L. M., Iams, J. D., Porter, K. & Glaser, R. **2012**. Epstein-Barr virus reactivation during pregnancy and postpartum: Effects of race and racial discrimination. *Brain, Behavior, and Immunity,* 26**, 1280-1287**.

Cleaveland, S., Kusiluka, L., Ole Kuwai, J., Bell, C. & Kazwala, R. **2001**. Assessing the impact of malignant catarrhal fever in Ngorongoro District, Tanzania. *Report to the DFID Animal Health Programme, Centre for Tropical Veterinary Medicine, University of Edinburgh*.

Cloutier, N. & Flamand, L. **2010**. Kaposi's sarcoma-associated herpesvirus latency-associated nuclear antigen inhibits interferon beta (IFN-β) expression by competing with IFN regulatory factor-3 for binding to IFN-β promoter. *Journal of Biological Chemistry***, jbc. M109. 018838**.

Coffin, J. M., Hughes, S. H. & Varmus, H. 1997. *Retroviruses,* Plainview, N.Y., Cold Spring Harbor Laboratory Press.

Commission, I. O. o. E. B. S. & Committee, I. O. o. E. I. **2008**. *Manual of diagnostic tests and vaccines for terrestrial animals: mammals, birds and bees*, Office international des épizooties.

Connolly, S. A., Jackson, J. O., Jardetzky, T. S. & Longnecker, R. **2011**. Fusing structure and function: a structural view of the herpesvirus entry machinery. *Nature Reviews Microbiology,* 9**, 369**.

Costa, E. A., Bomfim, M. R., da Fonseca, F. G., Drumond, B. P., Coelho, F. M., Vasconcelos, A. C., Furtini, R., Paixao, T. A., Tsolis, R. M., Santos, R. L. & Resende, M. **2009**. Ovine herpesvirus 2 infection in Foal, Brazil. *Emerg Infect Dis,* 15**, 844-5**.

Cotter II, M. A. & Robertson, E. S. **1999**. The latency-associated nuclear antigen tethers the Kaposi's sarcoma-associated herpesvirus genome to host chromosomes in body cavity-based lymphoma cells. *Virology,* 264**, 254-264**.

Cotter, M. A., 2nd, Subramanian, C. & Robertson, E. S. **2001**. The Kaposi's sarcoma-associated herpesvirus latency-associated nuclear antigen binds to specific sequences at the left end of the viral genome through its carboxy-terminus. *Virology,* 291**, 241-59**.

Coulter, L. J., Wright, H. & Reid, H. W. **2001**. Molecular genomic characterization of the viruses of malignant catarrhal fever. *J Comp Pathol,* 124**, 2-19**.

Crawford, T. B., Li, H., Rosenburg, S. R., Norhausen, R. W. & Garner, M. M. **2002**. Mural folliculitis and alopecia caused by infection with goat-associated malignant catarrhal fever virus in two sika deer. *J Am Vet Med Assoc,* 221**, 843-7, 801**.

Cunha, C. W., Gailbreath, K. L., O'Toole, D., Knowles, D. P., Schneider, D. A., White, S. N., Taus, N. S., Davies, C. J., Davis, W. C. & Li, H. **2012**. Ovine herpesvirus 2 infection in

American bison: virus and host dynamics in the development of sheep-associated malignant catarrhal fever. *Vet Microbiol,* 159**, 307-19**.
Cunha, C. W., Knowles, D. P., Taus, N. S., O'Toole, D., Nicola, A. V., Aguilar, H. C. & Li, H. **2015**. Antibodies to ovine herpesvirus 2 glycoproteins decrease virus infectivity and prevent malignant catarrhal fever in rabbits. *Vet Microbiol,* 175**, 349-55**.
Cunha, C. W., O'Toole, D., Taus, N. S., Knowles, D. P. & Li, H. **2013**. Are rabbits a suitable model to study sheep-associated malignant catarrhal fever in susceptible hosts? *Vet Microbiol,* 163**, 358-63**.
Cunha, C. W., Traul, D. L., Taus, N. S., Oaks, J. L., O'Toole, D., Davitt, C. M. & Li, H. **2008**. Detection of ovine herpesvirus 2 major capsid gene transcripts as an indicator of virus replication in shedding sheep and clinically affected animals. *Virus Res,* 132**, 69-75**.
Dai, C., Cao, Z., Wu, Y., Yi, H., Jiang, D. & Li, W. **2007**. Improved fusion protein expression of EGFP via the mutation of both Kozak and the initial ATG codon. *Cell Mol Biol Lett,* 12**, 362-9**.
Daniels, P., Sudurisman, W. & Ronohardjo, P. **1988**. Epidemiological aspects of malignant catarrhal fever in Indonesia. *Malignant Catarrhal Fever in Asian Livestock***, 20-31**.
Davison, A. J. **2010**. Herpesvirus systematics. *Veterinary Microbiology,* 143**, 52-69**.
Davison, A. J., Eberle, R., Ehlers, B., Hayward, G. S., McGeoch, D. J., Minson, A. C., Pellett, P. E., Roizman, B., Studdert, M. J. & Thiry, E. **2009**. The order Herpesvirales. *Arch Virol,* 154**, 171-7**.
Dettwiler, M., Stahel, A., Kruger, S., Gerspach, C., Braun, U., Engels, M. & Hilbe, M. **2011**. A possible case of caprine-associated malignant catarrhal fever in a domestic water buffalo (Bubalus bubalis) in Switzerland. *BMC Vet Res,* 7**, 78**.
Dewals, B., Boudry, C., Farnir, F., Drion, P. V. & Vanderplasschen, A. **2008**. Malignant catarrhal fever induced by alcelaphine herpesvirus 1 is associated with proliferation of CD8+ T cells supporting a latent infection. *PLoS One,* 3**, e1627**.
Dewals, B., Boudry, C., Gillet, L., Markine-Goriaynoff, N., de Leval, L., Haig, D. M. & Vanderplasschen, A. **2006**. Cloning of the genome of Alcelaphine herpesvirus 1 as an infectious and pathogenic bacterial artificial chromosome. *J Gen Virol,* 87**, 509-17**.
Dewals, B. G. & Vanderplasschen, A. **2011**. Malignant catarrhal fever induced by Alcelaphine herpesvirus 1 is characterized by an expansion of activated CD3+CD8+CD4- T cells expressing a cytotoxic phenotype in both lymphoid and non-lymphoid tissues. *Vet Res,* 42**, 95**.
DeWire, S. M. & Damania, B. **2005**. The latency-associated nuclear antigen of rhesus monkey rhadinovirus inhibits viral replication through repression of Orf50/Rta transcriptional activation. *Journal of virology,* 79**, 3127-3138**.
Doboro, F. A., Njiro, S., Sibeko-Matjila, K. & Van Vuuren, M. **2016**. Molecular Analysis of South African Ovine Herpesvirus 2 Strains Based on Selected Glycoprotein and Tegument Genes. *PLoS One,* 11**, e0147019**.
Domon, B. & Aebersold, R. **2006**. Mass spectrometry and protein analysis. *science,* 312**, 212-217**.
Domsic, J. F., Chen, H.-S., Lu, F., Marmorstein, R. & Lieberman, P. M. **2013**. Molecular basis for oligomeric-DNA binding and episome maintenance by KSHV LANA. *PLoS pathogens,* 9**, e1003672**.
Dong, X., Armstrong, S. D., Xia, D., Makepeace, B. L., Darby, A. C. & Kadowaki, T. **2017**. Draft genome of the honey bee ectoparasitic mite, Tropilaelaps mercedesae, is shaped by the parasitic life history. *GigaScience,* 6**, 1-17**.

Dry, I., Todd, H., Deane, D., Percival, A., McLean, K., Inglis, N. F., Manson, E. D., Haig, D. M., Nayuni, S., Hutt-Fletcher, L. M., Grant, D. M., Bartley, K., Stewart, J. P. & Russell, G. C. **2016**. Alcelaphine herpesvirus 1 glycoprotein B: recombinant expression and antibody recognition. *Arch Virol,* 161**, 613-9**.

Dunn, K. W., Kamocka, M. M. & McDonald, J. H. **2011**. A practical guide to evaluating colocalization in biological microscopy. *American Journal of Physiology-Cell Physiology,* 300**, C723-C742**.

Dupré, A., Boyer-Chatenet, L. & Gautier, J. **2006**. Two-step activation of ATM by DNA and the Mre11–Rad50–Nbs1 complex. *Nature Structural and Molecular Biology,* 13**, 451**.

Ebert, O., Finke, S., Salahi, A., Herrmann, M., Trojaneck, B., Lefterova, P., Wagner, E., Kircheis, R., Huhn, D. & Schriever, F. **1997**. Lymphocyte apoptosis: induction by gene transfer techniques. *Gene therapy,* 4**, 296**.

Eisenberg, R. J., Atanasiu, D., Cairns, T. M., Gallagher, J. R., Krummenacher, C. & Cohen, G. H. **2012**. Herpes virus fusion and entry: a story with many characters. *Viruses,* 4**, 800-32**.

Ensser, A., Pflanz, R. & Fleckenstein, B. **1997**. Primary structure of the alcelaphine herpesvirus 1 genome. *J Virol,* 71**, 6517-25**.

Epstein, M. A., Achong, B. G. & Barr, Y. M. **1964**. VIRUS PARTICLES IN CULTURED LYMPHOBLASTS FROM BURKITT'S LYMPHOMA. *Lancet,* 1**, 702-3**.

Fan, C., Dong, L., Zhu, N., Xiong, Y., Zhang, J., Wang, L., Shen, Y., Zhang, X. & Chen, M. **2012**. Isolation of siRNA target by biotinylated siRNA reveals that human CCDC12 promotes early erythroid differentiation. *Leuk Res,* 36**, 779-83**.

Fay, F. S., Taneja, K. L., Shenoy, S., Lifshitz, L. & Singer, R. H. **1997**. Quantitative digital analysis of diffuse and concentrated nuclear distributions of nascent transcripts, SC35 and poly (A). *Experimental cell research,* 231**, 27-37**.

Ferrer-Miralles, N., Saccardo, P., Corchero, J. L., Xu, Z. & García-Fruitós, E. **2015**. General introduction: recombinant protein production and purification of insoluble proteins. *Insoluble Proteins.* Springer.

Fields, B. N., Knipe, D. M. & Howley, P. M. **2007**. *Fields virology,* Philadelphia, Wolters Kluwer Health/Lippincott Williams & Wilkins.

Finkelshtein, D., Werman, A., Novick, D., Barak, S. & Rubinstein, M. **2013**. LDL receptor and its family members serve as the cellular receptors for vesicular stomatitis virus. *Proceedings of the National Academy of Sciences,* 110**, 7306-7311**.

Foyle, K. L., Fuller, H. E., Higgins, R. J., Russell, G. C., Willoughby, K., Rosie, W. G., Stidworthy, M. F. & Foster, A. P. **2009**. Malignant catarrhal fever in sika deer (Cervus nippon) in the UK. *Vet Rec,* 165**, 445-7**.

Fraser, S. J., Nettleton, P. F., Dutia, B. M., Haig, D. M. & Russell, G. C. **2006**. Development of an enzyme-linked immunosorbent assay for the detection of antibodies against malignant catarrhal fever viruses in cattle serum. *Vet Microbiol,* 116**, 21-8**.

Fujimori, T., Suno, R., Iemura, S. i., Natsume, T., Wada, I. & Hosokawa, N. **2017**. Endoplasmic reticulum proteins SDF 2 and SDF 2L1 act as components of the BiP chaperone cycle to prevent protein aggregation. *Genes to Cells,* 22**, 684-698**.

Gailbreath, K. L., Taus, N. S., Cunha, C. W., Knowles, D. P. & Li, H. **2008**. Experimental infection of rabbits with ovine herpesvirus 2 from sheep nasal secretions. *Vet Microbiol,* 132**, 65-73**.

Gallardo, H. F., Tan, C., Ory, D. & Sadelain, M. **1997**. Recombinant retroviruses pseudotyped with the vesicular stomatitis virus G glycoprotein mediate both stable gene transfer and pseudotransduction in human peripheral blood lymphocytes. *Blood,* 90**, 952-7**.

Gao, F., Bailes, E., Robertson, D. L., Chen, Y., Rodenburg, C. M., Michael, S. F., Cummins, L. B., Arthur, L. O., Peeters, M., Shaw, G. M., Sharp, P. M. & Hahn, B. H. **1999**. Origin of HIV-1 in the chimpanzee Pan troglodytes troglodytes. *Nature,* 397**, 436**.

Garber, A. C., Hu, J. & Renne, R. **2002**. Latency-associated nuclear antigen (LANA) cooperatively binds to two sites within the terminal repeat, and both sites contribute to the ability of LANA to suppress transcription and to facilitate DNA replication. *J Biol Chem,* 277**, 27401-11**.

García-Dorival, I., Wu, W., Dowall, S., Armstrong, S., Touzelet, O., Wastling, J., Barr, J. N., Matthews, D., Carroll, M. & Hewson, R. **2014**. Elucidation of the Ebola virus VP24 cellular interactome and disruption of virus biology through targeted inhibition of host-cell protein function. *Journal of proteome research,* 13**, 5120-5135**.

Gasper, D., Barr, B., Li, H., Taus, N., Peterson, R., Benjamin, G., Hunt, T. & Pesavento, P. A. **2012**. Ibex-associated malignant catarrhal fever-like disease in a group of bongo antelope (Tragelaphus eurycerus). *Vet Pathol,* 49**, 492-7**.

Gaudy, J., Willoughby, K., Lamm, C., Karavanis, E. & Logue, D. N. **2012**. Possible natural MCF-like disease in a domestic lamb in Scotland. *Vet Rec,* 171**, 563**.

Gelaye, E., Mekonnen, G., Jenberie, S. & Ayelet, G. **2013**. Detection of sheepassociated malignant catarrhal fever from clinical cases in Ethiopian cattle. *OIE Revue Scientifique et Technique,* 32**, 851-856**.

Gelgor, A., Gam ze Letova, C., Yegorov, Y., Kalt, I. & Sarid, R. **2018**. Nucleolar stress enhances lytic reactivation of the Kaposi's sarcoma-associated herpesvirus. *Oncotarget,* 9**, 13822-33**.

Giangaspero, M., Savini, G., Osawa, T. & Harasawa, R. **2013**. Serological survey to determine the occurrence of malignant catarrhal fever infection in the Japanese small ruminant population from northern districts. *J Vet Med Sci,* 75**, 815-8**.

Graham, F. L., Smiley, J., Russell, W. & Nairn, R. **1977**. Characteristics of a human cell line transformed by DNA from human adenovirus type 5. *Journal of General Virology,* 36**, 59-72**.

Graham, F. L. & van der Eb, A. J. **1973**. A new technique for the assay of infectivity of human adenovirus 5 DNA. *Virology,* 52**, 456-467**.

Grievink, H. W., Luisman, T., Kluft, C., Moerland, M. & Malone, K. E. **2016**. Comparison of three isolation techniques for human peripheral blood mononuclear cells: cell recovery and viability, population composition, and cell functionality. *Biopreservation and biobanking,* 14**, 410-415**.

Grinde, B. **2013**. Herpesviruses: latency and reactivation – viral strategies and host response. *Journal of Oral Microbiology,* 5**, 22766**.

Groves, A. K., Cotter, M. A., Subramanian, C. & Robertson, E. S. **2001**. The latency-associated nuclear antigen encoded by Kaposi's sarcoma-associated herpesvirus activates two major essential Epstein-Barr virus latent promoters. *Journal of virology,* 75**, 9446-9457**.

Grundhoff, A. & Ganem, D. **2003**. The latency-associated nuclear antigen of Kaposi's sarcoma-associated herpesvirus permits replication of terminal repeat-containing plasmids. *Journal of virology,* 77**, 2779-2783**.

Haig, D. M., Grant, D., Deane, D., Campbell, I., Thomson, J., Jepson, C., Buxton, D. & Russell, G. C. **2008**. An immunisation strategy for the protection of cattle against alcelaphine herpesvirus-1-induced malignant catarrhal fever. *Vaccine,* 26**, 4461-8**.

Hart, J., Ackermann, M., Jayawardane, G., Russell, G., Haig, D. M., Reid, H. & Stewart, J. P. **2007**. Complete sequence and analysis of the ovine herpesvirus 2 genome. *J Gen Virol,* 88**, 28-39**.

Headley, S. A., Sousa, I. K. F., Minervino, A. H. H., Barros, I. O., Barrêto Júnior, R. A., Alfieri, A. F., Ortolani, E. L. & Alfieri, A. A. **2012**. Molecular confirmation of ovine herpesvirus 2-induced malignant catarrhal fever lesions in cattle from Rio Grande do Norte, Brazil. *Pesquisa Veterinária Brasileira,* 32**, 1213-1218**.

Herring, A., Reid, H., Inglis, N. & Pow, I. **1989**. Immunoblotting analysis of the reaction of wildebeest, sheep and cattle sera with the structural antigens of alcelaphine herpesvirus-1 (malignant catarrhal fever virus). *Vet Microbiol,* 19**, 205-15**.

Heuschele, W. **1988**. Malignant catarrhal fever: a review of a serious disease hazard for exotic and domestic ruminants. *Zool. Garten. NF,* 58**, 123-133**.

Holliman, A. **2005**. Differential diagnosis of diseases causing oral lesions in cattle. *In practice,* 27**, 2**.

Hollingworth, R., Skalka, G. L., Stewart, G. S., Hislop, A. D., Blackbourn, D. J. & Grand, R. J. **2015**. Activation of DNA damage response pathways during lytic replication of KSHV. *Viruses,* 7**, 2908-2927**.

Honiball, E., Van Essen, L. & Du Toit, J. **2008**. *A review of malignant catarrhal fever in the Republic of South Africa*, Advisory Bureau for Development (Pty) Limited.

Hu, J., Garber, A. C. & Renne, R. **2002**. The latency-associated nuclear antigen of Kaposi's sarcoma-associated herpesvirus supports latent DNA replication in dividing cells. *J Virol,* 76**, 11677-87**.

Hu, Z. & Usherwood, E. J. **2014**. Immune escape of γ-herpesviruses from adaptive immunity. *Reviews in medical virology,* 24**, 365-378**.

Jacobsen, B., Thies, K., von Altrock, A., Forster, C., Konig, M. & Baumgartner, W. **2007**. Malignant catarrhal fever-like lesions associated with ovine herpesvirus-2 infection in three goats. *Vet Microbiol,* 124**, 353-7**.

Jacoby, R., Buxton, D. & Reid, H. **1988**. The pathology of wildebeest-associated malignant catarrhal fever in hamsters, rats and guinea-pigs. *Journal of comparative pathology,* 98**, 99-109**.

Jarosinski, K. W. **2017**. Interindividual Spread of Herpesviruses. *In:* OSTERRIEDER, K. (ed.) *Cell Biology of Herpes Viruses.* Cham: Springer International Publishing.

Jayawardane, G., Russell, G. C., Thomson, J., Deane, D., Cox, H., Gatherer, D., Ackermann, M., Haig, D. M. & Stewart, J. P. **2008**. A captured viral interleukin 10 gene with cellular exon structure. *Journal of General Virology,* 89**, 2447-2455**.

Jia, Q., Freeman, M. L., Yager, E. J., McHardy, I., Tong, L., Martinez-Guzman, D., Rickabaugh, T., Hwang, S., Blackman, M. A., Sun, R. & Wu, T. T. **2010**. Induction of protective immunity against murine gammaherpesvirus 68 infection in the absence of viral latency. *J Virol,* 84**, 2453-65**.

Johnston, C., Martin, B., Fichant, G., Polard, P. & Claverys, J.-P. **2014**. Bacterial transformation: distribution, shared mechanisms and divergent control. *Nature Reviews Microbiology,* 12**, 181**.

Kalunda, M., Ferris, D. H., Dardiri, A. H. & Lee, K. M. **1981**. Malignant catarrhal fever III. Experimental infection of sheep, domestic rabbits and laboratory animals with malignant catarrhal fever virus. *Can J Comp Med,* 45**, 310-4**.

Kedes, D. H., Lagunoff, M., Renne, R. & Ganem, D. **1997**. Identification of the gene encoding the major latency-associated nuclear antigen of the Kaposi's sarcoma-associated herpesvirus. *J Clin Invest,* 100**, 2606-10**.

Keel, M. K., Gage, P. J., Noon, T. H., Bradley, G. A. & Collins, J. K. **2003a**. Caprine Herpesvirus-2 in Association with Naturally Occurring Malignant Catarrhal Fever in Captive Sika Deer (Cervus Nippon). *Journal of Veterinary Diagnostic Investigation,* 15**, 179-183**.

Kim, O., Li, H. & Crawford, T. B. **2003**. Demonstration of sheep-associated malignant catarrhal fever virions in sheep nasal secretions. *Virus Res,* 98**, 117-22**.

Kim, T. K. & Eberwine, J. H. **2010**. Mammalian cell transfection: the present and the future. *Analytical and Bioanalytical Chemistry,* 397**, 3173-3178**.

Kleiboeker, S. B., Miller, M. A., Schommer, S. K., Ramos-Vara, J. A., Boucher, M. & Turnquist, S. E. **2002**. Detection and Multigenic Characterization of a Herpesvirus Associated with Malignant Catarrhal Fever in White-Tailed Deer (Odocoileus virginianus) from Missouri. *Journal of Clinical Microbiology,* 40**, 1311-1318**.

Krithivas, A., Fujimuro, M., Weidner, M., Young, D. B. & Hayward, S. D. **2002**. Protein interactions targeting the latency-associated nuclear antigen of Kaposi's sarcoma-associated herpesvirus to cell chromosomes. *Journal of virology,* 76**, 11596-11604**.

Kurien, B. T. **2012**. *Protein electrophoresis : methods and protocols,* New York, Humana Press.

Kurien, B. T. & Scofield, R. H. **2015**. Western blotting : methods and protocols.

Kwun, H. J., da Silva, S. R., Qin, H., Ferris, R. L., Tan, R., Chang, Y. & Moore, P. S. **2011**. The central repeat domain 1 of Kaposi's sarcoma-associated herpesvirus (KSHV) latency associated-nuclear antigen 1 (LANA1) prevents cis MHC class I peptide presentation. *Virology,* 412**, 357-365**.

Lachmanovich, E., Shvartsman, D., Malka, Y., Botvin, C., Henis, Y. & Weiss, A. **2003**. Co-localization analysis of complex formation among membrane proteins by computerized fluorescence microscopy: application to immunofluorescence co-patching studies. *Journal of microscopy,* 212**, 122-131**.

Lamarche, B. J., Orazio, N. I. & Weitzman, M. D. **2010**. The MRN complex in double-strand break repair and telomere maintenance. *FEBS Letters,* 584**, 3682-3695**.

Lankester, F., Lugelo, A., Kazwala, R., Keyyu, J., Cleaveland, S. & Yoder, J. **2015a**. The economic impact of malignant catarrhal fever on pastoralist livelihoods. *PLoS One,* 10**, e0116059**.

Lankester, F., Lugelo, A., Mnyambwa, N., Ndabigaye, A., Keyyu, J., Kazwala, R., Grant, D. M., Relf, V., Haig, D. M., Cleaveland, S. & Russell, G. C. **2015b**. Alcelaphine Herpesvirus-1 (Malignant Catarrhal Fever Virus) in Wildebeest Placenta: Genetic Variation of ORF50 and A9.5 Alleles. *PLoS One,* 10**, e0124121**.

Leight, E. R. & Sugden, B. **2000**. EBNA-1: a protein pivotal to latent infection by Epstein-Barr virus. *Rev Med Virol,* 10**, 83-100**.

Li, H., Brooking, A., Cunha, C. W., Highland, M. A., O'Toole, D., Knowles, D. P. & Taus, N. S. **2012**. Experimental induction of malignant catarrhal fever in pigs with ovine herpesvirus 2 by intranasal nebulization. *Vet Microbiol,* 159**, 485-9**.

Li, H., Cunha, C. W., Abbitt, B., deMaar, T. W., Lenz, S. D., Hayes, J. R. & Taus, N. S. **2013a**. Goats are a potential reservoir for the herpesvirus (MCFV-WTD), causing malignant catarrhal fever in deer. *J Zoo Wildl Med,* 44**, 484-6**.

Li, H., Cunha, C. W., Davies, C. J., Gailbreath, K. L., Knowles, D. P., Oaks, J. L. & Taus, N. S. **2008a**. Ovine herpesvirus 2 replicates initially in the lung of experimentally infected sheep. *J Gen Virol,* 89**, 1699-708**.

Li, H., Cunha, C. W., Gailbreath, K. L., O'Toole, D., White, S. N., Vanderplasschen, A., Dewals, B., Knowles, D. P. & Taus, N. S. **2011**. Characterization of ovine herpesvirus 2-induced malignant catarrhal fever in rabbits. *Vet Microbiol,* 150**, 270-7**.

Li, H., Cunha, C. W., O'Toole, D., Nicola, A. V., Knowles, D. P. & Taus, N. S. **2013b**. Development of an in vivo system to measure antibody-blocking of ovine herpesvirus 2 entry. *J Virol Methods,* 188**, 104-7**.

Li, H., Cunha, C. W., Taus, N. S. & Knowles, D. P. **2014**. Malignant catarrhal fever: inching toward understanding. *Annu Rev Anim Biosci,* 2**, 209-33**.

Li, H., Dyer, N., Keller, J. & Crawford, T. B. **2000**. Newly recognized herpesvirus causing malignant catarrhal fever in white-tailed deer (Odocoileus virginianus). *J Clin Microbiol,* 38**, 1313-8**.

Li, H., Gailbreath, K., Bender, L. C., West, K., Keller, J. & Crawford, T. B. **2003a**. Evidence of three new members of malignant catarrhal fever virus group in muskox (Ovibos moschatus), Nubian ibex (Capra nubiana), and gemsbok (Oryx gazella). *J Wildl Dis,* 39**, 875-80**.

Li, H., Gailbreath, K., Flach, E. J., Taus, N. S., Cooley, J., Keller, J., Russell, G. C., Knowles, D. P., Haig, D. M., Oaks, J. L., Traul, D. L. & Crawford, T. B. **2005a**. A novel subgroup of rhadinoviruses in ruminants. *J Gen Virol,* 86**, 3021-6**.

Li, H., Hua, Y., Snowder, G. & Crawford, T. B. **2001a**. Levels of ovine herpesvirus 2 DNA in nasal secretions and blood of sheep: implications for transmission. *Vet Microbiol,* 79**, 301-10**.

Li, H., Karney, G., O'Toole, D. & Crawford, T. B. **2008b**. Long distance spread of malignant catarrhal fever virus from feedlot lambs to ranch bison. *Can Vet J,* 49**, 183-5**.

Li, H., Keller, J., Knowles, D. P. & Crawford, T. B. **2001b**. Recognition of another member of the malignant catarrhal fever virus group: an endemic gammaherpesvirus in domestic goats. *J Gen Virol,* 82**, 227-32**.

Li, H., Keller, J., Knowles, D. P., Taus, N. S., Oaks, J. L. & Crawford, T. B. **2005b**. Transmission of caprine herpesvirus 2 in domestic goats. *Veterinary Microbiology,* 107**, 23-29**.

Li, H., McGuire, T. C., Muller-Doblies, U. U. & Crawford, T. B. **2001c**. A simpler, more sensitive competitive inhibition enzyme-linked immunosorbent assay for detection of antibody to malignant catarrhal fever viruses. *J Vet Diagn Invest,* 13**, 361-4**.

Li, H., O'Toole, D., Kim, O., Oaks, J. L. & Crawford, T. B. **2005c**. Malignant catarrhal fever-like disease in sheep after intranasal inoculation with ovine herpesvirus-2. *J Vet Diagn Invest,* 17**, 171-5**.

Li, H., Shen, D. T., Knowles, D. P., Gorham, J. R. & Crawford, T. B. **1994**. Competitive inhibition enzyme-linked immunosorbent assay for antibody in sheep and other ruminants to a conserved epitope of malignant catarrhal fever virus. *J Clin Microbiol,* 32**, 1674-9**.

Li, H., Snowder, G. & Crawford, T. B. **1999**. Production of malignant catarrhal fever virus-free sheep. *Vet Microbiol,* 65**, 167-72**.

Li, H., Snowder, G., O'Toole, D. & Crawford, T. B. **1998**. Transmission of ovine herpesvirus 2 in lambs. *J Clin Microbiol,* 36**, 223-6**.

Li, H., Snowder, G. D. & Crawford, T. B. **2002**. Effect of passive transfer of maternal immune components on infection with ovine herpesvirus 2 in lambs. *American journal of veterinary research,* 63**, 631-633**.

Li, H., Taus, N. S., Lewis, G. S., Kim, O., Traul, D. L. & Crawford, T. B. **2004**. Shedding of ovine herpesvirus 2 in sheep nasal secretions: the predominant mode for transmission. *J Clin Microbiol,* 42**, 5558-64**.

Li, H., Taus, N. S. & Oaks, J. L. **2006**. Sheep-associated malignant catarrhal fever virus: prospects for vaccine development. *Expert Rev Vaccines,* 5**, 133-41**.
Li, H., Wunschmann, A., Keller, J., Hall, D. G. & Crawford, T. B. **2003b**. Caprine herpesvirus-2-associated malignant catarrhal fever in white-tailed deer (Odocoileus virginianus). *J Vet Diagn Invest,* 15**, 46-9**.
Lim, C., Sohn, H., Gwack, Y. & Choe, J. **2000**. Latency-associated nuclear antigen of Kaposi's sarcoma-associated herpesvirus (human herpesvirus-8) binds ATF4/CREB2 and inhibits its transcriptional activation activity. *Journal of General Virology,* 81**, 2645-2652**.
Lodish, H. & Matsudaira, P. **2000**. *Molecular cell biology,* New York, Freeman.
Løken, T., Bosman, A.-M. & Van Vuuren, M. **2009**. Infection with Ovine herpesvirus 2 in Norwegian herds with a history of previous outbreaks of malignant catarrhal fever. *Journal of veterinary diagnostic investigation,* 21**, 257-261**.
Lung, O., Furukawa-Stoffer, T., Burton Hughes, K., Pasick, J., King, D. P. & Hodko, D. **2017**. Multiplex RT-PCR and Automated Microarray for Detection of Eight Bovine Viruses. *Transbound Emerg Dis,* 64**, 1929-1934**.
Mackintosh, C. **1993**. Importance of infectious diseases of New Zealand farmed deer. *Surveillance,* 20**, 24-26**.
Maclachlan, N., N. James Maclachlan, E. J. D. S. W. B. D. F. S. & Winton, J. R. **2016**. Fenner's Veterinary Virology (Fifth Edition).
Marcaccini, A., López Peña, M., Quiroga, M. I., Bermúdez, R., Nieto, J. M. & Alemañ, N. **2008**. Pseudorabies virus infection in mink: A host-specific pathogenesis. *Veterinary Immunology and Immunopathology,* 124**, 264-273**.
Marchisio, P. C. & Trusolino, L. **1999**. Immunofluorescence of cultured cells. *Methods Mol Biol,* 96**, 85-92**.
Mariggiò, G., Koch, S., Zhang, G., Weidner-Glunde, M., Rückert, J., Kati, S., Santag, S. & Schulz, T. F. **2017**. Kaposi sarcoma herpesvirus (KSHV) latency-associated nuclear antigen (LANA) recruits components of the MRN (Mre11-Rad50-NBS1) repair complex to modulate an innate immune signaling pathway and viral latency. *PLoS pathogens,* 13**, e1006335**.
Martins, M. S. N., Castro, A., Lima, M. D. S., Pinto, V., Silva, T. G. D., Fava, C. D., Depes, C. R., Okuda, L. H. & Pituco, E. M. **2017**. Malignant Catarrhal Fever in Brazilian cattle presenting with neurological syndrome. *Braz J Microbiol,* 48**, 366-372**.
Martucciello, A., Marianelli, C., Capuano, M., Astarita, S., Alfano, D. & Galiero, G. **2006**. An outbreak of malignant catarrhal fever in Mediterranean water buffalo (Bubalus bubalis). *Large Animal Review,* 12**, 21-24**.
Mason, J. M. & Arndt, K. M. **2004**. Coiled coil domains: stability, specificity, and biological implications. *Chembiochem,* 5**, 170-176**.
Mbole-Kariuki, M. N., Sonstegard, T., Orth, A., Thumbi, S. M., Bronsvoort, B. M., Kiara, H., Toye, P., Conradie, I., Jennings, A., Coetzer, K., Woolhouse, M. E., Hanotte, O. & Tapio, M. **2014**. Genome-wide analysis reveals the ancient and recent admixture history of East African Shorthorn Zebu from Western Kenya. *Heredity (Edinb),* 113**, 297-305**.
McGeoch, D. J., Rixon, F. J. & Davison, A. J. **2006**. Topics in herpesvirus genomics and evolution. *Virus Res,* 117**, 90-104**.
McIntosh, L. A., Marion, M. C., Sudman, M., Comeau, M. E., Becker, M. L., Bohnsack, J. F., Fingerlin, T. E., Griffin, T. A., Haas, J. P. & Lovell, D. J. **2017**. Genome-wide association

meta-analysis reveals novel juvenile idiopathic arthritis susceptibility loci. *Arthritis & Rheumatology,* 69**, 2222-2232**.
Meier-Trummer, C. S., Rehrauer, H., Franchini, M., Patrignani, A., Wagner, U. & Ackermann, M. **2009**. Malignant catarrhal fever of cattle is associated with low abundance of IL-2 transcript and a predominantly latent profile of ovine herpesvirus 2 gene expression. *PLoS One,* 4**, e6265**.
Mettenleiter, T. C., Klupp, B. G. & Granzow, H. **2006**. Herpesvirus assembly: a tale of two membranes. *Current Opinion in Microbiology,* 9**, 423-429**.
Mettenleiter, T. C. & Sobrino, F. 2008. *Animal viruses: molecular biology*, Horizon Scientific Press.
Metzler, A. E. **1991**. The malignant catarrhal fever complex. *Comp Immunol Microbiol Infect Dis,* 14**, 107-24**.
Milne, E. M. & Reid, H. W. **1990**. Recovery of a cow from malignant catarrhal fever. *Veterinary Record,* 126**, 640-641**.
Min, M., Mayor, U. & Lindon, C. **2013**. Ubiquitination site preferences in anaphase promoting complex/cyclosome (APC/C) substrates. *Open Biol,* 3**, 130097**.
Mitchell, E. S. & Scholes, S. F. **2009**. Unusual presentation of malignant catarrhal fever involving neurological disease in young calves. *Vet Rec,* 164**, 240-2**.
Mlilo, D., Mhlanga, M., Mwembe, R., Sisito, G., Moyo, B. & Sibanda, B. **2015**. The epidemiology of malignant catarrhal fever (MCF) and contribution to cattle losses in farms around Rhodes Matopos National Park, Zimbabwe. *Trop Anim Health Prod,* 47**, 989-94**.
Modesto, P., Grattarola, C., Biolatti, C., Varello, K., Casalone, C., Mandola, M. L., Caruso, C., Dondo, A., Goria, M., Rocca, F., Decaro, N., Leonardi, C., Iulini, B. & Acutis, P. L. **2015**. First report of malignant catarrhal fever in a captive pudu (Pudu puda). *Res Vet Sci,* 99**, 212-4**.
Modrow, S., Falke, D., Truyen, U. & Schätzl, H. 2013. *Molecular virology*, Springer.
Moore, D. A., Kohrs, P., Baszler, T., Faux, C., Sathre, P., Wenz, J. R., Eldridge, L. & Li, H. **2010**. Outbreak of malignant catarrhal fever among cattle associated with a state livestock exhibition. *J Am Vet Med Assoc,* 237**, 87-92**.
Mullis, K. B. **1990**. The unusual origin of the polymerase chain reaction. *Sci Am,* 262**, 56-61, 64-5**.
Münz, C. **2016**. Epstein Barr virus—a tumor virus that needs cytotoxic lymphocytes to persist asymptomatically. *Current opinion in virology,* 20**, 34-39**.
Mushi, E. & Wafula, J. **1983**. Infectivity of cell-free malignant catarrhal fever virus in rabbits and cattle. *Veterinary research communications,* 6**, 153-155**.
Mushi, E. Z. & Rurangirwa, F. R. **1981**. Epidemiology of bovine malignant catarrhal fevers, a review. *Vet Res Commun,* 5**, 127-42**.
Musser, J. M. **2004**. A practitioner's primer on foot-and-mouth disease. *Journal of the American Veterinary Medical Association,* 224**, 1261-1268**.
Myers, M. G. & Connelly, B. L. **1992**. Animal models of varicella. *Journal of Infectious Diseases,* 166**, S48-S50**.
Nelson, D. D., Davis, W. C., Brown, W. C., Li, H., O'Toole, D. & Oaks, J. L. **2010**. CD8(+)/perforin(+)/WC1(-) gammadelta T cells, not CD8(+) alphabeta T cells, infiltrate vasculitis lesions of American bison (Bison bison) with experimental sheep-associated malignant catarrhal fever. *Vet Immunol Immunopathol,* 136**, 284-91**.

Nelson, D. D., Taus, N. S., Schneider, D. A., Cunha, C. W., Davis, W. C., Brown, W. C., Li, H., O'Toole, D. & Oaks, J. L. **2013**. Fibroblasts express OvHV-2 capsid protein in vasculitis lesions of American bison (Bison bison) with experimental sheep-associated malignant catarrhal fever. *Vet Microbiol,* 166**, 486-92**.

Nicolas, C. S., Park, K.-H., El Harchi, A., Camonis, J., Kass, R. S., Escande, D., Mérot, J., Loussouarn, G., Le Bouffant, F. & Baró, I. **2008**. I Ks response to protein kinase A-dependent KCNQ1 phosphorylation requires direct interaction with microtubules. *Cardiovascular research,* 79**, 427-435**.

Nishimori, T., Ishihara, R., Kanno, T., Jayawardane, G. L., Nishimori, K., Uchida, I. & Imai, K. **2004**. Experimental transmission of ovine herpesvirus-2 in sheep. *J Vet Med Sci,* 66**, 1171-6**.

O'Toole, D. & Li, H. **2014**. The pathology of malignant catarrhal fever, with an emphasis on ovine herpesvirus 2. *Vet Pathol,* 51**, 437-52**.

O'Toole, D., Li, H., Miller, D., Williams, W. R. & Crawford, T. B. **1997**. Chronic and recovered cases of sheep-associated malignant catarrhal fever in cattle. *Vet Rec,* 140**, 519-24**.

O'Toole, D., Li, H., Sourk, C., Montgomery, D. L. & Crawford, T. B. **2002**. Malignant catarrhal fever in a bison (Bison bison) feedlot, 1993-2000. *J Vet Diagn Invest,* 14**, 183-93**.

O'Toole, D., Taus, N. S., Montgomery, D. L., Oaks, J. L., Crawford, T. B. & Li, H. **2007**. Intra-nasal inoculation of American bison (Bison bison) with ovine herpesvirus-2 (OvHV-2) reliably reproduces malignant catarrhal fever. *Vet Pathol,* 44**, 655-62**.

Odell, I. D. & Cook, D. **2013**. Immunofluorescence techniques. *J Invest Dermatol,* 133**, e4**.

Oehmig, A., Fraefel, C. & Breakefield, X. O. **2004**. Update on herpesvirus amplicon vectors. *Molecular Therapy,* 10**, 630-643**.

Ohteki, T. **2002**. Critical role for IL-15 in innate immunity. *Current molecular medicine,* 2**, 371-380**.

Okeson, D. M., Garner, M. M., Taus, N. S., Li, H. & Coke, R. L. **2007**. Ibex-associated malignant catarrhal fever in a bongo antelope (Tragelaphus euryceros). *J Zoo Wildl Med,* 38**, 460-4**.

Orzalli, M. H., Broekema, N. M., Diner, B. A., Hancks, D. C., Elde, N. C., Cristea, I. M. & Knipe, D. M. **2015**. cGAS-mediated stabilization of IFI16 promotes innate signaling during herpes simplex virus infection. *Proceedings of the National Academy of Sciences***, 201424637**.

Otter, A., Pow, I. & Reid, H. W. **2002**. Outbreak of malignant catarrhal fever in Welsh Black cattle in Carmarthenshire. *Vet Rec,* 151**, 321-4**.

Pagamjav, O., Sakata, T., Ibrahim el, S. M., Sugimoto, C., Takai, S., Paweska, J. T., Yamaguchi, T., Yasuda, J. & Fukushi, H. **2005**. Detection of novel gammaherpesviruses in wild animals of South Africa. *J Vet Med Sci,* 67**, 1185-8**.

Palmeira, L., Sorel, O., Van Campe, W., Boudry, C., Roels, S., Myster, F., Reschner, A., Coulie, P. G., Kerkhofs, P., Vanderplasschen, A. & Dewals, B. G. **2013**. An essential role for gamma-herpesvirus latency-associated nuclear antigen homolog in an acute lymphoproliferative disease of cattle. *Proc Natl Acad Sci U S A,* 110**, E1933-42**.

Palmer, M. V., Thacker, T. C., Madison, R. J., Koster, L. G., Swenson, S. L. & Li, H. **2013**. Active and latent ovine herpesvirus-2 (OvHV-2) infection in a herd of captive white-tailed deer (Odocoileus virginianus). *J Comp Pathol,* 149**, 162-6**.

Parameswaran, N., Dewals, B. G., Giles, T. C., Deppmann, C., Blythe, M., Vanderplasschen, A., Emes, R. D. & Haig, D. **2014**. The A2 gene of alcelaphine herpesvirus-1 is a

transcriptional regulator affecting cytotoxicity in virus-infected T cells but is not required for malignant catarrhal fever induction in rabbits. *Virus Res,* 188**, 68-80**.
Pellet, P. & Roizman, B. **2013**. Herpesviridae. *Fields Virology. Philadelphia: Lippincott Williams and Wilkins***, 1802-22**.
Petre, C. E., Sin, S. H. & Dittmer, D. P. **2007**. Functional p53 signaling in Kaposi's sarcoma-associated herpesvirus lymphomas: implications for therapy. *J Virol,* 81**, 1912-22**.
Petsch, D. & Anspach, F. B. **2000**. Endotoxin removal from protein solutions. *Journal of biotechnology,* 76**, 97-119**.
Pfeifer, A. & Verma, I. M. **2001**. Gene therapy: promises and problems. *Annual review of genomics and human genetics,* 2**, 177-211**.
Phillips, I. L., Cunha, C. W., Galbraith, D., Highland, M. A., Bildfell, R. J. & Li, H. **2018**. High copy number of ovine gammaherpesvirus 2 DNA associated with malignant catarrhal fever-like syndrome in a lamb. *J Vet Diagn Invest***, 1040638718766976**.
Piolot, T., Tramier, M., Coppey, M., Nicolas, J. C. & Marechal, V. **2001**. Close but distinct regions of human herpesvirus 8 latency-associated nuclear antigen 1 are responsible for nuclear targeting and binding to human mitotic chromosomes. *J Virol,* 75**, 3948-59**.
Plowright, W. **1965**. MALIGNANT CATARRHAL FEVER IN EAST AFRICA. II. OBSERVATIONS ON WILDEBEEST CALVES AT THE LABORATORY AND CONTACT TRANSMISSION OF THE INFECTION TO CATTLE. *Res Vet Sci,* 6**, 69-83**.
Plowright, W. **1968**. Malignant catarrhal fever. *J Am Vet Med Assoc,* 152**, 795-805**.
Plowright, W., Ferris, R. D. & Scott, G. R. **1960**. Blue wildebeest and the aetiological agent of bovine malignant catarrhal fever. *Nature,* 188**, 1167-9**.
Powers, J. G., VanMetre, D. C., Collins, J. K., Dinsmore, R. P., Carman, J., Patterson, G., Brahmbhatt, D. & Callan, R. J. **2005**. Evaluation of ovine herpesvirus type 2 infections, as detected by competitive inhibition ELISA and polymerase chain reaction assay, in dairy cattle without clinical signs of malignant catarrhal fever. *J Am Vet Med Assoc,* 227**, 606-11**.
Radkov, S. A., Kellam, P. & Boshoff, C. **2000**. The latent nuclear antigen of Kaposi sarcoma-associated herpesvirus targets the retinoblastoma–E2F pathway and with the oncogene Hras transforms primary rat cells. *Nature medicine,* 6**, 1121**.
Recillas-Targa, F. **2006**. Multiple strategies for gene transfer, expression, knockdown, and chromatin influence in mammalian cell lines and transgenic animals. *Molecular Biotechnology,* 34**, 337-354**.
Reid, H. W. & Bridgen, A. **1991**. Recovery of a herpesvirus from a roan antelope (Hippotragus equinus). *Vet Microbiol,* 28**, 269-78**.
Reid, H. W., Buxton, D., Pow, I. & Finlayson, J. **1986**. Malignant catarrhal fever: experimental transmission of the 'sheep-associated' form of the disease from cattle and deer to cattle, deer, rabbits and hamsters. *Res Vet Sci,* 41**, 76-81**.
Reid, H. W., Pow, I. & Buxton, D. **1989**. Antibody to alcelaphine herpesvirus-1 (AHV-1) in hamsters experimentally infected with AHV-1 and the 'sheep-associated' agent of malignant catarrhal fever. *Res Vet Sci,* 47**, 383-6**.
Riaz, A., Dry, I., Levy, C. S., Hopkins, J., Grey, F., Shaw, D. J. & Dalziel, R. G. **2014**. Ovine herpesvirus-2-encoded microRNAs target virus genes involved in virus latency. *J Gen Virol,* 95**, 472-80**.
Riaz, A., Murtaz-ul-Hasan, K. & Akhtar, N. **2017**. Recent Understanding of the Classification and Life Cycle of Herpesviruses: A Review. *Science Letters,* 5**, 195-207**.

Rosbottom, J., Dalziel, R. G., Reid, H. W. & Stewart, J. P. **2002**. Ovine herpesvirus 2 lytic cycle replication and capsid production. *J Gen Virol,* 83**, 2999-3002**.
Rossiter, P. B. **1981a**. Antibodies to malignant catarrhal fever virus in sheep sera. *J Comp Pathol,* 91**, 303-11**.
Rossiter, P. B. **1981b**. Immunofluorescence and immunoperoxidase techniques for detecting antibodies to malignant catarrhal fever in infected cattle. *Trop Anim Health Prod,* 13**, 189-92**.
Rossiter, P. B. **1982**. Attempts to protect rabbits against challenge with virulent, cell-associated, malignant catarrhal fever virus. *Vet Microbiol,* 7**, 419-25**.
Russell, G. C., Benavides, J., Grant, D. M., Todd, H., Thomson, J., Puri, V., Nath, M. & Haig, D. M. **2012**. Host gene expression changes in cattle infected with Alcelaphine herpesvirus 1. *Virus Res,* 169**, 246-54**.
Russell, G. C., Stewart, J. P. & Haig, D. M. **2009**. Malignant catarrhal fever: a review. *Vet J,* 179**, 324-35**.
Russell, G. C., Todd, H., Deane, D., Percival, A., Dagleish, M. P., Haig, D. M. & Stewart, J. P. **2013**. A novel spliced gene in alcelaphine herpesvirus 1 encodes a glycoprotein which isye secreted in vitro. *J Gen Virol,* 94**, 2515-23**.
Sambrook, J., Russell, D. W. & Maniatis, T. **2001**. Molecular cloning, vol. 1-3. *Cold Spring Habour Laboratory Press, New York*.
Sarek, G., Kurki, S., Enback, J., Iotzova, G., Haas, J., Laakkonen, P., Laiho, M. & Ojala, P. M. **2007**. Reactivation of the p53 pathway as a treatment modality for KSHV-induced lymphomas. *J Clin Invest,* 117**, 1019-28**.
Sarid, R., Flore, O., Bohenzky, R. A., Chang, Y. & Moore, P. S. **1998**. Transcription mapping of the Kaposi's sarcoma-associated herpesvirus (human herpesvirus 8) genome in a body cavity-based lymphoma cell line (BC-1). *Journal of virology,* 72**, 1005-1012**.
Schock, A., Collins, R. & Reid, H. **1998**. Phenotype, growth regulation and cytokine transcription in Ovine Herpesvirus-2 (OHV-2)-infected bovine T-cell lines. *Veterinary immunology and immunopathology,* 66**, 67-81**.
Schock, A. & Reid, H. W. **1996**. Characterisation of the lymphoproliferation in rabbits experimentally affected with malignant catarrhal fever. *Vet Microbiol,* 53**, 111-9**.
Schwam, D. R., Luciano, R. L., Mahajan, S. S., Wong, L. & Wilson, A. C. **2000**. Carboxy terminus of human herpesvirus 8 latency-associated nuclear antigen mediates dimerization, transcriptional repression, and targeting to nuclear bodies. *Journal of Virology,* 74**, 8532-8540**.
Sentsui, H., Nishimori, T., Nagai, I. & Nishioka, N. **1996**. Detection of sheep-associated malignant catarrhal fever virus antibodies by complement fixation tests. *J Vet Med Sci,* 58**, 1-5**.
Shapshak, P., Sinnott, J. T., Somboonwit, C. & Kuhn, J. H. **2015**. Global virology I : identifying and investigating viral diseases.
Shinohara, H., Fukushi, M., Higuchi, M., Oie, M., Hoshi, O., Ushiki, T., Hayashi, J.-I. & Fujii, M. **2002a**. Chromosome binding site of latency-associated nuclear antigen of Kaposi's sarcoma-associated herpesvirus is essential for persistent episome maintenance and is functionally replaced by histone H1. *Journal of virology,* 76**, 12917-12924**.
Shinohara, H., Fukushi, M., Higuchi, M., Oie, M., Hoshi, O., Ushiki, T., Hayashi, J. & Fujii, M. **2002b**. Chromosome binding site of latency-associated nuclear antigen of Kaposi's sarcoma-associated herpesvirus is essential for persistent episome maintenance and is functionally replaced by histone H1. *J Virol,* 76**, 12917-24**.

Si, H. & Robertson, E. S. **2006**. Kaposi's sarcoma-associated herpesvirus-encoded latency-associated nuclear antigen induces chromosomal instability through inhibition of p53 function. *J Virol,* 80**, 697-709**.

Si, H., Verma, S. C., Lampson, M. A., Cai, Q. & Robertson, E. S. **2008**. Kaposi's sarcoma-associated herpesvirus-encoded LANA can interact with the nuclear mitotic apparatus protein to regulate genome maintenance and segregation. *J Virol,* 82**, 6734-46**.

Sieber, V., Robert, N., Schybli, M., Sager, H., Miserez, R., Engels, M. & Ryser-Degiorgis, M. P. **2010**. Causes of mortality and diseases in farmed deer in Switzerland. *Vet Med Int,* 2010.

Simon, S., Li, H., apos, Toole, D., Crawford, T. B. & Oaks, J. L. **2003**. The vascular lesions of a cow and bison with sheep-associated malignant catarrhal fever contain ovine herpesvirus 2-infected CD8+ T lymphocytes. *Journal of General Virology,* 84**, 2009-2013**.

Sivachandran, N., Wang, X. & Frappier, L. **2012**. Functions of the Epstein-Barr virus EBNA1 protein in viral reactivation and lytic infection. *J Virol,* 86**, 6146-58**.

Slater, O. M., Peters-Kennedy, J., Lejeune, M., Gummer, D., Macbeth, B., Warren, A., Joseph, T., Li, H., Cunha, C. W. & Duignan, P. J. **2017**. Sheep-Associated Malignant Catarrhal Fever-Like Skin Disease in a Free-Ranging Bighorn Sheep ( Ovis canadensis ), Alberta, Canada. *J Wildl Dis,* 53**, 153-158**.

Sohn, S.-Y. & Hearing, P. **2012**. Adenovirus regulates sumoylation of Mre11-Rad50-Nbs1 components through a paralog-specific mechanism. *Journal of virology,* 86**, 9656-9665**.

Sood, R., Hemadri, D. & Bhatia, S. **2013**. Sheep associated malignant catarrhal fever: an emerging disease of bovids in India. *Indian J Virol,* 24**, 321-31**.

Spear, P. G., Eisenberg, R. J. & Cohen, G. H. **2000**. Three classes of cell surface receptors for alphaherpesvirus entry. *Virology,* 275**, 1-8**.

Stampfer, S. D., Lou, H., Cohen, G. H., Eisenberg, R. J. & Heldwein, E. E. **2010**. Structural basis of local, pH-dependent conformational changes in glycoprotein B from herpes simplex virus type 1. *Journal of virology,* 84**, 12924-12933**.

Stear, M. **2005**. OIE Manual of Diagnostic Tests and Vaccines for Terrestrial Animals (Mammals, Birds and Bees) 5th Edn. Volumes 1 & 2. World Organization for Animal Health 2004. ISBN 92 9044 622 6.€ 140. *Parasitology,* 130**, 727-727**.

Steen, H. & Mann, M. **2004**. The ABC's (and XYZ's) of peptide sequencing. *Nature reviews Molecular cell biology,* 5**, 699**.

Stenglein, M. D., Schumacher, A. J., LaRue, R. S. & Harris, R. S. 2009. Host Factors that Restrict Retrovirus Replication. *Viral Genome Replication.* Springer.

Stuhlmann, H., Cone, R., Mulligan, R. C. & Jaenisch, R. **1984**. Introduction of a selectable gene into different animal tissue by a retrovirus recombinant vector. *Proceedings of the National Academy of Sciences,* 81**, 7151-7155**.

Suavet, F., Champion, J. L., Bartolini, L., Bernou, M., Alzieu, J. P., Brugidou, R., Darnatigues, S., Reynaud, G., Perrin, C., Adam, G., Thiery, R. & Duquesne, V. **2016**. First Description of Infection of Caprine Herpesvirus 1 (CpHV-1) in Goats in Mainland France. *Pathogens,* 5.

Swa, S., Wright, H., Thomson, J., Reid, H. & Haig, D. **2001**. Constitutive activation of Lck and Fyn tyrosine kinases in large granular lymphocytes infected with the gamma-herpesvirus agents of malignant catarrhal fever. *Immunology,* 102**, 44-52**.

Swai, E. S., Kapaga, A. M., Sudi, F., Loomu, P. M. & Joshua, G. **2013**. Malignant catarrhal fever in pastoral Maasai herds caused by wildebeest associated alcelaphine herpesvirus-1: An outbreak report. *Vet Res Forum,* 4**, 133-6**.

Taus, N. S., Cunha, C. W., Marquard, J., O'Toole, D. & Li, H. **2015**. Cross-Reactivity of Neutralizing Antibodies among Malignant Catarrhal Fever Viruses. *PLoS One,* 10**, e0145073**.

Taus, N. S., Herndon, D. R., Traul, D. L., Stewart, J. P., Ackermann, M., Li, H., Knowles, D. P., Lewis, G. S. & Brayton, K. A. **2007**. Comparison of ovine herpesvirus 2 genomes isolated from domestic sheep (Ovis aries) and a clinically affected cow (Bos bovis). *J Gen Virol,* 88**, 40-5**.

Taus, N. S., O'Toole, D., Herndon, D. R., Cunha, C. W., Warg, J. V., Seal, B. S., Brooking, A. & Li, H. **2014**. Malignant catarrhal fever in American bison (Bison bison) experimentally infected with alcelaphine herpesvirus 2. *Vet Microbiol,* 172**, 318-22**.

Taus, N. S., Oaks, J. L., Gailbreath, K., Traul, D. L., O'Toole, D. & Li, H. **2006**. Experimental aerosol infection of cattle (Bos taurus) with ovine herpesvirus 2 using nasal secretions from infected sheep. *Vet Microbiol,* 116**, 29-36**.

Taus, N. S., Schneider, D. A., Oaks, J. L., Yan, H., Gailbreath, K. L., Knowles, D. P. & Li, H. **2010**. Sheep (Ovis aries) airway epithelial cells support ovine herpesvirus 2 lytic replication in vivo. *Vet Microbiol,* 145**, 47-53**.

Taus, N. S., Traul, D. L., Oaks, J. L., Crawford, T. B., Lewis, G. S. & Li, H. **2005**. Experimental infection of sheep with ovine herpesvirus 2 via aerosolization of nasal secretions. *J Gen Virol,* 86**, 575-9**.

Teankam, K., Tantilertcharoen, R., Boonserm, T., Suadsong, S. & Banlunara, W. **2006**. Malignant catarrhal fever in swamp buffaloes (Bubalus bubalis): A retrospective pathological study of outbreaks in Thailand. *The Thai Journal of Veterinary Medicine,* 36**, 19-30**.

Thonur, L., Russell, G. C., Stewart, J. P. & Haig, D. M. **2006**. Differential transcription of ovine herpesvirus 2 genes in lymphocytes from reservoir and susceptible species. *Virus Genes,* 32**, 27-35**.

Towbin, H., Staehelin, T. & Gordon, J. **1979**. Electrophoretic transfer of proteins from polyacrylamide gels to nitrocellulose sheets: procedure and some applications. *Proc Natl Acad Sci U S A,* 76**, 4350-4**.

Traul, D. L., Elias, S., Taus, N. S., Herrmann, L. M., Oaks, J. L. & Li, H. **2005**. A real-time PCR assay for measuring alcelaphine herpesvirus-1 DNA. *J Virol Methods,* 129**, 186-90**.

Traul, D. L., Taus, N. S., Lindsay Oaks, J., O'Toole, D., Rurangirwa, F. R., Baszler, T. V. & Li, H. **2007**. Validation of nonnested and real-time PCR for diagnosis of sheep-associated malignant catarrhal fever in clinical samples. *J Vet Diagn Invest,* 19**, 405-8**.

Tyanova, S., Temu, T., Sinitcyn, P., Carlson, A., Hein, M. Y., Geiger, T., Mann, M. & Cox, J. **2016**. The Perseus computational platform for comprehensive analysis of (prote) omics data. *Nature methods,* 13**, 731**.

Uppal, T., Banerjee, S., Sun, Z., Verma, S. & Robertson, E. **2014**. KSHV LANA—the master regulator of KSHV latency. *Viruses,* 6**, 4961-4998**.

van Steensel, B., van Binnendijk, E. P., Hornsby, C. D., Van der Voort, H., Krozowski, Z. S., de Kloet, E. R. & van Driel, R. **1996**. Partial colocalization of glucocorticoid and mineralocorticoid receptors in discrete compartments in nuclei of rat hippocampus neurons. *Journal of cell science,* 109**, 787-792**.

van Vuuren, M. **2004**. Malignant catarrhal fever (MCF).

Vázquez, E. D. L., Carey, V. J. & Kaye, K. M. **2013**. Identification of Kshv Lana regions important for episome segregation, replication and persistence. *Journal of virology*, **JVI. 01243-13**.

Verma, S. C., Cai, Q., Kreider, E., Lu, J. & Robertson, E. S. **2013**. Comprehensive analysis of LANA interacting proteins essential for viral genome tethering and persistence. *PLoS One,* 8**, e74662**.

Verma, S. C., Choudhuri, T., Kaul, R. & Robertson, E. S. **2006**. Latency-associated nuclear antigen (LANA) of Kaposi's sarcoma-associated herpesvirus interacts with origin recognition complexes at the LANA binding sequence within the terminal repeats. *Journal of virology,* 80**, 2243-2256**.

Verma, S. C. & Robertson, E. S. **2003**. Molecular biology and pathogenesis of Kaposi sarcoma-associated herpesvirus. *FEMS Microbiology Letters,* 222**, 155-163**.

Verma, S. P. & Armstrong-Altrin, J. S. **2013**. New multi-dimensional diagrams for tectonic discrimination of siliciclastic sediments and their application to Precambrian basins. *Chemical Geology,* 355**, 117-133**.

Vikøren, T., Li, H., Lillehaug, A., Monceyron Jonassen, C., Böckerman, I. & Handeland, K. **2006**. Malignant catarrhal fever in free-ranging cervids associated with OvHV-2 and CpHV-2 DNA. *Journal of wildlife diseases,* 42**, 797-807**.

Waldmann, T. A. **2006**. The biology of interleukin-2 and interleukin-15: implications for cancer therapy and vaccine design. *Nature Reviews Immunology,* 6**, 595**.

Wambua, L., Wambua, P. N., Ramogo, A. M., Mijele, D. & Otiende, M. Y. **2016**. Wildebeest-associated malignant catarrhal fever: perspectives for integrated control of a lymphoproliferative disease of cattle in sub-Saharan Africa. *Arch Virol,* 161**, 1-10**.

Weber, E., Anderson, W. F. & Kasahara, N. **2001**. Recent advances in retrovirus vector-mediated gene therapy: teaching an old vector new tricks. *Curr Opin Mol Ther,* 3**, 439-53**.

Wei, F., Gan, J., Wang, C., Zhu, C. & Cai, Q. **2016**. Cell Cycle Regulatory Functions of the KSHV Oncoprotein LANA. *Frontiers in Microbiology,* 7.

Wen, K. W., Dittmer, D. P. & Damania, B. **2009**. Disruption of LANA in rhesus rhadinovirus generates a highly lytic recombinant virus. *Journal of virology,* 83**, 9786-9802**.

Wessels, M., Harwood, D., Maley, M., Willoughby, K. & Balfour, C. **2011**. Malignant catarrhal fever in kune kune pigs in the UK. *Vet Rec,* 169**, 156**.

Wilkinson, J., Galea-Lauri, J. & Reid, H. **1992**. A cytotoxic rabbit T-cell line infected with a gamma-herpes virus which expresses CD8 and class II antigens. *Immunology,* 77**, 106**.

Williams, E. S. & Barker, I. K. **2008**. Infectious Diseases Of Wild Mammals.

Wilson, R. **2013**. Sensitivity and specificity: twin goals of proteomics assays. Can they be combined? *Expert review of proteomics,* 10**, 135-149**.

Wiyono, A., Baxter, S. I., Saepulloh, M., Damayanti, R., Daniels, P. & Reid, H. W. **1994**. PCR detection of ovine herpesvirus-2 DNA in Indonesian ruminants--normal sheep and clinical cases of malignant catarrhal fever. *Vet Microbiol,* 42**, 45-52**.

Ye, F., Lei, X. & Gao, S.-J. **2011**. Mechanisms of Kaposi's Sarcoma-Associated Herpesvirus Latency and Reactivation. *Advances in Virology,* 2011**, 19**.

Ye, F. C., Zhou, F. C., Yoo, S. M., Xie, J. P., Browning, P. J. & Gao, S. J. **2004**. Disruption of Kaposi's sarcoma-associated herpesvirus latent nuclear antigen leads to abortive episome persistence. *J Virol,* 78**, 11121-9**.

Yin, Y., Manoury, B. & Fåhraeus, R. **2003**. Self-Inhibition of Synthesis and Antigen Presentation by Epstein-Barr Virus-Encoded EBNA1. *Science,* 301**, 1371-1374**.

Zachary, J. **2012**. Bovine malignant catarrhal fever. *Pathologic basis of veterinary disease. 5th ed. St Louis, Missouri: Elsevier/Mosby***, 219-219**.

Zemljic, T., Pot, S. A., Haessig, M. & Spiess, B. M. **2012**. Clinical ocular findings in cows with malignant catarrhal fever: ocular disease progression and outcome in 25 cases (2007-2010). *Vet Ophthalmol,* 15**, 46-52**.

Zemljič, T., Pot, S. A., Haessig, M. & Spiess, B. M. **2012**. Clinical ocular findings in cows with malignant catarrhal fever: ocular disease progression and outcome in 25 cases (2007–2010). *Veterinary Ophthalmology,* 15**, 46-52**.

Zhang, D., Manna, M., Wohland, T. & Kraut, R. **2009**. Alternate raft pathways cooperate to mediate slow diffusion and efficient uptake of a sphingolipid tracer to degradative and recycling compartments. *Journal of cell science,* 122**, 3715-3728**.

Zhang, G., Chan, B., Samarina, N., Abere, B., Weidner-Glunde, M., Buch, A., Pich, A., Brinkmann, M. M. & Schulz, T. F. **2016a**. Cytoplasmic isoforms of Kaposi sarcoma herpesvirus LANA recruit and antagonize the innate immune DNA sensor cGAS. *Proc Natl Acad Sci U S A,* 113**, E1034-43**.

Zhang, G., Chan, B., Samarina, N., Abere, B., Weidner-Glunde, M., Buch, A., Pich, A., Brinkmann, M. M. & Schulz, T. F. **2016b**. Cytoplasmic isoforms of Kaposi sarcoma herpesvirus LANA recruit and antagonize the innate immune DNA sensor cGAS. *Proceedings of the National Academy of Sciences,* 113**, E1034-E1043**.

Zhang, Y.-J., Deng, J.-H., Rabkin, C. & Gao, S.-J. **2000**. Hot-spot variations of Kaposi's sarcoma-associated herpesvirus latent nuclear antigen and application in genotyping by PCR–RFLP. *Journal of General Virology,* 81**, 2049-2058**.

Zheng, C. **2018**. Evasion of cytosolic DNA-stimulated innate immune responses by herpes simplex virus 1. *Journal of virology,* 92**, e00099-17**.

Zinchuk, O., Fukushima, A., Zinchuk, V., Fukata, K. & Ueno, H. **2005**. Direct action of platelet activating factor (PAF) induces eosinophil accumulation and enhances expression of PAF receptors in conjunctivitis. *Mol Vis,* 11**, 114-123**.

Zinchuk, V. & Grossenbacher-Zinchuk, O. **2011**. Quantitative colocalization analysis of confocal fluorescence microscopy images. *Current protocols in cell biology,* 52**, 4.16. 1-4.16. 19**.

Zinchuk, V., Zinchuk, O. & Okada, T. **2007**. Quantitative colocalization analysis of multicolor confocal immunofluorescence microscopy images: pushing pixels to explore biological phenomena. *Acta histochemica et cytochemica,* 40**, 101-111**.